



HAL
open science

Antibody conjugates : integrated approach towards selective, stable and controllable bioconjugation

Igor Dovgan

► **To cite this version:**

Igor Dovgan. Antibody conjugates: integrated approach towards selective, stable and controllable bioconjugation. Organic chemistry. Université de Strasbourg, 2017. English. NNT : 2017STRAF036 . tel-02872896

HAL Id: tel-02872896

<https://theses.hal.science/tel-02872896>

Submitted on 18 Jun 2020

HAL is a multi-disciplinary open access archive for the deposit and dissemination of scientific research documents, whether they are published or not. The documents may come from teaching and research institutions in France or abroad, or from public or private research centers.

L'archive ouverte pluridisciplinaire **HAL**, est destinée au dépôt et à la diffusion de documents scientifiques de niveau recherche, publiés ou non, émanant des établissements d'enseignement et de recherche français ou étrangers, des laboratoires publics ou privés.

ÉCOLE DOCTORALE DES SCIENCES CHIMIQUES
UMR 7199, Laboratoire des Systèmes Chimiques Fonctionnels

THÈSE

présentée par :

Igor DOVGAN

soutenue le : **21 septembre 2017**

pour obtenir le grade de : **Docteur de l'Université de Strasbourg**

Discipline/ Spécialité : Chimie Organique

**Antibody conjugates: integrated approach
towards selective, stable and controllable
bioconjugation**

THÈSE dirigée par :

WAGNER Alain

Docteur, Université de Strasbourg

RAPPORTEURS :

BIOT Christophe
CHUDASAMA Vijay

Professeur, Université de Lille 1
Docteur, University College London

AUTRES MEMBRES DU JURY :

CIANFÉRANI Sarah

Docteur, Université de Strasbourg

Leonardo da Vinci:

“Where Nature finishes producing its own species man begins, with the help of Nature, to create an infinity of species”

ACKNOWLEDGMENTS

This PhD work has been carried out in the Laboratory of Functional Chemo-Systems (LFCS; currently BioFunctional Chemistry, BFC) of the Faculty of Pharmacy at the University of Strasbourg under the supervision of Dr. Alain Wagner and has received financial support from University of Strasbourg and Region Alsace. This work could not be possible also without acknowledging a number of people who supervised me, helped me and supported me over the past three years.

First of all, I would like to thank my PhD supervisor Dr. Alain Wagner for giving me an opportunity to work on the fascinating projects and for the freedom and confidence I was gained to realize them. I wish to acknowledge all his support and encouragement during my research and his constant enthusiasm towards my sometime naïve ideas.

I would also like to express my thanks to jury members: Prof. Christophe Biot from the University of Lille and Dr. Vijay Chudasama from the University College London for examining my work, Dr. Sarah Cianférani from the University of Strasbourg for the acceptance to be the President of this committee and Dr. Sergii Kolodych from Syndivia for his willingness to participate in the thesis discussion.

I am very grateful to those who helped me on my early stage in the lab: Oleksandr Koniev for the course of organic synthesis and experiment settings, for his invariable and relentless guidance to work hard; Sergii Kolodych for the wise supervision in bioconjugate chemistry and for our fruitful tea-time discussion about science and life.

I would like to express my gratitude to those who helped my research to be done; Sylvain Ursuegui for the generous sharing of his linkers, the synthesis of oligonucleotide derivative and for the constant readiness to help. The LSMBO group – Stephane Erb, Anthony Ehkirch, Steve Hessmann, Sarah Cianferani, and Alain van Dorsselaer – for the realisation of the screening project. Our new permanent, Guilhem Chaubet, for his help with the thesis proofread. All the colleges from our UMR; in particular Eric and Celia for the time spend together and our funny journey to Amsterdam, Manon for the successful projects done together.

Enormous thank you to all my friends from Strasbourg, who were always near to help or to have fun: Nina, Anna D, Anna Z, Natalia, Viktoriia, Diana, Olga, Kon'ko, Iiulia D. & Dima D., Simon, Vuk, Joe. To Kyong for making me his very tasty cappuccino during my thesis writing. To my friends from Toulouse: Roberto, Marie and Emmanuelito, thanks a lot guys for your friendship and our crazy parties! To my friends from Ukraine: Vetalka, Kolya, Magir, Danil, Viktor, Levko, Oleg for being in contact, even after so many years being in distance.

A special thanks to Artem Osypenko who has motivated me to come in France and for our perpetual philosophic evening spent together that I liked so much. To Dima Kandaskalov for his tutoring in chemistry during my preparation to chemical Olympiads (the best teacher ever).

I thank my wife for her love, her constant support and believe in me, for her patience and her courage. I would like to thank all my family, especially my mum and sister for their love and support throughout my life.

ABBREVIATIONS

ABF	<i>p</i> -Azidobenzoyl Fluoride
ABNHS	<i>p</i> -Azidobenzoyl <i>N</i> -Hydroxysuccinimide
ACs	Antibody Conjugates
ADCs	Antibody-Drug Conjugates
ADCC	Antibody-Dependent Cell-Mediated Cytotoxicity
AOCs	Antibody-Oligonucleotide Conjugates
APG	<i>p</i> -Azidophenyl Glyoxal Monohydrate
APN	3-Arylpropionitriles
BBS	Borate Buffered Saline
BCN	Bicyclo[6.1.0]Nonyne
BHQ	Black Hole Quencher
BME	B-Mercaptoethanol
CBTF	4-((4-(Cyanoethynyl)Benzoyl)Oxy)-2,3,5,6-Tetrafluorobenzenesulfonate
CuAAC	Copper(I)-Catalysed Alkyne-Azide Cycloaddition
DCC	<i>N,N'</i> -Dicyclohexylcarbodiimide
DCM	Dichloromethane
DIBO	Dibenzoazacyclooctyne
DIPEA	<i>N,N</i> -Diisopropylethylamine
DMF	Dimethylformamide
DoC	Average Degree Of Conjugation
DTT	Dithiothreitol
EDC, EDCI	1-Ethyl-3-(3-Dimethylaminopropyl)Carbodiimide
EDTA	Ethylenediaminetetraacetic Acid
Fab	Fragment Antigen-Binding
FBDP	Formylbenzene Diazonium Hexafluorophosphate
FcRn	Neonatal Fc Receptor
FDA	U.S. Food And Drug Administration
HATU	1-[Bis(Dimethylamino)Methylene]-1 <i>H</i> -1,2,3-Triazolo[4,5- <i>B</i>]Pyridinium3-Oxide Hexafluorophosphate
HBTU	<i>O</i> -Benzotriazole- <i>N,N,N',N'</i> -Tetramethyl-Uronium Hexafluorophosphate
HIV	Human Immunodeficiency Virus
HOBt	Hydroxybenzotriazole
HRMS	High Resolution Mass Spectrometry
IC50	Half Maximal Inhibitory Concentration
LCMS	Liquid Chromatography Mass Spectrometry
LRMS	Low Resolution Mass Spectrometry

mAb	Monoclonal Antibody
MAPN	<i>p</i> -(Maleimide)-Phenylpropiolonitrile
MDTF	Sodium 4-(Maleimidomethyl)-1,3-Dioxane-5-Carbonyl)Oxy)-2,3,5,6-Tetrafluorobenzenesulfonate
MS	Mass Spectroscopy
MWCO	Molecular Weight Cut Off
native-HRMS	High Resolution Native Mass Spectrometry
NHS	<i>N</i> -Hydroxysuccinimidyl
NMR	Nuclear Magnetic Resonance
PCR	Polymerase Chain Reaction
PB	Phosphate Buffer
PBS	Phosphate Buffered Saline
PEG	Polyethylene Glycol
PTAD	4-Phenyl-3h-1,2,4-Triazole-3,5(4h)-Dione
PyBOP	(Benzotriazol-1-Yloxy)Tripyrrolidinophosphonium Hexafluorophosphate
RNA	Ribonucleic Acid
SDS-PAGE	Sodium Dodecyl Sulfate - Polyacrylamide Gel Electrophoresis
SMCC	<i>N</i> -Succinimidyl-4-(Maleimidomethyl)-Cyclohexanecarboxylate
SPAAC	Strain-Promoted Alkyne–Azide Cycloadditions
STP	Sodium 2,3,5,6-Tetrafluoro-4-Hydroxybenzene-1-Sulfonate
TAMRA	Tetramethylrhodamine
TCEP	Tris(2-Carboxyethyl)Phosphine Hydrochloride
TFA	Trifluoroacetic Acid
THF	Tetrahydrofuran
TLC	Thin Layer Chromatography
Tris	Tris(Hydroxymethyl)Aminomethane
UV-Vis	Ultraviolet-Visible Spectrophotometry

TABLE OF CONTENTS

A. Introduction	1
1 Bioconjugate chemistry	1
2 Antibody conjugates	1
2.1 Antibodies	2
2.2 Antibody structure.....	3
2.3 Antibody-drug conjugates.....	5
3 Chemical approach for antibody conjugation.....	7
3.1 Bioorthogonal reaction and click chemistry	7
3.2 Strategies for antibody functionalisation	8
3.3 Aspartic and glutamic acid.....	9
3.4 Lysine residues.....	10
3.5 Cysteine residues.....	14
3.6 Disulfide rebridging	19
3.7 Tyrosine residues	23
3.8 Arginine residues	27
3.9 Tryptophan residues.....	28
3.10 Methionine residues	29
3.11 Glycan residues	31
4 Objectives	31
B. Towards a novel chemistry for bioconjugation	33
Part 1. Development of novel linker for bioconjugation	33
1.1 Introduction.....	33
1.2 Design of more hydrophilic linkers	34
1.3 Synthesis of MDTF	35
1.4 Stability of MD and MCC linkers in human plasma	35
1.5 Stability of MD and MCC linkers <i>in vitro</i>	37
1.6 Application of MDTF reagent for the preparation of antibody conjugates	38
Part 2. Screening and development of residue-selective reagents	40
2.1 Design of the screening system.....	40

2.2 Acyl fluoride for plug-and-play bioconjugation	45
2.3 Arginine-selective functionalisation of antibodies	54
Part 3. Mono-functionalised ACs	59
3.1 Introduction	59
3.2 Trans-tagging of proteins	61
3.3 Antibody conjugates with single payload	62
3.4 Stability of antibody-iSyd-Biotin conjugates on the column	64
3.5 Conclusions and perspectives	65
C. Experimental part.....	67
1 General Methods.....	67
1.1 Experimental procedures.....	67
1.2 Materials.....	67
1.3 Instrumentation	67
1.4 Software	69
2 General Procedures	69
2.1 Protein concentration measuring.....	69
2.2 Antibody conjugates purification.....	69
2.3 SDS PAGE analysis	70
2.4 Antibody conjugates preparation for MS analysis.....	70
2.5 Calculation of the DoC	70
2.6 Antibody conjugates affinity.....	70
2.7 Stability of P1 and P2 in human plasma and other media	71
2.8 Hydrolysis of succinimide of P1 and P2 in human plasma.....	71
2.9 Hydrolytic stability of R1-R20, ABF and ABNHS	71
2.10 Aminolysis of ABF, ABNHS, R2 and R4	71
2.11 Stability of T-TAMRA(R), C1 and C2 in human plasma.....	72
3 Bioconjugation.....	73
3.1 Maleimide dioxane linkage	73
3.3 Acyl fluoride chemistry	73
3.4 Phenyl glyoxal chemistry.....	74

3.5 Preparation of mono-functionalised ACs.....	75
4 Compounds synthesis	77
References	94
Annexes	105
Annex 1	105
Annex 2.....	106
Annex 3.....	107
Annex 4.....	110
Annex 5.....	122

A. INTRODUCTION

In this chapter the current developments in antibody conjugation techniques were highlighted. The various sites in native antibodies able for selective labelling have been surveyed with attention on most relevant among reported methods. Advantages and drawbacks of these methods with reference to efficacy, selectivity and conjugate stability have been discussed.

1 Bioconjugate chemistry

Bioconjugate chemistry is a chemical strategy to perform a stable covalent linkage between two molecules of interest, at least one of which is a biomolecule.¹⁻³ The resulting adduct – a bioconjugate – possesses the combined properties of its individual components and can serve as safer and more efficient therapeutics, assemblies for studying proteins in their biological context, new protein-based materials, microarrays, biologics, tools for immobilisation, or elucidation of the structure of proteins.³

The majority of bioconjugates consists of three main parts: a biomolecule, a linker and an attached entity called payload (Figure 1).

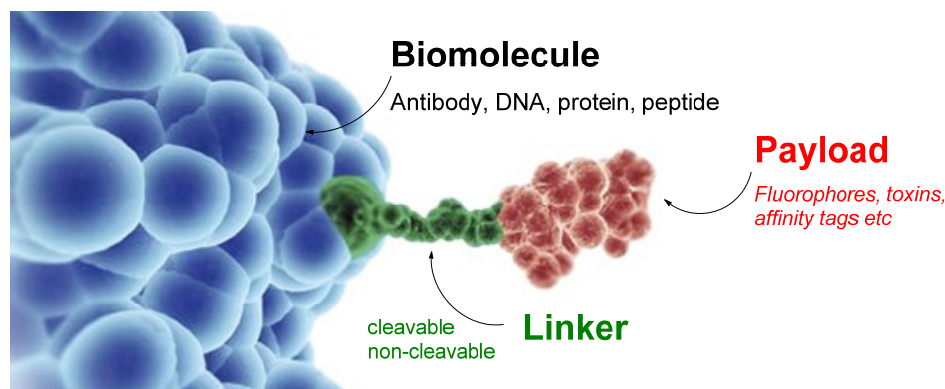


Figure 1. Three main components of bioconjugates. Adapted from www.syndivia.com

The biomolecule can vary starting from small peptides and ending with macromolecules, such as antibodies, DNA or viral capsids. The linker is an important component of the bioconjugates, as its main function is to firmly connect the entities together. The payload aims to enhance the functionality of biomolecules. For instance, a payload can be represented by fluorophores or radionuclides to make the conjugate traceable, by polyethyleneglycols to improve the solubility, by affinity tags to facilitate the affinity purification and detection, or by cytotoxic drugs for targeted delivery, when the biomolecule is represented by an antibody.

2 Antibody conjugates

Among a large variety of bioconjugates, antibody-drug conjugates (ADCs) have gained a great attention of scientific community during the last decade as more efficient and safer alternative to traditional cancer chemotherapies.^{4,5} ADC is comprised of three components: a monoclonal antibody

(mAb) against antigens overexpressed on cancer cells, a highly cytotoxic drug (often called a warhead) with subnanomolar half-maximal inhibitory concentration (IC₅₀) values and a linker that connects these two entities (Figure 2). In the ADC, the antibody acts as a vehicle allowing for delivery of the potent cytotoxic drug selectively to the tumour cells.

Another interesting type of antibody conjugates (ACs) is antibody-oligonucleotides conjugates (AOCs), which are powerful tools for antigen detection in immuno-PCR^{6,7} and are considered to be attractive for specific delivery of small interference RNA (siRNA) molecules into the cells.⁸

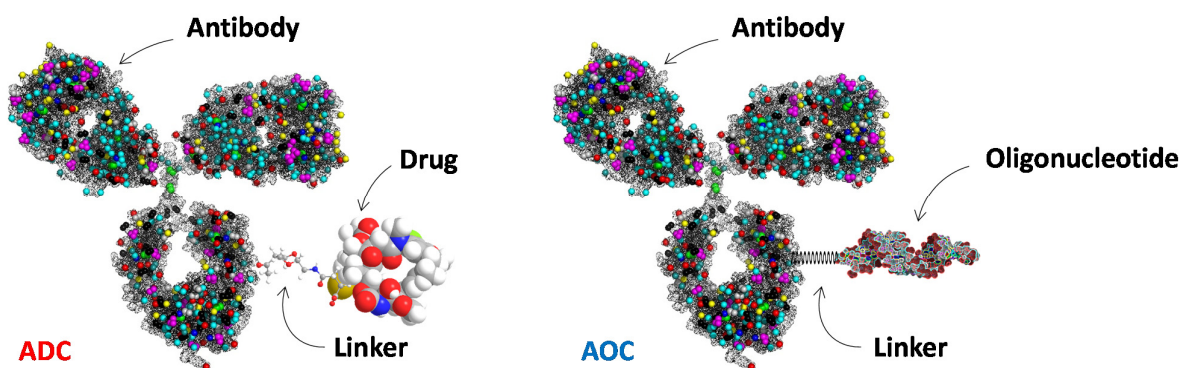


Figure 2. Representations of antibody-drug conjugates (ADCs) and antibody-oligonucleotide conjugates (AOCs).

In this regards, the development of reliable methodologies for ACs preparation is currently of high demand. The controllable conjugation and preparation of ACs with defined structure are still challenging due to high excess of reactive groups in antibody structure, which are accessible for conjugation (in Figure 2, the coloured dots on antibody represent these reactive functions).

In this work, we will focus on chemical approaches for the reliable antibody functionalisation, which enable the preparation of stable ACs conjugates with well-defined payload to antibody ratios. To this end, first of all the reader should be informed about the basis of antibody structure and properties, which is reviewed in the next sections.

2.1 Antibodies

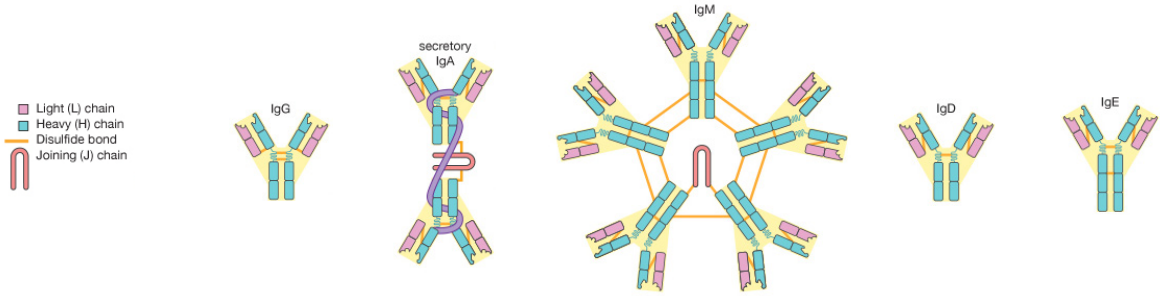
Antibodies, also known as immunoglobulins (Ig), are Y-shaped glycoproteins produced by immune system in B-cells in order to protect the organism against invading pathogens, such as bacteria and viruses. These macromolecules (*ca.* 150 kDa and above) can recognise a specific region on a harmful agent, called antigen, and bind it with high precision. Using this binding, an antibody can tag the pathogen for further attack by other components of the immune system or can neutralise the invader directly by blocking, for instance, its vital parts. Owing to high selectivity of the antigen recognition, antibodies have recently gained much attention as targeted therapeutics alone, *via* antibody-dependent cell-mediated cytotoxicity (ADCC), and as vehicles for drug delivery and imaging.

Depending on the structure of the constant domains of the heavy chain, antibodies are grouped into five classes, or isotypes: IgG, IgA, IgM, IgD and IgE (Table 1). The classes of antibody differ

not only in their structures, but also in the functions. For instance, the most common antibody, IgG, is present mostly in the blood and tissue fluids, while IgA is found in the mucous membranes lining the respiratory and gastrointestinal tracts. Some isotypes are also subdivided into Ig subclasses. There are four different types of IgG (IgG1, IgG2, IgG3 and IgG4) and two of IgA (IgA1 and IgA2) in humans, with more than 95% similarity in their sequences. In normal human serum, IgG1, IgG2, IgG3, and IgG4 are found in the approximate proportions of 65, 25, 5, and 5%, respectively.

Antibodies against the same antigen can be either polyclonal or monoclonal. Polyclonal antibodies are derived from different B cells and recognize different parts (called epitopes) on the same antigen. By contrast, monoclonal antibody is produced from a single B cell and it only binds to one unique epitope of the antigen.

Table 1. Five classes of human antibodies: their structures, characteristics and functions.



Class	IgG (γ)	IgA (α)	IgM (μ)	IgD (δ)	IgE (ϵ)
Structure	Monomer	Dimer	Pentamer	Monomer	Monomer
Percentage of total serum antibody	80%	10-15%	5-10%	0.2%	0.002%
Molecular weight	150 000	405 000	970 000	175 000	190 000
Half-life in serum	23 days	6 days	5 days	3 days	2 days
Function	Immunity to pathogens	Agglutination, immunity to pathogens	Agglutination, initiation of classical complement pathway	Activation of B cells	Allergy, immunity to parasites

2.2 Antibody structure

Antibodies are symmetrical glycoproteins comprising of four polypeptide chains: two light chains and two heavy chains, which interconnect by disulfide bonds (Figure 3). The first hundred amino acid residues of the both chains vary greatly from antibody to antibody (variable region), while their remaining parts consist of amino acids that are almost identical (the constant regions). Antibody can be divided enzymatically or chemically into several different fragments:

- **Fv fragment** (variable). This is the smallest fragment (*ca.* 25 kDa) that still can bind to a particular antigen. It is comprised of non-covalently connected V_L and V_H domains. More specifically, Fv fragments bind its antigen through β -loops that are referred as complementarity determining regions (CDRs).

- **Fab fragment** (antigen-binding). This fragment (*ca.* 50 kDa) can be obtained by papain cleavage and has the same affinity to the antigen as the full antibody. Fab consists of the whole light chain and of part of the heavy chain (V_H and C_{H1}), which are connected *via* one disulfide bond.
- **F(ab')₂ fragment**. This part of the antibody (*ca.* 110 kDa) can be prepared by pepsin cleavage and corresponds to the association of two Fab fragments linked together by two disulfide-bonds. In contrast to monovalent Fv and Fab, this fragment is bivalent just like the full antibody.
- **Fc fragment** (crystallisable). This fragment (*ca.* 50 kDa) possesses the biological properties of the antibodies, in particular its ability to interact with surface receptors of effector cell of the immune system or to activate the complement system. This region is also responsible for binding with neonatal Fc receptor (FcRn), which performs a recycling of the IgG from cellular compartments and thus prolong its half-life in serum. Fc are obtained together with Fab fragments during papain cleavage of the full antibody and for IgG1 it consists of two constant domain (C_{H2} and C_{H3}) connected by two disulfide bonds. Antibodies have one carbohydrate residue on each C_{H2} domain of Fc fragments, more precisely on Asn297. These *N*-glycans control the quaternary structure of the antibodies and can alter the affinity for Fc and other immune receptors.

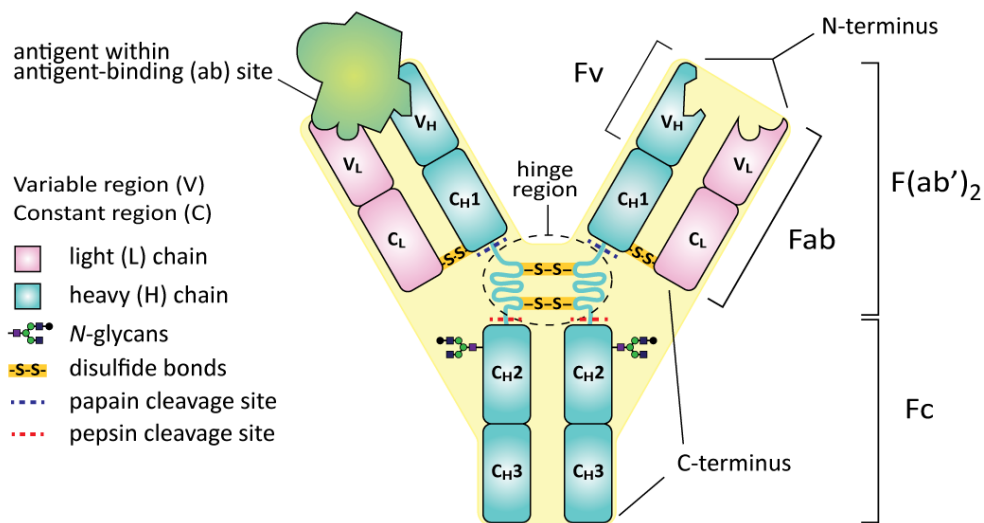


Figure 3. General structure of an IgG1 with its fragments highlighted. Adapted from Encyclopædia Britannica, Inc.

Owing to favourable pharmacokinetic of antibodies and their long half-life in serum, the conjugation of a drug molecule to them can increase the circulation time of the therapeutic agent and thus enhance its therapeutic effect. Moreover, high specificity of antibody-antigen recognition enables the possibility to use more potent drugs (IC₅₀ in subnanomolar range), which cannot otherwise be applied for conventional chemotherapy due to the high toxicity. All these exceptional properties of antibodies paved a way towards their application as targeted cancer therapies – antibody-drug conjugates.

2.3 Antibody-drug conjugates

In 1958, the first example of covalent attachment of a chemotherapeutic agent to an antibody was demonstrated by the research team of Jean Bernard at the Hérould Hospital in Paris.⁹ Namely, hamster IgGs were reacted with diazotised form of methotrexate and the resulting ADC was used against leukemia xenografts in hamsters (Figure 4). It was found that this immunoconjugate significantly prolonged animal survival compared with the unconjugated antibody, the drug, or a noncovalent mixture thereof. Thus, the covalent coupling of methotrexate to the targeting antibody demonstrated a beneficial clinical effect. In this case, the antibody molecules could be regarded as “guided missiles”, which carry and deliver cytotoxic agents specifically to the targeted cells.

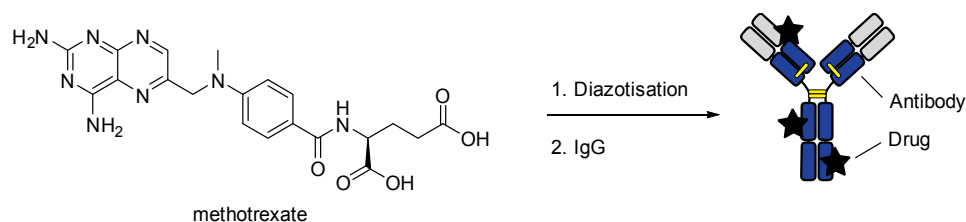


Figure 4. Preparation of the first reported ADC.

Since then, the technologies of antibody conjugation and ADC design have started to develop unceasingly. Non-covalently and covalently linked ADCs were tested in animal models in the 1970's followed less than decade later by the first clinical trial with the antimetabolic vinca alkaloid vindesine as cytotoxic payload.¹⁰ Despite promising results, these early attempts relied exclusively on available at that time polyclonal murine antibodies, which caused significant immune reactions in humans. These issues were overcome in the 1990's by designing ADCs based on chimeric and humanised monoclonal antibodies (mAbs).¹¹ Subsequently, the rational target selection and increase of the drug potency provided more efficient ADCs.¹² This led to the first-generation ADC (Mylotarg®, gemtuzumab ozogamicin, developed by Pfizer) approved for the first time by US Food and Drug Administration (FDA) in 2000 (Figure 5).¹³

Despite initially promising clinical results, Mylotarg® was withdrawn from the market in 2010 due to a lack of clinical benefit over standard chemotherapy (in early 2017 Pfizer reapplied for US and EU approval). However, very soon two second-generation ADCs gained FDA approval: Adcetris®, brentuximab vedotin (developed by Seattle Genetics)^{14–16} in 2011 and Kadcyla®, trastuzumab emtansine (also known as T-DM1 and ado-trastuzumab emtansine; developed by Roche and Immunogen)^{17,18} in 2013. Currently, there are more than 60 ADCs in the clinical trials and their market is expected to increase in the future.

One of the important parameters of an ADC is the average drug to antibody ratio (average DAR), because it determines the overall amount of drug that can be delivered to the target cells and can directly correlate with both safety and efficacy. For bioconjugate chemistry in general, this term corresponds to the average degree of conjugation (hereinafter, we will shortcut it as DoC).

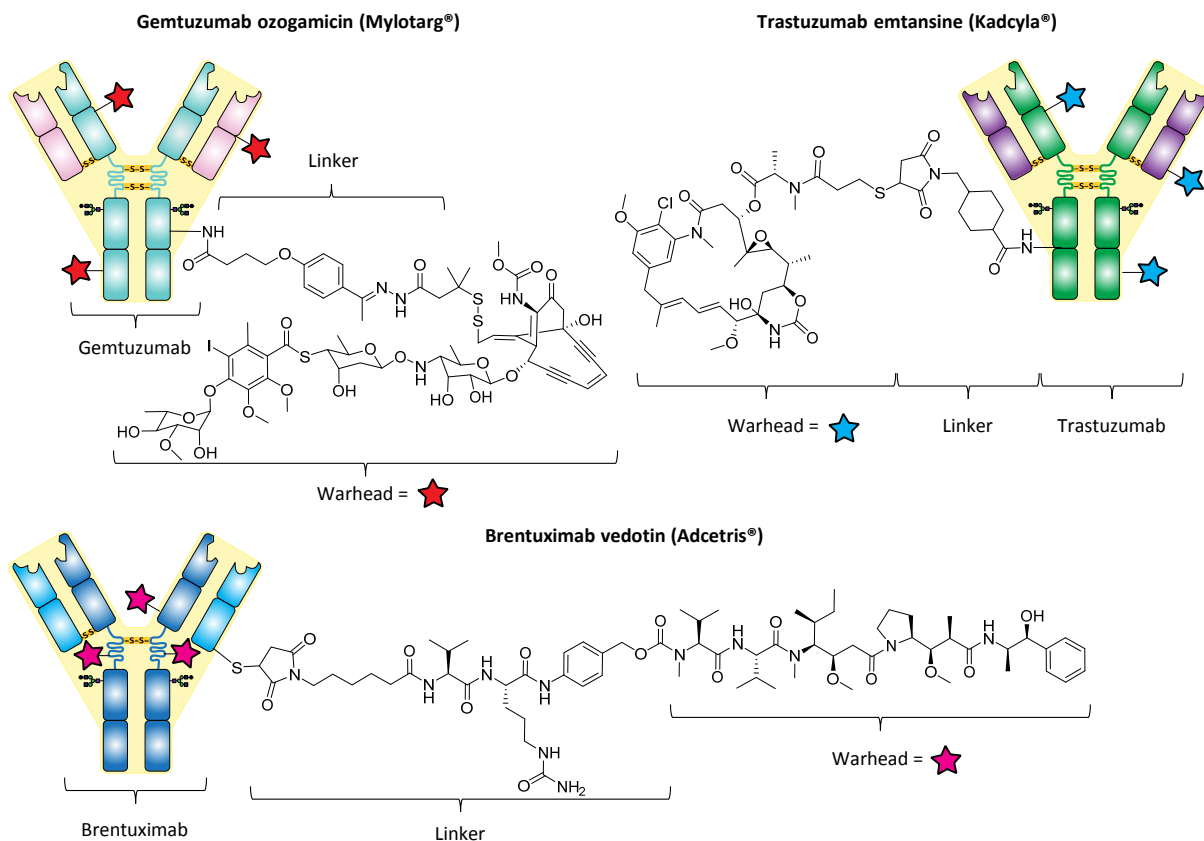


Figure 5. Structures of FDA approved ADCs.

Kadcyla® is prepared by attaching the cytotoxic microtubule-inhibiting, maytansine derivative, DM1 to the accessible lysine residues of the anti-HER2 antibody, trastuzumab (Herceptin). Due to availability of 90 lysine residues in trastuzumab, such classical, non-specific modification leads to highly heterogeneous ADC, with up to 10^6 distinct species statistically possible when targeting DAR of 2 – 4.¹⁹ According to mass spectrometry (MS), Kadcyla® has the average DAR value of 3.5 and is composed of a mixture of antibody species with different individual DARs ranging from 0 to 8 (Figure 6). Notably, the observed drug load distribution can be described statistically using Poisson distribution or binominal distribution models.^{20,21} Detailed characterisation of the distribution profile is important, because different drug-loaded forms may have different pharmacokinetic and/or toxicological profiles.²²

To decrease compositional heterogeneity of ADC, in 1993 Willner *et al.* exploited an approach based on drug-linker conjugation to cysteine residues generated by complete reduction of the four interchain disulfide bonds of the antibody.²³ Using this approach, scientists from Seattle Genetics prepared near-homogeneous ADC with DAR of 8.²⁴ Afterwards, it was showed that antibody species with such high drug loads suffer from low tolerability, high plasma clearance rates, and decreased efficacy *in vivo*.²² Therefore, Adcetris® was prepared using a partial reduction of the disulfide bonds to afford the ADC with average DAR of about 4, which was found to be an optimal value in terms of efficacy and safety. Adcetris® consists of a highly potent synthetic payload, monomethyl auristatin E

(MMAE), conjugated to an anti-CD30 antibody, brentuximab, through a protease-cleavable valine-citrulline linker with a self-immolative *p*-aminobenzylcarbamate spacer (vc-PABC). Cys-directed approach provided a significant improvement over lysine modification strategies in terms of reduced heterogeneity, however still giving *ca.* 15 distinct species for DoC value of ~ 4 . Such modification of cysteine residues also leaves the original disulfides unbridged leading to structurally disintegrated conjugates, which may decrease the stability of the ADC.

There is a growing interest for site-specific methods of antibody conjugation as a way to overcome wide DAR distributions. In this context, antibody engineering and enzymatic approaches have been actively developed.^{25,4} Although these processes have been successfully applied for the preparation of homogeneous ADC, most of them are not applicable to native antibodies and require costly protein engineering techniques.

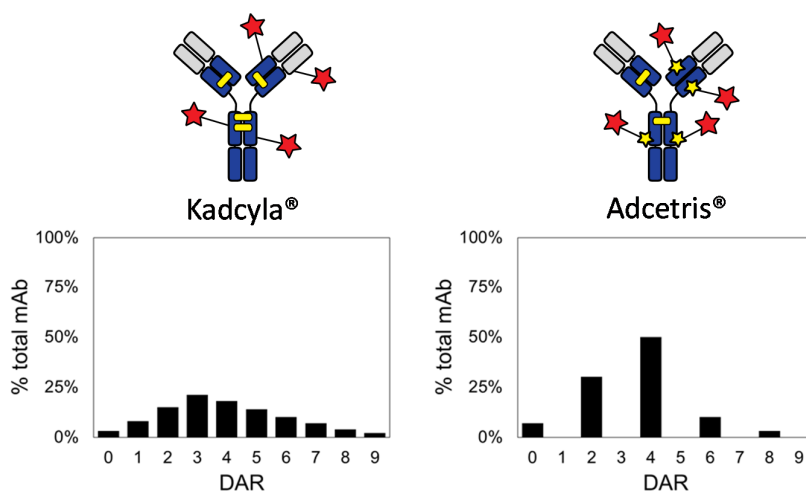


Figure 6. Main drawbacks in existing technologies: heterogeneity and loss of structural disulfide bonds.

The majority of ADCs in clinical trials are based on the same linking technologies, which are used for the preparation of FDA approved ADCs. However, their drawbacks, such as lack of selectivity and/or loss of structural integrity, forced scientists to search for more stable, effective and controllable conjugation strategies.

3 Chemical approach for antibody conjugation

3.1 Bioorthogonal reaction and click chemistry

The antibody functionalisation is usually performed in two steps. On the first stage, the antibody is decorated with reactive handles, which are then used for chemical ligation of payload during the second step. Such approach (plug-and-play) allows for the precise control of the conjugation step and provides versatility for the functionalisation step. The handles should have low reactivity, *i.e.* be orthogonal, towards reactive groups present on antibody surface, otherwise by-side reactions may occur leading to intra- or inter-molecular cross-linking. Such reactive functionalities are called bioorthogonal if their corresponding modification can occur selectively and fast inside biological

system without interfering with native biochemical processes or functionalities.^{26–28} Moreover, the bioorthogonal functions should be stable and non-toxic under physiological conditions.

The bioorthogonal groups should undergo chemical transformation efficiently using click chemistry, which is known to be modular, stereospecific, high yielding, and generating only inoffensive by-products.²⁹ One of the most popular click reaction of such kind is the copper-catalysed azide–alkyne Huisgen cycloaddition (CuAAC), which requires often addition of ligands that chelate and stabilise catalytic Cu(I) ions, in order to accelerate the reaction (Figure 7).²⁷ However, Cu(I) ions were associated with formation of reactive oxygen species (ROS), the presence of which can affect the structural and functional integrity of biomolecules, causing degradation of amino acids and cleavage of peptide chains.³⁰ These issues promoted the development of copper-free version of CuAAC, strain-promoted alkyne-azide cycloaddition (SPAAC), which although being non-stereospecific is often applied owing to its catalyst-free condition.^{31,32} Both CuAAC and SPAAC can be performed in aqueous media and have fast kinetics along with high degree of bioorthogonality. These reactions are frequently used for functionalisation of such complex proteins as antibodies.^{33–36}

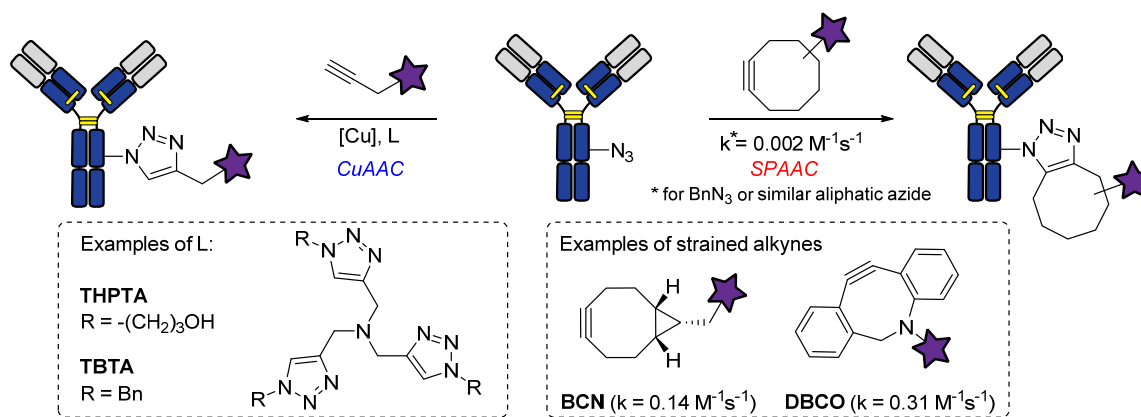


Figure 7. CuAAC and SPAAC for antibody functionalisation. DBCO dibenzoazacyclooctyne, BCN bicyclononyne, THPTA tris(hydroxypropyltriazolyl)methylamine, , TBTA tris(benzyltriazolyl)methylamine.

3.2 Strategies for antibody functionalisation

In general, two strategies, namely chemical and biochemical, are applied to construct ADCs. In the chemical approach, native antibodies are used for conjugation, and fine drug-linker design or/and delicate tuning of reaction conditions are performed in order to modulate the chemoselectivity, site-specificity and DoC parameters of the reaction. The biochemical approach on the contrast, is based on a proper antibody design achieved by means of antibody engineering and/or a use of specific enzymes in order to define both the location of conjugation sites and their number. Despite being challenging, the chemical approach remains very attractive due to its simplicity and straightforwardness, it requires no complex antibody engineering process or enzyme development. In our work we thus decided to focalise on the chemical approaches for the development of more efficient, stable and well-defined ACs.

In this review, we will survey the methodology of the chemical strategy for antibody conjugation. We will mainly focus on known naturally occurring conjugation sites on antibodies with an emphasis on reaction conditions, reagent selectivity and efficacy, along with conjugate stability. For more details of the biochemical strategy, the reader is referred to several recent reviews on this topic.^{25,4,37}

3.3 Aspartic and glutamic acid

Among reactive residues aspartic (Asp, D) and glutamic (Glu, E) amino acids have relatively high abundance in proteins.³⁸ Being the only amino acids with negatively charged side chains under physiological pH, they play an important role for properties related to protein solubility. Suggesting greater hydration of acidic amino acids, the recent works found that negatively charged amino acid on protein surface contribute strongly to protein solubility and aggregation resistance.^{39,40}

Owing to low reactivity of carboxylic acids in water towards nucleophiles, it is generally difficult to selectively target Asp and Glu residues in proteins. Commonly, prior to reaction with nucleophiles the pre-activation of carboxylic functions into activated esters is performed using activating agents. Carbodiimide-based reagents are the oldest and most extensively used activating agents for carboxylic acid modification in proteins.^{41,42} They can transform carboxyl groups to afford activated O-acyl-isoureas, which can efficiently react with different nucleophiles, in particular with amines, resulting in stable amide bond formation (Figure 8). While water-insoluble *N,N'*-dicyclohexylcarbodiimide (DCC) activating agent is widely applied for peptide coupling in organic solvents, the water-soluble alternatives such as 1-ethyl-3-(3-dimethylaminopropyl)carbodiimide (EDC)⁴³ and Woodward's reagent K (*N*-ethyl-5-phenylisoxazolium-3'-sulfonate)⁴⁴ were developed for acid-selective conjugation in aqueous media. *N*-hydroxysuccinimide (NHS) is often included in the activation protocol to yield more stable NHS activated esters, which improves the efficacy of the conjugation step.

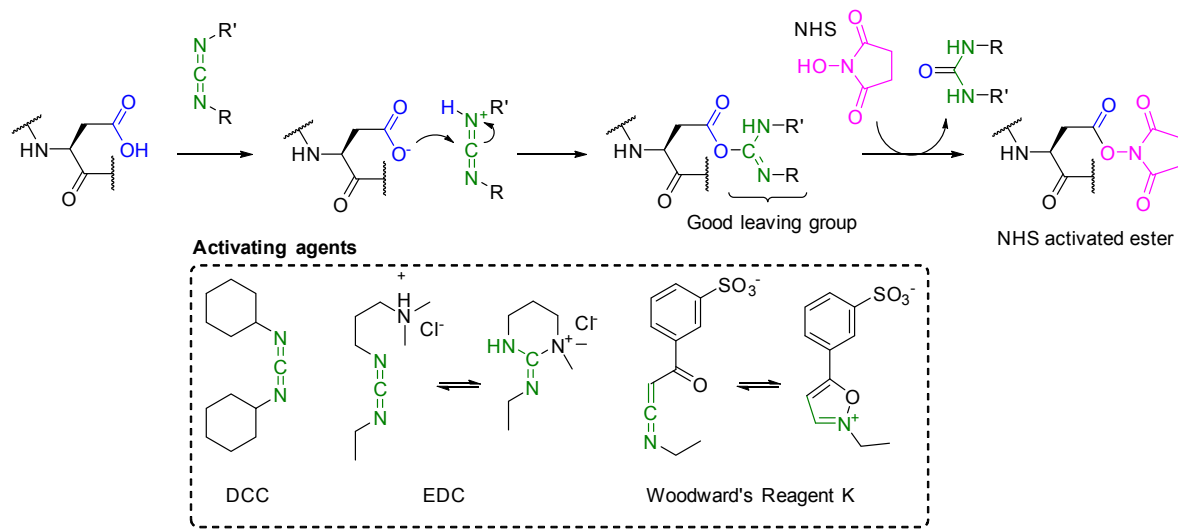


Figure 8. Activation of carboxylic acids and preparation of NHS activated esters.

The carbodiimide-mediated amide linkage was employed in the very first reports of the covalent conjugation of drugs to the antibodies.^{45–47} The methodologies exploited Asp, Glu, and the C-termini of the antibodies for the coupling with amine-containing drugs. However, due to cross-reactivity of the activated acids with lysine side chains, a high degree of antibody cross-linking was observed with this methodology, especially when an excess amount of activating reagents was used. This resulted in precipitation and conjugate aggregation leading to poor circulation times of the resulting ADCs *in vivo*.⁴⁸ These main drawbacks led to a withdrawal of the methodology from ADC field and its substitution with milder methods including lysine-selective conjugation with NHS activated ester.

3.4 Lysine residues

Lysine (Lys, K) is one of the most abundant amino acid in proteins. Given a pKa of ~10, the ϵ -amine of lysine is mainly present in its protonated form at neutral pH and thus occurs mainly on solvent-accessible surface of the antibody. Displaying a great number of charged lysine residues in part contributes to antibody aqueous solubility. For instance, trastuzumab has 90 lysine residues in its structure, of which 40-70 are solvent-exposed and thus can react easily with exogenous reagents.^{20,49}

Owing to this facile accessibility of lysine residues in proteins, the very first methodologies in bioconjugate chemistry exploited their selective modification. Consequently, these approaches were applied in the first examples of ADCs construction and, despite heterogeneous nature of the final products, are frequently used even today. Approximately a third of all ADCs currently in the clinical trials is prepared using lysine conjugation.

Deprotonation of the ϵ -amine of lysine provides a powerful nucleophilic centre. In general, only moderate elevation of pH is needed to produce enough free amino groups that can react rapidly with different electrophiles. The detailed review of lysine bioconjugation methodologies was published by Hermanson.³ In context of ADCs production, the common approaches include lysine amidation with activated esters, reductive amination with aldehyde/sodium borohydride or nucleophilic reaction with isothiocyanate.

3.4.1 Activated esters

Reaction of activated ester with lysine residue is probably the most efficient and straightforward approach for covalent attachment of drug moieties to an antibody. This is the method of choice for the preparation of lysine-linked ADCs currently undergoing clinical trials. Moreover, among myriad activated esters, the NHS ester or its more water-soluble sulfonate form (sulfo-NHS) is favoured and the most applied for the synthesis of ACs. Indeed, clinically approved ADC, trastuzumab emtansine, is prepared using a two-step approach (plug-and-play) using NHS activated ester (Figure 9). On the first stage, lysine residue of the trastuzumab antibody is conjugated with *N*-Succinimidyl-4-(maleimidomethyl)cyclohexanecarboxylate (SMCC) to yield T-MCC bearing maleimide handles, which is able to react further with a thiol-containing drug (mertansine, DM1) to afford the ADC. However, selectivity issues can arise during the first step of the bioconjugation, with lysine residues

reacting with maleimide groups; this side reaction was reported to be responsible for intra-antibody cross-linked species observed by MS analysis.⁵⁰

Recently, site-specific lysine conjugation of DNA to native antibodies was achieved using their metal binding sites for affinity labelling.⁵¹ Although being conceptually interesting, this strategy is technically limited for the scale-up.

The preference of NHS activated esters is often explained by their relatively high hydrolytic stability and high efficacy in reaction with lysine residues. The resulting isopeptide bond formed in the reaction is considered stable under normal physiological pH, which is ideal for maintaining the drug covalently attached to the antibody. However, unspecific reactions of NHS activated esters may also occur with tyrosine and cysteine residues.⁵² They were suggested to occur during the preparation of the lysine-linked ADC resulting in labile adducts, which were unstable in the aqueous media (pH 4.0–7.2) and deconjugated up to 5% of the payload in the form of drug–linker–COOH.⁵³ Another important issue with lysine amidation is inevitable loss of charge during the transformation of primary amino groups into amide residues, which leads to decrease of the total charge on the protein surface and may therefore reduce its solubility. To overcome this issue, reductive amination of lysine residues was proposed.

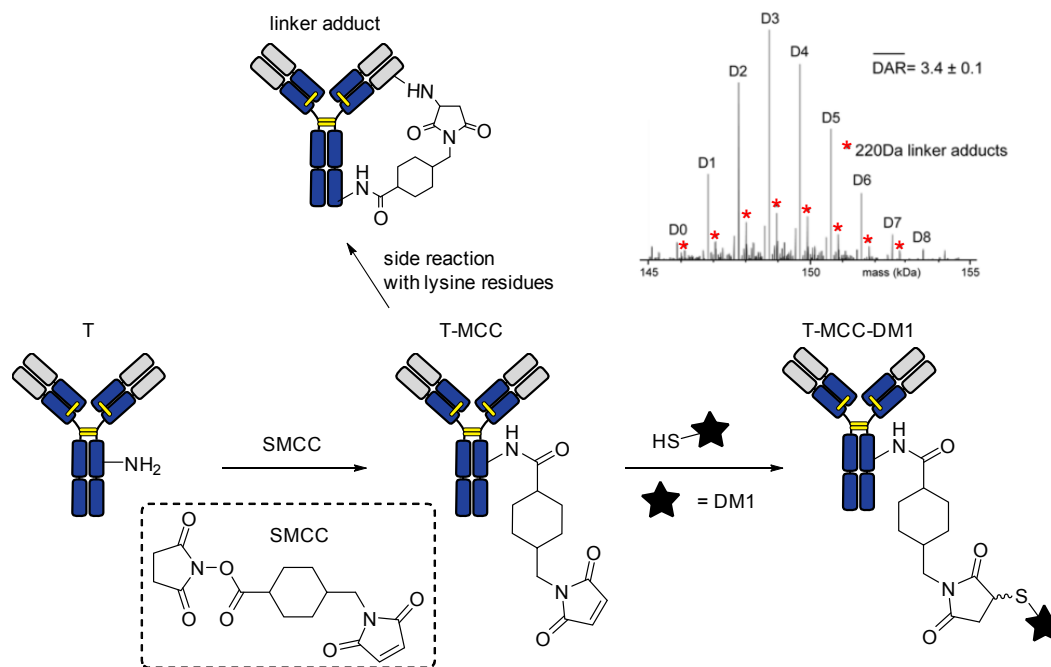


Figure 9. Two-step process for the preparation of Kadcyla® and by-products observed in its mass spectrum. MS spectrum is adapted from ref.⁵⁴

3.4.2 Reductive amination

The primary amine on the side chain of lysine residue reacts readily with aldehyde functionalities forming an imine. In solution the imine is present in equilibrium with both the hydrated hemi-aminal and the free aldehyde, but the labile link can be transformed into a stable secondary

amine upon reduction using water-soluble hydride donors NaBH_4 , NaBH_3CN , or $\text{NaBH}(\text{OAc})_3$. This approach is therefore can be used as an alternative to lysine amidation. For example, a propylene dialdehyde reagent affords a stable piperidine-linked conjugate (Figure 10).⁵⁵

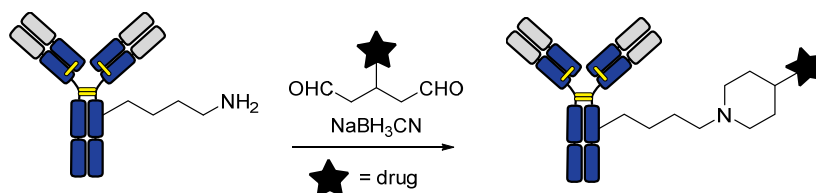


Figure 10. Preparation of ADC through reductive amination with propylene dialdehydes.

Although the methodology is quite simple and straightforward, the utilisation of reducing agents may potentially cause the reduction of disulfide bonds within antibodies therefore disrupting their structure.

3.4.3 Isothiocyanates

Amine group of lysine can undergo irreversible nucleophilic addition with isothiocyanates to readily yield stable thioureas. The reaction was generally used for radioactive and fluorescent labelling of IgG and was performed in carbonate–bicarbonate buffer with elevated pH to achieve higher efficacy (Figure 11).^{56–60} Several groups elaborated the methodology for antibody ligation with chelating agents using phenylisothiocyanate-containing reagents for further radionuclide labelling.^{60–62} Wilbur *et al.* pursued isothiocyanate-mediate antibody radiolabelling and developed a series of trifunctional reagents containing, in addition to the isothiocyanate moiety, a chelating functionality and a biotin tag.⁶³ The resulting radionuclide-containing ACs can be virtually removed from patient blood using affinity adsorption, which enables the elimination of harmful irradiation on demand.

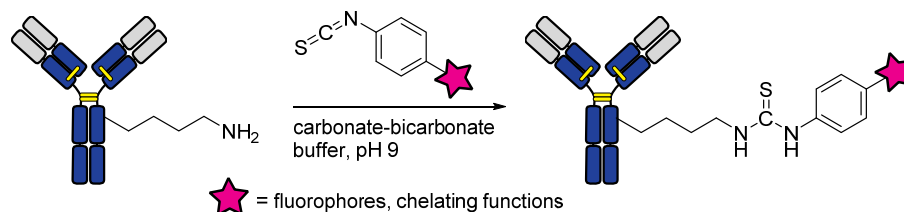


Figure 11. Isothiocyanate-mediated conjugation of fluorophore and chelating functionality with lysine of antibodies.

3.4.4 Squaramide esters

Diester derivatives of squaric acid are one of handful chemical entities comprising functionality, stability and simplicity. Their first ester group can be easily substituted by amines at slightly basic pH to produce a squaramide ester, while the substitution of the second ester function requires elevation of pH up to 9 to occur, which affords diamide of squaric acid (Figure 12A).

This homobifunctional reagents were applied for amine-to-amine bioconjugation with pH-resolved control.^{64–66} Because of high hydrolytic stability of both the conjugating reagent and the resulting squaramide moiety this method of cross-linking started to gain popularity.⁶⁷ Recently, the

squaramide ester derivative bearing chelating functionality was used for the preparation of zirconium-89 radiolabelled ACs (Figure 12B).⁶⁸

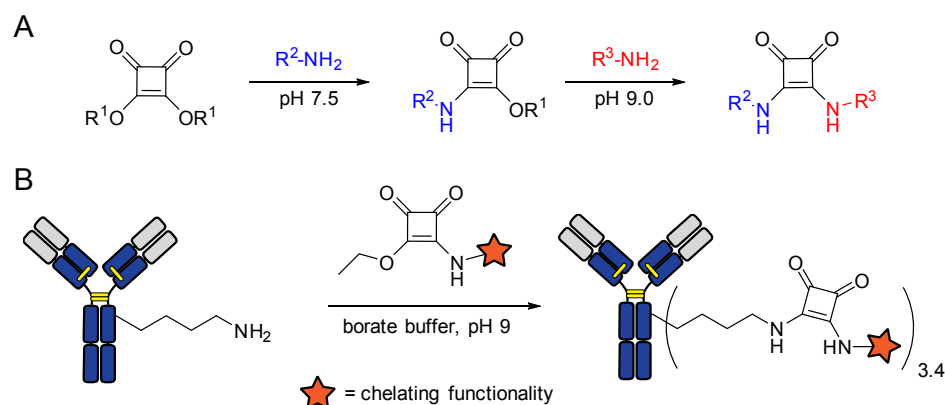


Figure 12. (A) Sequential reaction of diester derivatives of squaric acid with amines. (B) Preparation of radiolabelled ACs using squaramide ester reaction with lysine residues of the antibody.

Interestingly, depending of the microenvironment, the basicity and nucleophilicity of Lys can vary substantially, making some residues more reactive than others. The increased reactivity of the hot-spot lysines was exploited by Barbas group for antibody chemical programming using β -lactam conjugation.

3.4.5 Beta-lactams

In 2009 Barbas and coworker applied β -lactam conjugation for irreversible chemical programming of monoclonal aldolase antibody 38C2. This antibody possesses a reactive lysine residue in the heavy chain (LysH93) with an unusually low pKa of ~ 6 and is important for the catalytic properties of the antibody. Using β -lactam conjugation, selective modification of these lysine residues was achieved and a cyclic-RGD peptide as a targeting module for integrin receptors was covalently attached to the mAb. The resulting ACs bound specifically to the integrin expressed on human melanoma cells demonstrating the applicability of this approach towards preparation of chemically programmed antibodies.

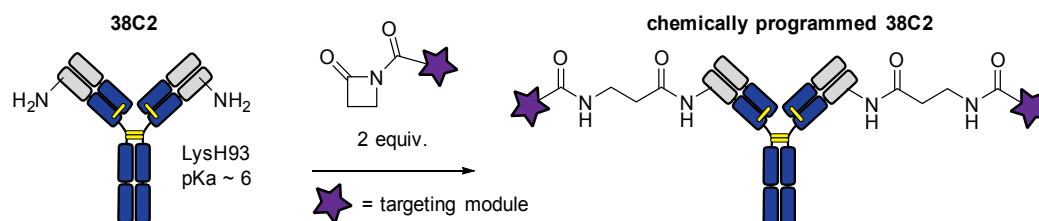


Figure 13. Chemical programming of aldolase antibody using β -lactam/lysine conjugation.

Another reactive functionalities for selective conjugation of LysH93 of 38C2 antibody included β -diketone,^{69–71} acid anhydride⁷² and an acetone aldol adduct of a vinylketone.^{73–75}

In summary, classic lysine conjugation remains a popular method for the preparation of ADCs, especially when the site-selectivity is not required. Given high amount of lysine residues, their targeting allows also for much higher drug loading on antibodies, which virtually should result in ADCs with higher potency. This was especially useful for ADCs comprising of drugs that were only moderately potent, such as anthracycline derivatives having IC₅₀ in micromolar range. For instance, even though with a low yield, preparation of *N*-Ac melphalan-based ADCs with DoC ranging from 10 to 30 was possible.⁷⁶ However, even with these high DoCs, the resulting ADCs showed only modest efficacy *in vivo*, which provoked development and employment of more cytotoxic drugs having IC₅₀ in picomolar range, such as auristatin and maytansinoid derivatives.

However, because of great excess of reactive sites compared with commonly desired DoC of 4, this lysine-directed bioconjugation leads to highly heterogeneous mixtures of species with DAR ranging from 0 to 10. Statistically, assuming the presence of 70 accessible lysine residues with the same reactivity, one can find that the ADC with DAR 4 theoretically may contain up to $70 \cdot 69 \cdot 68 \cdot 67 = 2 \cdot 10^7$ possible regioisomers, each with its own pharmacological properties.⁷⁷ Moreover, this complicated structural and pharmacological characterisation of the ADC. This forced to shift the conjugation methodology towards the modification of less abundant amino acid residues present in antibodies, such as cysteines, which can be easily obtained by reduction of disulfide bonds.

3.5 Cysteine residues

Cysteine (Cys, C) is one of rarest amino acid (1-2%) occurring predominantly in a form of disulfide bonds and only scarcely in its free form (0.2 %) in proteins. Owing to its rarity and the highest nucleophilicity of its sulfhydryl (-SH) side chain among other proteinogenic residues at physiological pH, cysteine modification opens a route for the selective and site-specific bioconjugation. Furthermore, the site-directed mutagenesis allows for facile cysteine insertion at a specific position on a protein. All these factors make cysteine-directed bioconjugation one of the most frequently applied among other approaches. In context of ADC production, more than half of ADCs currently in clinical trials and one on the market (Adcetris®) are prepared using Cys-selective conjugation.

There are 32 cysteine residues in IgG1 structure, however all of them are involved in formation of inter- and intrachain disulfide bonds (4 and 12, respectively) and thus antibodies do not possess ready for conjugation thiol groups in their structures. Nevertheless, the free sulfhydryl groups can be easily generated through selective reduction of the interchain disulfide bonds with reducing reagents such as dithiothreitol (DTT), 2-mercaptoethanol (β -mercaptoethanol), or tris[2-carboxyethyl]phosphine (TCEP). These mild reagents do not affect buried intrachain disulfides and only reduce the solvent-accessible interchain disulfide bonds. This results in a maximum of 8 reactive thiol groups per antibody, which once deprotonated can be readily modified with a variety of electrophiles through nucleophilic addition or substitution reaction. Historically, maleimide and haloacetamide reagents were the first electrophiles used for Cys-directed antibody conjugation.

3.5.1 Iodoacetamide

Haloacetyl electrophiles, namely iodoacetamides, are some of the oldest reagent for Cys-selective antibody labelling (Figure 14). Iodoacetamides enable rapid modification of cysteine to form stable alkyl thioether linkage. Given possible side reactions with other residues, including His, Lys, and Met, the conjugation of sulfhydryl groups is most specific at pH 8.3. Iodoacetamide derivatives were used predominantly for radiolabelling of antibodies⁷⁸ and nowadays they started to reappear as more stable alternative to classical maleimide conjugation. For instance, more recently, iodoacetamide drug derivatives were applied for the preparation of stable and potent ADCs through their reaction with engineered selenocysteine residues on the antibody.⁷⁹

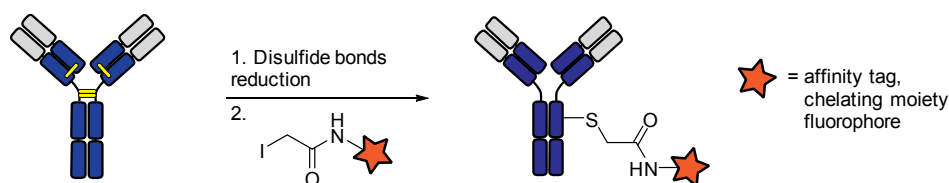


Figure 14. Antibody labeling with iodoacetamide derivatives.

3.5.2 Maleimide

One of the most frequently used cysteine-selective reagent is maleimide, which reacts fast and efficiently with thiolate nucleophiles through Michael addition. Maleimide-thiol conjugation was applied for the preparation of both ADCs currently on the market (Kadcyla® and Adcetris®). For the preparation of Kadcyla®, it is used during the second step, when trastuzumab-MCC reacts with thiol-containing mertansine to afford T-MCC-DM1. Adcetris®, in contrast, is prepared by partial reduction of disulfide bonds of anti-CD30 antibody followed by a subsequent reaction of the resulting free cysteines with maleimide-containing drug-linker (Figure 15A).

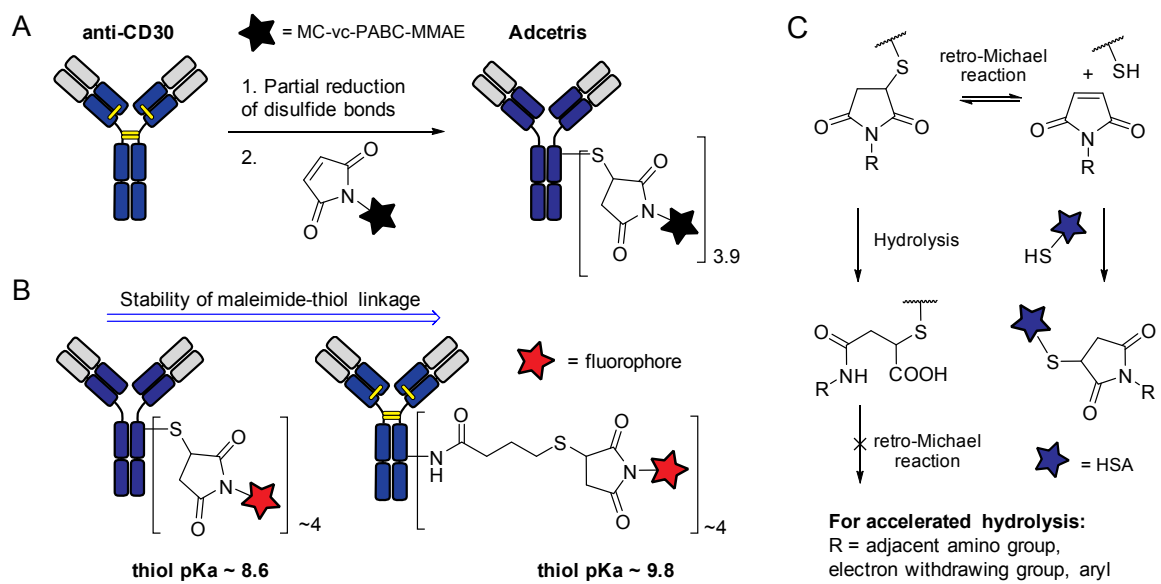


Figure 15. (A) Preparation of clinically approved ADC using maleimide-thiol conjugation. (B) Differences in thiosuccinimide stability related to thiol pKa. (C) Thio-maleimide linkage stabilisation by hydrolysis

Although maleimide-thiol reaction is fast and efficient, the obtained adduct is known to be unstable in serum. Due to the cleavage of the thiosuccinimide linkage by retro-Michael reaction, the exchange with human serum albumin (HSA) and other thiols present in plasma is possible. This leads to gradual deconjugation of cytotoxic drug during ADC circulation in blood, therefore increasing toxicity for normal tissue. Recently, scientists from ImmunoGen showed that the thiosuccinimide linkage in T-MCC-DM1 conjugates is more stable and presents a slower rate of drug deconjugation compared to rate reported for thiosuccinimide linkage in Cys-linked ADCs.⁸⁰ They explained this fact by different pKa value of two thiols forming thiosuccinimide linkage: ~9.8 for DM1 thiol and ~8.6 for cysteine thiol and confirmed this by testing the stability of similar antibody-fluorophore conjugates (Figure 15B). Thus, thio-maleimide adducts prepared from thiols with higher pKa values are more stable.⁸¹

Actually, the stabilisation of maleimide-thiol conjugates can be achieved by hydrolysis of the thiosuccinimide ring into thiosuccinamic acid, which is resistant to thiol exchange (Figure 15C). Notably, it has earlier been reported that it can be induced by modulation of the site of conjugation to an antibody^{82,83} by an amino group adjacent to the maleimide^{84,85}, by electron withdrawing *N*-substituents^{86,87} or by using *N*-aryl maleimides.⁸⁸ In most cases, buffers with high pH values are required to achieve hydrolysis.^{86,87} Alternatively, to enable access to serum stable conjugates, maleimide can be replaced by other thiol-reactive groups such as 3-arylpropionitrile^{89,90} or phenyloxadiazole sulfones⁹¹

3.5.3 Arylpropionitriles

Recently, in our group a novel class of reagents, 3-arylpropionitriles (APN), was developed for cysteine-selective conjugation. In 2014 Koniev *et al* introduced this remarkably stable reagents for selective irreversible tagging of cysteine residues in aqueous media (Figure 16).⁹⁰ Series of traceable amino acid derivatives was used for benchmarking the APN function against other cysteine-selective methods to show high efficacy and relatively fast kinetic ($3.1 \text{ M}^{-1}\text{s}^{-1}$) of cysteine-tagging. The selectivity of APN-mediated conjugation was further investigated on peptide mixture resulted from trypsin digestion of lysozyme. Following LC-MS/MS analysis confirmed successful attachment of APN-tag to all detectable cysteine-containing peptides, while cysteine-free peptides were unaffected. Additionally to improved efficacy and selectivity, high stability of APN conjugates was demonstrated in different aqueous media, human plasma and living cells.

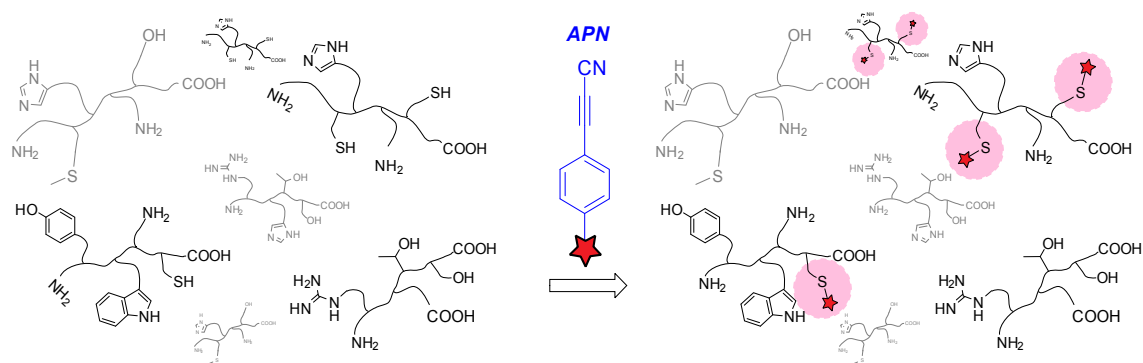


Figure 16. Irreversible coupling of cysteine residues with 3-arylpropionitriles (APN).

Continuing investigation of this functionality, Kolodych *et al* published a work describing an APN-containing reagent for amine-to-thiol conjugation in context of ACs production (Figure 17).⁸⁹ This heterobifunctional reagent, sodium 4-((4-(cyanoethyl)benzoyl)oxy)-2,3,5,6-tetrafluorobenzenesulfonate (CBTF), contains an activated ester group (STP) for the reaction with amines and the APN moiety for subsequent thiol-conjugation. CBTF was used for the preparation of serum-stable antibody-fluorophore conjugates and was proposed as an improved alternative to classical maleimide conjugation.

In 2015 Koniev *et al* introduced another APN-based reagent, p-(maleimide)-phenylpropionitrile (MAPN), for kinetically resolved thiol-to-thiol conjugation (Figure 17).⁵⁴ MAPN comprises of two thiol-specific function: APN and maleimide, which have distinctive reaction rates with sulfhydryl groups ($k > 50 \text{ M}^{-1} \text{ s}^{-1}$ for maleimide vs $k = 3.1 \text{ M}^{-1} \text{ s}^{-1}$ for APN). Considering at least 10-fold faster reaction of maleimide, this allowed MAPN application for the covalent heterocoupling of two thiol-containing molecules in controllable fashion. In particular, using thiol of mertansine and the cysteines of trastuzumab, MAPN was applied for the preparation of thiol-thiol ADC, which was a more homogeneous analogue of trastuzumab emtansine (Kadcyla®).

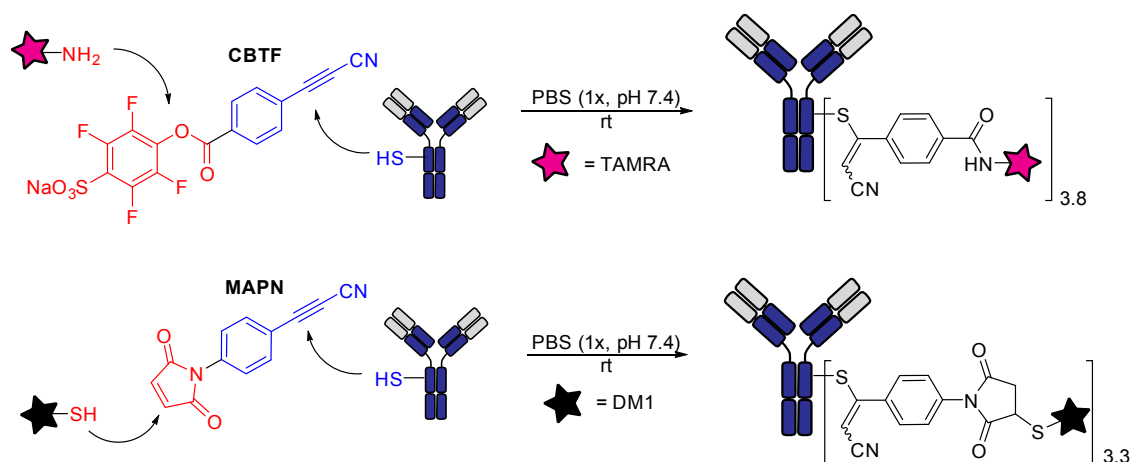


Figure 17. CBTF and MAPN reagents for amine-to-thiol and thiol-to-thiol conjugation, respectively.

Distinctive stability properties of APN-based conjugates resulted in commercialisation of a grand variety of APN-containing reagents for heterocoupling, in which the secondary function can represent a primary amine, strained alkyne (BCN), azide, aldehyde etc.

3.5.4 Sulfone reagents

Generation of serum-stable Cys-linked ACs can be also achieved by using vinyl sulfone reagents, which, while being water stable, can react almost quantitatively with thiolates through Michael-type addition (Figure 20). Selectivity of the vinyl sulfones can be modulated by changing buffer pH. For instance, vinyl sulfone derivative was used for selective radiolabeling of antibodies either through their Cys residue at pH 7 or through lysine residues at pH 9, showing versatility of vinyl sulfones in terms of conjugation options.⁹²

Mono-sulfone derivatives are also reactive towards Cys residues and were employed for selective PEGylation of Fab antibody fragment and anti-HER2 affibody.⁹³ In this reaction, performed under mild reaction conditions, mono-sulfones were more efficient than maleimide and other common thiol-selective reagents including vinyl sulfone, acrylate, and halo-acetamide derivatives.

Additionally, phenyloxadiazole sulfone functional group was applied for selective labelling of engineered cysteine and selenocysteine residues in antibodies (Figure 18).^{91,94} The resulting ACs demonstrated improved stability in human plasma compared with their maleimide analogues. Moreover, depending on location of Cys-engineered sites on an antibody, different reactivity of their thiol group towards phenyloxadiazole sulfone linker was observed, which was exploited for kinetically controlled dual labelling of the antibody.⁹¹

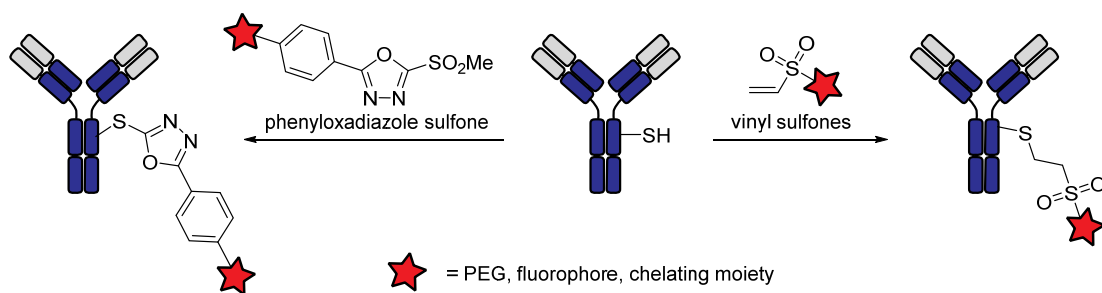


Figure 18. Sulfone reagents for antibody labelling.

3.5.6 Palladium-based conjugation

Arylation of Cys residues of the antibodies by means of transition-metal-based reaction has also recently been introduced for the preparation of stable Cys-linked ADC (Figure 19).⁹⁵ To this end, drug-containing palladium(II) complexes were applied to form stable conjugates under mild conditions that maintained the binding capacity of the native antibody. Alternatively, other groups have employed palladium-catalysis for efficient and selective labelling of Cys residues in trastuzumab antibody.⁹⁶

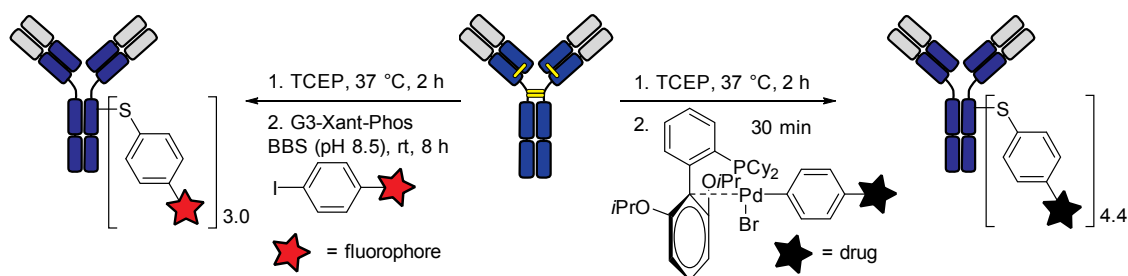


Figure 19. Palladium-based Cys-selective conjugation of antibodies.

3.5.7 *N*- or *C*-terminus modifications

To allow site-specific conjugation the Cys residues can be engineered at the *N*- and *C*-terminus of antibodies. For more details of the conjugation chemistry, the reader is referred to a recent review by Bernardes group on the construction of homogeneous ADCs.³⁷

3.6 Disulfide rebridging

Despite high efficiency and selectivity, Cys-modification approaches mentioned above leave the original disulfides unbridged resulting in structurally disintegrated ADCs, which may potentially increase instability of the conjugates. To preserve the integrity of Cys-linked ADCs, Brocchini *et al.* pioneered the development of bis-sulfone reagents, that enable functionalisation of native antibodies through disulfide rebridging (Figure 20).^{97,98} These bis-sulfones can react with two antibody cysteines to conjugate a payload through a stable three-carbon bridge. Conventional rebridging reagents enable insertion of a single payload per disulfide bond, thus decreasing the maximal DAR to 4, which is commonly considered to be an optimal value for the ADCs.²² Moreover, depending on the drug-linker design, the synthesis of near-homogeneous ADCs with other format of DAR is also possible: DAR 2, 2xDAR4 (dual payloading) or DAR 8.^{99,35,100} Enabling to afford near-homogeneous ADCs without any antibody engineering, the disulfide rebridging strategy is of great interest for the bioconjugation and several types of reagent have been developed in this context. Recently, an excellent review of common reagents for disulfide rebridging was made by Weil group.¹⁰¹ Concerning ADC, they mainly include bis-sulfones, dibromomaleimides and dibromopyridazinediones.

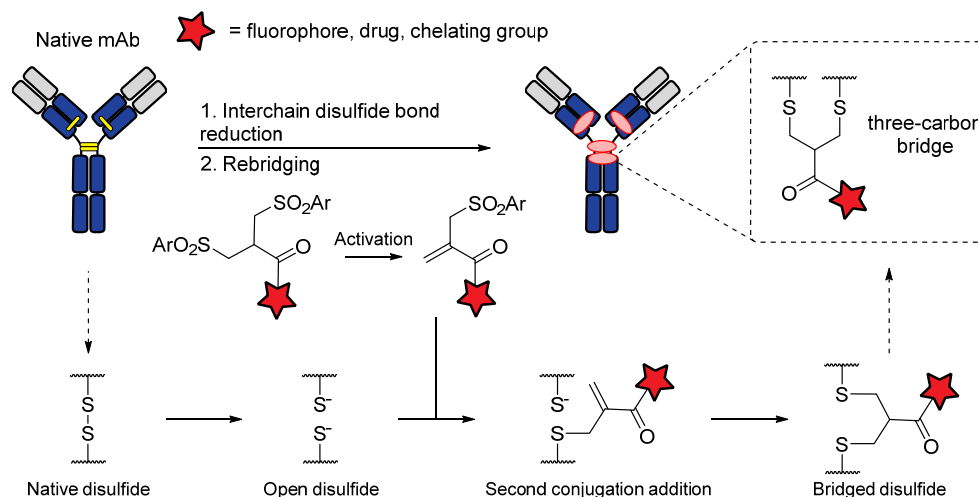


Figure 20. Disulfide rebridging with bis-sulfone reagent.

3.6.1 Bis-sulfones

In 1990, two consecutive articles were published on bis-sulfone reagents and their application for mAb rebridging in order to obtain more stable and homogeneous ACs.^{97,98} To this end, functionalised bis-sulfone reagents were synthesised bearing either fluorophore moiety or chelating group for radiolabelling. Using these reagents, the authors demonstrated successful rebridging and functionalisation of the partially reduced native antibodies, which resulted in ACs with increased stability *in vivo*. It is worth noting, that depending on payload structure, in some cases inter-antibody cross-linking was observed in parallel with intra-antibody.⁹⁸ Despite the potential of this strategy, it was rarely employed for ADC,¹⁰² being mainly applied for site-selective protein PEGylation,^{103–105} until the breakthrough in this field made by Badescu *et al.* from PolyTherics. Using a bis-sulfone reagent comprising MMAE, they efficiently (> 78%) transformed trastuzumab antibody into ADC with DAR of 4 and no sign of unconjugated antibody.¹⁰⁶ The resulting conjugates were stable in serum and showed potent and antigen-selective cancer cell killing *in vitro* along with high efficacy *in vivo*.¹⁰⁷

Since then, many other rebridging platforms have been developed. For instance, very recently, Weil group introduced a water-soluble allyl sulfones for dual site-specific labelling of protein as an alternative to classic bis-sulfone reagents.¹⁰⁸ These reagents do not require activation step as bis-sulfones, which offer more effective disulfide rebridging.

3.6.2 Dibromo- and dithiomaleimides

Another class of compounds allowing for the generation of Cys-bridged ADCs is dibromomaleimide, which was originally described as a reagent for efficient PEGylation of proteins.¹⁰⁹ This approach was used for the preparation of near-homogeneous ADC containing predominantly four drugs per antibody (Figure 21).¹¹⁰ The resulting ADCs were compared to analogous conventional heterogeneous ADCs and showed improved pharmacokinetics and superior

efficacy *in vivo*. Beside ADCs, dibromomaleimide functionalities were applied for generation of homogeneous bispecific antibodies *via* reaction of reduced antibody fragments with bis-dibromomaleimide linkers.¹¹¹ The main disadvantage of these linkers is the presence of maleimide moiety that is known to be instable in serum resulting in premature payload release. To overcome this issue, Morais *et al.* described an optimised protocol for the accelerated post-conjugation hydrolysis of the maleimide into maleamic acid in Cys-bridged ADCs.¹¹²

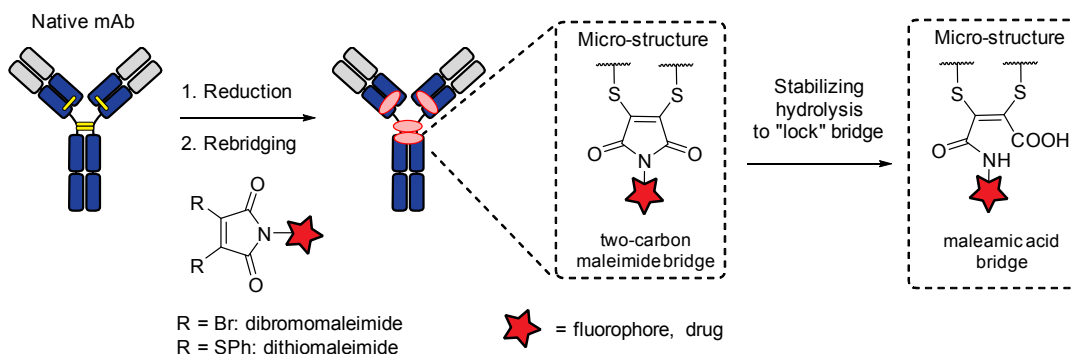


Figure 21. Native antibodies functionalisation using dibromo- or dithiomaleimide derivatives

Recently, several groups (*i.e.* Chudasama, Baker and Caddick) have described methodologies for efficient insertion of functionalised maleimide into disulfidesulphide bond of antibodies and their fragments.^{113–115} Using dithiophenolmaleimide–MMAE reagents, ADCs with narrow distribution of DAR, with DoC close to four were synthesised.¹¹⁴ The resulting maleimide bridge was further hydrolysed under mild conditions to afford serum stable conjugates. It was shown that the obtained ADCs had the potent and selective tumour cell killing activity *in vitro*¹¹⁴ and *in vivo*.¹¹⁶

3.6.3 Dibromopyridazinediones

A good alternative to dibromomaleimide rebridging reagents is dibromopyridazinediones (diBrPD), which while being hydrolytically stable can generate a stable Cys-bridge ADCs without any need of post-hydrolysis. Using this platform, Chudasama group enabled to achieve a number of scientifically interesting concepts. First of all, they introduced plug-and-play approach for dual conjugation of antibodies with two different payloads (Figure 22).

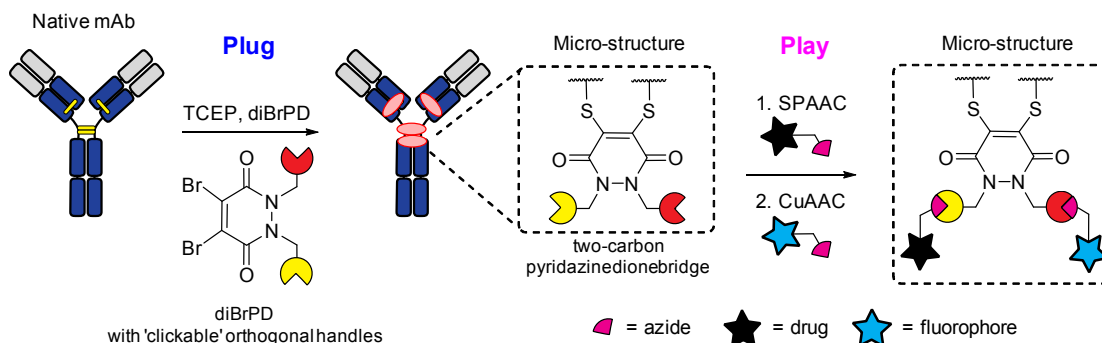


Figure 22. Plug-and-play approach for the preparation of ADC bearing both a cytotoxic drug and fluorophore.

This was possible using diBrPD derivatives bearing two bioorthogonal clickable handles, which enabled for consecutive SPAAC and CuAAC functionalisations of resulting pyridazinedione bridged ACs. They demonstrated successful preparation of dually modified ADC possessing two different payloads, with payload/antibody ratio of about four. This strategy potentially enables preparation of near-homogeneous ADCs bearing two cytotoxic agents with different mode of actions, which can be useful for cancer therapy of resistant tumours.

In other work, the authors decided to combine reduction and functional rebridging in one reagent.¹¹⁷ To this end, they synthesised TCEP derivative of dithiopyridazinedione and used it for functionalisation of Fab fragment of trastuzumab (Figure 23). Interestingly, this approach enabled generation of ACs without disulfide scrambling, which was usually observed when other rebridging reagents were used.

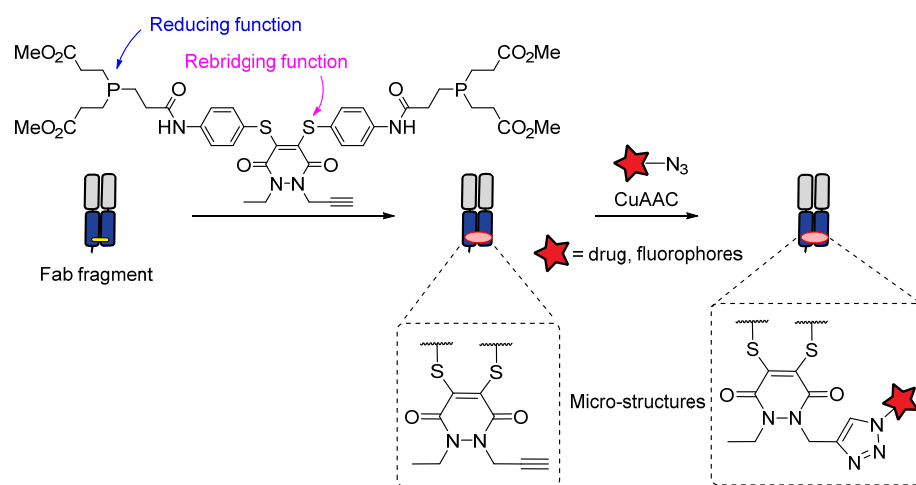


Figure 23. Pyridazinedione platform for disulfide scrambling-free functional rebridging.

More recently, using pyridazinedione platform, Lee *et al.* have demonstrated the controlled assembly of ACs with a loading of two modules without antibody engineering.⁹⁹ For this, bis-diBrPD linkers bearing diBrPD moiety on each terminals and one “clickable” handle were designed and synthesised (Figure 24). The length of these linkers was appropriate for simultaneous rebridging of interchain disulfide bonds both of hinge region and Fab domain. By reacting these linkers with reduced native antibodies, the authors managed to prepare ADC with DAR of two.

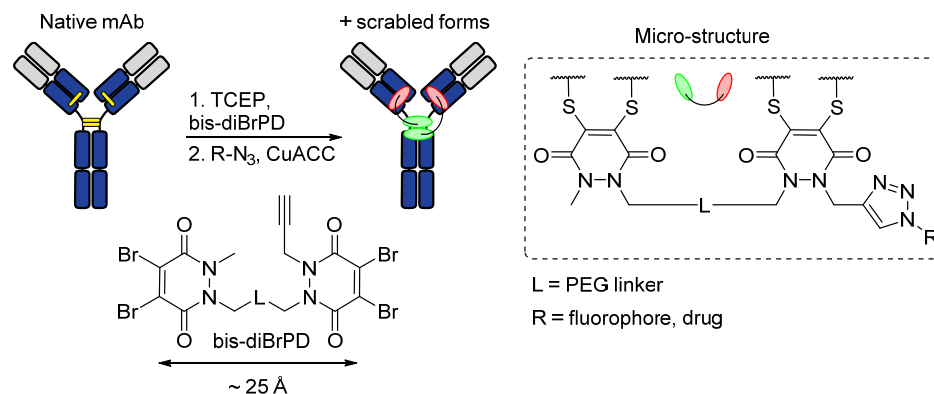


Figure 24. Enabling the loading of two payloads per antibody using bis-diBrPD linkers.

Finally, using pyridazinedione platform, Robinson *et al.* have succeeded in preparing the stable MMAE-based ADC with four drugs per antibody, which demonstrated a potent cancer cell killing activity *in vitro*, along with high efficacy *in vivo*.¹¹⁶

3.6.4 Pt-based linker

Very recently, platinum (II)-based linker was developed for the interchain disulfide rebridging of an antibody and construction of camptothecin-based ADC (Figure 25). The strong platinum-sulfur interaction provided more serum-stable ADCs compared with a similar maleimide-linked ADC. Containing approximately eight drug moieties per antibody (estimated by UV), these ADCs demonstrated increased anticancer efficacy *in vitro* and *in vivo*.

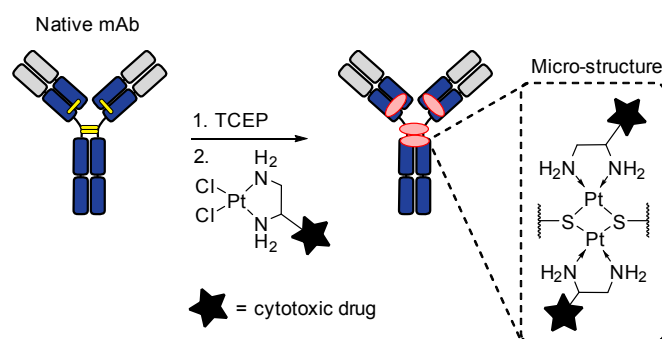


Figure 25. Platinum(II)-based linker allows for loading eight cytototoxic drug per antibody.

In summary, disulfide rebridging in bioconjugate chemistry is a relatively novel approach, especially for ADCs construction. It is a chemical strategy for antibody conjugation enabling controllable preparation of near-homogeneous ADCs without need of antibody engineering. Although disulfide scrambling seems to be the main issue of disulfide rebridging methodologies, it is believed that further investigation in this field may provide a novel drug-linker design with improved control and robustness of the conjugation process.

3.7 Tyrosine residues

In contrast to the abundance of lysine, tyrosine (Tyr, Y) residues occur with intermediate frequency on a native antibody (62 for trastuzumab). The majority of tyrosines are partially or completely buried into protein due to their relative hydrophobicity combined with a tendency of π - π stacking of the aromatic rings.¹¹⁸ The buried residues have limited exposure and thus left only a small fraction of tyrosines accessible for a solvent. Rare abundance of the tyrosine on the protein surface makes it an attractive target for bioconjugation. The known tyrosine-selective methodologies exploit either its electron-rich aromatic ring as a conjugation site in ene-type reaction under acidic/neutral conditions, or the alkylation/acylation of the oxygen atom of the tyrosine's hydroxyl group under basic condition.

The nucleophilicity of the aromatic ring of tyrosine is fairly different compared with lysine or cysteine residues, which provides a springboard for selective chemistries. The great contribution to the development of tyrosine bioconjugation was made by Francis and coworkers, who described tyrosine-specific reactions based on π -allyl palladium catalysis,¹¹⁹ the Mannich reaction,^{120–122} cerium oxidation.¹²³ Later, the work was pursued by Barbas group, who elaborated tyrosine click reaction mild enough for its application in the field of ADCs.

3.7.1 Diazodicarboxamides

In 2010, Barbas group reported the tyrosine-selective bioconjugation on various proteins including trastuzumab antibody using cyclic diazodicarboxamides (Figure 26A), like derivatives of 4-phenyl-3H-1,2,4-triazole-3,5(4H)-dione (PTAD).¹²⁴ These type of reagents are quite unstable and should be utilised immediately after oxidation of the corresponding precursors. The authors applied the tyrosine/ene-type reaction for the preparation of trastuzumab conjugated to integrin binding cyclic RGD peptide. The obtained trastuzumab-RGD conjugate preserved antibody's antigen binding activity.

In the following work, the authors have developed and used a versatile class of stable PTAD precursors, bearing different reactive function.¹²⁵ It was found that the selectivity of PTAD reagents can be improved by performing the bioconjugation in TRIS (tris(hydroxymethyl)aminomethane) buffer. The latter was hypothesised to act as a scavenger of an isocyanate by-product produced during PTAD decomposition in aqueous buffer (Figure 26A).

The authors showed the tyrosine click conjugation of trastuzumab with a small molecule HIV entry inhibitor, aplaviroc (Figure 26B). The portion addition of 25 equiv. of PTAD bearing aplaviroc entity resulted in trastuzumab-aplaviroc with a DoC of 1.3 according to MALDI-TOF spectrometry. The tyrosine/PTAD reaction was relatively fast, but not efficient (5.2 %) based on reported results. It was mentioned that, as determined by ELISA, no significant loss in trastuzumab binding was observed for the conjugate.

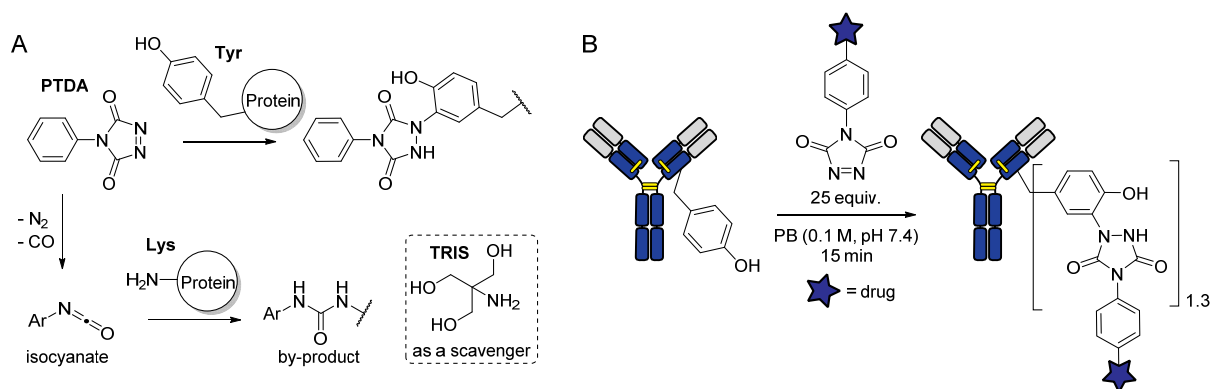


Figure 26. (A) Tyrosine conjugation with PTDA reagent and its decomposition to isocyanate, which may react with Lys residues on proteins. Side reaction can be eliminated using TRIS buffer. (B) Selective tyrosine modification of mAb.

3.7.2 Diazonium salts

The first application of diazonium reagents for tyrosine coupling was described by Pauly in 1915. Since then, it was shown that in order to perform Tyr-selective modification of proteins and avoid concurrent reaction with Lys and His residues, highly electrophilic diazonium salts should be applied. Such reactive diazonium salts can be obtained by introduction of electron withdrawing groups in their structure.

The diazotation reaction was employed for the preparation of the first ADCs.⁹ However, because of high aggregation and precipitation of the ADCs prepared using this approach, it was replaced promptly by milder methods employing lysine conjugation or carbohydrate targeting.¹²⁶

In 2012, Barbas group developed formylbenzene diazonium hexafluorophosphate (FBDP) reagent for the introduction of an aldehyde bioorthogonal tag through a tyrosine residues of proteins and antibodies (Figure 27). The aldehyde group is capable for future bioorthogonal modifications using oxime or hydrazone chemistry.¹²⁷ FBDP represents an elegant example of a stable plug-and-play reagent for tyrosine labelling.¹²⁸

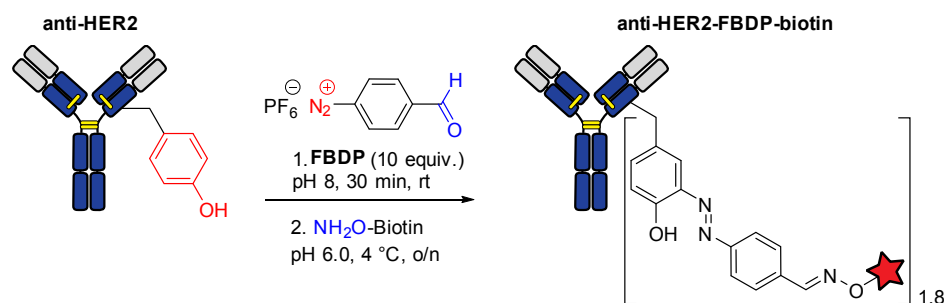


Figure 27. Diazonium salt application for tyrosine-selective functionalisation of trastuzumab.

The potential of the FBDP methodology was studied for the labelling of the trastuzumab antibody in two steps with a biotin tag. Using an optimised protocol, the antibody was first modified with 10 eq. of FBDP and then reacted with 20 eq. of biotin-oxyamine. This afforded trastuzumab-biotin conjugate with the DoC of 1.8 according to MS analysis. The MS spectrum showed the distribution of species with 0 to 3 payloads per antibody. The authors stated that this chemical modification did not affect antigen recognition of the obtained conjugate according to ErbB2 binding ELISA.

However, the recent investigation of the reaction between diazonium salts and trastuzumab showed that the majority of conjugated tyrosine residues are located on the heavy chain in the Fv region.¹²⁹ The same residues also belong to the binding site of the antibody and are likely to be involved in HER2 binding. Further studies should be done to evaluate the influence of this chemistry on the trastuzumab's antigen binding.

3.7.3 Luminol derivatives

Despite high utility of PTAD derivatives for protein functionalisation, they are unstable under physiological conditions. PTAD derivatives gradually decompose in aqueous media producing

reactive isocyanates, which can further react with lysine residues and N-terminal amino groups of proteins (Figure 26A). These side reactions are supposed to be the main reason of relatively low selectivity of PTAD reagents for a tyrosine residue.

In 2015, reactive luminol derivatives, which do not generate an electrophilic by-product, were envisioned for the Tyr-selective modification. As a result, N-methylated luminol derivatives activated *in situ* were proposed for tyrosine-specific chemical modification of peptides and proteins.¹³⁰ The authors applied this method for anti-tubulin antibody functionalisation with biotin and fluorophores using plug-and-play approach (Figure 28).

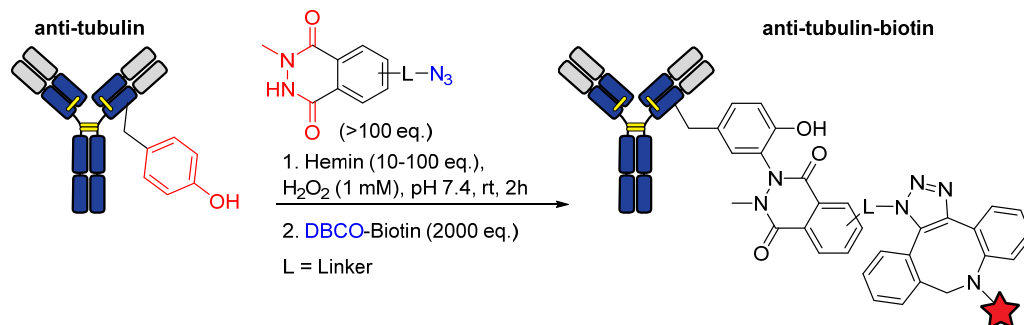


Figure 28. Tyrosine-specific anti-tubulin antibody modification with azide-containing luminol derivative activated *in situ* by hemin (an iron–protoporphyrin IX complex) and H₂O₂.

On the first step, the antibody was conjugated with azide-containing N-methylated luminol derivative (>100 eq.) under oxidative conditions in the presence of hemin and H₂O₂. On the second step, the resulting conjugate was functionalised with biotin tag by copper-free click chemistry using a large excess of dibenzocyclooctyne-biotin (DBCO-biotin). This afforded anti-tubulin-biotin conjugate, which had deteriorated antigen selectivity, but still could recognize tubulin in HeLa cell lysate. The decrease of antibody's antigen selectivity was probably due to oxidative damage of the antibody's structure under such harsh oxidative conditions (1 mM H₂O₂). The strong oxidative conditions and low efficacy are the main drawbacks, which significantly limit the applicability of the methodology.

Recently, van Delft group pursued tyrosine-selective bioconjugation and reported enzymatic approach of genetically encoded tyrosine tag (Y-tag) oxidation.¹³¹ The Y-tags were incorporated into C-terminus of the light chains of the antibody and were oxidised with mushroom tyrosinase. The resulting 1,2-quinone can react with different BCN derivatives through strain-promoted oxidation-controlled quinone–alkyne cycloaddition (SPOCQ). The authors demonstrated successful site-specific labelling of antibodies with fluorophore and cytotoxic derivatives, however occasionally they observed the presence of some unlabelled material, which may be due to a competitive reaction of quinone with lysine or histidine residues.

3.8 Arginine residues

Arginine (Arg, R) residues with their pKa of above 12 are positively charged under physiological pH and found with intermediate to low frequency in proteins. A decreased ratio of arginine to lysine content (RK ratio) is a common feature of highly abundant proteins with elevated solubility, such as antibodies and human serum albumin (HSA).¹³² For instance, trastuzumab antibody had more than twice lower arginine content compared with lysine content (40 vs 90), which makes arginine an attractive target for bioconjugation.

3.8.1 Glyoxal reagents

It was known for a long time that arginine residues are sites of glycation in Maillard reaction with glyoxal – and more generally dicarbonyl – derivatives reacting selectively with the side-chain guanidine groups.¹³³ To this end, 2,3-butanedione,¹³⁴ 1,2-cyclohexanedione,¹³⁵ malonaldehyde,¹³⁶ phenylglyoxal,¹³⁷ methylglyoxal,¹³⁸ or even the simpler glyoxal,¹³⁹ have long been employed, even though the exact nature of the resulting products has proven to be elusive.^{140,141} The selectivity of such transformation has been rationalised by a thermodynamic factor, favouring the formation of arginine condensation adducts over lysine and cysteine ones. Reactions with the latter have been observed in some occasions though, albeit in negligible amounts, and yielded less stable adducts. This arginine selectivity has notably been employed to generate mPEG-protein adducts,¹⁴⁰ to inactivate enzymes,^{142,143} or to probe the surface topology of proteins.¹³⁵ However, application of arginine-glyoxal reaction mainly resides in the study of native proteins glycation mechanisms.^{133,138,144,145}

Only few examples of glyoxal-based bioconjugation strategies can be found in the literature. Among them, phenylglyoxal reagents have been reported for specific citrulline modification at low pH in order to study the citrullinated proteins in complex biological systems.^{146–148} Concerning arginine residues, Dawson *et al.* have recently demonstrated that *p*-azidophenylglyoxal monohydrate and its derivatives were efficient reagents for the functionalisation of two model proteins (RNase A and Lysozyme).¹⁴⁹

To the best of our knowledge, there is only one report of arginine residues modification on a native antibody. It concerns the arginine modification by methylglyoxal, which was attributed to the post-translational modification of mAb in CHO cells.¹⁵⁰ Methylglyoxal can be produced enzymatically or nonenzymatically from glucose in CHO cells and was shown to cause arginine modification of the recombinant mAbs. Such modification affords two arginine adducts: dihydroxyimidazolidine resulted after primary addition of methylglyoxal and more stable hydroxyimidazolone produced after water elimination (Figure 29). The both forms had lower calculated pKa value compared with original arginine and were attributed to acidic species of mAb. Recently, phenylglyoxal derivatives were used for releasable and traceless PEGylation of arginine-rich peptides.¹⁵¹ It was shown that dihydroxyimidazolidine adduct was not stable under physiological pH with half-life of approximately 10 hours, while the dehydrated adduct, hydroxyimidazolone, was stable in the same conditions.

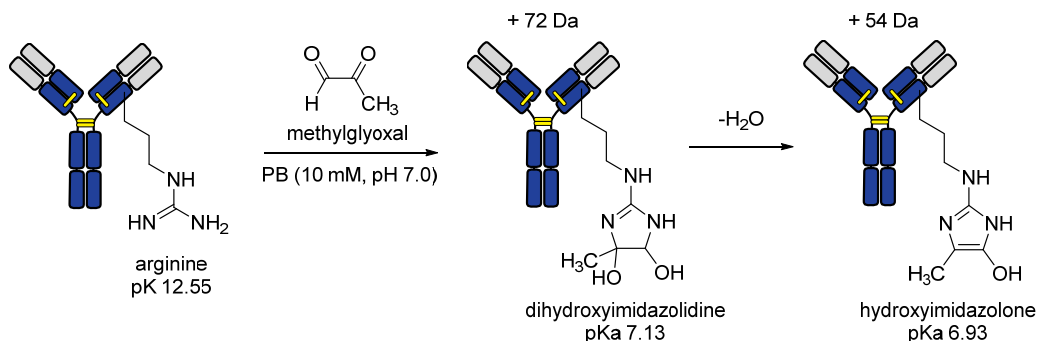


Figure 29. Arginine reaction with methylglyoxal as a post-modification of the recombinant mAbs leading to acidic species.

In summary, despite the methodology of arginine modification is comparatively old and many examples exist in the literature, the arginine bioconjugation in the context of ACs production seems disregarded, with no mention of any selective approach of antibody functionalisation with useful payloads.

3.9 Tryptophan residues

Among 21 natural amino acids, tryptophan (Trp, W) is the least abundant (~1%),³⁸ meanwhile approximately 90% of native proteins possess at least one Trp residue.¹⁵² Apparently, decreasing the number of reactive sites should translate into better control of protein conjugation and improved homogeneity of the final product. In this regard, the selective tryptophan targeting seems to be a promising strategy. Nevertheless, methodology of Trp-selective bioconjugation is still elusive. The approaches reported in the literature often require application of toxic heavy metals or biochemically harsh conditions.^{153–157} Moreover, the utilisation of these methods can be limited by their low selectivity towards tryptophan residues and cross-reaction with tyrosine. Despite the challenge, a metal-free method for tryptophan-selective functionalisation of proteins has been recently developed. This methodology relies on an organoradical reagent applied under the mild conditions and exhibits low levels of cross-reactivity.¹⁵⁸

3.9.1 Organoradical reagent

In 2016, Kanai group demonstrated that organoradical like 9-azabicyclo[3.3.1]nonane-3-one-N-oxyl (keto-ABNO) can selectively modify the tryptophan residue on proteins in the presence of NaNO₂ in an aqueous medium containing 0.1% acetic acid for 30 min in the absence of transition metal salts. It was suggested that in this reaction oxoammonium is a possible reactive intermediate produced by acid-promoted disproportionation and oxidation by NO_x, which in turn is generated from NaNO₂ and acetic acid. The method was effectively employed on a number of Trp-containing peptides and proteins and the resulting conjugates were chemically and thermally more stable than similar products based on Cys-bioconjugation. The methodology was also applied for the conjugation of anti- Aβ_{1–16} antibody (6E10) with fluorescein derivatives of keto-ABNO (Figure 30).

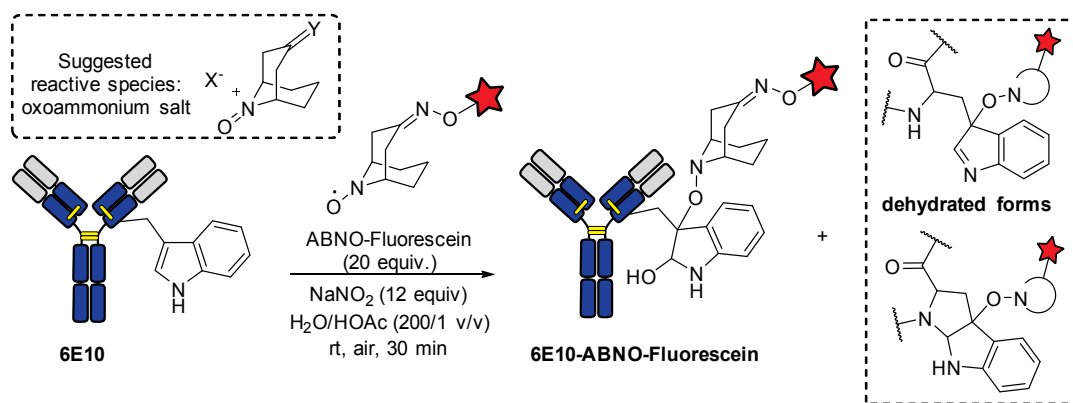


Figure 30. Preparation of antibody-fluorophore conjugates using tryptophan-selective organoradical reagent.

The resulting antibody-fluorophore conjugate was analysed by SDS PAGE, which revealed fluorescence of light and heavy chains of the antibody. This shows that despite low content of tryptophan residues in the antibody, the methodology still provides the heterogeneous ACs. The intact functionality of the antibody was demonstrated by dot blot assays targeting amyloid beta. Although the metal-free approach revealed the low cross-reactivity, the methodology required relatively strong acidic condition. Indeed, the water/acetic acid solution at used proportion gives pH of 2.9 going beyond the recommended pH values for antibody conjugation ranging from 4 to 9. This factor should be considered in cases, when the technique is employed on sensitive biomolecules.

3.10 Methionine residues

Methionine (Met, M) is one of the most hydrophobic and the third rarest amino acid (after Cys and Trp), which are preferably hidden inside the protein core.³⁸ This limits the amount of surface-accessible methionines making them potentially attractive for selective protein modification.

Owing to the relatively weak nucleophilicity of methionine residues, their selective modification is complicated in the presence of more nucleophilic amino acids such as cysteine, lysine, tyrosine, or serine.^{159,160} Consequently, the development of mild methionine-selective bioconjugation methodology is extremely challenging. The majority of reported approaches are based on alkylation of Met residues under acidic conditions ($\text{pH} < 3$). At such low pH all of the nucleophilic groups in protein, except methionine, are protonated, which greatly reduce their reactivity. As a result, this enables to discriminate methionine residues from other reactive centres making possible their selective alkylation. Kramer and Deming have recently demonstrated this approach for a reversible chemoselective tagging of methionine in peptides and polypeptides using alkyl bromide as a reactive group.¹⁵⁹ However, the bioconjugation of more complex substrates such as proteins and antibodies at pH lower 4 could represent an issue. Deterioration of proteins and their dysfunction are likely to happen in acidic media, which restrict the methodology for the ACs preparation.

Another remarkable feature of the methionine residues is their elevated susceptibility for the oxidation to methionine sulfoxide. Actually, the facile oxidation of methionine residues often creates a concern for ACs prepared using oxidative reaction. For example, oxidation of methionine residues

located near the FcRn binding site is commonly an issue during carbohydrate oxidation with sodium periodate used at high concentration (see section below). This over-oxidation is known to affect FcRn binding, which in its turn decrease the ACs half-life in serum.¹⁶¹

3.10.1 Oxaziridine reagents

Inspired by easiness of methionine oxidation, Chang group recently described oxidative sulfur imidation reaction as an alternative strategy for methionine bioconjugation. The methodology termed redox-activated chemical tagging (ReACT) employed plug-and-play oxaziridine-based reagents to provide highly selective and fast methionine labeling under pH-neutral conditions (Figure 31A).

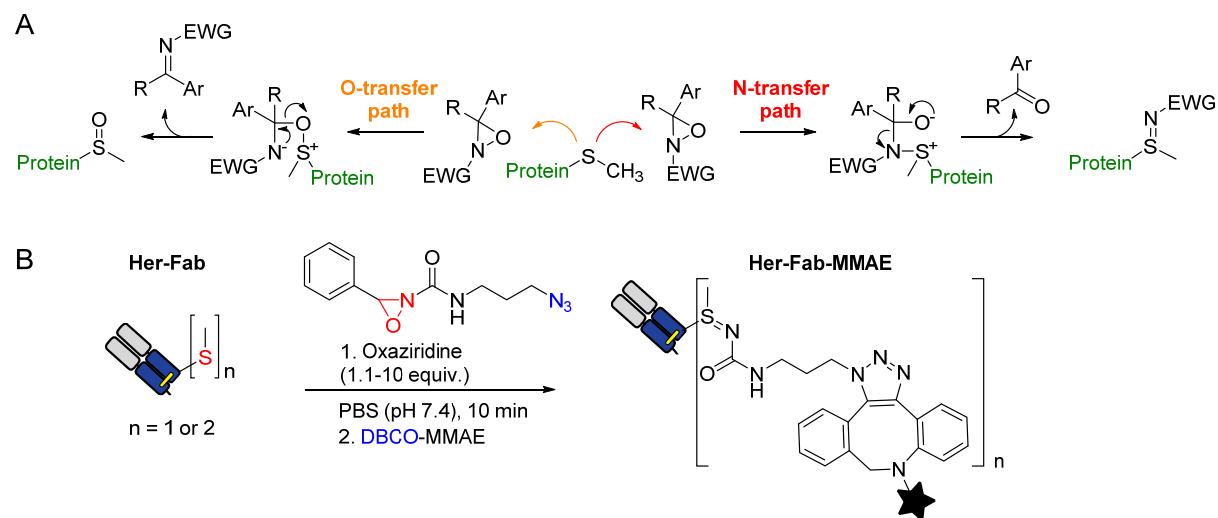


Figure 31. (A) Reaction mechanism between methionine and oxaziridine. (B) Selective methionine labeling of the engineered Her-Fab using plug-and-play oxaziridine-based reagent.

The ReACT was applied for the precise modification of proteins and preparation of ADCs using Fab fragment of Herceptin (Her-Fab). Despite the presence of several methionine residues in Her-Fab, none of them were solvent-accessible, thus ReACT did not label the wild type Fab antibody. To this end, engineered Her-Fab platforms carrying one or two methionine residues at the C terminus of the light chain were designed (Figure 31). On the plug stage, the reaction of the engineered Her-Fab with oxaziridine-azide reagent resulted in near quantitative addition of one or two azide groups to antibody, respectively (Figure 31B). On the play stage, the resulting azide handles were functionalised with MMAE using click chemistry.

The resulting Her-Fab-MMAE were tested *in vitro* to demonstrate selective toxicity towards HER2 positive breast cancer cells providing an evidence of unaffected antibody function. Although, ReACT can enable synthesis of ADCs with a defined DAR, in many cases methionine sulfoxide was detected as the major by-product. Therefore, application of ReACT methodology for the full antibodies may lead to oxidation of methionine residues found close to the FcRn binding site, which consequently reduces the half-life of the ADC in serum.

3.11 Glycan residues

All antibodies belong to glycoproteins and thus possess an *N*-glycosylation site at the conserved Asn297 residue of the Fc region. Therefore, there are only two glycan chains per antibody making them attractive target for bioconjugation. The main advantage of glycan residues modification is their distant location from the antibody's antigen binding region. Thus modification of antibody through these residues should have little or no effect on the antibody activity. However, glycan residues play an important role for enhancement the effector functions of the antibodies by altering antibody's affinity for Fc and other immune receptors.

One of the first method of glycan modification relied on oxidation of *cis*-diol functionality on the sugar residues. This reaction affords aldehyde or ketone groups, which can be easily targeted by oxime or hydrazone chemistry. Actually, the glycosylation of antibodies greatly contributes to their heterogeneity providing a mixture of antibody glycoforms bearing different glycan types. Given the different combination of oligosaccharide sequences in mammalian IgG,¹⁶² there is a potential to create 8-12 aldehydes per carbohydrate chain in the absence of any sialic acid and 6-10 aldehydes per chain when both terminal sialic acids are present. In this context, Hage and coworker showed that depending the reaction time, temperature and amount of the oxidizing agent, the antibody can be modified to different extent providing from 1 to 8 conjugation sites per antibody. The classical oxidising agent for glycan oxidation is sodium periodate applied at high concentration (100-1000 fold excess). This protocol was commonly used for ligation of hydrazine-containing drugs to antibodies and afforded relatively homogenous ADCs.¹⁶³ However, the antibodies are not stable under harsh oxidative conditions. Decreased antigen affinity and disruption of protein structure was often observed for the resulting conjugates prepared by this method.

Recently, a great amount of novel glycan conjugation methods appeared for the construction of near-homogeneous ADCs. All of them are based on enzymatic approaches for either reconstruction the native heterogeneous glycan population to homogenize them (glycolengineering)^{164,165,36} or/and for incorporation of bioorthogonal handles, namely azides, which could serve as clickable sites for further antibody functionalisation.¹⁶⁶

4 Objectives

From this review one can make a conclusion that the majority of the current linkage techniques for native antibody conjugation are not ideal and suffer from heterogeneity, loss of structural characteristics of antibodies, low efficacy or/and stability.

This project aims to find more reliable bioconjugation techniques and pursuits the following objectives (Figure 32):

- Overcoming the low stability and the hydrophobicity of linkage obtained using current maleimide-based heterobifunctional reagents for antibody conjugation (Part I).
- Design and development of a general screening system for reliable comparison of different functional group reactivity with the native antibodies. For the groups with the best

- characteristics in terms of efficacy, reactivity and/or selectivity, development of the plug-and-play reagents (Part II).
- Resolving the heterogeneity issues, design and development of conjugation strategies, which can provide a high control over conjugation affording ACs with defined degree of conjugation (Part III).
- This project involves the development, synthesis and biological evaluation of new, efficient and versatile linker technologies for the preparation of more stable and well-defined ACs.

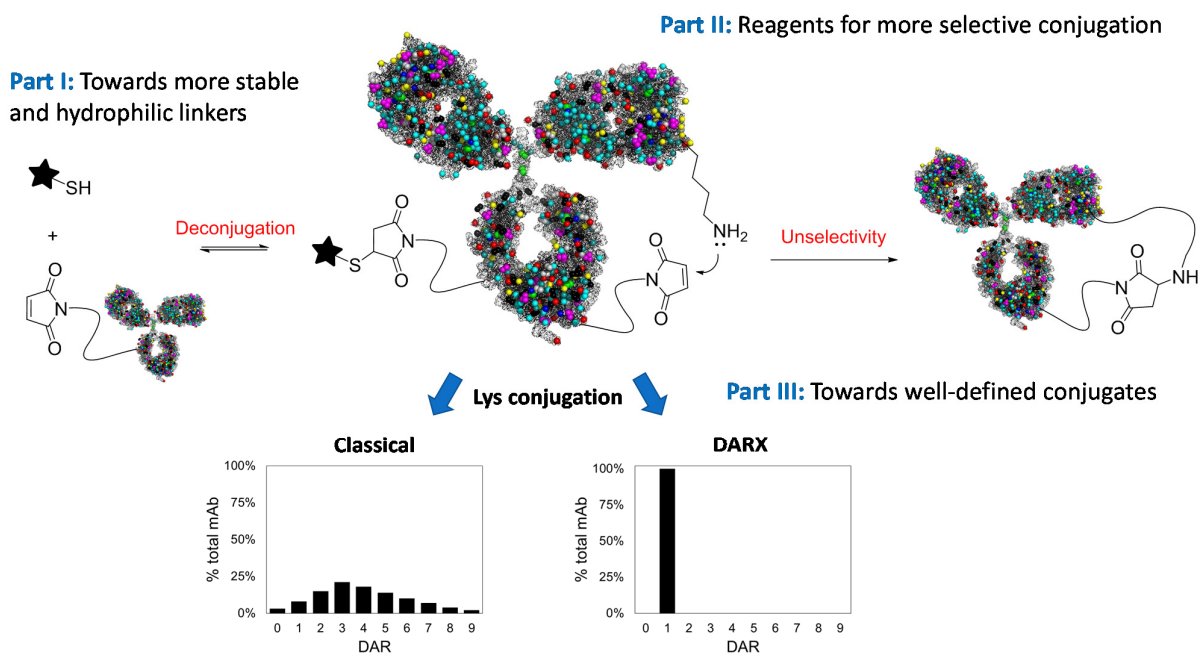


Figure 32. Three main project aims.

B. TOWARDS A NOVEL CHEMISTRY FOR BIOCONJUGATION

This chapter consists of three parts. The first part is devoted to design and development of maleimide-dioxane reagents as self-hydrolysable and serum-stable alternative to classical maleimide chemistry. The second part is dedicated to a screening approach for evaluation of residue-selective functionalities in reactions with an antibody using high resolution native mass spectrometry (native-HRMS). Finally, in the third part we introduce a novel technology, which enables efficient preparation of the antibody conjugates with a defined degree of conjugation and particularly monofunctionalisation of biomolecules.

Part 1. Development of novel linker for bioconjugation

This part of the chapter is devoted to the design, synthesis and evaluation of more stable maleimide-based linkers for bioconjugation. To address the hydrophobicity issue of MCC linker, we have developed a heterobifunctional analogue of a SMCC reagent, i.e., sodium 4-(maleimidomethyl)-1,3-dioxane-5-carbonyloxy)-2,3,5,6- tetrafluorobenzenesulfonate (MDTF) for amine-to-thiol conjugation (Figure 33). By replacing the cyclohexyl ring in the MCC structure with the 1,3-dioxane, we increased the hydrophilicity of the linker. A FRET probe based on maleimide-dioxane (MD) linker was prepared and showed superior stability compared to the MCC linker in human plasma, as well as in a variety of aqueous buffers and *in cell*. A detailed investigation demonstrated an accelerated succinimide ring opening for MD linker, resulting in stabilised conjugates. Finally, the MDTF reagent was applied for the preparation of serum stable antibody-fluorophore conjugate.

1.1 Introduction

The development of new linkers and conjugation techniques is of great interest in the construction of ADCs.^{167,168} The vast majority of them are prepared through amine-to-thiol conjugation.⁴ To date, SMCC has been one of the most frequently applied amine-to-thiol linker for the preparation of ADCs and other functionally enhanced proteins.¹⁶⁹

This heterobifunctional reagent contains an NHS ester that reacts with amines, yielding a peptide bond and a maleimide group that reacts with thiols, resulting in the formation of a thioether. Both groups are joined together by a cyclohexyl ring, which has been shown to increase the aqueous stability of the maleimide group.¹⁷⁰ Due to the high abundance of both amines (e.g., lysine residues) and thiols (e.g., cysteine residues) in biological molecules, the SMCC reagent has become an indispensable tool for the modification of biomolecules.

The applications of SMCC include preparation of hapten-carrier conjugates,¹⁷¹ antibody-enzyme conjugates,^{172–174} immunotoxins¹⁷⁵ and perhaps the most advanced application to date, generation of ADC^{176,177}. Indeed, one of the two marketed ADCs, trastuzumab emtansine¹⁸, as well as other antibody-maytansinoid conjugates in clinical development, are prepared *via* SMCC-mediated

conjugation,^{4,167} in which a highly potent drug is directly linked to an antibody through the MCC linker.

Despite its high applicability, some issues arise from the relatively hydrophobic character of SMCC. Precipitation of the linker in aqueous media, as well as aggregation and precipitation of resulting bioconjugates may occur, decreasing both conjugation efficiency and yield. This issue is of particular importance for the development of mertansine-based ADCs, where the drug is connected to an antibody through the MCC linker, without additional cleavable peptides or other elements that can increase water solubility.

To address the issue of reagent precipitation, a sulfo-SMCC linker containing a sulfonate group on the NHS ring was developed.¹⁷⁸ However, the linker structure remained unchanged and thus, the problem pertaining to linker innate hydrophobicity (causing aggregation and precipitation of bioconjugates) remained unsolved.

1.2 Design of more hydrophilic linkers

In an effort to address this issue, we designed a new SMCC-like reagent **5** with increased hydrophilicity of the linker core structure. This was achieved by substitution of the cyclohexyl ring by the 1,3-dioxane analogue to afford MD linker (Figure 33). By fitting two oxygen atoms into the structure, the calculated LogP value of the linker decreased by 1.67 units. Additionally, as the 1,3-dioxane ring contains in fact an acetal function, by doing such exchange, we expected also to obtain pH sensitive linker. This acid-cleavable linker could be interesting in context of ADCs, which should be stable under physiological pH during their circulation, but liberate the drug in acid interior of the lysosomes (pH 4.5-5) after their internalisation into the target cell. Moreover, we replaced the sulfo-NHS-activated ester with the 4-sulfotetrafluorophenylester in order to increase the solubility of the final product in water, which is an important parameter for biological applications.¹⁷⁹

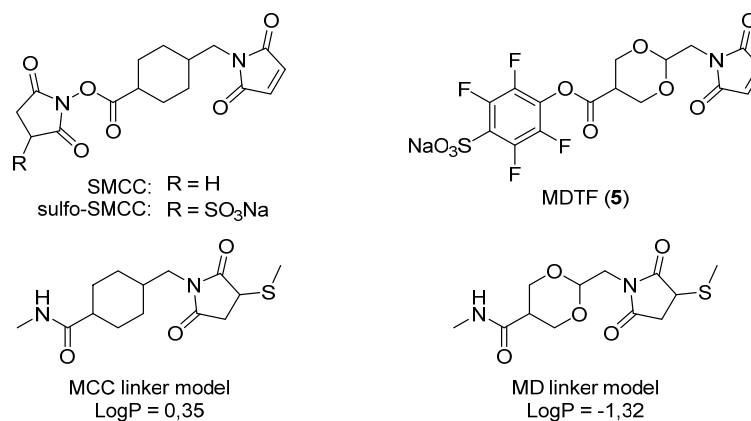
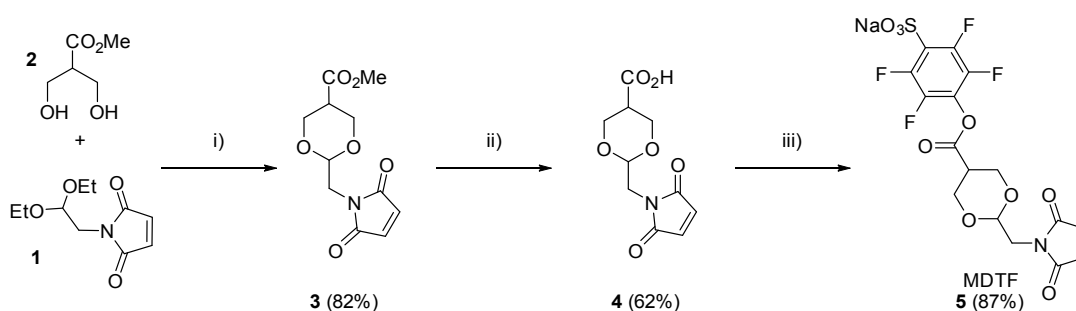


Figure 33. SMCC and MDTF reagents, the resulting linker models and their calculated LogP values. LogP values indicate higher hydrophilicity of the MD linker model.

1.3 Synthesis of MDTF

We prepared a new heterobifunctional reagent, the sodium 4-(maleimidomethyl)-1,3-dioxane-5-carboxylate **5** (MDTF) in three steps from readily available precursors **1** and **2** (Scheme 1). First, the reaction between **1** and **2** was carried out by refluxing their mixture in toluene, in the presence of a catalytic amount of *p*-TsOH in order to give 1,3-dioxane **3** in 82% yield. Then, hydrolysis of **3** with lithium hydroxide solution (THF/water) led to simultaneous de-esterification of carboxyl function and maleimide ring opening. The latter was then transformed into **4** using previously reported reaction conditions¹⁷⁰ in 62% yield. Finally, the activation of the carboxylic function of **4** with sodium salt of 4-sulfo-2,3,5,6-tetrafluorophenol (STP) gave the target activated ester **5** in 44% overall yield. It was notable that MDTF was completely soluble in water at 10 mM concentration, which is an important parameter for bioconjugation.



Scheme 1. Synthesis of MDTF reagent (in 44% overall yield): i) *p*-TsOH (cat.), toluene, reflux, 2 h, 82%; ii) LiOH, H₂O/THF, 25 °C, 30 min, then HCl to pH 2 and NaOAc, Ac₂O, 80 °C, 2 h, 62%; iii) 4-sulfo-2,3,5,6-tetrafluorophenol, DCC, DMF, 25 °C, 16 h, 87 %.

1.4 Stability of MD and MCC linkers in human plasma

In order to assess the stability of the linker in biological media and at different pH we synthesised two FRET probes **P1** and **P2** using MDTF and sulfo-SMCC reagents, respectively, through amine-to-thiol conjugation of 1 equiv. of fluorophore-amine (TAMRA-NH₂) and 1 equiv. of quencher-thiol (BHQ-2-SH). The probes were purified using semi-preparative HPLC in order to remove all traces of the starting materials. These probes were not fluorescent, as the quencher and the fluorophore were linked together through MD or MCC linker, but cleavage of the linker or substitution of BHQ-2-SH by other thiol-containing molecules such as human serum albumin (HSA) resulted in the appearance of the fluorescence signal.

To test the stability of the linkers we incubated probes **P1** and **P2** (1 μM) in different buffers (TRIS, PB) at various pH (from 5.5 to 9.0), as well as in human plasma (pH 7.4) and in 1 M aqueous solution of HCl at 37 °C (Figure S1, Annex 1). The appearance of fluorescence was monitored at 580 nm over 15 h and normalised using a solution of TAMRA-NH₂ (1 μM) and BHQ-2-SH (1 μM) in appropriate media as a positive control.

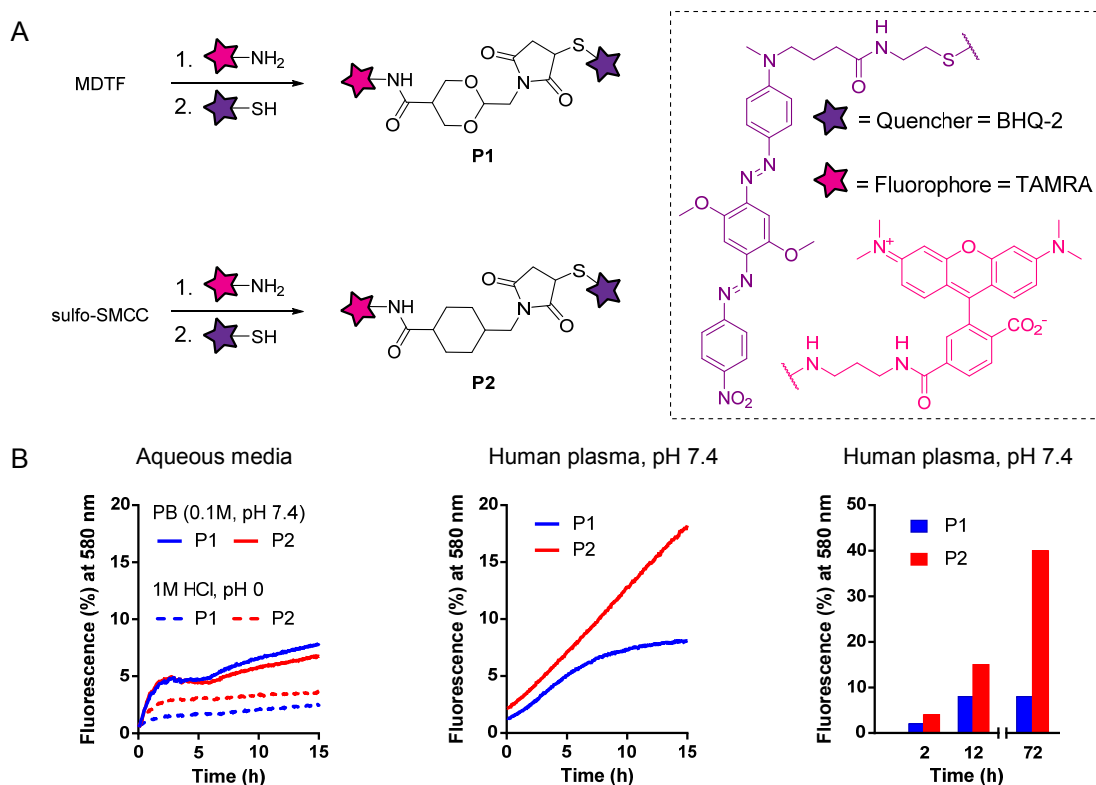


Figure 34. (A) Preparation of FRET probes **P1** and **P2**. (B) Stability of probes **P1** and **P2**.

Interestingly, despite the presence of an acetal function in its structure, the MD linker appeared to be more stable than MCC, even at pH 0 (Figure 34 B). We also found that the fluorescence observed during incubation of **P1** in human plasma reached a plateau after 12 hours (Figure 34 B), while **P2** exhibited linearly increasing fluorescence. The latter was demonstrated as being the result of a gradual exchange of BHQ-2-SH by the thiol of human serum albumin (HSA) present in human plasma.¹⁸⁰ This linear fluorescence increase in **P2** was maintained and after 72 hours provided 40% of linker cleavage. In contrast, the fluorescence of **P1** remained unchanged after reaching a plateau.

We hypothesised that the difference in behavior of similar scaffolds was due to the hydrolysis of the succinimide motif in the case of **P1**, which led to the succinamic acid **hP1**, which is known to be stable toward thiol exchange (Figure 35). To confirm this hypothesis, we measured the succinimide hydrolysis rates in human plasma of **P1** and **P2** using LC-MS analysis. Hence, probes **P1** and **P2** (50 μL each) were incubated in human plasma containing 10% of DMSO at 37 $^{\circ}\text{C}$. Aliquots at different time points were analysed by LC-MS after the precipitation of proteins by the addition of acetonitrile. As expected, a peak corresponding to succinamic acid **hP1** was observed for the probe **P1** and the reaction was almost complete after 29 hours, while for the probe **P2**, only a trace amount of hydrolysed product **hP2** could be detected after 29 hours (Figure 36). MD-based linkers therefore appear to offer an interesting possibility for self-stabilisation of the resulting conjugates *via* a succinimide ring opening.

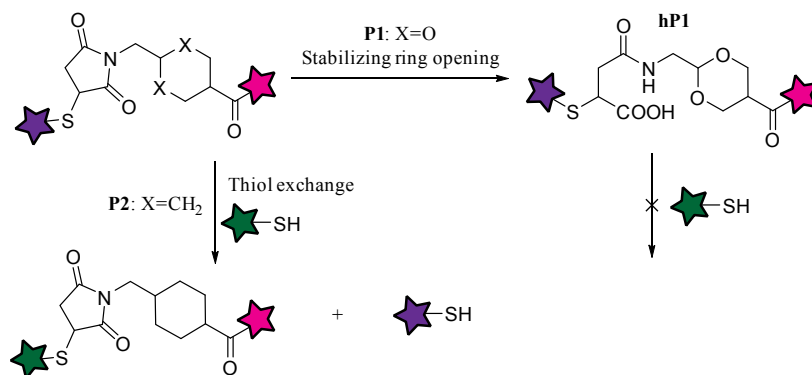


Figure 35. Hydrolysis of the succinimide of **P1** led to succinamic acid **hP1**, which did not undergo thiol exchange. In the case of **P2**, thiol exchange occurred faster than the stabilizing succinimide hydrolysis.

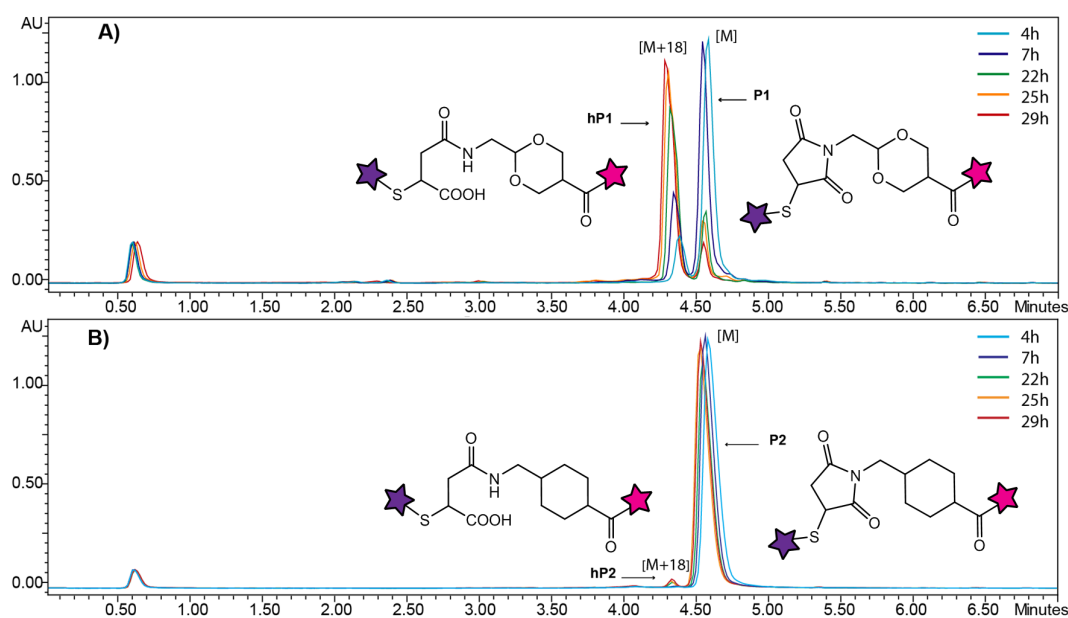


Figure 36. Incubation of FRET probes **P1** and **P2** (50 μ M) in human plasma at 37 $^{\circ}$ C and subsequent analysis of mixture composition by LC-MS analysis at 550 nm. (A) Hydrolysis of succinimide of the MD-based probe **P1** yielding succinamic acid **hP1**. (B) Only trace amount of hydrolysed product was observed for the MCC-based probe **P2**.

1.5 Stability of MD and MCC linkers *in vitro*

Stability of the FRET probes **P1** and **P2** (MD and MCC non-cleavable linkers respectively) was then evaluated *in vitro* on liver cells (BNL CL.2 cell line) using a confocal fluorescence microscopy (Figure 37). As a positive control we used a FRET probe of TAMRA and BHQ-2 connected through a lysosome cleavable linker. It was found again that probe **P1** was more stable *in cell* than probe **P2**, probably because of lower thiol exchange with such molecules as cysteine and glutathione presented in cytoplasm. This confirms that MDTF reagent can be applied for the construction of bioconjugates with non-cleavable stable linker.

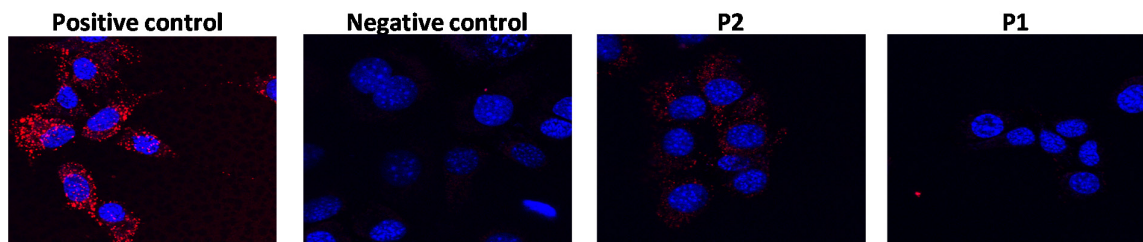


Figure 37. *In vitro* stability of FRET probes with cleavable linker (positive control) and non-cleavable linkers (**P1** and **P2**) evaluated on BNL CL.2 cell line. Viable cell imaging was carried out by first staining with the different probes (1 μ M, 90 min) followed by staining with Hoechst 33258 (5 μ g/mL, 30 min). Confocal fluorescence microscopy imaging of viable cells was performed at a magnification of 630 \times .

1.6 Application of MDTF reagent for the preparation of antibody conjugates

Encouraged by these results, we then decided to test the MDTF reagent for the preparation of homogenous antibody-fluorophore conjugate and to evaluate whether self-hydrolysis properties of MD linker can be used to prepare conjugates stable in human plasma. To this end, a side-by-side comparison with a sulfo-SMCC reagent was carried out (Figure 38). As an antibody platform we used anti-HER2 antibody, trastuzumab (T), used in clinic for breast cancer therapy and a component of FDA-approved ADC (Kadcyla®).

First, a reaction between MDTF or sulfo-SMCC and TAMRA-NH₂ was performed using classical conjugation conditions to afford MD-TAMRA and MCC-TAMRA adducts, respectively. In parallel, a complete reduction of the interchain disulfide bonds of trastuzumab was achieved using TCEP reagent. The resulting MD-TAMRA and MCC-TAMRA were then conjugated with reduced trastuzumab. The corresponding conjugates were purified by gel filtration chromatography to afford homogeneous T-MD-TAMRA and T-MCC-TAMRA conjugates. The ESI-MS analysis¹⁸¹ confirmed the fluorophore-to-antibody ratio value of 8 for both conjugates. To trigger succinimide hydrolysis, the conjugates were maintained in the PBS buffer (1x, pH 7.4) at 37 °C for 3 days (1 day for BBS buffer with pH 8.5) to afford conjugates **C1** and **C2**. Then, both conjugates were incubated in human plasma for five days. Aliquots were taken every 24 hours and analysed by SDS PAGE. In addition to the two lanes corresponding to the labelled heavy (HC) and light chains (LC) of the antibody, the MCC-based conjugate showed the gradual appearance of a third lane, corresponding to the transfer of the fluorophore to the HSA.¹⁸⁰

In summary, we have developed a new heterobifunctional reagent (MDTF) for amine-to-thiol conjugation that indicates similar reactivity towards sulfhydryl-containing molecules as the SMCC. Substitution of a cyclohexyl ring by a dioxane ring increased hydrophilic character in the new MD linker compared to the classical MCC linker. Interestingly, the MD linker underwent self-stabilisation in mild conditions via a succinimide ring opening. The resulting succinamic acid-containing linker is not prone to the undesirable thiol exchange reaction. In fact, a MD-based FRET probe incubated in human plasma showed a considerably higher self-stabilisation rate compared to the MCC-based

probe. This hydrolytic stabilisation process was shown to be efficient for the preparation of serum stable antibody conjugates.

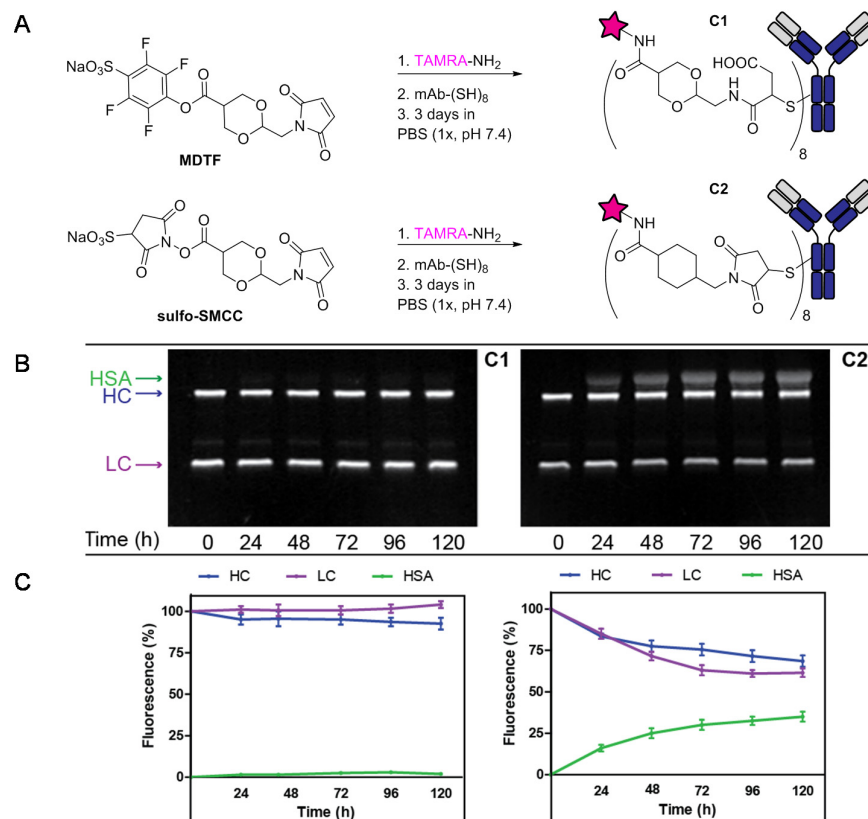


Figure 38. (A) Preparation of antibody-fluorophore conjugates **C1** and **C2**. (B) Fluorescent reducing SDS-PAGE analysis of **C1** and **C2** after incubation in human plasma. (C) Quantitative analysis of conjugate stability in human plasma demonstrated 38% of payload transfer to HSA over 120 hours for the MCC-based conjugate **C2** in contrast to 3% for the MD-based conjugate **C1**.

These results have been recently published.¹⁸² The further study of linkers containing cyclo-dioxo maleimide is currently ongoing in our group. Particularly, we investigate how a size of spacer between dioxo ring and maleimide and size of the dioxo ring influence on the ability of the linker to self-hydrolysis and stability at acidic pH.

Part 2. Screening and development of residue-selective reagents

In this part of the chapter the design of a screening system for evaluation of selectivity and efficacy of various functional groups in reaction with an antibody is discussed. A library of 3,4-dimethoxyphenyl derivatives bearing different electrophilic functions was synthesised and reacted with mAb to evaluate their efficacy and selectivity using native-HRMS. Comparing the resulting MS profiles allowed us to select the most interesting examples and further develop them as residue-selective reagents for antibody conjugation.

2.1 Design of the screening system

Among the myriad reactive functionalities available for bioconjugation,^{3,160,169} the NHS activated esters are the most frequently used for the preparation of ACs *via* lysine residue conjugation. However, to the best of our knowledge, the systematic investigation of the efficacy, selectivity and stability of different reactive groups in the context of ACs production has not been described in the literature yet. The evaluation of these parameters for reactive groups is of great interest for the effective preparation of stable protein conjugates in a selective fashion.

In an effort to address these questions, we designed a screening approach using a native-HRMS analysis, which allows for precise, controllable and reliable evaluation of the ACs composition.^{181,183,184} In this direct approach, the electrophiles were reacted with mAb and the resulting ACs mixtures were analysed after purification by native-HRMS. This screening system was developed in close collaboration with our colleagues from the Laboratory of Bioorganic Mass Spectrometry (LSMBO), who, in particular, performed all MS experiments.

It should be mentioned that another type of structure-reactivity study exists; in this case, the reagents are first tested on a library of amino acids, in order to determine hit candidates. The latter would then be evaluated in reactions with model peptides and then proteins.^{90,185} However, during this amino-acid-to-protein translation, some interesting candidates can be lost and not reach the final phase with protein test. For instance, the negative results with an amino acid could be deemed negative for proteins too, despite the fact that the presence of surrounding nucleophiles at the surface of the proteins might modulate the reactivity of the residue. Such microenvironments are a reason why same type of residues (for instance, Lys) differ in their reactivity on a protein surface, creating those so-called “hot-spot residues”.⁴⁹ Exploration of these peculiar microenvironments and determination of the hot-spots are thus only possible when a direct approach is employed. Reacting various electrophiles directly with mAb represents one of such approach.

For the screening, we decided to employ trastuzumab as a model and small electrophiles (100-300 Da). Given the differences in molecular mass between those species, the application of native-HRMS analysis was vital, because of its capacity to discriminate between antibody species with minimal mass changes. In order to be able to compare the reactivity profiles of different functionalities, their core structure was kept the same and every experimental parameters were fixed

(buffer composition and pH, temperature, time of conjugation, amount of added reagents and their concentrations).

To this end, a library consisting in 3,4-dimethoxyphenyl derivatives **R1-R20** was synthesised (Figure 39 B). The 3,4-dimethoxyphenyl core was chosen thanks to its UV absorbance, MS response and synthetic availability. The reactive functionalities were chosen based on a literature research of residue-selective groups^{3,160,169} and the purity of the resulting reagents **R1-R20** was confirmed by NMR spectroscopy and LC-MS analysis.

2.1.1 Library design

The majority of the library compounds (**R1-R4**, **R6-R9**, **R11**, **R12**, **R18-R20**) corresponds to the activated esters of 3,4-dimethoxybenzoyl. These activated esters have been frequently applied to the conjugation of lysine residues.¹⁸⁶⁻¹⁸⁸ Other reagents, such as oxazolone **R5**,³ squaramide **R10**,⁶⁶ and isothiocyanate **R16**,¹⁶⁹ belong to other classes of functional groups described for the modification of lysine residues.

Interestingly, isoxazolium salt **R17** is an analog of Woodward's Reagent K, which has been classically employed for carboxylate activation in peptide synthesis,¹⁸⁹ but was also known to covalently and unspecifically label proteins at histidine, lysine, cysteine, and tyrosine residues under appropriate conditions.¹⁹⁰ In the presence of bases, isoxazolium moieties can be deprotonated and converted into keto-ketenimines, which react fast with amines and carboxylic groups.

Alkyne **R13**,¹⁹¹ allene **R15**,¹⁹² or maleimide **R9**³ are known to react with thiol groups of cysteine residues. While free thiols are absent in non-reduced native antibodies, these reagents are still interesting to explore in order to determine their selectivity towards other amino acid residues on the antibody.

Despite the fact that phenylglyoxals have been actively applied for the arginine residues modification of peptides and proteins, they were never studied in the context of antibodies functionalisation. This motivated us to include the commercially available glyoxal **R14** to the library list in order to evaluate its reactivity profile in the reaction with the antibody.

2.1.2 Screening of the library reagents, determination of their efficacy

In the screening experiments, mAb (trastuzumab, 5 mg/mL) was treated in parallel with 10 equivalents of reagents **R1-R20** for 16 h at 25 °C. After purification by gel filtration chromatography, the resulting ACs were subjected for native-HRMS in order to find DoC, which can be transformed into the reagent efficacy parameter (Figure 39 A). The corresponding mass spectra were performed in triplicates in order to obtain more reliable results.

To the exception of reagents **R19** and **R20**, all the tested reagents demonstrated ability to modify the antibody to some extent. According to MS analysis, the resulting ACs were the heterogeneous mixtures of antibody species with 0, 1, 2 ... *n* add-on molecules per antibody (Annex 4). Distribution mass profile in most cases fitted well with binominal distribution model described

previously for the statistical analysis of ADCs.²¹ A mean of the distribution corresponds to the DoC value, from which the efficacy of the reagents can be found.

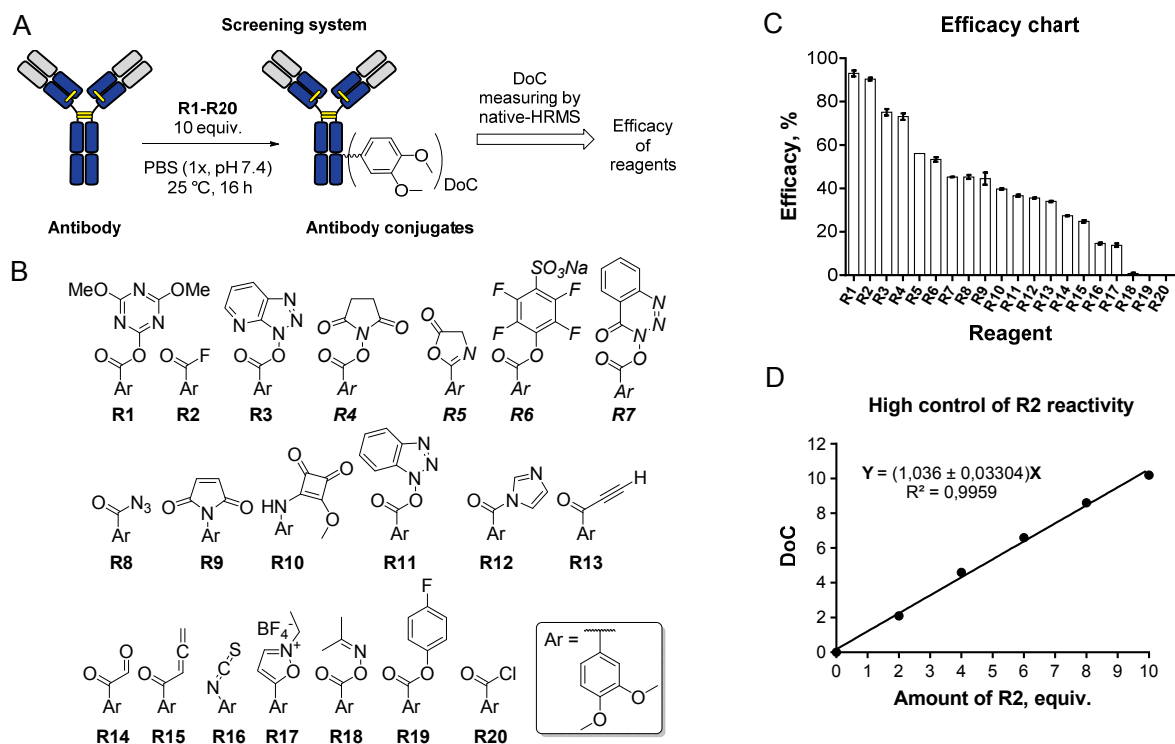


Figure 39. (A) The screening system for evaluation of residue-selective reaction by native-HRMS. (B) Library of the screened reagents **R1-R20**. (C) Efficacy chart based on the measured DoC value of the resulting ACs. Efficacy was calculated as DoC/amount of used reagent (*i.e.* 10 equiv.). DoC measurement was performed in triplicates. (D) DoC vs amount of **R2** displayed controllable and efficient conjugation properties of the acyl fluoride **R2**.

As seen from the efficacy chart, reagents **R1-R20** were classified by decreasing efficacy. These results were reproduced twice with efficacy errors smaller than 10% in most cases. The efficacy chart revealed that reagents **R1** and **R2** were interesting candidates for further investigation. In particular, the acyl fluoride **R2** showed high efficacy and was attractive due to its simplicity. Therefore, we decided to evaluate the influence of the number of equivalents of **R2** employed on the MS profile of the resulting ACs and their corresponding DoC values. This test demonstrated high control of **R2** reactivity, showing linear correlation between the DoC and number of used equivalents of **R2** (Figure 39 D). The slope of the curve revealed quantitative modification of mAb for each equivalent of **R2**. For each amount of **R2** tested, the obtained MS profiles fitted correctly with the binomial distribution model.

Interestingly, despite reported application of alkyne **R13**, allene **R15** and maleimide **R9** for thiol conjugation, these reagents demonstrated the ability to modify other amino acids on mAb's surface under our conditions. In particular, the reactivity of maleimide **R9** function can be comparable with that of activated ester **R7**.

It is notable that phenylglyoxal **R14**, a supposedly arginine-selective reagent, showed higher efficacy than amine-selective isothiocyanate **R16**. Interestingly, MS profile of **R14** reaction showed

also a quite narrow distribution of peaks. This prompted us to investigate the glyoxal chemistry in more details. Particularly, we focused our interest on selectivity and reactivity properties of phenylglyoxal moiety and applied this chemistry to antibody functionalisation using plug-and-play approach. These investigations are described in section 2.3.

It is worth noticing that not all reagents **R1-R20** are stable in aqueous media. In this case, low efficacy can be due to their fast hydrolysis in PBS buffer, competing with their reaction with mAb's residues. This means that, in first approximation, the efficacy value is a function of two parameters: hydrolysis rate and conjugation rate. This fact stimulated us to measure stability parameters for the reagents **R1-R20**.

2.1.3 Hydrolytic stability of the library reagents

To assess the stability of the reagents under the conditions used for the screening, we measured their hydrolysis rate in PBS buffer (1x, pH 7.4) using LC-MS analysis (Figure S4). The pseudo-first order kinetic rate constants were then converted into the stability half-life values, which are shown in Table 2.

Table 2. Stability of screening reagents **R1-R20** in PBS buffer (1x, pH 7.4) and their efficacy in reaction with mAb. The corresponding $t_{1/2}$ values were highlighted in colour for simplicity (green: $t_{1/2}>5$; blue: $1<t_{1/2}<5$; yellow: $0.2<t_{1/2}<1$; red: $0.2<t_{1/2}$; "n.h." – no hydrolysis, "-" – not evaluated).

Reagent:	R1	R2	R3	R4	R5	R6	R7	R8	R9	R10
Hydrolysis in PBS buffer: $t_{1/2}$, h	4.89	0.26	0.93	4.3	0.16	68.3	0.98	30.3	0.36	n.h.
Efficacy of mAb modification, %	93.0	90.4	75.1	73.1	56.1	53.4	45.3	45.3	44.5	39.7
Reagent:	R11	R12	R13	R14	R15	R16	R17	R18	R19	R20
Hydrolysis in PBS buffer: $t_{1/2}$, h	0.35	5.6	n.h.	-	10.4	n.h.	0.01<	n.h.	n.h.	-
Efficacy of mAb modification, %	36.6	35.6	34	27.4	24.8	14.6	13.8	0.8	0	0

Unexpectedly, acyl fluoride **R2** was found to be quite unstable, with $t_{1/2}$ of 0.26 h. Thus, its high efficacy should be due to its high reactivity towards amine groups, which was confirmed by measuring aminolysis rate with BnNH_2 under the same conditions (Figure S6, Table S2, Annex 3).

Low efficacy of isoxazolium salt **R17** was probably due to its fast hydrolysis. In contrast, for the reagents hydrolytically stable, low efficacy of mAb modification could be explained by low reactivity with surface accessible residues of mAb (examples **R13**, **R16**, **R18**, **R19**). Interestingly, classical NHS activated ester had moderate stability with $t_{1/2}$ of 4.3 and good efficacy of 73.1%, but probably slower kinetics of mAb modification compared to acyl fluoride. This motivated us to study the reactivity of acyl fluoride further.

As a result, two reactive groups were selected: acyl fluoride as fast and efficient reagents for Lys-directed conjugation and phenylglyoxal as an Arg-selective reagent for antibody functionalisation. The systematic evaluation of their reactivity profiles enabled us to develop a versatile plug-and-play methodology for the preparation of ACs. This strategy consists in the ligation of an azide group to the biomolecule in the first step (plug), followed by its subsequent

functionalisation using SPAAC chemistry during the second step (play). Our findings are described in the next section.

2.2 Acyl fluoride for plug-and-play bioconjugation

In this section, we introduced a plug-and-play strategy for the preparation of functionally enhanced antibodies with a defined DoC using acyl fluoride chemistry. The first stage (plug) allows the controllable and efficient installation of azide groups on lysine residues of a native antibody using 4-azidobenzoyl fluoride. The second step (play) allows for versatile antibody functionalisation with a single payload or combination of payloads, such as a toxin, a fluorophore, or an oligonucleotide, via copper-free strainpromoted azide–alkyne cycloaddition (SPAAC). It is notable that in comparison to a classical *N*-hydroxysuccinimide ester (NHS) strategy, benzoyl fluorides show faster and more efficient acylation of lysine residues in a PBS buffer. This translates into better control of the DoC and enables the efficient and fast functionalisation of delicate biomolecules at low temperature.

2.2.1 Efficacy assessment of antibody modification with 4-azidobenzoyl fluoride

In order to evaluate the efficacy of the lysine acylation of the antibody with 4-azidobenzoyl fluoride (ABF) we used trastuzumab as our model platform. Trastuzumab (T) was reacted with various amounts of ABF in a PBS buffer (1x, pH 7.4) at 25 °C for 18 h (Figure 40). The resulting trastuzumab-azide conjugates (T-N₃) were purified by gel filtration chromatography and analysed by native-HRMS to find their DoC values.

Plotting the measured DoC vs the number of **ABF** equivalents added per mAb resulted in a linear correlation, from which an efficacy of 72% could be deduced. To our surprise, a corresponding NHS ester of 4-azidobenzoic acid (**ABNHS**) under the same conditions proved to be much less efficient (49% efficacy).

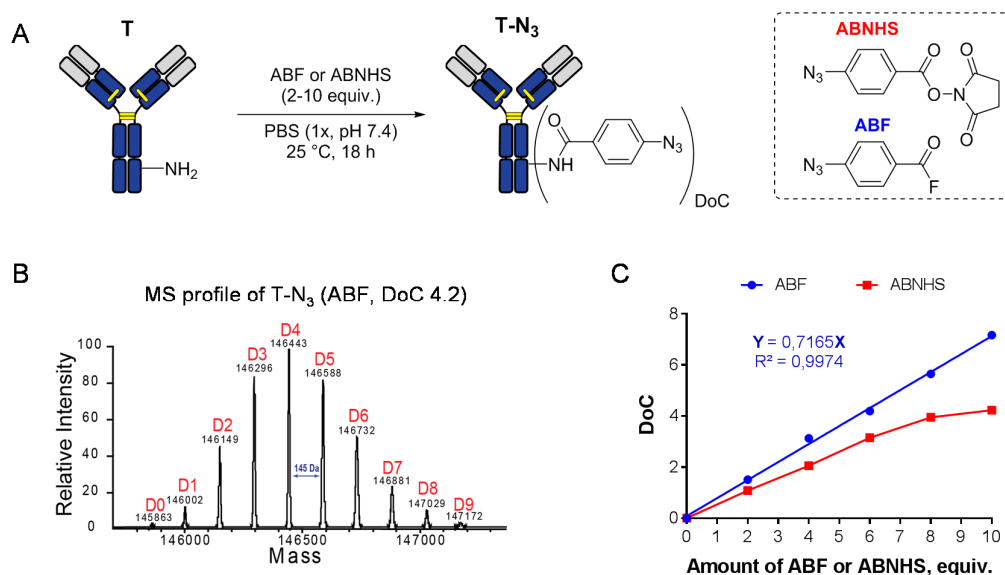


Figure 40. (A) Efficacy evaluation of mAb (**T**) modification with **ABF** and **ABNHS**. (B) Example of a deconvoluted mass spectrum of **T-N₃** conjugate with DoC 4.20; (C) Plot of DoC vs amount of **ABF** (72% efficacy).

It has been known for decades that the acylation reactivity of acyl fluorides is unlike that reported for other acyl halides, and instead can be compared to that of activated esters in aminolysis

reactions.¹⁹³ Most applications of acyl fluoride electrophiles have been reported in organic solvents,¹⁹⁴ where they served as peptide coupling reagents,^{195–197} and peptidomimetics,^{198,199} or in the construction of heterocycles,²⁰⁰ and the synthesis of biologically active molecules.^{201,202} Recently, Sintès *et al.* and Kielland *et al.* have reported water-stable mesoionic acyl fluorides for the fluorescent derivatisation of amine-containing biomolecules under biological conditions.^{203,204}

Consequently, it was decided to measure the stability of **ABF** in a PBS buffer (1x, pH 7.4) used for the conjugation. In contrast to our expectations, based on the report by Sintès *et al.*, **ABF** proved to be quite unstable in PBS buffer with a pseudo-first-order hydrolysis constant $k_1 = 2.46 \cdot 10^{-3} \text{ s}^{-1}$ ($t_{1/2} = 4.7 \text{ min}$). We then hypothesised that the high efficacy of **ABF** for lysine acylation could be explained by a much faster reaction rate with amines. Indeed, the second-order rate constant of the acylation of benzylamine with **ABF** in PBS buffer (1x, pH 7.4) was found to be $k_2 = 87.9 \text{ M}^{-1} \cdot \text{s}^{-1}$ ($t_{1/2} = 1.9 \text{ min}$, Table S2). Notably, we didn't observe any degradation of **ABF** over months, when it was kept in a solid state at $-20 \text{ }^\circ\text{C}$.

For comparison, **ABNHS** showed a pseudo-first-order hydrolysis constant $k_1 = 7.70 \cdot 10^{-5} \text{ s}^{-1}$ ($t_{1/2} = 150 \text{ min}$) under the same conditions and a second-order rate constant for benzylamine acylation of $k_2 = 2.72 \text{ M}^{-1} \cdot \text{s}^{-1}$ ($t_{1/2} = 62 \text{ min}$). In the case of the **ABNHS** hydrolysis, an unusual peak of *N*-(4-azidobenzoyloxy)-succinamic acid was detected by LC-MS (Figure S5, Annex 3). As previously reported by Romieu *et al.* the latter did not react with excess amounts of benzylamine and was slowly converted into its benzoic acid derivative.²⁰⁵

2.2.2 Kinetic study of the modification of an antibody with 4-azidobenzoyl fluoride

It was then decided to evaluate whether the high reactivity of 4-azidobenzoyl fluoride towards amines would translate into more efficient antibody conjugation by measuring the DoC at different reaction times. We therefore carried out a plug-and-play conjugation in parallel with **ABF** and **ABNHS** (Figure 41A).

In the first step, trastuzumab (1 mg/mL at $4 \text{ }^\circ\text{C}$ or $25 \text{ }^\circ\text{C}$) was treated separately with 4 equiv. of each reagents. The aliquots were then withdrawn at regular time intervals (1, 7.5, 15, 30, 60 and 120 min). At each point in time the aliquot was quickly purified by gel filtration chromatography to stop the reaction. The resulting conjugates **T-N₃** were subjected to SPAAC reaction with TAMRA-BCN (1.5 equiv. per an azide group) overnight at $25 \text{ }^\circ\text{C}$, to give trastuzumab-TAMRA conjugates **T-TAMRA** after purification by gel filtration chromatography. For a quantitative comparison of the conjugation efficacy, the antibody-dye conjugates (0.1 mg/mL) were analysed using SDS PAGE (Figure 41B). Coomassie Blue staining showed the same intensity of lines corresponding to the antibody in all sets of the experiment.

As expected, the negative control (lanes T and T+TAMRA-BCN) did not show any fluorescence, whilst the fluorescence signal of the **ABF**-based **T-TAMRA** indicated an almost complete conversion of acyl fluoride after 1 min at both $4 \text{ }^\circ\text{C}$ and $25 \text{ }^\circ\text{C}$. In contrast, the gel fluorescence of the **ABNHS**-based **T-TAMRA** revealed that conjugation did not take place at $4 \text{ }^\circ\text{C}$, while only a moderate efficacy could be obtained after 30 min at $25 \text{ }^\circ\text{C}$. It thus appeared that despite

a fast hydrolysis rate, the higher reactivity of acyl fluoride towards amine nucleophiles resulted in more efficient conjugation. In order to quantify this efficacy more precisely, we performed a native-HRMS analysis of the **T-TAMRA** conjugates. The native-HRMS analysis first confirmed the complete SPAAC modification of trastuzumab-azide conjugates **T-N₃** with TAMRA-BCN (Figure 42 A, as an example of MS profile of **T-TAMRA** prepared using 3 equiv. of **ABF**). The DoC of the **ABF** conjugates was found to be 2.9 (72% efficacy) at both 15 min and 2 h at 25 °C, indicating completion of the reaction after 15 min. In accordance with SDS PAGE analysis, the DoC measured using native-HRMS for **ABNHS** conjugates was only 0.3 (7% efficacy) and 1.8 (45% efficacy) after 15 min and 2 h at 25 °C respectively, thus confirming a much slower reaction (Figure 42B).

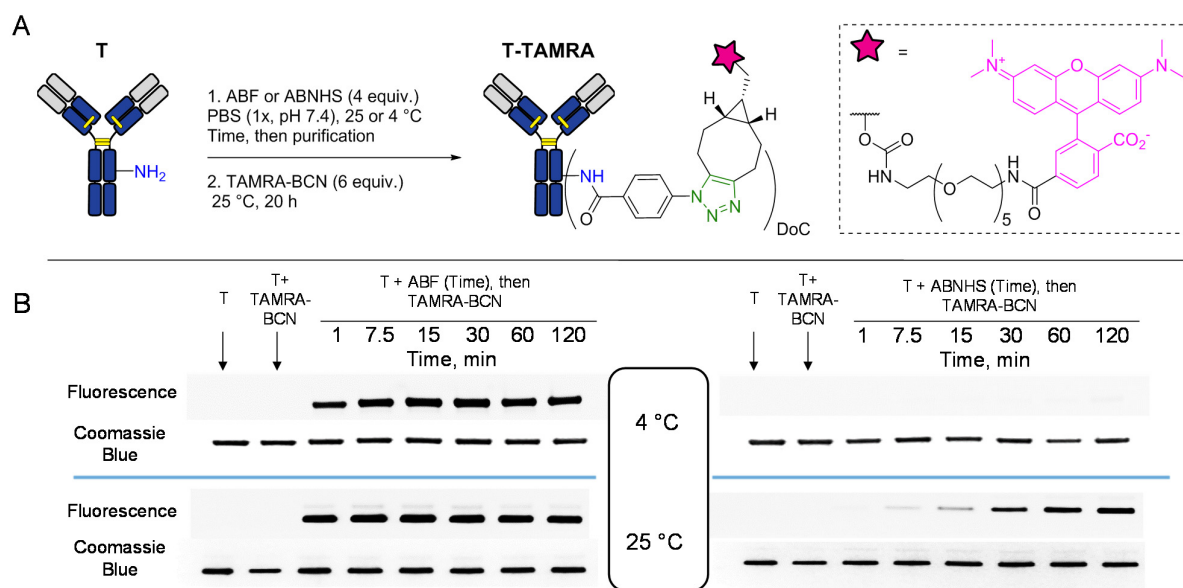


Figure 41. (A) Kinetic study of antibody modification with **ABF** or **ABNHS**. Over time, the aliquots of the reaction mixture were withdrawn, purified, and subjected to SPAAC with TAMRA-BCN. (B) SDS PAGEs analysis of the resulting conjugates: gel fluorescence and Coomassie Blue staining.

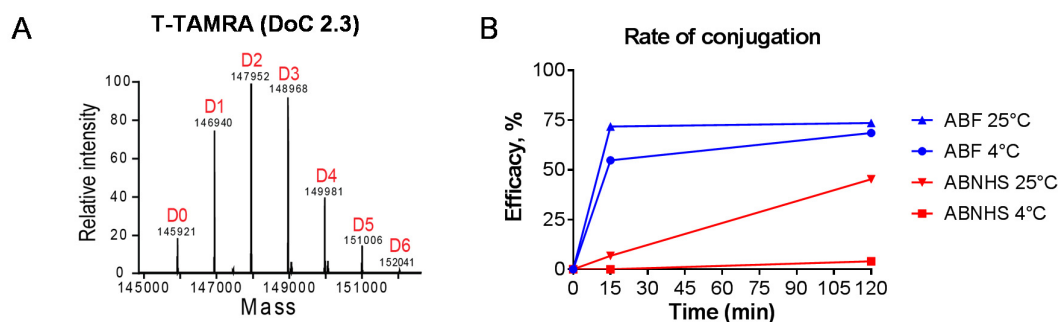


Figure 42. (A) Example of MS profile of **T-TAMRA** conjugate prepared using 3 equiv. of **ABF**. (B) Efficacy of conjugation at different time points measured by native-HRMS analysis of **T-TAMRA** conjugates.

2.2.3 ADC affinity

In order to test whether our chemistry would affect antigen recognition, we measured the affinity of antibody-dye conjugate **T-TAMRA** (DoC 2.9) using flow cytometry on two breast adenocarcinoma cell lines: HER2⁺ SKBR-3 (Figure 43B) and HER2⁻ MDA-MB-231 cell lines (Figure S7, Annex 3). Trastuzumab, the native antibody, was used as a reference in the expected median fluorescence intensity (MFI) and trastuzumab emtansine (T-DM1), a commercialised ADC, was used as a benchmark. As clearly shown by the MFIs, no significant change in antibody binding affinity was observed for **T-TAMRA** compared to our reference (Figure 43C).

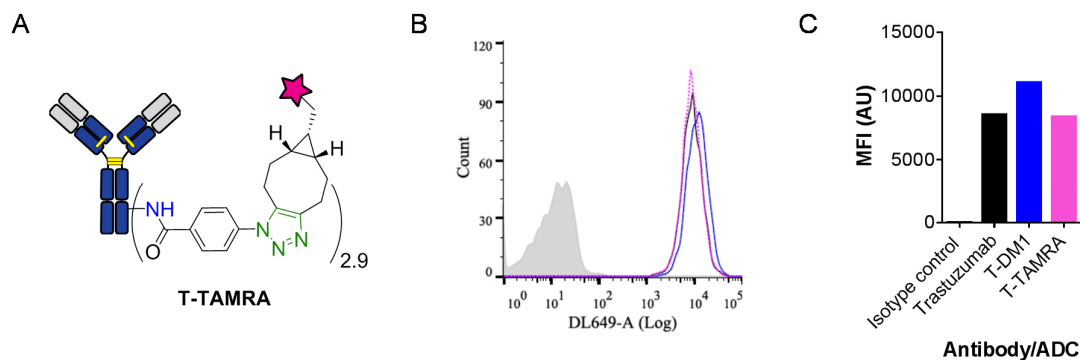


Figure 43. (A) Structure of **T-TAMRA** (DoC 2.9). (B) Estimate of antibody affinities of the prepared **T-TAMRA** (pink, DoC 2.9), the benchmark T-DM1 (blue, DoC 3.6) and the reference native antibody trastuzumab (black). The plot displays the superimposition of the fluorescence profile of each compound. (C) The bar-plot displays the median fluorescence intensity (MFI) of these profiles. Rituximab was used as isotype control (grey). All the antibodies and ADCs were tested at the concentration of 2 $\mu\text{g/mL}$. The fluorescence profile and the MFI of **T-TAMRA** was comparable to that of trastuzumab. These plots are representative of two independent experiments.

2.2.4 Versatility of the plug-and-play strategy

We then turned our attention to the “play” stage of the process and found that the copper-free azide-alkyne click reaction with bicyclononynes (BCN) was both efficient and appropriate for biological conditions.^{31,32} To illustrate the versatility of the plug-and-play strategy, it was decided to utilize different types of payloads bearing BCN groups at this step.

2.2.4.1 Antibody-oligonucleotide conjugates

The construction of AOCs is increasingly used in academia and industry for such application as immune-PCR⁶ and proximity-dependent DNA ligation assays.^{7,206} Therefore, to demonstrate versatility of the plug-and-play strategy, we first focused our attention on the preparation of AOCs. In order to do this, trastuzumab (1 mg/mL) was conjugated with 3 equiv. of **ABF** followed by functionalisation in the presence of 4.5 equiv. of **BCN-ON1** at 25 °C for 20 h to give **T-ON1** (Figure 44 A). This conjugate was further hybridised with complementary oligonucleotide **ON2** to yield **T-ON1-ON2**.

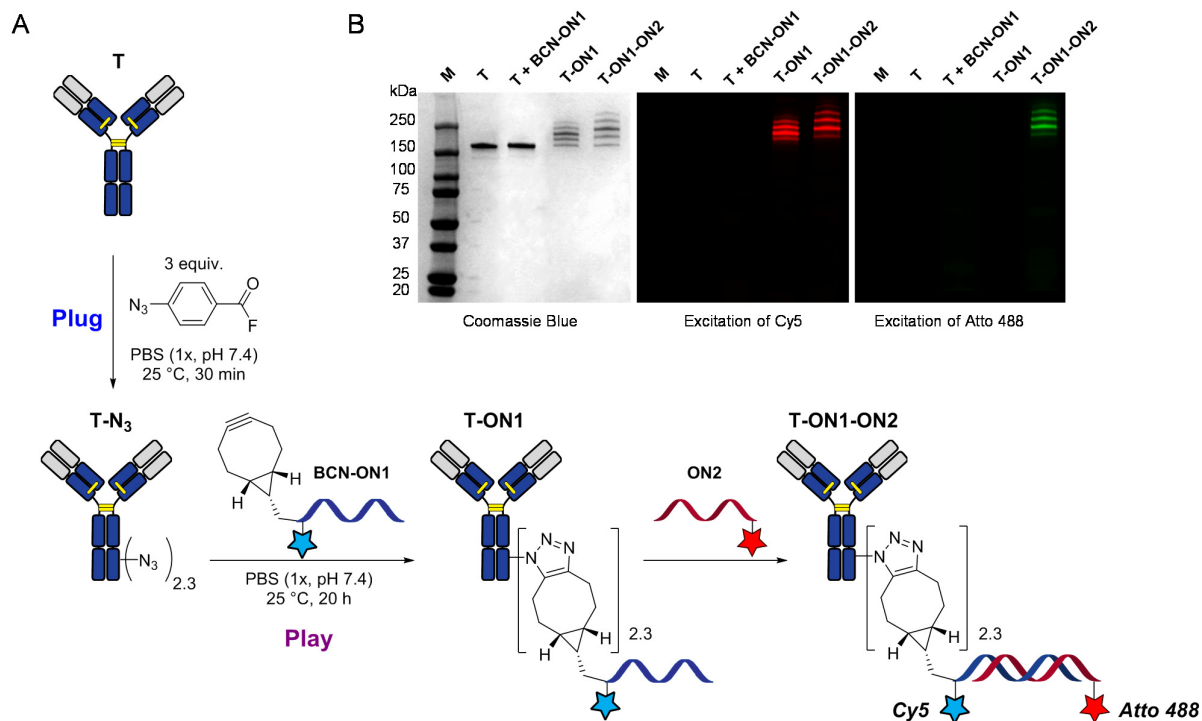


Figure 44. (A) Construction of AOCs **T-ON1** and its hybridisation. (B) Non-reducing SDS PAGEs analysis showed successful antibody-oligonucleotide conjugation and hybridisation (M: molecular weight marker; T+ON1: mixture of trastuzumab with ON1).

To verify the efficacy of the play stage, the conjugates were analysed using SDS PAGE (Figure 44 B). On the Coomassie Blue stained gel, the conjugate **T-ON1** had a number of lines corresponding to the expected species having ON1/mAb loads ranging from 0 to 4. Interestingly, calculations based on the integration of the fluorescence intensity of these lines after Cy5 excitation indicated a DoC value of 2.4, in close correlation with the DoC of the plug stage. This again indicates the high efficacy of the click reaction (the non-fluorescent line corresponding to load 0 accounts for the slightly higher DoC).

The **T-ON1-ON2** had the same number of lines as **T-ON1**, however these were more widely spread, because of the higher mass of the payload. The successful hybridisation could be estimated by the fluorescence of these lines under Atto 488 excitation.

2.2.4.2 Antibody-drug conjugate

To expand the scope of the functionalisation step, the antibody-drug conjugate trastuzumab-MMAE was prepared. For this purpose, the antibody conjugate **T-N₃** (DoC 2.16, using 3 equiv. of **ABF**) was reacted with the BCN-MMAE (Figure 45). After purification, the resulting conjugates **T-MMAE** were subjected to native-HRMS analysis, which confirmed the complete SPAAC modification with preservation of the DoC (DoC 2.10).

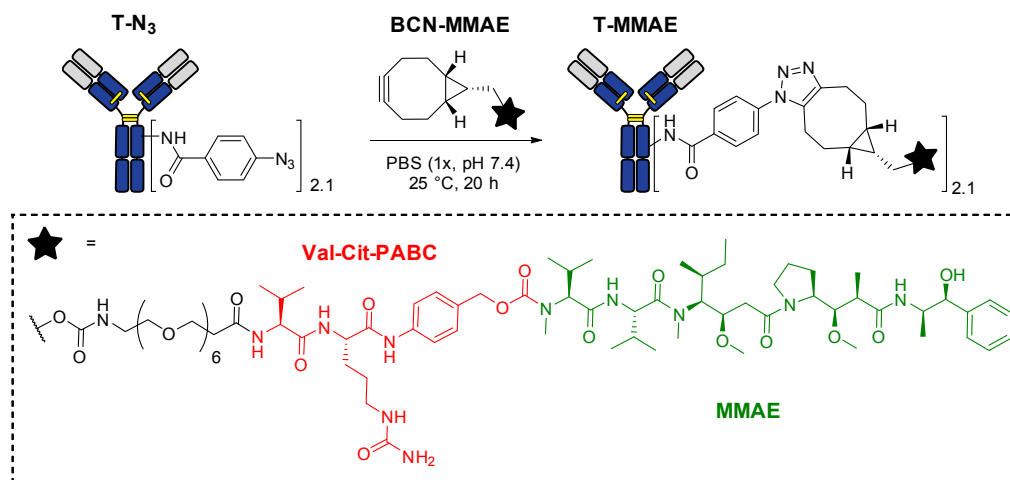


Figure 45. Preparation of ADC, trastuzumab-MMAE, using plug-and-play approach with ABF (3 equiv).

2.2.4.3 Dual antibody functionalisation

Recently, dual modification of biomolecule have gained a great attention of scientific community.³³ Finally, it was decided to demonstrate the controllable dual modification of the antibody by employing various ratios of two payloads in the play step. Our assumption was that two payloads bearing the same strain alkyne would react with similar kinetic rates; thus, their relative amounts in the reaction media would determine their final ratio on the resulting bioconjugate. The trastuzumab-azide conjugate **T-N₃** (DoC 2.3) was therefore reacted with a solution containing a mixture of TAMRA-BCN and Cy5-BCN at different ratios (Figure 46 A).

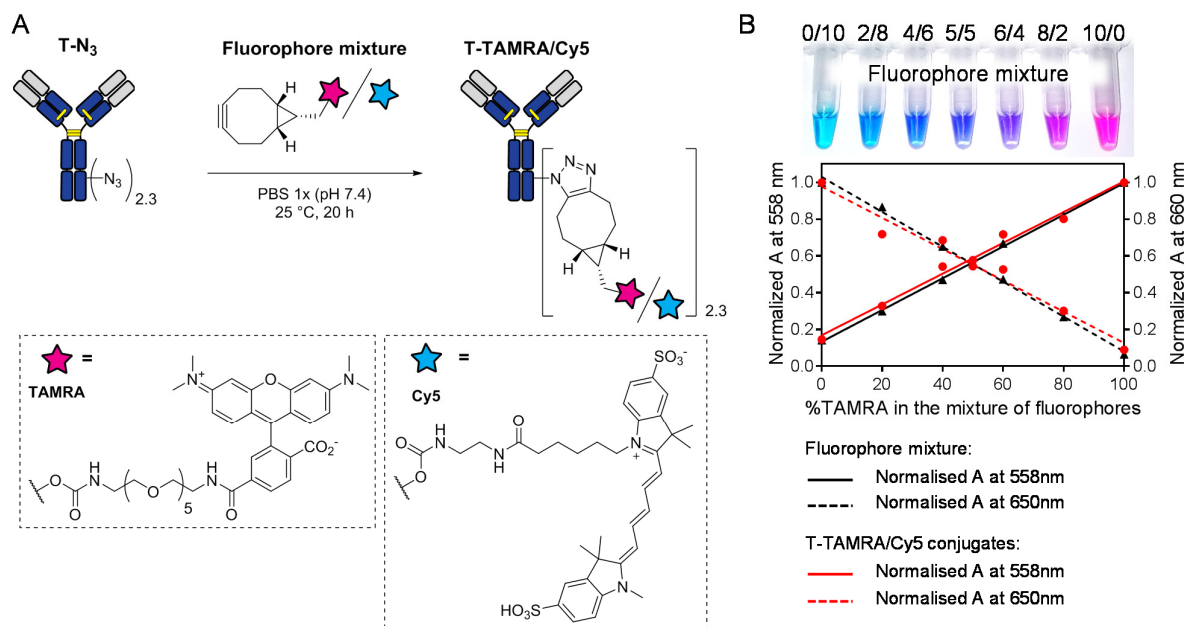


Figure 46. (A) Dual modification of antibody-azide conjugate with a mixture of TAMRA-BCN and Cy5-BCN. (B) Preservation of fluorophore ratio in fluorophore mixtures and in **T-TAMRA/Cy5** conjugates.

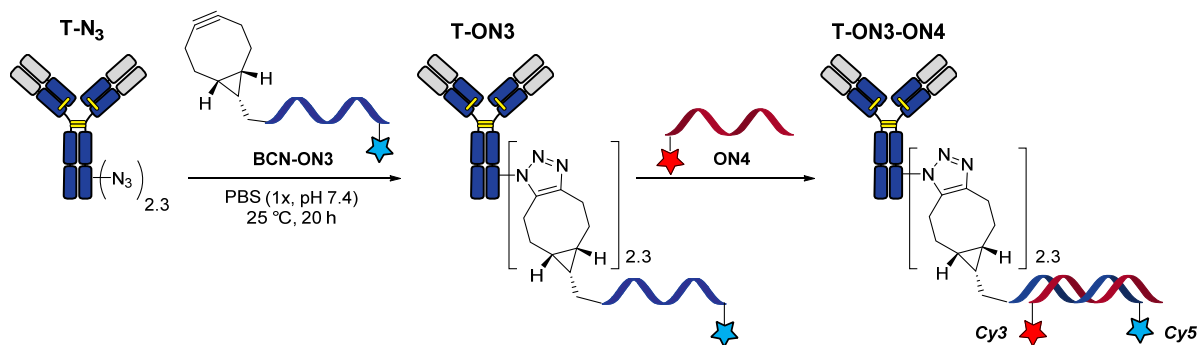
The excess of the reagents was removed by gel filtration chromatography after 20 h, and the absorptions at both 558 nm and 650 nm were measured for each antibody conjugate prepared at different fluorophore ratios (Figure 46 B, red lines). A standard curve was obtained by measuring the absorption of the mixture of two fluorophores in corresponding ratio (Figure 46 B, black lines). The standard lines agreed well with the lines corresponding to the absorption of antibody conjugates, showing that the bioconjugates displayed the same ratio of fluorophores as in the mixture used for the conjugation. This simple procedure opens up interesting prospects for the routine preparation of multi-labelled antibodies.

2.2.5 Stability of antibody-oligonucleotide conjugates in human plasma

Because of the increasing application of antibody-siRNA for gene-silencing *in vivo*,^{8,207} it is important to know the stability of the AOCs in human plasma and how their serum half-life can be extended. Indeed, human plasma contains special enzymes called nucleases that cleave the chains of oligonucleotides into smaller units.^{208,209} These enzymes degrade quickly the therapeutic siRNA causing their fast clearance and, consequently, resulting in their higher dose administration. In order to improve pharmacokinetic profile of siRNA, classical PEGylation strategies can be applied.²¹⁰ However, the influence of mAb conjugation on the stability of ON in serum has not been studied.

To investigate how the conjugation of ON to mAb impacts on the stability of the resulting conjugates in serum, we prepared trastuzumab-ON3 conjugates consisting in an ON with a terminal fluorophore Cy5 (Scheme 2). Once again, we exploited the plug-and-play strategy and the resulting **T-ON3** conjugate was purified using AKTA Pure chromatography system to remove the excess of **ON3** and unlabelled mAb (ON loading of 0). The hybridisation of **T-ON3** using complementary ON resulted in **T-ON3-ON4** conjugate. For **T-ON3** conjugate, the cleavage of ON linker by nucleases should be accompanied by a decrease in fluorescence of the AOCs, which could be quantified by fluorescence analysis in gel. To test their stability, conjugate **T-ON3** was incubated in human plasma at 37 °C. For comparison, the **ON3** and **T-ON3-ON4** were tested in parallel under the same experimental conditions (Figure 47A). Aliquots of each probes were taken every 24 h, diluted with water and frozen at -20 °C. The resulting probes were then analysed by SDS PAGEs to evaluate the change in fluorescence intensity of AOCs bands on the gel over time.

It was found that the fluorescence band of **ON3** gradually disappeared over incubation time in human plasma (Figure 47 C). In addition, a blur appeared under the band of **ON3** corresponding to the smaller fragments of ON. The fragmentation resulted in Cy5 fluorophore migrating with the front. The preservation of the fluorescence intensity from **ON3** band in lane 0 to the front band in lane 7 indicated a stability of the Cy5 fluorophore under those conditions. Therefore, the decrease in fluorescence of the ON band was not caused by degradation of the fluorophore fragment, but by ON cleavage into smaller fragments. Based on the integration of the fluorescence band of **ON3**, it was found that unconjugated **ON3** had a half-life of 0.87 days in human plasma (Figure 47 B).



Scheme 2. Preparation of AOCs containing a terminal Cy5 fluorophore.

Interestingly, the half-life of the ON in human plasma doubled when it was conjugated to the antibody, with **T-ON3** conjugate having a $t_{1/2}$ value of 1.79 days. This could be explained by a steric factor of the antibody, which protects the ON from the nuclease cleavage by shielding it from degrading enzymes.^{210,211} The further increase in ON stability in human plasma was achieved by hybridisation of **T-ON3** conjugate with a complementary **ON4**. Indeed, as seen from the stability curve of the **T-ON3-ON4** conjugate, the double-strained AOCs is three times more stable than the single-strained **T-ON3**. It is notable that in this case a distinct band of **ON3-ON4** was observed on the fluorescence gel (Figure 47 C, third gel). This was confirmed by an electrophoretic mobility value of the band and its fluorescence under Cy3 excitation (Figure S8, Annex 3). Preservation of sharp lines for **T-ON3-ON4** over time was especially well observed under Cy3 excitation of the gel. The specific mass loss of the payload and appearance of the distinct band of **ON3-ON4** should suggest that the nuclease cleavage site is located near the 5' terminus of **ON3**.

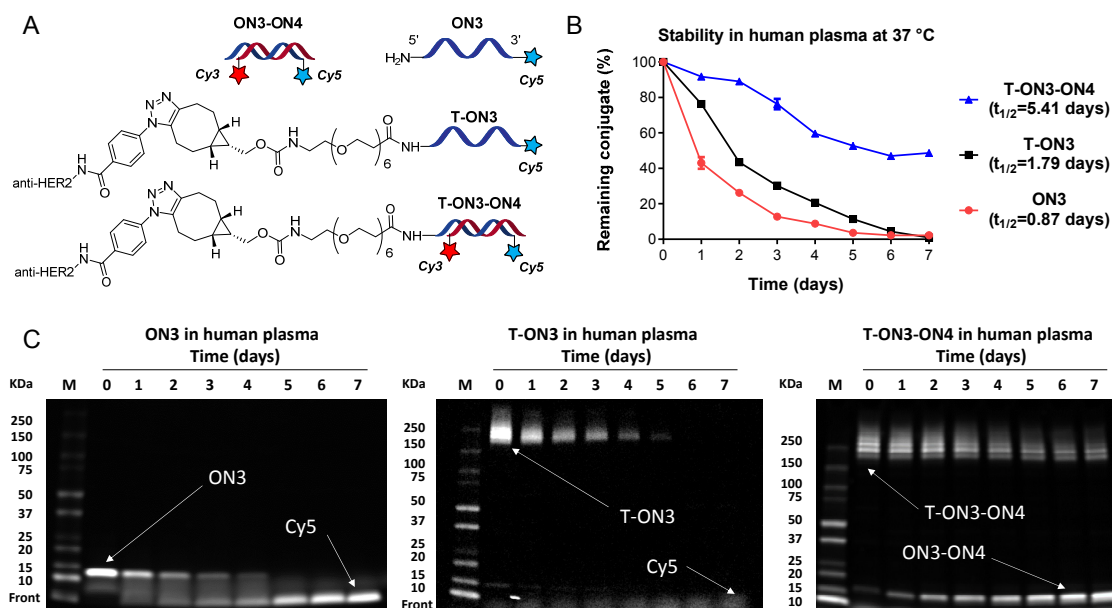


Figure 47. (A) Structures of ON and AOC probes. (B) Stability chart of the probes in human plasma at 37 °C. (C) Fluorescent gel (Cy5 excitation, non-reducing SDS PAGEs).

These results showed that the stability of the double-strained ON linker is close to the Ab-MCC format (38% degradation after 5 days, Figure 38), which enables potentially its application as a linkage in ADCs. Further investigations and improvements of AOCs stability are currently being carried out in our group. Development of novel ADCs comprising a double-strained ON linkage between the antibody and the drug is en route. In this regard, the ON-based ADCs could be interesting for fast screening of new drug candidates and study of the ON impact on ADCs properties.

In summary, we introduced 4-azidobenzoyl fluoride (**ABF**) as an efficient and fast reagent for the lysine modification of native antibodies. The efficient and rapid acylation of the antibody with **ABF** under biological conditions makes acyl fluoride chemistry interesting for bioconjugation chemistry and biological applications. The decoupling of the conjugation and functionalisation steps allows the antibody modification with azide groups in a controllable and reliable manner at the plug stage, using highly reactive acyl fluoride. These pre-functionalised antibodies can then be stored and further derivatised on demand, in a versatile way. For this purpose, the copper-free SPAAC reaction with BCN derivatives appeared to be highly practical and facile because of the good chemical stability/reactivity/bioorthogonality balance of both the azide and BCN functions. This approach was illustrated using a variety of representative payloads such as fluorophores, toxin and oligonucleotide, with good DoC reproducibility. Moreover, this direct strategy for dual conjugation opens up interesting prospects for the routine preparation of multi-labelled antibodies.

2.3 Arginine-selective functionalisation of antibodies

In this section, we introduced 4-azidophenyl glyoxal (APG) as an efficient plug-and-play reagent for selective arginine conjugation of antibodies. The reaction of APG with arginine residues permits ligation of azide groups on native antibodies. The reactivity-efficacy parameters of this step were studied for trastuzumab, as an example of monoclonal IgG1 antibody. These pre-functionalised antibody-azide conjugates have been further functionalised with strained alkynes comprising TAMRA fluorophore or an oligonucleotide. It is notable that the resulting conjugates preserved antibody-antigen recognition ability and affinity and have good stability in human plasma. We envision phenylglyoxal-based reagents for arginine selective modification orthogonally to lysine or/and cysteine conjugation approaches.

2.3.1 Efficacy evaluation of 4-azidophenylglyoxal in reaction with antibody.

To evaluate efficacy of trastuzumab modification with APG, the antibody was reacted with various amount of APG (from 2 to 20 equiv.) in PBS buffer (1x, pH 7.4) for 16 h (Figure 48 A). The resulting T-N₃(R) conjugates (R is denoted the arginine modification) were purified by gel filtration chromatography and were subjected for native-HRMS to measure average DoC.^{181,184} The MS spectra of T-N₃(R) conjugates had a distribution of peaks corresponding to different APG to antibody ratios (Annex 4). The mass difference between the peaks was 157 Da, which suggest a loss of two molecule of water during the reaction (Figure 48 B).^{149,151} Plotting the measured DoC (triplicate) vs amount of used APG reagent resulted in linear correlation from which 27% efficacy was found (Figure 48 C).

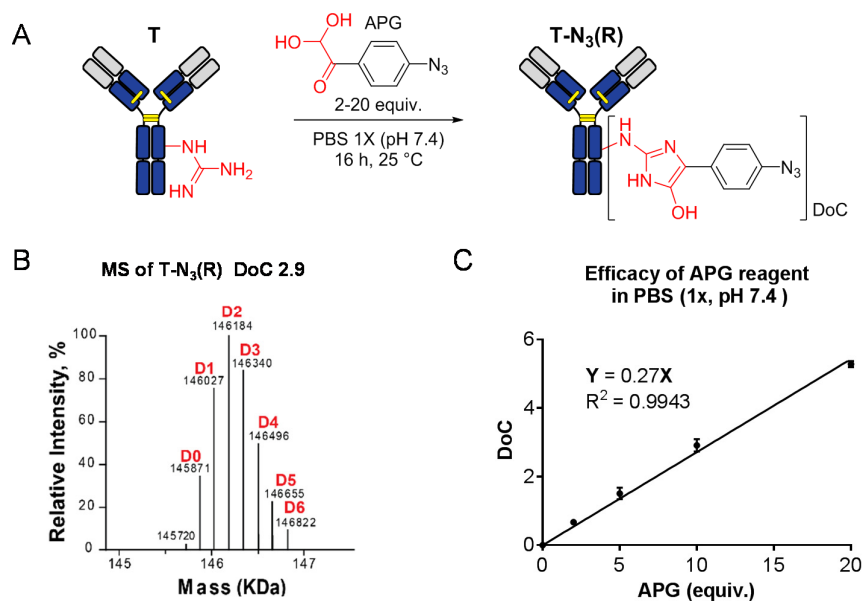


Figure 48. (A) Efficacy evaluation of APG. (B) Example of deconvoluted spectrum of T-N₃(R) conjugate (the peaks correspond to antibody species with different payload to antibody ratio ranging from 0 to 6). (C) Plot of DoC vs amount of added APG, the DoC was measured in triplicate.

It's notable that efficacy can be increased by changing buffer composition and pH,¹⁴⁹ for instant in HEPES/K₂CO₃ buffer (50 mM each, pH 8.7) the efficacy of **APG** was 68%.

2.3.2 Reaction rate evaluation of the antibody modification with **APG**.

To determine the rate of antibody modification with **APG**, we prepared antibody-fluorophore conjugates in different time points of antibody reaction with **APG**. The conjugation between antibody and **APG** (11 equiv.) was performed in PBS buffer (1x, pH 7.4). In certain time points the aliquots were taken and the reaction was stopped by removing excess of **APG** using gel filtration chromatography. The resulted **T-N₃(R)** conjugates were functionalised with TAMRA-BCN to give **T-TAMRA(R)** (Figure 49 A). The concentration of the conjugates was measured by BCA and adjusted to 0.5 mg/mL prior to measure their absorption at 558 nm. Plotting the absorption vs time displayed a plateau after 6 h indicating to reaction termination (Figure 49 B).

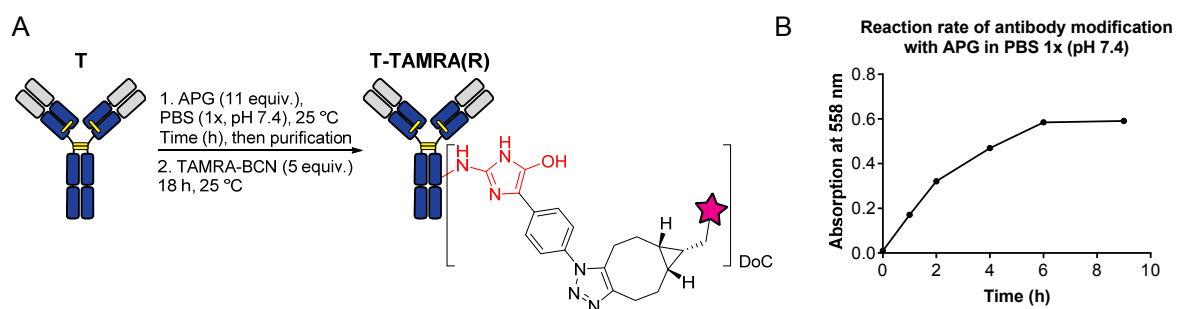


Figure 49. (A) Evaluation of reaction rate by preparation of antibody-fluorophore conjugates **T-TAMRA(R)**. Reaction between antibody and **APG** was stopped in certain time points and **T-N₃(R)** conjugates were functionalised using TAMRA-BCN. (B) Plot of absorption of **T-TAMRA(R)** conjugates at 558 nm vs time of antibody conjugation with **APG**.

2.3.3 Selectivity evaluation of **APG** towards arginine residue.

Trastuzumab – either alone or in the presence of an excess of L-arginine or L-lysine – was first reacted with various amounts of **APG** reagent (5, 8 or 11 equiv.) in PBS buffer (1x, adjusted to pH 7.5), followed by gel filtration chromatography to produce the **T-N₃(R)** conjugates (Figure 50 A). Those were further functionalised with TAMRA-BCN to yield the antibody-fluorophore conjugates **T-TAMRA(R)**, which were analysed using SDS PAGE (Figure 50 B).

Whilst reacting trastuzumab with increasing amounts of **APG** provoked a fluorescence intensification (Figure 50 C, lanes 3 to 5), reacting it with 5 equivalents of **APG** in the presence of an excess of L-arginine led to almost no fluorescence after SPAAC functionalisation (lane 6). Interestingly, we observed a fluorescence restoration when the same experiment was performed with an excess of L-lysine (lane 7). Altogether, this suggests that L-arginine, contrary to L-lysine, acted as an **APG** scavenger during the first stage of antibody modification, thus showing the discriminatory nature of **APG** reagent towards arginine and lysine residues.

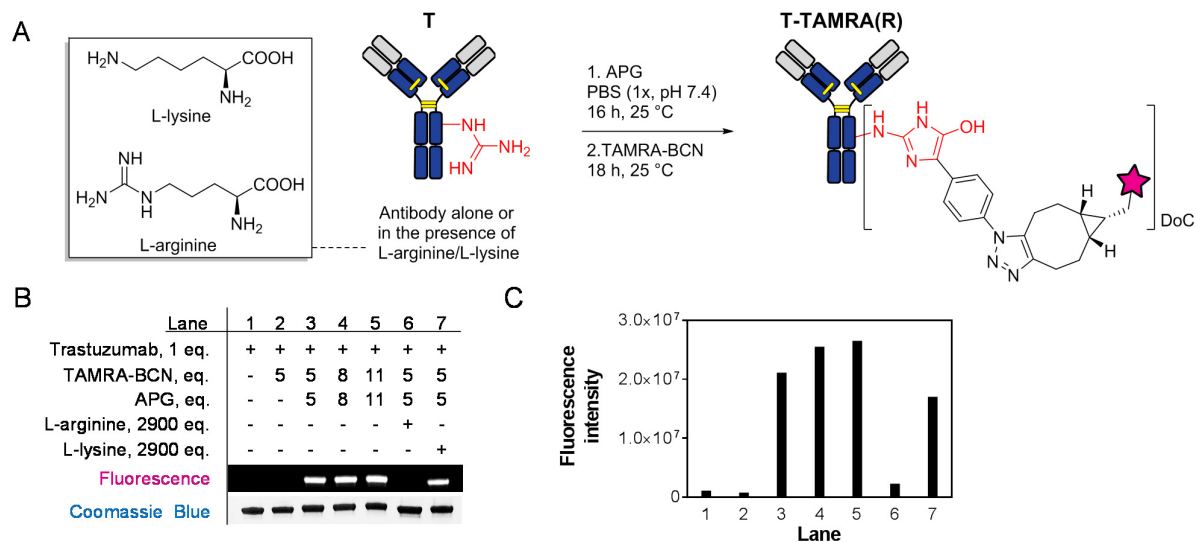


Figure 50. (A) Preparation of **T-TAMRA(R)** conjugates using **APG** reagent with either the simple antibody or a mixture of antibody and excess of L-arginine/L-lysine amino acids. (B) SDS PAGE analysis of antibody conjugates: gel fluorescence and Coomassie Blue staining. (C) Fluorescence intensity of the lanes.

2.3.4 Stability of APG-based antibody conjugates in human plasma.

Native-HRMS of the **T-TAMRA(R)** (based on 8 and 11 eq. of APG) confirmed complete SPAAC reaction giving DoC values of 2.6 and 3.2 respectively (Figure 51). The stability of the **T-TAMRA(R)** was then evaluated in human plasma at 37 °C during 7 days (Figure 51 B).

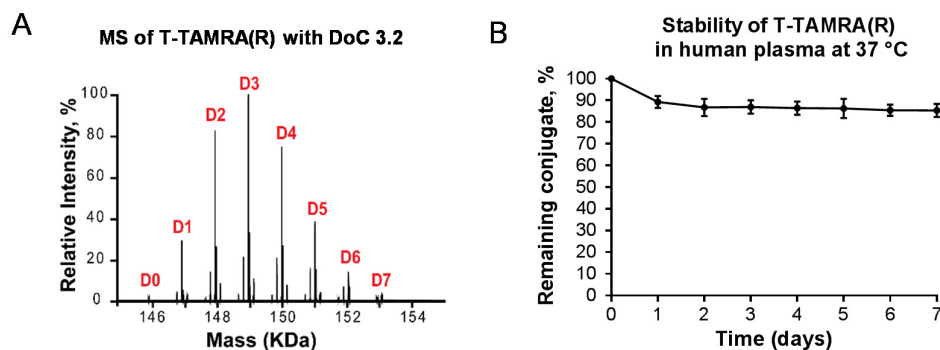


Figure 51. (A) Deconvoluted mass spectrum of **T-TAMRA(R)** (peaks D0-D7 correspond to different TAMRA to antibody ratio). (B) Stability of **T-TAMRA(R)** conjugate in human plasma at 37 °C according to integration of **T-TAMRA(R)** bands on the fluorescent gel.

The aliquots of the **T-TAMRA(R)** conjugates incubated in human plasma were withdrawn every 24 h and then were analysed by SDS PAGE. The fluorescence intensity of antibody bands on gel displayed about 10% of fluorophore transfer to human serum albumin (HSA) after 1 day of incubation before reaching a plateau. In comparison, trastuzumab-MCC-TAMRA conjugates prepared through maleimide-thiol coupling displayed 38% of fluorophore transfer to HSA after 5 days under the same conditions (Figure 38).

2.3.5 Affinity of the APG-based antibody conjugates.

In order to test whether modifications of arginine residue of antibody would affect antigen recognition, many of these amino acids being in close vicinity to and/or within the paratope (Figure 52A), we measured the affinity of **T-TAMRA (R)** and **T-N₃ (R)**, with DoC 3.5 and 3.6 respectively, using flow cytometry on two breast adenocarcinoma cell lines: HER2⁺ SKBR-3 (Figure 52B) and HER2⁻ MDA-MB-231 cell lines (Figure S9). Trastuzumab was used as a reference in the expected median fluorescence intensity (MFI) and T-DM1 was used as a benchmark. As clearly shown by the MFIs, no significant change in antibody binding affinity was observed for either Arg-linked ACs compared to our reference.

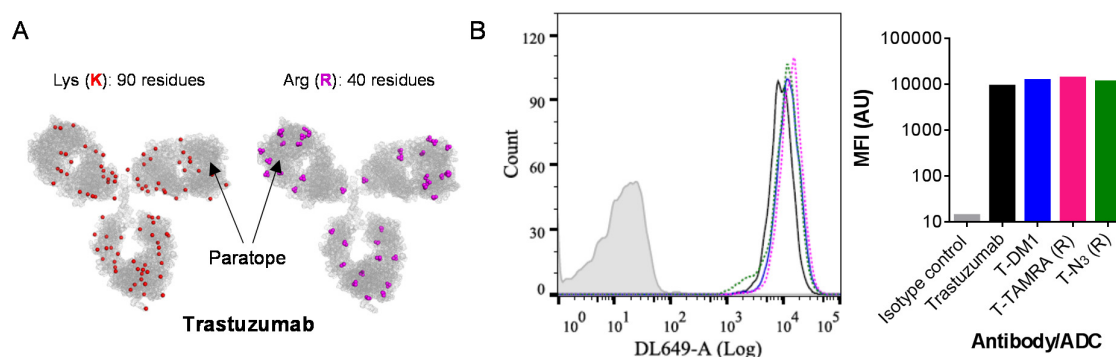


Figure 52. (A) Position of Lys and Arg residues in trastuzumab model (Nitrogen are represented by red and pink spheres respectively) displaying the high abundance of arginine residues near paratope of the antibody. (B) Estimate of antibody affinities of the **T-TAMRA(R)** (pink, DoC 3.5) and **T-N₃(R)** (green, DoC 3.6), the reference **T-DM1** (blue, DoC 3.6), the trastuzumab (black) and rituximab (isotype control, grey). The plot on the left displays the superimposition of the fluorescence profile of each compound. The bar-plot on the right displays the median fluorescence intensity (MFI) of these profiles. These plots are representative of two independent experiments.

2.3.6 Preparation of APG-based antibody-oligonucleotide conjugates.

To demonstrate the applicability of the plug-and-play approach with **APG** for this purpose, we decided to prepare AOC using arginine residues of antibody as conjugation sites. To this end, **T-N₃(R)** conjugates with varying DoC (from 0.7 to 2.9) were treated with **BCN-ON5** for 18 h (Figure 53). After purification by gel filtration chromatography the AOCs **T-ON5** were hybridised with complementary oligonucleotide **ON6** and the resulting conjugates were analysed by SDS PAGE. Gel stained with Coomassie Blue showed successful functionalisation and hybridisation of the **T-N₃(R)** and **T-ON5** conjugates, respectively. According to mobility of the lines on the gel, the increasing of DoC of **T-N₃(R)** led to **T-ON5** with higher average oligonucleotide per antibody loading.

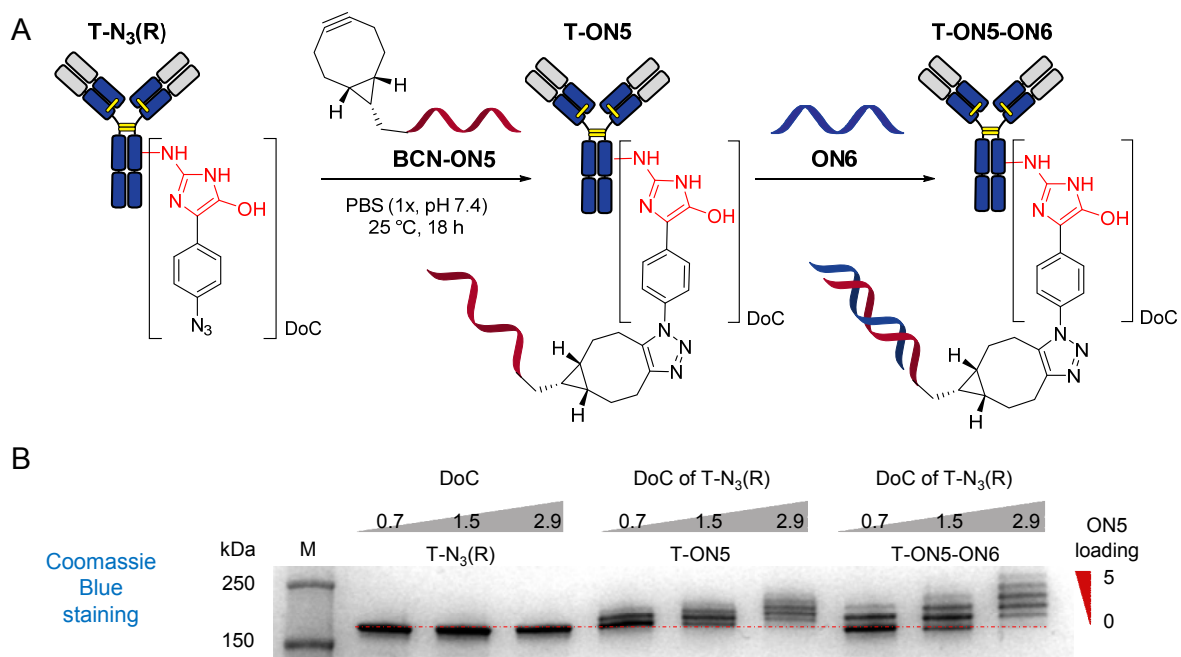


Figure 53. (A) Preparation of AOCs **T-ON5** and their subsequent hybridisation to afford **T-ON5-ON6**. **T-N₃(R)** conjugates with DoC of 0.7, 1.5 and 2.9 were used for functionalisation with **BCN-ON5**. (B) SDS PAGE displayed successful functionalisation with DoC increasing giving higher oligo loading per antibody (M: molecular weight marker).

In summary, we demonstrated that **APG** is a reliable plug-and-play reagent for the selective modification of arginine residues of antibodies. The resulting antibody-azide conjugates can be further functionalised in demand with strained alkynes bearing various payloads. These arginine-based conjugates maintain antibody affinity towards antigens and showed high stability in human plasma. In perspective, phenylglyoxal-based reagents can be used for Arg-selective modification of proteins orthogonally to lysine or/and cysteine conjugation approaches.

Part 3. Mono-functionalised ACs

This part is devoted to a technology enabling mono-modification of mAb through Lys residues. The technology was used for the preparation of ACs with a single payload per antibody. To demonstrate the versatility of this technique, various payloads were installed: small molecules (BCN-OH), fluorophores (TAMRA and Cy5), oligonucleotide derivatives, and BCN functions for further post-modification with azide-containing molecules. The obtained ACs were characterised by native-HRMS and showed a single peak in the MS spectra corresponding to species with a 1/1 payload/antibody ratio. The mAb-oligonucleotide conjugate was successfully hybridised with complementary ON, according to native-HRMS. The mAb-BCN was post-labelled with TAMRA, using TAMRA-N₃ derivative, which was confirmed by fluorescent gel analysis and native-HRMS.

3.1 Introduction

Despite a great advance in site-specific methods of bioconjugation, there is still no general strategy for functionalisation of biomolecules with defined number of payload per biomolecule. Concerning ADCs, there are mainly four chemical approaches: Lys-conjugation, Cys-conjugation, rebridging of disulfide bonds, and conjugation using engineered Cys-handles (Figure 54).

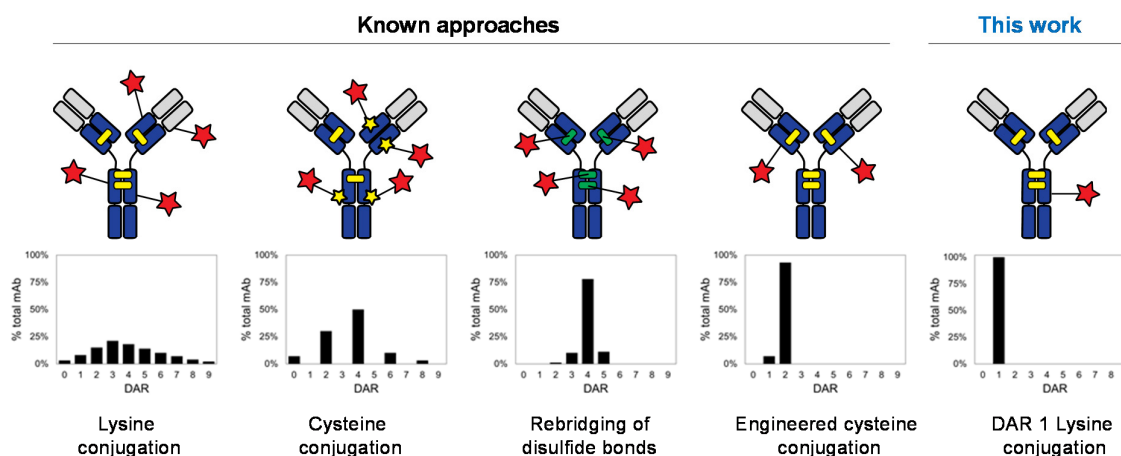


Figure 54. Classical approaches for antibody functionalisation and MS profiles of their ADCs. This work represents controllable monofunctionalisation (DAR 1) using Lys residues of mAb.

The first two methods are often used for ADCs production²¹² as demonstrated by the two FDA-approved ADCs currently on the market: Kadcyla® and Adcetris®. Nevertheless, these two methods afford heterogeneous ADCs with wide distribution in payload-to-antibody ratios ranging from 0 to 8. In contrast, engineered cysteine conjugation gives near-homogeneous ADCs with drug-to-antibody ratio (DAR) of 2. This method is highly applicable nowadays, but requires antibody engineering, which is expensive and time-consuming. Moreover, this technique is not universal and needs optimisation for each biomolecule. Among all the methods, rebridging of disulfide bonds might be the best chemical way to modify native antibodies in controllable fashion. It gives near-homogeneous DAR distribution and, depending on the chemistry employed, gives access to antibodies bearing 2, 4

or 8 drug molecules.^{99,100,106} It is worth mentioning that the rebridging strategy cannot be considered as a general method for bioconjugation because of its limitation to biomolecules containing solvent accessible disulfides only. As can be noticed, the approaches enabling narrow distribution MS profiles (*i.e.* rebridging, engineered Cys) can result only in even numbers of loaded molecules (2, 4 and 8). It is due to the symmetrical nature of mAb, and the duplication of each amino acid residue in the structure, making the bioconjugation of an odd number of payload per antibody (*i.e.* mono- or trifunctionalisation) a challenging task.

The scientific interest and the challenge of ACs construction with narrow distribution MS profile impelled us to find a way for efficient mono-payloading of antibodies. Mono-functionalisation of mAbs could be of great interest for a number of applications. For instance, it could enable preparation of mono-loaded AOCs, which are desired for precise immune-PCR.^{6,7} Monolabelled antibody-fluorophore conjugates are also valuable, when quantification is needed, because they should not suffer from FRET effect. By analogy with the study of protein-DNA complex using atomic-force microscopy, another useful application of monoloaded AOCs could be the study of mAb's aggregation.²¹³

Among myriad of bioconjugation techniques there are no methods for efficient mono-modification of antibodies. Although, some advance was made in this direction using the metal-binding region of the native antibodies and template-directed covalent conjugation,⁵¹ this method suffered mainly from low efficacy and difficulty in scalability.

Another interesting approach on this subject was reported by Weil group in 2012.²¹⁴ They succeeded in site-selective lysine modification of native proteins and peptides using kinetically controlled conjugation. A single lysine residue on the proteins was reacted with an activated biotinylation reagent added in low amount (0.5 equiv.) in 100 equal portions (Figure 55). Such kinetically controlled modification allowed for site-selective conjugation of hot-spot lysine residue and resulted in a mixture of mono-labelled (21%) and unlabelled biomolecule (79%) with no sign of bis-labelled product in MS spectra. After affinity purification, the obtained monobiotinylated proteins were functionalised by click chemistry, using an ethynyl functional group present in the biotinylation reagent. This methodology was used successfully for the modification of two model proteins, namely RNase A and lysozyme C.

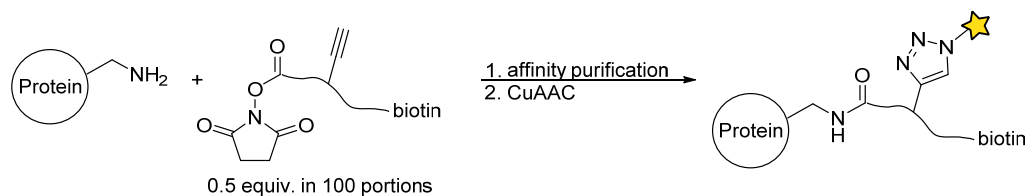


Figure 55. The site-selective lysine bioconjugation. Proteins (RNase A, lysozyme C) are biotinylated in low conversion and then the mono-labelled form is purified by affinity chromatography and functionalised with a payload using click chemistry.

One of the evident drawbacks of this biotinylation reagent is the linker structure, which is unable to release the biotin tag after purification. Indeed, the presence of biotin in the final bioconjugates could represent an issue due to its numerous biological functions. An ideal solution would be to substitute directly the biotin group by a payload of choice, an approach referred to as trans-tagging hereafter.

Thus, for mono-functionalisation of antibodies, we decided to adopt the low-conversion method for the modification of the biomolecule in combination with a trans-tagging reaction.

3.2 Trans-tagging of proteins

In this work we introduced a novel concept, a trans-tagging reaction, which is a bioorthogonal substitution reaction enabling a replacement of one payload by another. Of the many requirements for effective trans-tagging reactions include bioorthogonality, fast kinetics of the reaction, and the generation of stable products under biological conditions. Figure 56 illustrates the identified potential trans-tagging reactions appropriate for protein modification.

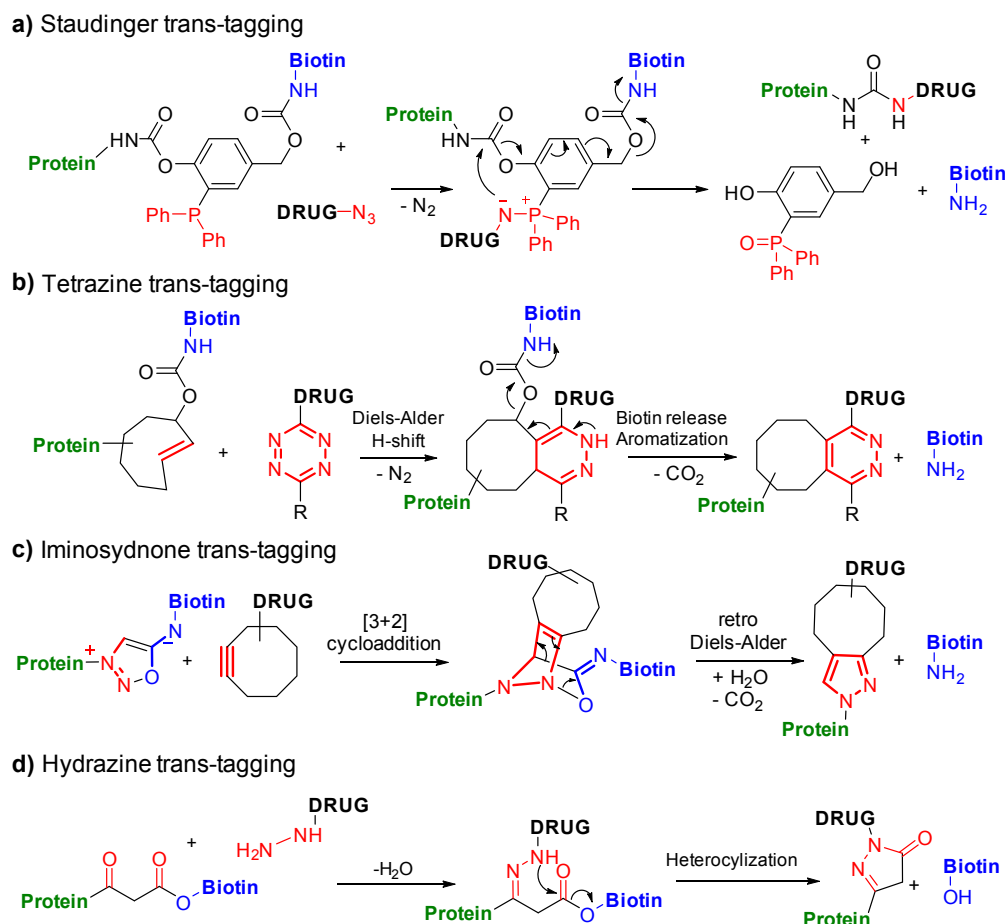


Figure 56. Representation of the potential strategies for trans-tagging of proteins.

The first reaction is based on traceless Staudinger ligation and use a drug-azide derivative as a trans-tagging partner (Figure 56a). This reaction might be hampered by slow kinetic and oxidation of

triphenylphosphines. Nevertheless, until recently, modified Staudinger reactions were the only available bioorthogonal release reactions.

In contrast, the tetrazine/*trans*-cyclooctene reaction is very fast and has been previously applied to the *in vitro*^{215,216} and *in vivo* drug release.²¹⁷

Recently, Taran group from Paris has developed a novel iminosydnone/strained alkyne chemistry for click-and-release applications (unpublished results). Remarkably, iminosydnone (iSyd) are stable under physiological conditions and have a good reaction rate, comparable to that of azides, when reacting with BCN group. In this regard, in collaboration with Taran group, we decided to utilize iminosydnone as *trans*-tagging partner for the preparation of mono-functionalised ACs. To this end, we synthesised a NHS-iSyd-biotin trifunctional reagent containing a NHS activated ester for lysine conjugation, iSyd moiety for *trans*-tagging and a biotin tag for purification.

3.3 Antibody conjugates with single payload

We envisioned the mono-functionalisation of antibodies using a three-step protocol (Figure 57). Trastuzumab was used as the model protein. In the first step, the trastuzumab was reacted with NHS-iSyd-biotin reagent such as to obtain Ab-iSyd-biotin conjugates with the DoC of 0.1. Theoretically, by applying Poisson distribution model to trastuzumab,²⁰ a DoC of 0.1 signifies there are 90.5% of unconjugated antibody, 9% of mono-labelled ACs and less than 0.5% of bis- and higher labelled ACs. This prediction was partially confirmed by MS analysis of the resulting ACs, even though only mono- and unconjugated products were detected in the spectra (data not shown). In the second step, the reaction mixture, composed of the mAb and the monobiotinylated AC, was loaded on streptavidin affinity column to capture the AC and the eluted mAb was recycled and submitted again to the first step. Finally, in the third step, the AC captured in the column was *trans*-tagged using BCN derivatives containing the desired payload to afford mono-functionalised ACs. All those steps can be performed either manually, using syringe, or automatically using AKTA Pure chromatography, which enables control of the process by UV measuring of protein concentration.

To demonstrate the versatility of this technique, the streptavidin column (1 mL), pre-loaded with trastuzumab-iSyd-biotin (1.5 mg), was equilibrated with the solution of a BCN derivate (0.1 eq.) bearing either a small substituent (R = OH) or fluorophore moieties (R = Cy5 or TAMRA) as illustrated on Figure 58. The column was left overnight for the reaction to proceed, before being washed with PBS 1x to afford the corresponding ACs with good yields. The obtained ACs were concentrated, purified using gel filtration chromatography and subjected to MS analysis. In each case, the MS spectra displayed one peak with MW value corresponding to mono-functionalised ACs.

Only a tiny peak of mAb was observed in some cases (Figure 58) which can be explained by some remaining mAb left in the affinity column, because of an insufficient number of washing steps and/or low-scale loading of the column. This was confirmed by the acquisition of cleaner spectra when an excess of BCN derivatives was employed. Application of the excess amount of BCN derivatives provides also a quantitative release-functionalisation of ACs demonstrating high efficacy of the *trans*-tagging strategy.

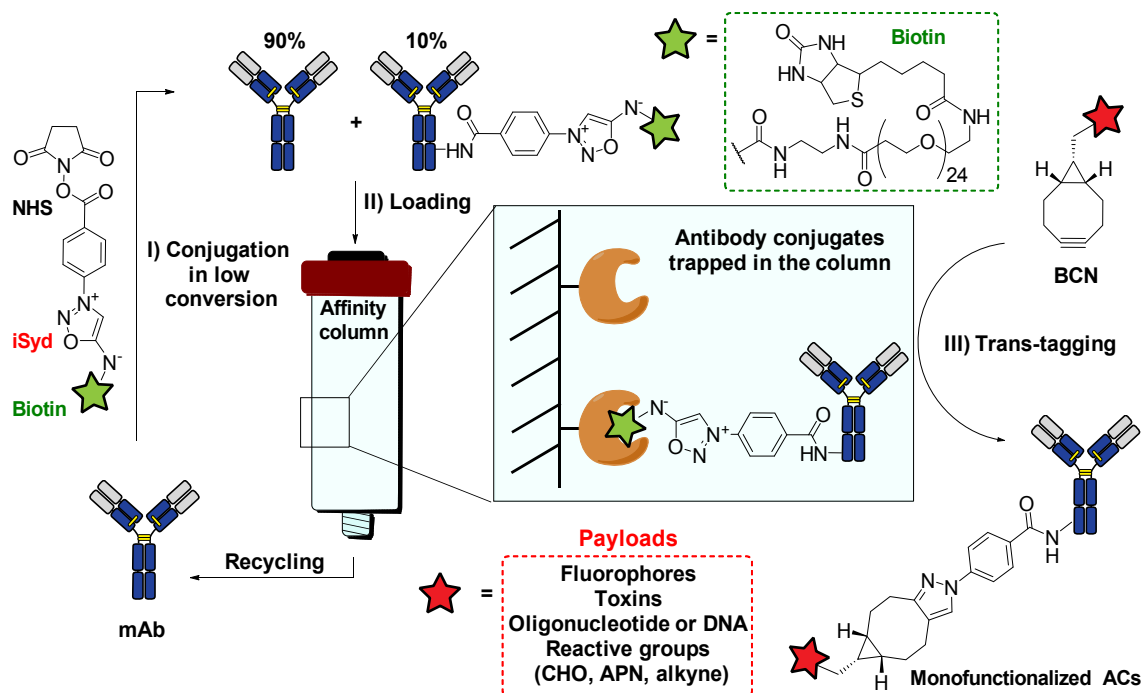


Figure 57. Preparation of monofunctionalised ACs. Step I: the conjugation of the mAb at low conversion with a reagent bearing three functional modules: a reactive group (NHS), a trans-tagging group (iminosydnone, iSyd) and an affinity group (Biotin). Step II: the reaction mixture, composed of the mAb and the monobiotinylated AC, is passed through an affinity column to capture the AC and the eluted mAb is recycled (re-subjected to Step I). Step III: the AC in the column is trans-tagged using strained alkyne derivatives containing payload to give monofunctionalised ACs.

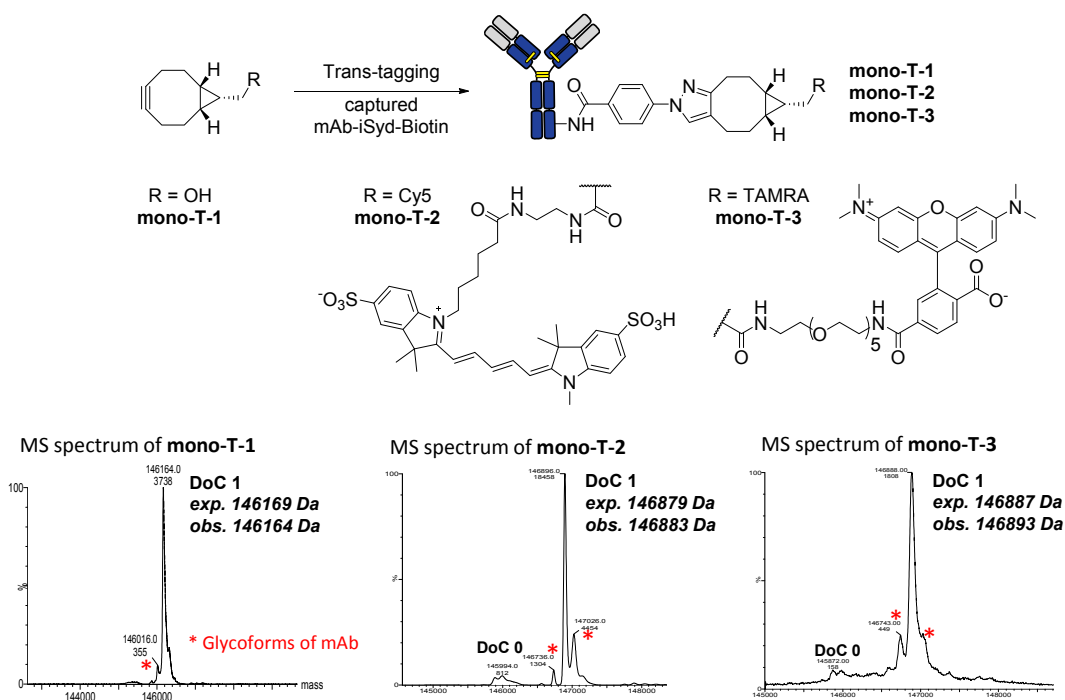


Figure 58. Trans-tagging of the captured trastuzumab-iSyd-Biotin with BCN (product **mono-T-1**), BCN-Cy5 (product **mono-T-2**) and BCN-TAMRA (product **mono-T-3**). The MS spectra of the obtained ACs revealed a single peak corresponding to mono-loaded species.

We also tested the trans-tagging with other strained alkynes and used simple DBCO derivatives for exemplification. As previously observed, the reaction resulted in mono-functionalised ACs only, which was confirmed by MS analysis (Figure S10, Annex 5).

Encouraged by these results, we then decided to examine the feasibility of this technique with more complex derivatives: either with a BCN bearing a 21-base oligonucleotide payload ($R_1 = \text{ON5}$) or with a bis-BCN group ($R_1 = \text{sBCN}$). We anticipated that in the second case the envisioned mAb-sBCN product will react much slowly with mAb-iSyd-biotin compared to BCN-sBCN, mainly due to steric hindrance and slower rotation of big macromolecule, which should allow a selective trans-tagging reaction. In both cases the trans-tagging afforded mono-functionalised ACs according to MS (Figure 59). Moreover, no mAb-sBCN-mAb adduct was observed in Coomassie Blue stained gel after SDS PAGE analysis of **mono-T-6** (Figure S11, Annex 5). The obtained ACs were then used for post-modifications such as: 1) hybridisation in the case of AOCs and 2) SPAAC chemistry with TAMRA- N_3 in the case of ACs bearing free secondary BCN function. Again, successful post-modifications were confirmed by SDS PAGEs and MS analysis.

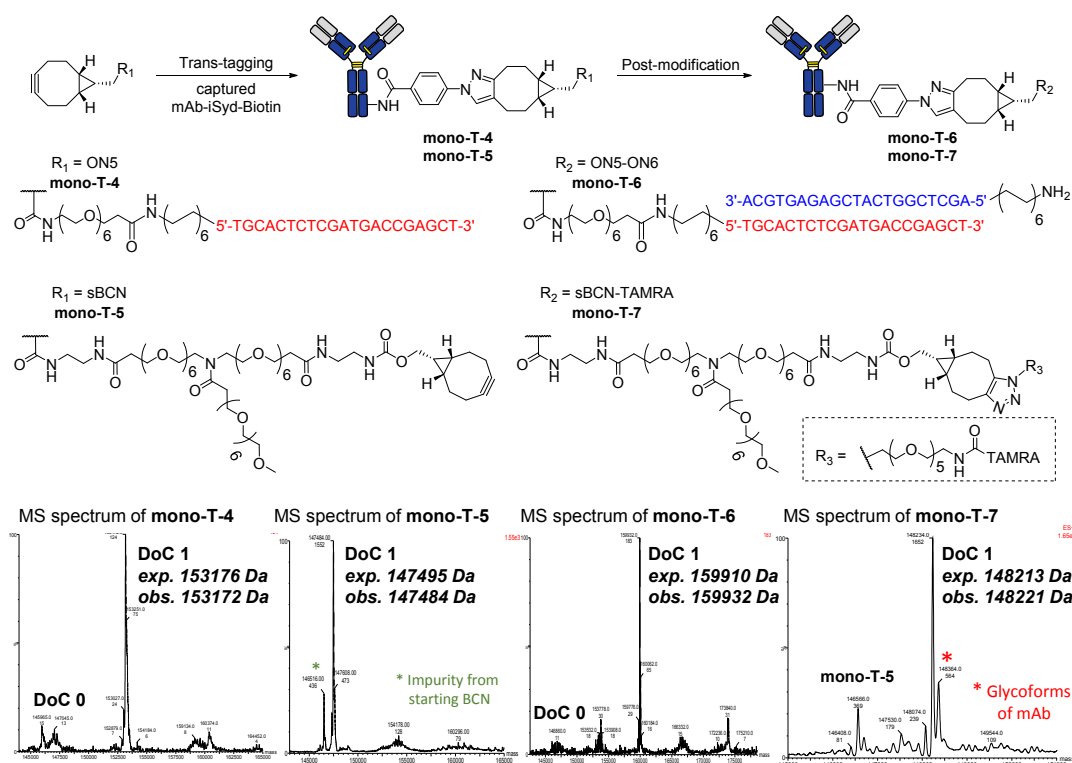


Figure 59. Trans-tagging of the captured trastuzumab-iSyd-Biotin using BCN-ON5 (**mono-T-4**), BCN-sBCN (**mono-T-5**) and the corresponding post-modification of these products with complementary ON (**mono-T-6**) and TAMRA- N_3 (**mono-T-7**), respectively. The MS spectra confirmed the above transformations showing the major peaks of mono-payloaded ACs.

3.4 Stability of antibody-iSyd-Biotin conjugates on the column

To test the stability of the mAb-iSyd-Biotin conjugates on the affinity column, HiTrap Streptavidin HP columns loaded with antibody-iSyd-Biotin conjugates (1.5 mg) were stored in the

dark at 4 °C and subjected to the trans-tagging reaction with BCN-TAMRA after one day, two weeks and one month (Figure 60A). The resulting **T-TAMRA(1)** conjugates were analysed by SDS PAGE. Gel stained with Coomassie Blue showed no sign of degradation of the immobilised mAb-iSyd-biotin conjugates over time (Figure 60B).

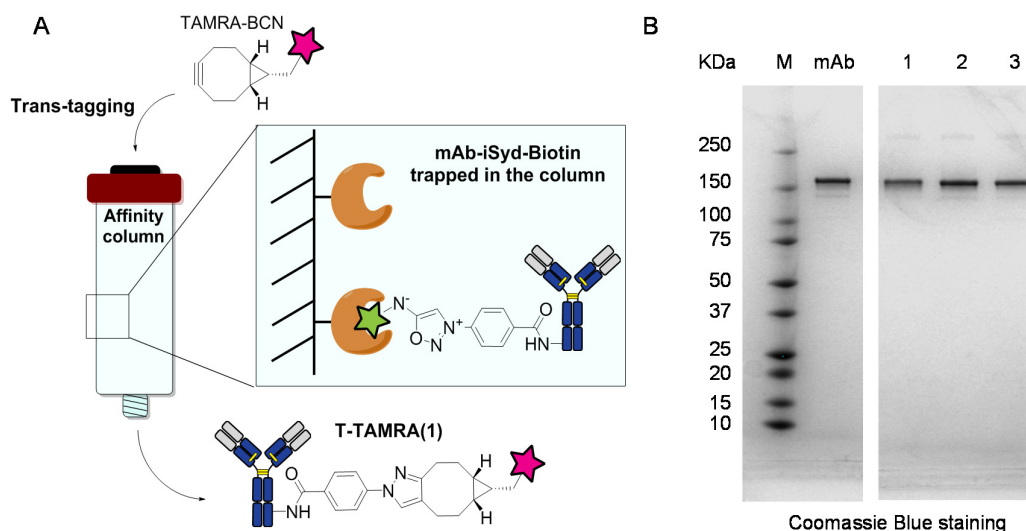


Figure 60. (A) Stability of mAb-iSyd-Biotin on the streptavidin column monitored by trans-tagging reaction with TAMRA-BCN after 1, 14 and 28 days of AC loading on the column. The column was kept in the dark at 4 °C. (B) SDS PAGE analysis of resulting antibody conjugates displayed no sign of degradation of antibody over one month (M: molecular weight marker; mAb: trastuzumab; 1-3: **T-TAMRA(1)** conjugates prepared using trans-tagging reaction after 1, 14 and 28 days, respectively).

3.5 Conclusions and perspectives

In summary, we developed a novel technology for the mono-functionalisation of native antibodies using lysine residues as conjugation sites. The versatility of this approach was demonstrated by the efficient preparation of a series of mono-labelled monodisperse ACs with various payloads ranging from small molecules (BCN, DBCO) to big entities (fluorophores or oligonucleotide). The intermediate trastuzumab-iSyd-biotin was shown to be stable over a month in a streptavidine column. Taking into account the stability and efficacy of this approach, we expect successful applications of this technology (called currently DARX) to the mono-functionalisation of other biomolecules.

The next development would be the preparation of mono-drug ADCs and the comparison of their biological properties (such pharmacokinetic, toxicity and efficacy *in vivo*) with site-specific ADCs. Moreover, the DARX technology is suitable for the preparation of well-defined ADCs bearing two drugs with different modes of action (Figure 61), which may potentially enable the treatment of some resistant cancer forms.^{218,219}

Another interesting application would be the controllable preparation of protein-protein or antibody-nanoparticle conjugates having equimolar ratio between the entities, which can be useful for biomedical applications.²²⁰ We also envision the use of DARX technology for the construction

of bispecific antibodies using two different mAb, each mono-functionalised with an ON or a reactive function. We believe that the current technology will find an application in a variety of domains where controllable and defined bioconjugation is needed.

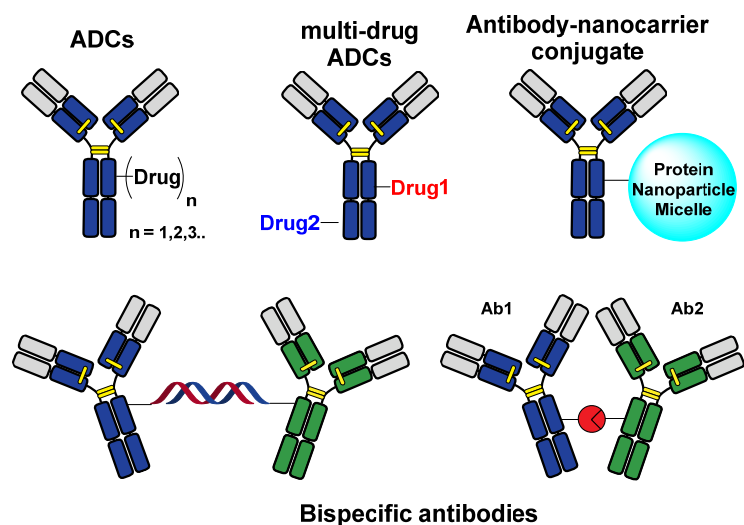


Figure 61. Potential applications of DARX technology

C. EXPERIMENTAL PART

1 General Methods

1.1 Experimental procedures

Unless otherwise indicated, reactions were carried out under an atmosphere of argon in flame-dried glassware with magnetic stirring. Air- and/or moisture-sensitive liquids were transferred *via* syringe. When required, solutions were degassed by bubbling of argon through a needle. Organic solutions were concentrated by rotary evaporation at 25-60 °C at 15-30 torr. Analytical thin layer chromatography (TLC) was performed using plates cut from glass sheets (silica gel 60F-254 from Merck). Visualisation was achieved under a 254 or 365 nm UV light and by immersion in an appropriate revelation solution. Melting point of compounds was determined on Büchi B-540.

1.2 Materials

All reagents were obtained from commercial sources (Aldrich, Alfa Aesar, Acros, TCI or Apollo Scientific) and were used without further purification. Dry solvents were obtained from Sigma-Aldrich or Alfa Aesar. Column flash chromatography was carried out using silica gel G-25 (40-63 µm) from Macherey-Nagel.

1.3 Instrumentation

1.3.1 NMR

¹H and ¹³C NMR spectra were recorded at 23 °C on Bruker 400 and 500 spectrometers. Recorded shifts are reported in parts per million (δ) and calibrated using residual non-deuterated solvent. Data are represented as follows: chemical shift, multiplicity (s = singlet, d = doublet, t = triplet, q = quartet, quint = quintet, m = multiplet, br = broad), coupling constant (J, Hz) and integration.

1.3.2 HPLC

Analytical LC-MS were conducted with Waters Alliance LC with Cortecs® C18 2.7 µM 4.6x50 mm column (Waters) coupled to an Acquity QDa Mass Detector (Waters). Chromatographic separation was performed as follows: elution at 1 mL/min flow rate and a gradient from 5 to 95% of mobile phase B for 5 min, followed by 1 min at 95% of mobile phase and post time of 1 min. Mobile phase A was 0.05% TFA in water (mQ) (v/v), mobile phase B was acetonitrile (HPLC grade).

Preparative HPLC procedures were performed on semi-preparative HPLC Shimadzu (pump: Shimadzu LC-8A, UV-Vis detector: Shimadzu SPD-10A, collector: Shimadzu fraction collector FRC-10A) or Waters (pump: Waters 600, detector: Waters 2489, collector: Waters fraction collector

III, 5 mL sample loop) using a Sunfire C18 (150 mm × 19 mm i.d., 5 µm, Waters) at a flow of 17 mL/min. The samples (1 mL) were injected and water/ACN containing 0.05% TFA was used as eluent system. The gradient applied was 5% to 95% ACN in 40 minutes and 10 minutes of re-equilibration. Detection was done at 550 nm for TAMRA derivatives and at 254 nm in other cases.

1.3.3 Microscopy.

Fluorescence images were recorded on an inverted widefield microscope DM IRB (Leica Microsystems) equipped with a mercury metal halide EL 6000 (Leica Microsystems) for fluorescence excitation and a variety of objectives (x10/x20/x40/x63) have been applied. Filter cubes utilised were A4 for Hoechst imaging (BP 360/40 – 400 – BP 470/40) and Cy3 for TAMRA imaging (BP 545/40 – 565 – BP 610/75). Confocal images were recorded on a TCS SPE-II (Leica Microsystems) using HXC PL APO 20x/0.7 CS (x20) and HXC PL APO 63x/1.40 OIL CS (x63) objectives. Excitation was done with 405 nm (Hoechst experiment), 488 nm (Oregon Green experiment) or 561 nm (TAMRA experiment) and fluorescence was detected from 430 – 480 nm (Hoechst), 500 – 560 nm (Oregon Green) and 570 – 625 nm (TAMRA).

1.3.4 Mass spectrometry

High resolution mass spectra (HRMS) were obtained using a Agilent Q-TOF (time of flight) 6520 and low resolution mass spectra using a Agilent MSD 1200 SL (ESI/APCI) with a Agilent HPLC1200 SL. Antibody MS experiments were performed on an electrospray time-of-flight mass spectrometer MS (LCT, Waters, Manchester) coupled to an automated chip-based nanoelectrospray device (Triversa Nanomate, Advion Biosciences, Ithaca, U.S.A.) operating in the positive ion mode.

1.3.5 Native-LRMS analysis

MS experiments were performed on an electrospray time-of-flight mass spectrometer MS (LCT, Waters, Manchester) coupled to an automated chip-based nanoelectrospray device (Triversa Nanomate, Advion Biosciences, Ithaca, U.S.A.) operating in the positive ion mode. For native MS experiments, external calibration of the ESI-TOF instrument was performed using singly charged ions produced by a 2 mg/mL solution of cesium iodide in 2-propanol/water (1v/1v). Tuning parameters of the mass spectrometer were carefully optimised to improve desolvation and ion transfer as well as maintaining weak interactions. Particularly, the sample cone voltage V_c was set to 120 V and the backing pressure P_i was increased to 6 mbar to improve ion collisional cooling and maintain non-covalent interaction for averaging DoC calculation. Native MS data interpretation was performed using MassLynx 4.1 (Waters, Manchester, UK.).

1.3.6 Native-HRMS analysis

High resolution native mass spectrometry (native-HRMS) was performed on an Exactive Plus EMR (Thermo Fisher Scientific, Bremen, Germany) coupled to an automated chip-based nanoelectrospray

device (Triversa Nanomate, Advion, Ithaca, USA). Electrospray ionisation was conducted at a capillary voltage of 1.86 kV and nitrogen nanoflow of 0.15 psi.

Native MS experiments were performed using classical interface tuning parameters of the mass spectrometer with a nominal resolution of either 17,500 or 35,000 and in the positive ion mode. The in-source collision-induced dissociation and the higher-energy collisional dissociation cells were set to 200 eV and 50 eV respectively. The trapping gas pressure was set to 3 a.u. (which corresponds to an Ultra High Vacuum of 4.10^{-10} mbar approximatively). In order to improve the transmission of the high mass species the voltages on the injection, inter and bent flatpole were fixed to 8, 7 and 6 V respectively.

External calibration was performed using singly-charged ions produced by a 2 mg/mL solution of cesium iodide in 2-propanol/water (50/50 v/v) and samples were infused at 5 μ M in NH₄OAc 150 mM pH 7.4. MS data interpretations and deconvolutions were performed using Protein Deconvolution 4.0 available on BiopharmaFinder SP1 (Thermo Fisher, Bremen, Germany). The parameters of software were optimised for each spectrum.

1.4 Software

Chemical structures and schemes were drawn using ChemDraw Professional 16.0. The LogP values were calculated using algorithms from fragment-based methods developed by the Medicinal Chemistry Project and BioByte (ChemOffice 2015). Protein structures were visualised using PyMol software. Graphical charts were performed in GraphPad Prism 6. Gel images were treated in Image Studio Lite ver 5.2. Confocal microscopy data was carried out with ImageJ 1.50i. Figures were constructed in PowerPoint 2013.

2 General Procedures

2.1 Protein concentration measuring

Protein concentration of a stock solution of antibody (PBS 1/20X, pH 7.4) was determined by UV absorbance using a NanoDrop One spectrophotometer (Thermo Fisher Scientific).

Protein concentration of antibody conjugates was measured using BCA Protein Assay Kit (Thermo Fisher Scientific) according to the manufacturer's protocol. As a standard protein solution, Trastuzumab stock solution was used.

2.2 Antibody conjugates purification

Antibody conjugates were purified by gel filtration chromatography using Bio-spin P-30 Columns (Bio-Rad, Hercules, U.S.A.) equilibrated with PBS (1/20x, pH 7.4). Antibody-oligonucleotide conjugates were purified by size-exclusion chromatography using AKTA Pure chromatography.

Concentration of the ACs was performed using micro-concentrators (Vivaspin, 10, 30 or 50 kD MWCO, Sartorius, Gottingen, Germany).

2.3 SDS PAGE analysis

Reducing and non-reducing glycine-SDS-PAGE was performed on 4–15% Mini-PROTEAN® TGX™ Gel (Bio-Rad ref 4561084) following standard lab procedures. To samples containing antibody conjugates (24 µL, 0.1 mg/mL in H₂O) was added 8 µL of loading buffer (4x reducing (ref J60015) or non-reducing (ref J63615) Laemmli SDS sample buffer, Alfa Aesar) and heated at 95 °C for 5 minutes. The gel was run at constant voltage (200 V) for 35 min using TRIS 0.25 M - Glycine 1.92 M - SDS 1% as a running buffer. Fluorescence was visualised on GeneGenius bio-imaging system (Syngene) prior to staining with Coomassie Blue.

2.4 Antibody conjugates preparation for MS analysis

Prior to native MS experiments, antibody conjugates were desalted against 150 mM ammonium acetate solution buffered at pH 7.4 using six cycles of concentration/dilution on micro-concentrators (Vivaspin, 30 kD cutoff, Sartorius, Gottingen, Germany). ACs deglycosylation was achieved by incubating (37 °C, 2h) 0.4 units of Remove-iT® Endo S (New England Biolabs, Ipswich, U.S.A.) per microgram of ADC prior to buffer exchange desalting step.

2.5 Calculation of the DoC

The average Degree of Conjugation (DoC) values from native MS were calculated by using eq. 1. These results were derived from the relative peak intensities in deconvoluted mass spectra.

$$(Eq. 1) \quad DoC = \frac{\sum_{i=0}^n i * I(ML_i)}{\sum_{i=0}^n I(ML_i)}$$

Where $I(ML_i)$ is relative peak intensity of conjugate species with i molecules loaded (ML) per antibody.

2.6 Antibody conjugates affinity

The antibody affinity of the different T-TAMRA was determined using flow cytometry on two breast adenocarcinoma cell lines: (i) HER2⁺ SKBR-3 cells; (ii) HER2⁻ MDA-MB-231 cells. A single cell suspension was obtained after incubating the adherent cells in 0.25 % trypsin for 1-2 min at 37 °C. Subsequent steps were performed at 4 °C. Briefly, 2 x 10⁵ cells were blocked in 10 % BSA for 15 min and washed in FACS buffer (5 % BSA, 0.1 % NaN₃). Then the cells were incubated for 15 min with the following antibodies/ADCs (20 µg/mL in FACS buffer): Trastuzumab, T-DM1, T-TAMRA or IgG1 isotype control. Subsequently, the cells were washed and incubated for 15 min with DyLight649-conjugated goat anti-human IgG antibody (Novus Biologicals, Littleton, CO, USA). The

samples were analysed on the Guava® easyCyte 12HT (Merck Millipore, Molsheim, France) and the data analysis was performed using FlowJo X.0.7 (Tree Star, Ashland, OR, USA).

2.7 Stability of P1 and P2 in human plasma and other media

Aliquots of stock solutions of probes **P1** and **P2** (10 mM in DMSO, stored at -80 °C) were diluted with DMSO to give 40 µM working solutions. 25 µL of each working solution was added to 975 µL of human plasma or other media, vortexed and distributed onto 96-well plates (in triplicates). The fluorescence was measured every 3 minutes for 15 hours and normalised according to the fluorescence of a solution of TAMRA-NH₂ (1 µM) and BHQ-2-SH (1 µM) in appropriate media (positive control). Obtained results are shown in Figure S1, Annex 1. Normalised fluorescence of probes **P1** and **P2** after 12h and 72h in different media is shown in Table S1, Annex 1.

2.8 Hydrolysis of succinimide of P1 and P2 in human plasma

Solutions (2 mL) of **P1** and **P2** (50µM, in human plasma, DMSO 10%) were incubated at 37 °C. After defined intervals of time 100µL aliquots were taken and mixed with 100µL of acetonitrile, allowing the precipitation of proteins. The resulting mixture was centrifuged and the supernatant was analysed by HPLC. Results are shown in Figure 36.

2.9 Hydrolytic stability of R1-R20, ABF and ABNHS

The acylating reagents (1 mM or 0.5 mM) in PBS buffer (1x, pH 7.4) containing 5% of DMSO were analysed by LC-MS at 254 nm (Figure S1). Pseudo-first-order rate constant for the reaction was determined by plotting $\ln(A_t)$ versus time and analyzing by linear regression, where A is the area under the peak of acylating reagents. The observed pseudo-first-order rate constant, k_1 , was reproducible to within ±5% and was measured for two different concentrations of the acylating reagent. The average of two or more runs were normally taken. The resulting data is contained in Table 2.

2.10 Aminolysis of ABF, ABNHS, R2 and R4

The acylation was conducted under pseudo-first order conditions with benzylamine in a 10-fold excess comparing to the acylating reagent in PBS buffer (1x, pH 7.4) with 2% of DMSO in the final solution. Aliquots of reaction mixture were taken after certain intervals of time and quenched with the same volume of water containing 5% v/v of TFA. The samples were then analysed by LC-MS at 254 nm (Figure S2). The second order rate constant, k_2 , for the reaction was determined from linear plot of $\ln(A_\infty - A_t)$ versus time using the following formula: $\ln(A_\infty - A_t) = -kt + \ln A_\infty$, where $k = k_1 + k_2 \cdot C_0(\text{BnNH}_2)$; A is the area under the peak of the amide product; k_1 is a pseudo-first order rate constant of hydrolysis in PBS 1x (pH 7.4); $C_0(\text{BnNH}_2)$ is a concentration of benzylamine. The determined second order constant, k_2 , was reproduced for two or more different concentrations of

acylating reagent, and the average of two runs were normally taken. The resulting data is contained in Table S2.

2.11 Stability of T-TAMRA(R), C1 and C2 in human plasma

Antibody-fluorophore conjugates (1 mg/mL, 50 μ L in water) was mixed with 50 μ L of human plasma and incubated at 37 °C. Every 24 h aliquots (2 μ L) were taken and diluted with water (98 μ L) in order to decrease a concentration of proteins in the mixture to 1 mg/mL. The resulting probes were stored at -20 °C prior to SDS PAGE analysis.

3 Bioconjugation

3.1 Maleimide dioxane linkage

3.1.1 Preparation of C1 and C2

Reduction of the antibody

Trastuzumab was dissolved in PBS (1x, pH 7.4) containing EDTA (2 mM) to give 5 mg/mL solution. To this solution was added a solution of TCEP (4.8 eq., 100 mM in H₂O). The mixture was incubated at 37 °C for 2 h and used in the next without further purification.

Conjugation with cysteines

To 100 µL of the solution of the reduced trastuzumab was added the solution of **MD-TAMRA** (30 eq., 4.13µL, 25 mM in DMF) or **MCC-TAMRA** (20 eq., 2.75µL, 25 mM in DMF) at 0 °C. The resulting mixture was incubated at 4 °C for 1 h and then purified using Bio-Spin P-30 Columns (Bio-Rad, Hercules, U.S.A.) equilibrated with PBS (1x, pH 7.4). Conjugates were subjected for MS analysis to confirm DoC of 8.1 and 8.3 for T-MD-TAMRA and T-MCC-TAMRA, respectively (Figure S2). Prior to stability test in human plasma the both conjugates were maintained at 37 °C in PBS buffer (1x, pH 7.4) for 3 days (or in BBS buffer with pH 8.5 for 1 day) to afford the conjugates **C1** and **C2**.

3.3 Acyl fluoride chemistry

3.3.1 Preparation of ACs using ABF

Conjugation step

To a solution of trastuzumab (1 eq, 1 mg/mL, 90 µL in PBS 1x (pH 7.4)) was added DMSO (5 µL) and **ABF** or **ABNHS** (2,3,4,6,8 or 10 eq. in 2.47 µL of DMSO) at 25 °C and the reaction mixture was incubated at 25 °C for 18 h. The excess of reagents was then removed by gel filtration chromatography using Bio-spin P-30 Columns (Bio-Rad, Hercules, U.S.A.) pre-equilibrated with PBS 1/20x (pH 7.4) to give a solution of trastuzumab-azide (T-N₃), which was used in the functionalisation step.

Functionalisation step

BCN-payload (1.5 eq per 1 eq. of acylating reagent on conjugation stage) was added to the solution of T-N₃ in PBS 1/20x and the reaction mixture was incubated at 25 °C for 20 h. BCN-MMAE and TAMRA-BCN were used as 1 mM solution in DMSO, Oligonucleotide-BCN derivatives were used as 350 µM solution in H₂O. The excess of reagents was then removed by gel filtration chromatography using Bio-spin P-30 Columns (Bio-Rad, Hercules, U.S.A.) equilibrated with PBS 1/20x (pH=7.3). The average yield over two steps was 65-80%. The protein concentration of antibody conjugates was determined by BCA assay (ref 23225, ThermoFisher Scientific).

3.3.2 Dual conjugation with mixture of two fluorophores

To a solution of trastuzumab (1 eq, 1 mg/mL, 2000 μ L in PBS 1x (pH 7.4)) was added **ABF** (3 eq., 41.1 μ L, 1 mM in DMSO) at 25 °C and the reaction mixture was incubated at 25 °C for 30 min. The aliquots of reaction mixture (100 μ L) were taken and were reacted with mixture of TAMRA-BCN and Cy5-BCN (4.5 eq. total, 6.17 μ L, 0.5 mM in DMSO), where the ratio between two fluorophores was 0/10; 2/8; 4/6; 5/5; 6/4; 8/2 and 10/0 respectively. The samples were incubated at 25 °C for 20 h. The excess of reagents was then removed by gel filtration chromatography using Bio-spin P-30 Columns (Bio-Rad, Hercules, U.S.A.) equilibrated with PBS 1/20x (pH 7.4) to yield (65-80%) trastuzumab-TAMRA/Cy5 conjugates, that were further analysed by UV-Vis spectroscopy (SAFAS Xenius XC) at 558 nm and 650 nm (100 μ L of antibody conjugates, 0.5 mg/mL in 96-well plate). The protein concentration of antibody conjugates was determined by BCA assay (ref 23225, ThermoFisher Scientific).

3.3.3 Kinetic of antibody acylation with ABF and ABNHS

Kinetic study was performed with **ABF** and **ABNHS** in parallel. Further described is the protocol for **ABF**; the same protocol was used for **ABNHS**.

To a solution of trastuzumab (1 eq, 1 mg/mL, 1000 μ L in PBS 1x (pH 7.4)) was added DMSO (10 μ L) and **ABF** (4 or 3 eq., 1 mM in DMSO) at 4 °C or 25 °C. After incubation at 4 °C or 25 °C for 1 min, 7.5 min, 15 min, 30 min, 60 min, or 120 min, aliquots (100 μ L) were taken and purified by gel filtration chromatography using Bio-spin P-30 Columns pre-equilibrated with PBS 1/20x (pH 7.4). The resulting conjugates were subjected to SPAAC with TAMRA-BCN (6 eq., 4.11 μ L, 1 mM in DMSO) at 25 °C for 20 h. The excess of reagents was then removed by gel filtration chromatography using Bio-spin P-30 Columns pre-equilibrated with PBS 1/20x (pH 7.4) to yield (65-80%) trastuzumab-TAMRA conjugates (T-TAMRA), that were further analysed by SDS PAGEs and native-HRMS (Figure 41 and Table S3).

3.4 Phenyl glyoxal chemistry

3.4.1 Efficacy of APG

APG (2, 5, 10 or 20 eq. in 6.86 μ L of DMSO) was added to a solution of trastuzumab (1 eq., 5 mg/mL, 100 μ L) in PBS 1x (pH 7.4) at 4 °C and the reaction mixture was incubated at 25 °C for 16 h. The excess of reagents was then removed by gel filtration chromatography using Bio-spin P-30 Columns pre-equilibrated with PBS 1/20x (pH 7.4) to give a solution of trastuzumab-azide conjugates **T-N₃(R)**, which were subjected to native HRMS for a measurement of the average degree of conjugation (DoC). The DoC values (triplicates) were plotted vs amount of added APG reagent as present on **Error! Reference source not found.** MS spectra are represented in Annex 4

3.4.2 Preparation of APG-based AOCs

A solution of **T-N₃(R)** conjugates (from step above, 2 mg/mL, 50 μ L in PBS (1x, pH 7.4)) with DoC (0.7, 1.5 or 2.9) was treated with **BCN-ON5** (1.3 eq. per azide groups, 249 μ M in H₂O) at 25 °C for 18 h. The excess of reagents was then removed by gel filtration chromatography using Bio-spin P-30 Columns pre-equilibrated with PBS 1/20x (pH 7.4) to give a solution of **T-ON5**, which were characterised by SDS PAGE (Figure 53). The hybridisation to **T-ON5-ON6** was evaluated by SDS PAGE analysis using a sample of **T-ON5** (1 eq., 0.1 mg/mL, 24 μ L) containing 6 eq. (98 pmol) of complementary oligonucleotide **ON6**.

3.4.3 Kinetic of antibody modification with APG

One after another DMSO (10 μ L) and APG (11 eq., 25.14 μ L, 15 mM in DMSO) were added to a solution of trastuzumab (1 eq, 5 mg/mL, 1000 μ L) in PBS (1x, pH 7.4) at 25 °C and the reaction mixture was incubated at 25 °C. At certain time points (1 h, 2 h, 4 h, 6 h, 9 h and 32 h) aliquots (100 μ L) were taken and purified by gel filtration chromatography using Bio-spin P-30 Columns pre-equilibrated with PBS 1/20x (pH 7.4). The resulting conjugates were subjected to SPAAC with TAMRA-BCN (5 eq., 1.14 μ L, 15 mM in DMSO) at 25 °C for 18 h. The excess of the reagent was then removed by gel filtration chromatography using Bio-spin P-30 Columns pre-equilibrated with PBS 1/20x (pH 7.4) to yield (70-95%) T-TAMRA(R). Concentration of the conjugates was adjusted to 0.5 mg/mL and absorption at 558 nm was measured in a quartz cuvette (chamber volume 160 μ L, ref. Z600318, Sigma-Aldrich) using UV-Vis spectrophotometer (Varian Cary 100 Bio). The resulting absorption values were plotted vs time as present on Figure 50B.

3.4.4 Selectivity of APG

APG (5 eq. (1.72 μ L), 8 eq. (2.75 μ L) or 11 eq. (3.78 μ L), 10 mM in DMSO) was added to a solution of trastuzumab (1 eq, 5 mg/mL, 100 μ L) in PBS 1x (pH 7.4) at 4 °C. In a parallel test, a solution of L-arginine or L-lysine (2900 eq., 10 μ L, 1 M) in PBS 1x (adjusted to pH 7.4 by 1M HCl solution) was added to a solution of trastuzumab (1 eq, 5 mg/mL, 100 μ L) and then APG (5 eq., 1.72 μ L, 10 mM in DMSO) was added 4 °C. The samples were incubated at 25 °C for 16 h. The excess of reagents was then removed by gel filtration chromatography using Bio-spin P-30 Columns pre-equilibrated with PBS 1/20x (pH 7.4) to give a solution of **T-N₃(R)**. The resulting conjugates were subjected to SPAAC with TAMRA-BCN (5 eq., 1.14 μ L, 15 mM in DMSO) at 25 °C for 18 h. As a negative control, a solution of trastuzumab (1 eq, 5 mg/mL, 100 μ L) was treated with TAMRA-BCN (5 eq., 1.14 μ L, 15 mM in DMSO) at 25 °C for 20h. The excess of the reagent was then removed by gel filtration chromatography using Bio-spin P-30 Columns pre-equilibrated with PBS 1/20x (pH 7.4) to afford **T-TAMRA(R)** in 70-90% yield. The conjugates were analysed by SDS PAGE (at 0.5 mg/mL Ab) and native-HRMS (samples based on 8 eq. and 11 eq. of APG).

3.5 Preparation of mono-functionalised ACs

3.5.1 General procedure A for the preparation of ACs with unique DoC 1 comprises three parts:

Part I. Preparation of antibody conjugates with affinity tag in low conversion

Part II. Loading of antibody conjugates into the affinity column

Part III. Trans-tagging reaction

Part I. Preparation of antibody-iSyd-Biotin conjugates

DMSO (15 μ L) followed by NHS-iSyd-Biotin reagent (1 eq., 10 x 21 μ L, 500 μ M in DMSO) were added to a solution of trastuzumab (1 eq., 5 mg/mL, 3mL in PBS 1x, pH 7.4) at 25 °C. The reaction mixture was maintained at 25 °C for 2 h. The reaction mixture was washed 3 times with PBS (1x, pH 7.4) using Vivaspin 20 centrifugal filtration unit (MWCO 30 kD, Sartorius).

Part II. Loading of antibody conjugates into the affinity column

Trastuzumab-iSyd-Biotin conjugate (3 mL in PBS 1x, pH 7.4) was loaded on HiTrap Streptavidin HP column (1 mL, GE Healthcare Life Sciences, Ref. 17-5112-01) equilibrated with PBS (1x, pH 7.4) using ÄKTA Pure chromatography system (GE Healthcare Life Sciences) at flow rate of 0.2 mL/min. The column was then washed with PBS (1x, pH 7.4, 0.2 mL/min, 20 CV) and the fractions of unconjugated antibody were collected and concentrated on using Vivaspin 20 centrifugal filtration unit (MWCO 30 kD, Sartorius) for use in subsequent cycles.

Part III. Trans-tagging reaction

Trans-tagging reaction was performed in the streptavidin column using bicyclononyne (BCN) derivatives bearing fluorophores (TAMRA, Cy5), oligonucleotide or BCN as secondary functionality. The column was equilibrated with the solution of a BCN derivative (10 μ M, 5 mL in PBS 1x, pH 7.4 containing 5% of DMSO) at flow rate of 1 mL/min. The column was incubated at 25 °C for 24 h and then eluted with PBS (1x, pH 7.4, 10 mL) at flow rate of 0.5 mL/min using ÄKTA Pure chromatography system (GE Healthcare Life Sciences). The collected fraction of the functionalised antibody conjugate was concentrated using Vivaspin 500 centrifugal filtration unit (MWCO 50 kD, Sartorius) and then purified by gel filtration chromatography on Bio-Spin P-30 Columns equilibrated with PBS (1x, pH 7.4). The general yield was 150-500 μ g of antibody conjugates per trans-tagging reaction. The resulting conjugates (50 μ g) were subjected to MS analysis according to General Procedure C.

General procedure B for post-modification of protein conjugates

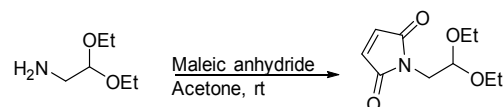
Protein conjugates (1 eq., 50 μ L, 1 mg/mL in PBS 1x, pH 7.4) obtained following General Procedure A were reacted with post-modification reagent (2 eq., 1.36 μ L, 0.5 mM) for 18 hours at 25 °C. The conjugates were purified by gel filtration chromatography on Bio-Spin P-30 Columns equilibrated with PBS (1x, pH 7.4) and subjected to native-LRMS analysis.

3.5.2 Stability of antibody-iSyd-Biotin conjugates on streptavidin column

HiTrap Streptavidin HP column loaded with antibody-iSyd-Biotin conjugates (1.5 mg) was subjected to the trans-tagging reaction (Part III) with BCN-TAMRA after 1, 14, 28 days. Between the trans-tagging reactions the column was kept in dark at 4 °C. The resulting T-TAMRA conjugates were analysed by SDS PAGE. Gel stained with Coomassie Blue showed no sign of degradation of the immobilised antibody-iSyd-Biotin conjugates over the period of one month (Figure 60).

4 Compounds synthesis

(2Z)-3-[(2,2-diethoxyethyl)carbamoyl]prop-2-enoic acid (1)

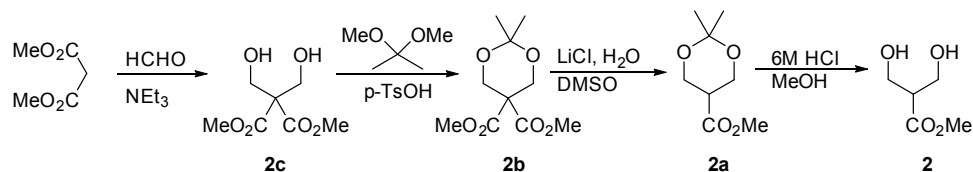


Maleic anhydride (1 eq., 10 g, 101 mmol) and 2,2-diethoxyethylamine (1 eq., 13.6 g, 14.8 mL, 101 mmol) were stirred in acetone (75 mL) at room temperature overnight. The solvent was evaporated and the residue was recrystallised from propan-2-ol. The resulting product was treated with sodium acetate (1.2 eq., 10 g, 122 mmol) in acetic anhydride (100 mL). The reaction mixture was stirred for 1h at r.t., then for 2h at 90 °C. After evaporation of acetic anhydride the residue was dissolved in EtOAc and filtered. The filtrate was concentrated *in vacuo* and the residue was purified by flash chromatography (EtOAc/Cyclohexane gradient: 0/100 to 100/0) to give 1-(2,2-diethoxyethyl)-2,5-dihydro-1H-pyrrole-2,5-dione (15.2 g, 71.4 mmol, 70 %) as a yellow oil.

¹H NMR (400MHz, CDCl₃, δ ppm): 6.72 (s, 2 H), 4.76 (t, J=5.8 Hz, 1 H), 3.68 - 3.75 (m, 2 H), 3.67 (d, J=5.8 Hz, 2 H), 3.48 - 3.56 (m, 2 H), 1.17 ppm (t, J=7.0 Hz, 6 H)

¹³C NMR (100MHz, CDCl₃, δ ppm): 170.4, 134.1, 98.4, 61.8, 39.6, 15.2

methyl 3-hydroxy-2-(hydroxymethyl)propanoate (2)



2c: 1,3-dimethyl 2,2-bis(hydroxymethyl)propanedioate

1,3-dimethyl 2,2-bis(hydroxymethyl)propanedioate was synthesised according to the literature procedure.²²¹

2b: 5,5-dimethyl 2,2-dimethyl-1,3-dioxane-5,5-dicarboxylate

To a solution of 1,3-dimethyl 2,2-bis(hydroxymethyl)propanedioate (1 eq., 20 g, 104 mmol) in 2,2-dimethoxypropane (90.3 mL) was added TsOH·H₂O (10 %, 1.98 g, 10.4 mmol) at 25 °C. After the reaction mixture was maintained at room temperature for 1 h and was poured into a 5% (w/v) aqueous solution of NaHCO₃ (70 mL) and toluene (100 mL). The resulting organic layer was washed with brine (100 mL) and evaporated to afford the desired 5,5-dimethyl 2,2-dimethyl-1,3-dioxane-5,5-dicarboxylate (22.7 g, 97.7 mmol, 94 %) as a transparent oil, which was used in the next step without purification.

¹H NMR (400MHz, CDCl₃, δ ppm): 4.31 (s, 4 H), 3.79 (s, 6 H), 1.43 (s, 6 H).

¹³C NMR (100MHz, CDCl₃, δ ppm): 168.4, 98.6, 62.5, 53.8, 53.0, 23.5.

MS(ESI) m/z : 232.09 [M+H]⁺.

2a: methyl 2,2-dimethyl-1,3-dioxane-5-carboxylate

To a solution of 5,5-dimethyl 2,2-dimethyl-1,3-dioxane-5,5-dicarboxylate (1 eq., 21.4 g, 92.1 mmol) in DMSO (34 mL) were added LiCl (2 eq., 7.81 g, 184 mmol) and H₂O (1 eq., 1.66 g, 1.66 mL, 92.1 mmol). The reaction mixture was heated to 160 °C and stirred for 2 h, then cooled to 0 °C. To the reaction mixture were added water (120 mL) and EtOAc (240 mL), and the resulting mixture was filtered. To the filtrate was added EtOAc (40 mL), the organic layer was washed with brine (40 mL) and concentrated carefully under reduced pressure (the product is volatile) to afford methyl 2,2-dimethyl-1,3-dioxane-5-carboxylate (10.8 g, 61.7 mmol, 67%), which was used in the next step without purification.

¹H NMR (400MHz, CDCl₃, δ ppm): 4.02 - 4.12 (m, 4 H), 3.72 (s, 3 H), 2.78 - 2.86 (m, 1 H), 1.42 (s, 3 H), 1.45 ppm (s, 3 H) according to the literature²²².

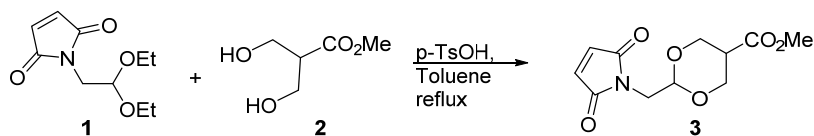
2: methyl 3-hydroxy-2-(hydroxymethyl)propanoate

To a solution of methyl 2,2-dimethyl-1,3-dioxane-5-carboxylate (1 eq., 5.8 g, 33.3 mmol) in MeOH (42.1 mL) was added 0.086 mL of 6M HCl (0.56 eq., 1.84 g, 1.53 mL, 18.6 mmol) at 25 °C. The mixture was stirred for 12 h at 25 °C, and then NaHCO₃ (6.48 eq., 18.1 g, 215 mmol) was added. The reaction mixture was filtered and washed with EtOAc (50 mL) twice. The filtrate was concentrated *in vacuo* and the residue was purified by flash chromatography (EtOAc/Cyclohexane gradient: 0/100 to 100/0, then DCM 100%) to give methyl 3-hydroxy-2-(hydroxymethyl)propanoate (4.26 g, 31.6 mmol, 95 %) as a yellow oil.

¹H NMR (400MHz, CDCl₃, δ ppm): 3.99 (dd, J=12.2, 4.1 Hz, 4 H), 3.77 (s, 3 H), 2.74 (t, J=4.9 Hz, 1 H), 2.63 (br. s., 2 H).

¹³C NMR (100MHz, CDCl₃, δ ppm): 173.7, 61.7, 52.1, 48.8.

methyl 2-[(2,5-dioxo-2,5-dihydro-1H-pyrrol-1-yl)methyl]-1,3-dioxane-5-carboxylate (3)



A solution of **1** (1 eq., 2 g, 9.38 mmol), **2** (1 eq., 1.26 g, 9.38 mmol) and monohydrate of *p*-toluenesulfonic acid (0.2 eq., 0.357 g, 1.88 mmol) was refluxed in toluene (100 mL) and EtOH formed during the reaction was separated as the toluene azeotrope. After 2h the toluene was evaporated, the residue was dissolved in EtOAc, washed with saturated solution of NaHCO₃, brine and dried over MgSO₄. The solvent was evaporated and the residue was purified by flash chromatography (EtOAc/Cyclohexane gradient: 0/100 to 100/0) to give methyl 2-[(2,5-dioxo-2,5-dihydro-1H-pyrrol-1-yl)methyl]-1,3-dioxane-5-carboxylate (1.96 g, 7.69 mmol, 82 %) as a mixture of *cis*- and *trans*-isomers (4:6). Individual isomers were separated for characterisation.

cis-methyl-2-[(2,5-dioxo-2,5-dihydro-1H-pyrrol-1-yl)methyl]-1,3-dioxane-5-carboxylate:

¹H NMR (400MHz, CDCl₃, δ ppm): 6.72 (s, 2 H), 4.81 (t, J=5.0 Hz, 1 H), 4.58 (d, J=10.8 Hz, 2 H), 3.82 - 3.89 (m, 2 H), 3.80 (s, 3 H), 3.68 (d, J=5.3 Hz, 2 H), 2.32 (br. s., 1 H)

¹³C NMR (100MHz, CDCl₃, δ ppm): 171.4, 170.3, 134.1, 97.9, 66.6, 52.3, 40.8, 39.8

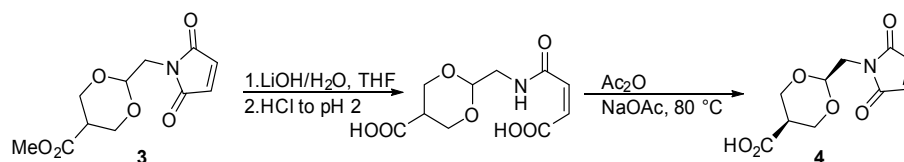
MS(ESI) *m/z*: 256.07 [M+H]⁺

trans-methyl-2-[(2,5-dioxo-2,5-dihydro-1H-pyrrol-1-yl)methyl]-1,3-dioxane-5-carboxylate:

¹H NMR (400MHz, CDCl₃, δ ppm): 6.74 (s, 2 H), 4.69 (t, J=5.1 Hz, 1 H), 4.31 (dd, J=11.8, 4.8 Hz, 2 H), 3.69 - 3.76 (m, 4 H), 3.67 (s, 3 H), 3.04 (m, 1 H)

¹³C NMR (100MHz, CDCl₃, δ ppm): 170.3, 170.0, 134.2, 97.5, 67.4, 51.9, 40.5, 39.7

MS(ESI) *m/z*: 256.07 [M+H]⁺

cis-2-[(2,5-dioxo-2,5-dihydro-1H-pyrrol-1-yl)methyl]-1,3-dioxane-5-carboxylic acid (4)

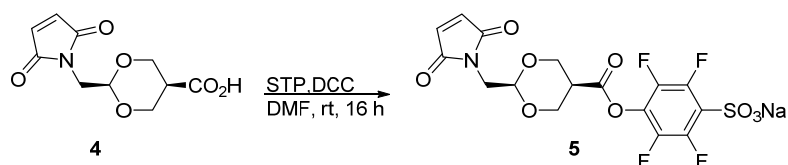
A solution of LiOH (4 eq., 0.526 g, 22 mmol) in H₂O (10 mL) was added to a solution of **3** (1 eq., 1.4 g, 5.49 mmol) in THF (20 mL) at rt. After stirring for 30min at r.t., EtOAc was added and the mixture was acidified to pH=2 with HCl. The mixture was extracted with EtOAc (3x), and the combined organic layer was washed with H₂O and brine, dried over MgSO₄ and concentrated to give corresponding carboxylic acid (1.38 g, 5.33 mmol, 97 %) as a mixture of cis- and trans- isomers (4:6). The mixture (1 eq., 1.38 g, 5.33 mmol) was treated with sodium acetate (2.4 eq., 1.05 g, 12.79 mmol) in acetic anhydride (20 mL). The reaction mixture was stirred 15 min at r.t. and then for 2 h at 80°C. Acetic anhydride was evaporated and water (15 mL) was added to the mixture. The mixture was stirred for 30 min and extracted with EtOAc. The organic layer was washed with brine and dried over MgSO₄. The solvent was evaporated and the residue was dissolved in a small amount of hot propan-2-ol and activated carbon was added. The resulting mixture was filtered off and the filtrate was kept at 0 °C for 15 hours. The mixture was filtered, the precipitate was washed with cold propan-2-ol and dried to afford (2*s*,5*s*)-2-[(2,5-dioxo-2,5-dihydro-1*H*-pyrrol-1-yl)methyl]-1,3-dioxane-5-carboxylic acid (820 mg, 3.40 mmol, 62 % overall in two steps) as a white solid (*t_m*=178 °C).

¹H NMR (400MHz, Methanol-d₄, δ ppm): 6.72 (s, 2 H), 4.72 (t, J=5.1 Hz, 1 H), 4.38 (d, J=10.8 Hz, 2 H), 3.78 (dd, J=11.8, 3.3 Hz, 2 H), 3.46 (d, J=5.3 Hz, 2 H), 2.25 (br. s., 1 H).

¹³C NMR (100MHz, Methanol-d₄, δ ppm): 172.7, 170.5, 134.6, 97.2, 66.2, 40.3, 39.1

MS(ESI) *m/z*: 242.07[M+H]⁺.

2,3,5,6-tetrafluoro-4-{[(2*s*,5*s*)-2-[(2,5-dioxo-2,5-dihydro-1*H*-pyrrol-1-yl)methyl]-1,3-dioxan-5-yl]carbonyloxy}benzene-1-sulfonate (5)



To the solution of **4** (1 eq., 500 mg, 2.07 mmol) and sodium 2,3,5,6-tetrafluoro-4-hydroxybenzene-1-sulfonate (1 eq., 555 mg, 2.07 mmol) in dry DMF (5 mL) was added DCC (1.05 eq., 471 mg, 2.17 mmol) at 0 °C. The resulting mixture was stirred at 25 °C for 16 h, then cooled to 0 °C, stirred for 1h and filtered off. The filtrate was diluted with cold dry Et₂O (75 mL) to precipitate the product. The mixture was filtered and the precipitate was washed with cold Et₂O and dried to give **5** (884 mg, 1.80 mmol, 87 %) as a white solid (*t_m*>250 °C)

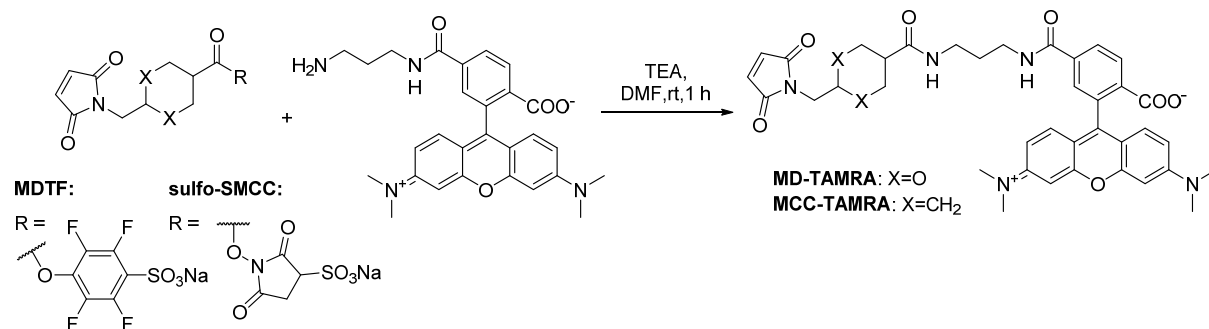
¹H NMR (400MHz, DMSO-d₆, δ ppm): 7.05 (s, 1 H), 4.86 (t, *J*=4.9 Hz, 1 H), 4.44 (d, *J*=11.5 Hz, 1 H), 4.04 (d, *J*=10.3 Hz, 1 H), 3.48 (d, *J*=4.8 Hz, 1 H), 3.18 ppm (br. s., 1 H)

¹⁹F NMR (376MHz, DMSO-d₆, δ ppm): -139.36 (dd, *J*=25.18, 9.16 Hz), -153.63 (dd, *J*=25.18, 10.31 Hz).

¹³C NMR (126MHz, DMSO-d₆, δ ppm): 170.4, 168.1, 134.6, 97.4, 65.9, 40.3, 39.6.

MS(ESI) *m/z*: 468.25 [M-Na]⁻.

MD-TAMRA and MCC-TAMRA



To the solution of **5** (1 eq., 0.035 mmol, 350 μL, 100 mM in DMF) was added a solution of N-(3-aminopropyl)-5-tetramethylrhodamine-1-carboxamide (1 eq., 0.035 mmol, 350 μL, 100 mM in DMF) followed by the solution of triethylamine (3 eq., 0.105 mmol, 105 μL, 1M in DMF). The mixture was incubated at 25°C for 1 hour and purified by preparative HPLC to afford **MD-TAMRA** (22.3 mg, 0.0315 mmol, 90%) as a red solid.

¹H NMR (400MHz, Acetonitrile-d₃, δ ppm): 8.32 (d, *J*=8.3 Hz, 1 H), 8.09 - 8.18 (m, 1 H), 7.79 - 7.83 (m, 1 H), 7.75 - 7.79 (m, 1 H), 7.11 (d, *J*=9.5 Hz, 2 H), 7.06 (br. s., 1 H), 6.91 (dd, *J*=9.4, 2.4 Hz, 2 H), 6.82 (d, *J*=2.5 Hz, 2 H), 6.72 (s, 2 H), 4.76 (t, *J*=4.9 Hz, 1 H), 4.19 (d, *J*=11.8 Hz, 2 H), 3.85 - 3.94 (m, 2 H), 3.55 (d, *J*=4.8 Hz, 2 H), 3.41 (q, *J*=6.1 Hz, 2 H), 3.30 (q, *J*=6.3 Hz, 2 H), 3.21 - 3.26 (m, 12 H), 2.16 (br. s., 1 H), 1.68 - 1.76 (m, 2 H)

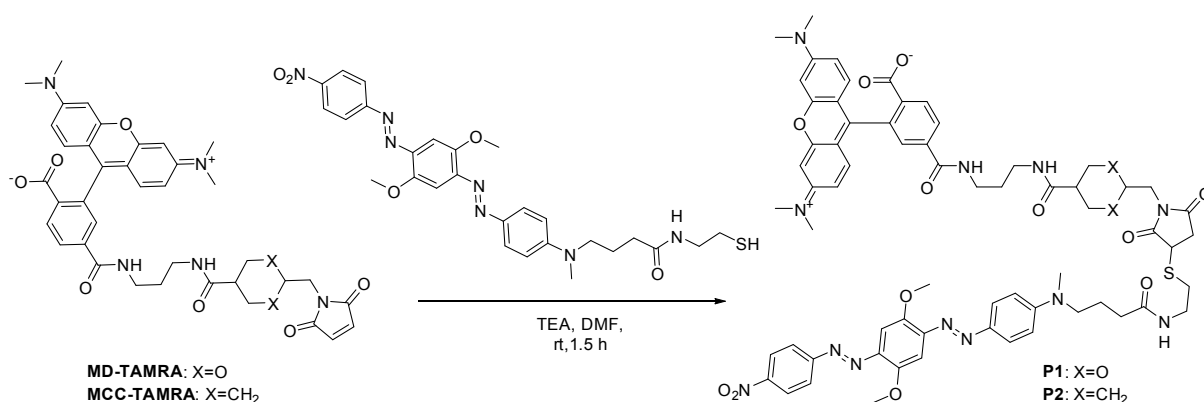
HR-ESI-MS: C₃₈H₃₉N₅O₉, 709.27478; found 709.27593

For the preparation of **MCC-TAMRA** the same protocol was used with the commercial sulfo-SMCC instead of **5** to give **MCC-TAMRA** (22.9 mg, 0,0325 mmol, 93%) as a red solid.

¹H NMR (400MHz, Methanol-d₄, δ ppm): 8.69 (m, 1H), 8.33 (m, 1H), 8.14 (m, 1H), 7.71-7.87 (m, 2 H), 7.08 (d, *J*=8.8 Hz, 2 H), 6.94 (d, *J*=9.5 Hz, 2 H), 6.87 (d, *J*=1.8 Hz, 2 H), 6.70 (s, 2 H), 3.31 (t, *J*=6.5 Hz, 2 H), 3.22-3.25 (m, 2H), 3.20 (s, 12 H), 3.13 (t, *J*=6.7 Hz, 2 H), 1.93 - 2.05 (m, 1 H), 1.62 - 1.75 (m, 4 H), 1.58 (d, *J*=13.3 Hz, 2 H), 1.46 - 1.54 (m, 1 H), 1.15 - 1.34 (m, 2 H), 0.80 - 0.95 (m, 2 H)

HR-ESI-MS: C₄₀H₄₃N₅O₇, 705.31625; found 705.31785

Probes P1 and P2



To the solution of **MD-TAMRA** (1 eq., 0.015 mmol, 300 μL, 50 mM in DMF) was added a solution of **BHQ-2-SH** (1 eq., 0.015 mmol, 300 μL, 50 mM in DMF) followed by the solution of triethylamine (3 eq., 0.045mmol, 45 μL, 1M in DMF). The mixture was incubated at 25°C for 1.5 hour and purified by preparative HPLC to give **P1** (16.2 mg, 0,0128 mmol, 85%) as a violet solid.

¹H NMR (400MHz, DMSO-d₆, δ ppm): 8.81 (t, *J*=5.3 Hz, 1 H), 8.43 (d, *J*=8.8 Hz, 2 H), 8.29 - 8.33 (m, 1 H), 8.24 - 8.29 (m, 1 H), 8.00 - 8.12 (m, 3 H), 7.95 (s, 1 H), 7.80 (d, *J*=9.0 Hz, 2 H), 7.72 (t, *J*=5.4 Hz, 1 H), 7.42 (s, 1 H), 7.36 (s, 1 H), 7.03 (s, 4 H), 6.91 (s, 2 H), 6.87 (d, *J*=9.0 Hz, 2 H), 4.75 (t, *J*=5.1 Hz, 1 H), 4.29 (d, *J*=11.5 Hz, 2 H), 4.02 - 4.07 (m, 1 H), 3.99 (s, 3 H), 3.94 (s, 3 H), 3.81-3.84 (m, 2H), 3.44 - 3.51 (m, 4 H), 3.30 - 3.36 (m, 4 H), 3.24 (s, 12H), 3.20 (d, *J*=8.3 Hz, 2 H), 3.07 (s, 3 H), 2.84 (dt, *J*=13.0, 6.4 Hz, 1 H), 2.71 (dt, *J*=13.2, 6.7 Hz, 1 H), 2.55-2.57 (m, 2H), 2.34 (br.s, 1H), 2.18 (d, *J*=5.5 Hz, 2 H), 1.76 - 1.86 (m, 2 H), 1.66 - 1.76 (m, 2 H)

HR-ESI-MS: C₆₅H₇₀N₁₂O₁₄S, 1274.48552; found 1274.48491.

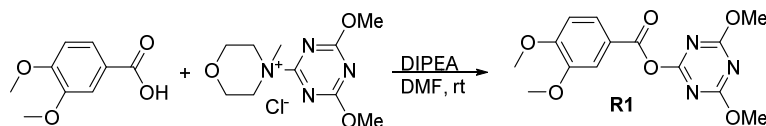
For the preparation of **P2** the same protocol was used with **MCC-TAMRA** to give **P2** (15.4 mg, 0,0122 mmol, 81%) as a violet solid.

¹H NMR (400MHz, DMSO-d₆, δ ppm): 8.74 (t, *J*=5.1 Hz, 1 H), 8.42 (d, *J*=8.8 Hz, 2 H), 8.29 (d, *J*=8.3 Hz, 1 H), 8.23 (d, *J*=7.5 Hz, 1 H), 8.04 (d, *J*=8.8 Hz, 3 H), 7.92 (s, 1 H), 7.81 (d, *J*=8.8 Hz, 2 H), 7.71 (t, *J*=5.1 Hz, 1 H), 7.42 (s, 1 H), 7.35 (s, 1 H), 7.01 (br. s., 4 H), 6.84 - 6.93 (m, 4 H), 4.01 - 4.06 (m, 1 H), 3.99 (s, 3 H), 3.93 (s, 3 H), 3.47 (t, *J*=6.3 Hz, 1 H), 3.17-3.32 (m, 18 H), 3.03-3.10

(m, 5 H), 2.70 - 2.93 (m, 2 H), 2.55-2.57(m, 2H), 2.13 - 2.22 (m, 2 H), 1.81 (br. s., 2 H), 1.58-1.72 (m, 6H), 1.20 - 1.28 (m, 4 H), 0.82 - 0.96 (m, 2 H)

HR-ESI-MS: C₆₇H₇₄N₁₂O₁₂S, 1270.52699; found 1270.52364

dimethoxy-1,3,5-triazin-2-yl 3,4-dimethoxybenzoate (R1)



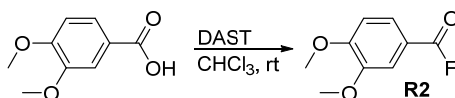
To a solution of 3,4-dimethoxybenzoic acid (1 eq., 143 mg, 0.785 mmol) in DMF (2.26 mL), 4-(4,6-dimethoxy-1,3,5-triazin-2-yl)-4-methyl morpholinium chloride (1 eq., 226 mg, 0.785 mmol) was added followed by DIPEA (3 eq., 304 mg, 0.389 mL, 2.35 mmol) and the solution was stirred at room temperature for 30 minutes. The reaction mixture was diluted with EtOAc, washed with saturated solution of NaHCO₃, water, dried over MgSO₄ and the solvent was evaporated under reduced pressure. The crude product was recrystallised from EtOAc to give **R1** (150 mg, 0.467 mmol, 59 %)

¹H NMR (400 MHz, CDCl₃, δ ppm): 7.83 (d, J=8.3 Hz, 1 H), 7.62 (br. s., 1 H), 6.94 (d, J=8.3 Hz, 1 H), 4.08 (s, 6 H), 3.94 (s, 3 H), 3.97 ppm (s, 3 H)

¹³C NMR (101 MHz, CDCl₃, δ ppm): 174.2, 171.0, 162.2, 154.4, 148.9, 125.4, 120.3, 112.6, 110.4, 56.1, 56.1, 55.8.

MS(ESI) m/z: 344.27 [M+Na]⁺.

3,4-dimethoxybenzoyl fluoride (R2)



To a solution of 3,4-dimethoxybenzoic acid (1 eq., 712 mg, 3.91 mmol) in CHCl₃ (17.8 mL) was added DAST (1.1 eq., 692 mg, 0.527 mL, 4.3 mmol) at rt. The mixture was stirred for 15 min and then solvent was evaporated under reduced pressure. The crude product was purified by flash chromatography (Cyclohexane 2 min, then Cyclohexane to EtOAc in 18 min) to yield **R2** (651 mg, 3.53 mmol, 90 %).

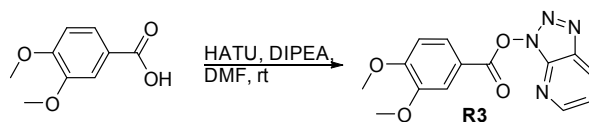
¹H NMR (400 MHz, CDCl₃, δ ppm): 7.72 (d, J=8.3 Hz, 1H), 7.49 (s, 1H), 6.95 (d, J=8.5 Hz, 1H), 3.89 - 4.04 (m, 6H)

¹³C NMR (101 MHz, CDCl₃, δ ppm): 159.0, 155.6, 155.0, 149.2, 126.2, 126.2, 117.2, 116.6, 113.1, 113.1, 110.7, 56.2, 56.1

¹⁹F NMR (376 MHz, CDCl₃, δ ppm): 15.66

MS (ESI) m/z: 185.12 [M+H]⁺.

3H-[1,2,3]triazolo[4,5-b]pyridin-3-yl 3,4-dimethoxybenzoate (R3)



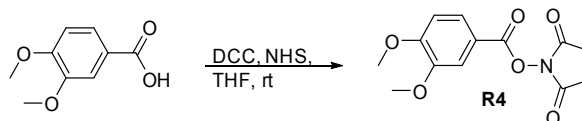
To a solution of 3,4-dimethoxybenzoic acid (1 eq., 76.9 mg, 0.422 mmol) in DMF (1.54 mL) is added HATU (1.3 eq., 208 mg, 0.549 mmol) followed by DIPEA (3.5 eq., 191 mg, 0.244 mL, 1.48 mmol) and the solution was stirred at room temperature for 30 minutes. The reaction mixture was diluted with EtOAc, washed with saturated solution of NaHCO₃, water, dried over MgSO₄ and the solvent was evaporated under reduced pressure. The crude product was recrystallised from EtOAc to give **R3** (120 mg, 0.4 mmol, 95 %).

¹H NMR (400 MHz, CDCl₃, δ ppm): 8.69 - 8.83 (m, 1H), 8.40 - 8.54 (m, 1H), 8.00 (dd, *J*=8.4, 1.9 Hz, 1H), 7.71 (d, *J*=2.0 Hz, 1H), 7.46 (dd, *J*=8.3, 4.5 Hz, 1H), 7.03 (d, *J*=8.5 Hz, 1H), 3.97 (s, 3H), 4.02 (s, 3H)

¹³C NMR (101 MHz, CDCl₃, δ ppm): 162.2, 155.2, 151.7, 149.2, 140.8, 135.1, 129.5, 125.8, 120.8, 116.5, 112.6, 110.8, 56.2, 56.2

MS (ESI) *m/z*: 301.12 [M+H]⁺.

2,5-dioxopyrrolidin-1-yl 3,4-dimethoxybenzoate (R4)



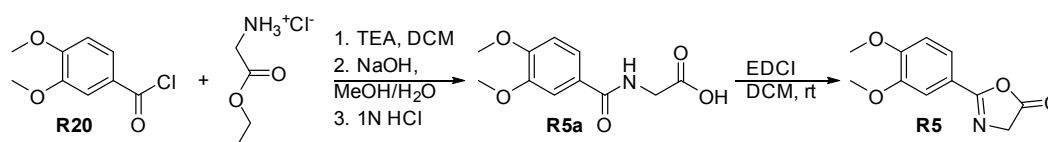
To a solution of 3,4-dimethoxybenzoic acid (1 eq., 100 mg, 0.549 mmol) and N-hydroxysuccinimide (1.05 eq., 66.3 mg, 0.576 mmol) in anhydrous THF (3.37 mL) was added DCC (1 eq., 113 mg, 0.549 mmol) at 0 °C. The reaction mixture was stirred for 5 h at room temperature, then was filtrated and the solvent was evaporated under reduced pressure. The crude product was purified by flash chromatography (Cyclohexane 2 min, then Cyclohexane to EtOAc in 18 min) to give **R4** (35 mg, 0.125 mmol, 23 %) as a white solid.

¹H NMR (400 MHz, CDCl₃, δ ppm): 7.80 (dd, *J*=8.4, 1.9 Hz, 1H), 7.55 (d, *J*=1.8 Hz, 1H), 6.93 (d, *J*=8.5 Hz, 1H), 3.95 (s, 3H), 3.92 (s, 3H), 2.88 (br. s., 4H)

¹³C NMR (101 MHz, CDCl₃, δ ppm): 169.4, 161.5, 154.7, 148.9, 125.3, 117.1, 112.4, 110.6, 56.1, 56.0, 25.6

MS (ESI) *m/z*: 280.10 [M+H]⁺.

2-(3,4-dimethoxyphenyl)-4,5-dihydro-1,3-oxazol-5-one (R5)



R5a: 2-[(3,4-dimethoxyphenyl)formamido]acetic acid

3,4-dimethoxybenzoyl chloride (1 eq., 1.5 g, 7.48 mmol) was slowly added to a suspension of glycine ethyl ester hydrochloride (1 eq., 1.04 g, 7.48 mmol) and TEA (2.4 eq., 1.82 g, 2.49 mL, 17.9 mmol) in DCM (24 mL) at 0 °C under argon atmosphere. The reaction mixture was allowed to warm up to room temperature and stirred at the same temperature for 20 hours before being quenched with 1 N HCl. The organic layer was washed with 1 N HCl, saturated aqueous NaHCO₃ solution, and brine, which was then dried over MgSO₄, filtered, and concentrated in vacuo to afford crude ester as a yellow crystalline solid. The crude ester and NaOH (1.6 eq., 0.478 g, 12 mmol) were dissolved in mixed solvent of H₂O (7 mL) and MeOH (24 mL), and the reaction mixture was stirred at room temperature for 1 h. After concentration of MeOH under reduced pressure, the residue was washed with DCM twice. The aqueous layer was acidified to pH 1 using 1 N HCl and brine was added to initiate precipitation, the mixture was left in the refrigerator overnight to provide white precipitate, which was collected by filtration and dried at 40 °C to yield **R5a** (1100 mg, 4.6 mmol, 61 %) as a white solid.

¹H NMR (400 MHz, MeOD-d₄, δ ppm): 7.43 - 7.56 (m, 2H), 7.02 (d, J=8.3 Hz, 1H), 4.08 (s, 2H), 3.88 (s, 6H)

¹³C NMR (101 MHz, MeOD-d₄, δ ppm): 153.9, 150.5, 127.7, 122.2, 112.3, 56.7, 56.6, 42.5

MS (ESI) m/z: 240.07 [M+H]⁺, 262.04 [M+Na]⁺.

R5: 2-(3,4-dimethoxyphenyl)-4,5-dihydro-1,3-oxazol-5-one

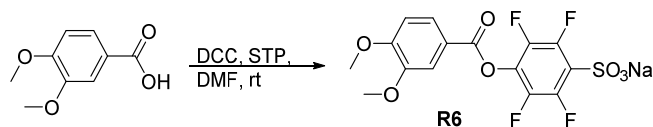
2-[(3,4-dimethoxyphenyl)formamido]acetic acid (1 eq., 785 mg, 3.28 mmol) and EDCI (1.3 eq., 817 mg, 4.27 mmol) were dissolved in DCM (7.85 mL) and stirred at room temperature for 5h under argon atmosphere. Then, the reaction was quenched with water. The organic layer was separated, and washed twice with water and once with brine. The organic layer was dried over MgSO₄ and the solvent was removed under reduced pressure. The crude product was purified by flash chromatography (Cyclohexane 2 min, then Cyclohexane to EtOAc in 18 min) to afford **R5** (350 mg, 1.58 mmol, 48 %) as a yellow solid.

¹H NMR (400 MHz, CDCl₃, δ ppm): 7.57 (d, J=8.3 Hz, 1H), 7.48 (s, 1H), 6.93 (d, J=8.5 Hz, 1H), 4.39 (s, 2H), 3.94 (d, J=3.5 Hz, 6H)

¹³C NMR (101 MHz, CDCl₃, δ ppm): 176.0, 163.2, 152.9, 149.1, 121.9, 118.2, 110.7, 109.7, 56.0, 54.9

MS (ESI) m/z: 222.13 [M+H]⁺.

sodium 4-[(3,4-dimethoxyphenyl)carboxyloxy]-2,3,5,6-tetrafluorobenzene-1-sulfonate (R6)

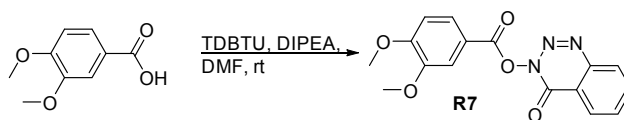


To a solution of 3,4-dimethoxybenzoic acid (1 eq., 116 mg, 0.642 mmol) in DMF (1.59 mL) is added sodium 2,3,5,6-tetrafluoro-4-hydroxybenzene-1-sulfonate (1 eq., 172 mg, 0.642 mmol) followed by DCC (1 eq., 132 mg, 0.642 mmol) at 0 °C and the solution is stirred at room temperature for 3h. The

reaction mixture was filtrated. The filtrate was mixed with 10x volume of diethyl ether resulting in precipitation. The precipitate was filtrated to afford **R6** (100 mg, 0.231 mmol, 36 %) as a white solid.
¹H NMR (400 MHz, DMSO-d₆, δ ppm): 7.87 (d, J=7.3 Hz, 1 H), 7.62 (s, 1 H), 7.22 (d, J=8.5 Hz, 1 H), 3.87 (s, 3 H), 3.91 ppm (s, 3 H).

¹⁹F NMR (376 MHz, DMSO-d₆, δ ppm): -139.35 (dd, J= 25.18, 9.15), -154.17 (dd, J= 25.18, 9.15).

4-oxo-3,4-dihydro-1,2,3-benzotriazin-3-yl 3,4-dimethoxybenzoate (**R7**)

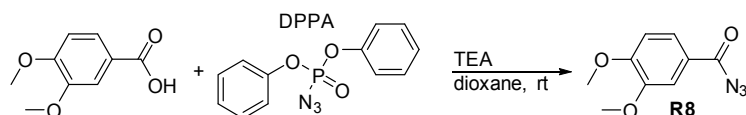


To a solution of 3,4-dimethoxybenzoic acid (1 eq., 100 mg, 0.549 mmol) in DMF (2 mL) is added [(dimethylamino)[(4-oxo-3,4-dihydro-1,2,3-benzotriazin-3-yl)oxy]methylidene]dimethylazanium; tetrafluoroboranuide (1.05 eq., 201 mg, 0.576 mmol) followed by DIPEA (3.5 eq., 248 mg, 0.318 mL, 1.92 mmol) and the solution is stirred at room temperature for 30 minutes. The reaction mixture is diluted with EtOAc, washed with water, and dried over anhydrous MgSO₄, filtered and concentrated at reduced pressure. The concentrated solution was maintained overnight at 4 °C, then the precipitation was filtered and washed with cold EtOAc to yield **R7** (120 mg, 0.367 mmol, 67 %).
¹H NMR (400 MHz, CDCl₃, δ ppm): 8.43 (d, J=8.0 Hz, 1H), 8.27 (d, J=8.0 Hz, 1H), 8.04 (t, J=7.7 Hz, 1H), 7.97 (dd, J=8.3, 1.8 Hz, 1H), 7.87 (t, J=7.5 Hz, 1H), 7.70 (d, J=1.8 Hz, 1H), 7.01 (d, J=8.5 Hz, 1H), 3.98 (s, 3H), 4.01 (s, 3H)

¹³C NMR (101 MHz, CDCl₃, δ ppm): 162.4, 154.8, 150.5, 149.1, 144.4, 135.3, 132.7, 129.0, 125.8, 125.5, 122.3, 117.4, 112.6, 110.7, 56.2, 56.1

MS (ESI) m/z: 328.12 [M+H]⁺.

3,4-dimethoxybenzoyl azide (**R8**)



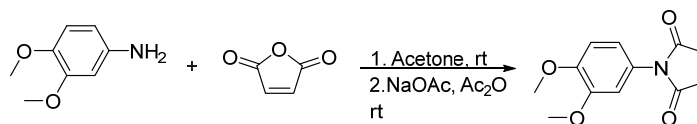
To a stirred solution of 3,4-dimethoxybenzoic acid (1 eq., 581 mg, 3.19 mmol) in dioxane (15.9 mL), diphenylphosphoryl azide (1 eq., 877 mg, 0.689 mL, 3.19 mmol) and TEA (1.1 eq., 354 mg, 0.488 mL, 3.51 mmol) were added. The reaction mixture was stirred at room temperature for 30 min. Then, the solution was poured into 10 ml water and extracted with cyclohexane (3 x 30 ml). The organic layers were combined, washed with water (1 x 10 ml), brine (1 x 10 ml) and dried over MgSO₄ before evaporating *in vacuo*. The crude product was purified by recrystallisation to give **R8** (409 mg, 1.98 mmol, 62 %)

¹H NMR (400 MHz, CDCl₃, δ ppm): 7.68 (d, J=8.3 Hz, 1 H), 7.52 (s, 1 H), 6.88 (d, J=8.5 Hz, 1 H), 3.93 (s, 3 H), 3.95 (s, 3 H).

¹³C NMR (101 MHz, CDCl₃, δ ppm): 171.6, 154.3, 148.9, 124.0, 123.3, 111.5, 110.3, 56.1, 56.0.

MS (ESI) m/z: 208.14 [M+H]⁺

1-(3,4-dimethoxyphenyl)-2,5-dihydro-1H-pyrrole-2,5-dione (R9)



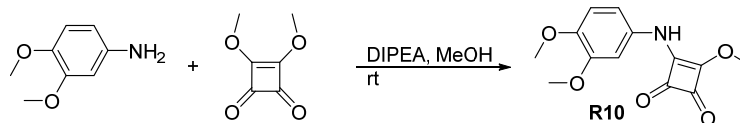
Maleic anhydride (1 eq., 320 mg, 0.216 mL, 3.26 mmol) and 4-aminoveratrole (1 eq., 500 mg, 3.26 mmol) were stirred in acetone (12 mL) at room temperature for 1h. The solvent was evaporated and the resulting product was treated with sodium acetate (1.1 eq., 294 mg, 3.59 mmol) in acetic anhydride (5 mL). The reaction mixture was stirred for 1h at room temperature. After evaporation of acetic anhydride the residue was dissolved in EtOAc and filtered. The filtrate was concentrated *in vacuo* and the residue was recrystallised from propanol-2 to give **R9** (350 mg, 1.5 mmol, 46 %) as a yellow solid.

¹H NMR (400 MHz, CDCl₃, δ ppm): 7.37 (d, J=5.0 Hz, 1 H), 7.22 (d, J=8.0 Hz, 1 H), 7.17 (br. s., 1 H), 6.88 (d, J=8.5 Hz, 1 H), 6.63 (d, J=5.0 Hz, 1 H), 3.92 ppm (br. s., 6 H).

¹³C NMR (101 MHz, CDCl₃, δ ppm): 167.5, 149.1, 149.0, 148.5, 143.4, 136.6, 126.6, 120.0, 110.9, 110.2, 56.0, 55.9.

MS (ESI) m/z: 234.14 [M+H]⁺.

3-[(3,4-dimethoxyphenyl)amino]-4-methoxycyclobut-3-ene-1,2-dione (R10)



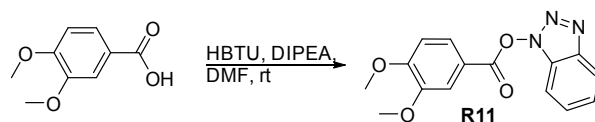
To a solution of 4-aminoveratrole (1 eq., 107 mg, 0.704 mmol) with DIPEA (1 eq., 90.9 mg, 0.116 mL, 0.704 mmol) in MeOH (1.5 mL) was added a solution of 3,4-dimethoxy-3-cyclobutene-1,2-dione (1 eq., 100 mg, 0.704 mmol) in MeOH (1.5 mL) resulting in precipitation of the product. The precipitate was filtered off and washed with MeOH to yield **R10** (150 mg, 0.57 mmol, 81 %) as a white solid.

¹H NMR (400 MHz, CDCl₃, δ ppm): 6.97 (br.s, 1H), 6.76 - 6.86 (m, 2H), 4.49 (s, 3H), 3.87 (s, 3H), 3.90 (s, 3H)

¹³C NMR (101 MHz, CDCl₃, δ ppm): 183.7, 167.3, 149.7, 146.8, 130.5, 111.7, 104.1, 60.9, 56.2, 56.0

MS (ESI) m/z: 264.17 [M+H]⁺.

1H-1,2,3-benzotriazol-1-yl 3,4-dimethoxybenzoate (R11)



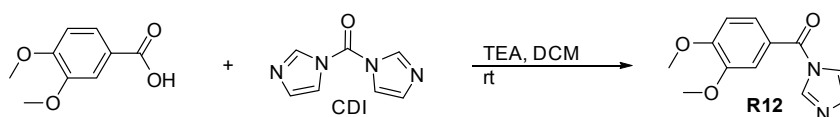
To a solution of 3,4-dimethoxybenzoic acid (1 eq., 200 mg, 1.1 mmol) in DMF (4 mL) is added HBTU (1.05 eq., 437 mg, 1.15 mmol) followed by DIPEA (3.5 eq., 496 mg, 0.635 mL, 3.84 mmol) and the solution is stirred at room temperature for 30 minutes. The reaction mixture is diluted with EtOAc, washed with water, dried over MgSO_4 and concentrated under reduced pressure. The concentrated solution was kept overnight at 4 °C, then the precipitation was filtered and washed with cold EtOAc to yield **R11** (224 mg, 0.748 mmol, 68 %).

^1H NMR (400 MHz, CDCl_3 , δ ppm): 8.11 (d, $J=8.3$ Hz, 1H), 7.95 - 8.02 (m, 1H), 7.69 (s, 1H), 7.42 - 7.59 (m, 3H), 7.04 (d, $J=8.5$ Hz, 1H), 3.98 (s, 3 H), 4.02 (s, 3H)

^{13}C NMR (101 MHz, CDCl_3 , δ ppm): 162.7, 155.5, 149.6, 143.9, 129.2, 129.0, 125.9, 125.1, 120.8, 117.0, 112.8, 111.2, 108.7, 56.6, 56.5

MS (ESI) m/z : 300.09 $[\text{M}+\text{H}]^+$.

1-(3,4-dimethoxyphenyl)buta-2,3-dien-1-one (R12)



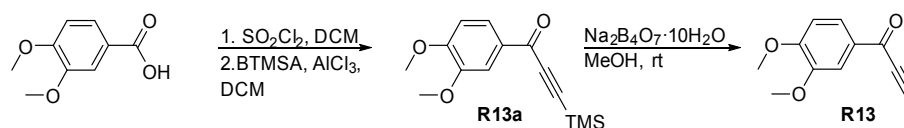
To a solution of 3,4-dimethoxybenzoic acid (1 eq., 200 mg, 1.1 mmol) and TEA (1 eq., 111 mg, 0.153 mL, 1.1 mmol) in dichloromethane was added CDI (1 eq., 178 mg, 1.1 mmol) at room temperature. After 30 min at room temperature, the solution was washed several times with dilute sodium bicarbonate solution, organic phase was dried over MgSO_4 and concentrated under reduced pressure. The residue was recrystallised from n-heptane to give **R12** (100 mg, 0.431 mmol, 39 %) as a white solid.

^1H NMR (400 MHz, CDCl_3 , δ ppm): 8.09 (s, 1H), 7.54 (s, 1H), 7.32 - 7.49 (m, 2H), 7.15 (s, 1H), 6.96 (d, $J=8.3$ Hz, 1H), 3.94 (s, 3H), 3.98 (s, 3H)

^{13}C NMR (101 MHz, CDCl_3 , δ ppm): 165.4, 153.8, 149.3, 138.1, 130.6, 124.4, 123.9, 118.2, 112.5, 110.4, 56.2, 56.1

MS (ESI) m/z : 233.11 $[\text{M}+\text{H}]^+$.

1-(3,4-dimethoxyphenyl)prop-2-yn-1-one (R13)



R13a: 1-(3,4-dimethoxyphenyl)-3-(trimethylsilyl)prop-2-yn-1-one

SOCl₂ (7 eq., 8.27 g, 5.05 mL, 69.5 mmol) was added to 3,4-dimethoxybenzoic acid (1 eq., 1.81 g, 9.94 mmol) in DCM (9.05 mL) in a dry flask and the mixture allowed to reflux for 15 min. The excess of thionyl chloride and solvent were then removed at reduced pressure to provide the acid chloride. The residue was dissolved in DCM (40 mL), bis(trimethylsilyl)acetylene (1.1 eq., 1.86 g, 2.48 mL, 10.9 mmol) was then added and the temperature of the solution was lowered to 0 °C. AlCl₃ (1.16 eq., 1.54 g, 11.5 mmol) was added by portion and the reaction mixture was stirred for 1h at 0 °C. The reaction was carefully quenched by pouring the reaction mixture into a beaker containing ice (50 mL). The organic layer was separated, washed with saturated aqueous NaHCO₃ (2 × 20 mL), brine (2 × 20 mL), dried over MgSO₄, and the solvent was evaporated under reduced pressure to give spectroscopically pure **R13a** (2250 mg, 8.58 mmol, 86 %) as a yellow oil.

¹H NMR (400 MHz, CDCl₃, δ ppm): 7.86 (dd, J=8.4, 1.4 Hz, 1H), 7.63 (s, 1H), 6.95 (d, J=8.5 Hz, 1H), 3.94 (s, 3H), 3.97 (s, 3H), 0.32 (s, 9H)

¹³C NMR (101 MHz, CDCl₃, δ ppm): 176.3, 154.4, 149.0, 130.1, 125.8, 110.3, 110.1, 100.9, 99.5, 56.2, 56.0, -0.35

MS (ESI) m/z: 263.18 [M+H]⁺.

R13: 1-(3,4-dimethoxyphenyl)prop-2-yn-1-one

To a solution of **R13a** (1 eq., 500 mg, 1.91 mmol) in MeOH (10 mL) was added a aqueous solution of Na₂B₄O₇·10H₂O (0.383 eq., 0.1 M, 7.3 mL, 0.73 mmol). After stirring for 2 minutes at room temperature a precipitate formed rapidly and the mixture was poured in a solution of THF and 1 N aq. HCl (1:1). The phases were separated by adding brine, and the organic phase was dried over MgSO₄ and concentrated under reduced pressure to give a crude product, which was recrystallised from n-heptane to yield **R13** (258 mg, 1.36 mmol, 71 %) as a yellowish solid.

¹H NMR (400 MHz, CDCl₃, δ ppm): 7.89 (dd, J=8.5, 1.5 Hz, 1H), 7.62 (s, 1H), 6.94 (d, J=8.3 Hz, 1H), 3.95 (s, 4H), 3.98 (s, 3H), 3.39 (s, 1H)

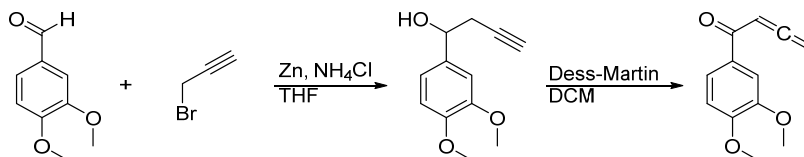
¹³C NMR (101 MHz, CDCl₃, δ ppm): 175.9, 154.7, 149.1, 129.8, 126.1, 110.2, 110.2, 80.4, 79.9, 56.2, 56.0

MS (ESI) m/z: 191.06 [M+H]⁺.

3,4-Dimethoxyphenylglyoxal hydrate (R14)

Reagent **R14** is commercially available and was supplied by Alfa Aesar.

1-(3,4-dimethoxyphenyl)buta-2,3-dien-1-one (R15)



R15a: 1-(3,4-dimethoxyphenyl)but-3-yn-1-ol

To a stirred suspension of veratraldehyde (1 eq., 0.80 g, 4.81 mmol), 3-bromopropyne (2 eq., 1.43 g, 1.07 mL, 9.63 mmol) and Zn (5 eq., 1.57 g, 24.1 mmol) in THF (16 mL) at 0 °C was added to a saturated aqueous NH₄Cl solution dropwise. The mixture was allowed to warm up to room temperature and was stirred until full conversion was detected by TLC. The mixture was filtered over celite and the filter cake was rinsed with DCM. The filtrate was washed with a saturated aqueous solution of NH₄Cl, distilled water and dried under MgSO₄. Evaporation of the solvent under reduced pressure yielded the crude product, which was purified by flash column chromatography (20 minutes gradient Cyclohexane/EtOAc) to give **R15a** (720 mg, 3.49 mmol, 73 %).

¹H NMR (400 MHz, CDCl₃, δ ppm): 6.98 (s, 1H), 6.93 (d, J=8.5 Hz, 1H), 6.82 - 6.88 (m, 1H), 4.84 (t, J=6.1 Hz, 1H), 3.90 (d, J=8.0 Hz, 7H), 2.65 (dd, J=6.4, 2.4 Hz, 2H), 2.33 (br. s., 1H), 2.09 (br. s., 1H)

¹³C NMR (101 MHz, CDCl₃, δ ppm): 149.1, 148.8, 135.1, 118.0, 111.0, 108.9, 80.8, 72.2, 70.9, 55.9, 55.9, 29.5

MS (ESI) m/z: 206.13 [M+H]⁺.

R15: 1-(3,4-dimethoxyphenyl)buta-2,3-dien-1-one

To a solution of **R15a** (1 eq., 300 mg, 1.45 mmol) in DCM (6.06 mL) was added Dess-Martin (1.1 eq., 678 mg, 1.6 mmol) at 0 °C and the solution warmed up to room temperature. After stirring for 1h the solvent was partially removed under reduced pressure at low temperature and directly purified by flash chromatography (20 minutes gradient Cyclohexane/EtOAc) to afford **R15** (200 mg, 0.979 mmol, 67 %) as a yellow solid.

¹H NMR (400 MHz, CDCl₃, δ ppm): 7.60 (d, J=8.3 Hz, 1H), 7.52 (s, 1H), 6.89 (d, J=8.3 Hz, 1H), 6.48 (t, J=6.5 Hz, 1H), 5.26 (d, J=6.5 Hz, 2H), 3.95 (d, J=5.0 Hz, 6H)

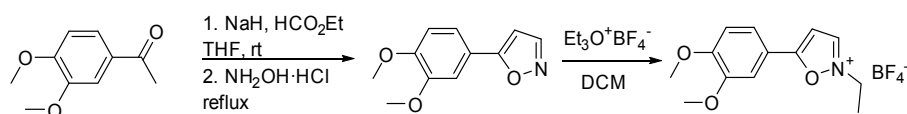
¹³C NMR (101 MHz, CDCl₃, δ ppm): 216.4, 153.3, 149.0, 130.5, 123.3, 111.0, 109.9, 92.7, 79.0, 56.1, 56.0

MS (ESI) m/z: 205.09 [M+H]⁺.

3,4-dimethoxyphenyl isothiocyanate (R16)

Reagent **R16** is commercially available and was obtained from Acros.

5-(3,4-dimethoxyphenyl)-2-ethyl-1,2-oxazol-2-ium tetrafluoroboranuide (R17)



R17a: 5-(3,4-dimethoxyphenyl)-1,2-oxazole

To a stirred mixture of sodium hydride in oil (2.01 eq., 0.89 g, 22.3 mmol), ethyl formate (3.25 eq., 2.67 g, 2.91 mL, 36.1 mmol) in THF (18.3 mL) was added 3',4'-dimethoxyacetophenone (1 eq., 2 g, 11.1 mmol) in tetrahydrofuran (10 mL) at 0°C. The reaction mixture was stirred for 2.5 h at room

temperature forming a precipitate of sodium enolate, then diluted with water and washed with ethyl acetate (3x). The aqueous layer was separated and hydroxylamine hydrochloride (1 eq., 774 mg, 11.1 mmol) was added. The reaction was heated to reflux for 3 h. The mixture was allowed to cool to room temperature before being acidified with glacial acetic acid, diluted with water and extracted 3x with DCM. The organic fractions were washed with brine, dried over MgSO₄ and the solvent was evaporated at reduced pressure. The crude product was purified by flash chromatography (20 minutes gradient Cyclohexane/EtOAc) to yield 5-(3,4-dimethoxyphenyl)-1,2-oxazole (933 mg, 4.55 mmol, 41 %).

¹H NMR (400 MHz, CDCl₃, δ ppm): 8.26 (s, 1H), 7.34 - 7.40 (m, 1H), 7.32 (s, 1H), 6.94 (d, J=8.3 Hz, 1H), 6.42 (s, 1H), 3.95 (m, 6H)

¹³C NMR (101 MHz, CDCl₃, δ ppm): 169.3, 150.9, 150.8, 149.3, 120.3, 119.2, 111.3, 108.8, 97.5, 56.1, 56.0

MS (ESI) m/z: 206.16 [M+H]⁺.

R17: 5-(3,4-dimethoxyphenyl)-2-ethyl-1,2-oxazol-2-ium salt of tetrafluoroborate

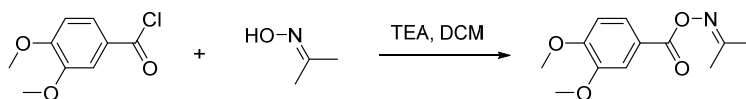
Triethyloxonium tetrafluoroborate (1 eq., 92.6 mg, 0.487 mmol) and 5-(3,4-dimethoxyphenyl)-1,2-oxazole (1 eq., 100 mg, 0.487 mmol) were dissolved in DCM (1 mL) and mixture was allowed to stand overnight at room temperature under argon. After the solvent had been removed at reduced pressure, the solid residue was crystallised by being dissolved in warm acetone and precipitated with diethyl ether to give 5-(3,4-dimethoxyphenyl)-2-ethyl-1,2-oxazol-2-ium tetrafluoroborate (110 mg, 0.343 mmol, 70 %) as a yellow solid.

¹H NMR (400 MHz, DMSO-d₆, δ ppm): 9.68 (d, J=2.5 Hz, 1H), 7.79 (d, J=2.5 Hz, 1H), 7.66 - 7.73 (m, 1H), 7.52 - 7.61 (m, 1H), 7.25 (d, J=8.5 Hz, 1H), 4.72 (q, J=7.1 Hz, 2H), 3.89 (s, 3H), 3.89 (s, 3H), 1.60 (t, J=7.1 Hz, 3H)

¹³C NMR (101 MHz, DMSO-d₆, δ ppm): 171.3, 153.5, 149.4, 149.0, 121.6, 115.3, 112.3, 109.8, 102.3, 56.0, 56.0, 50.0, 12.7

MS (ESI) m/z: 234.12 [M-BF₄]⁺.

(propan-2-ylidene)amino 3,4-dimethoxybenzoate (R18)



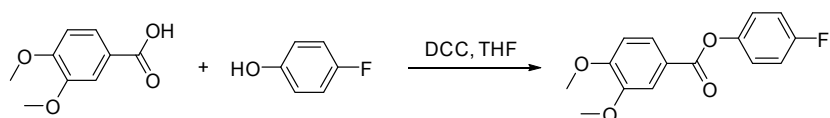
Acetone oxime (1.3 eq., 71 mg, 0.0789 mL, 0.972 mmol) in DCM (2.4 mL) was added to a solution of 3,4-dimethoxybenzoyl chloride (1 eq., 150 mg, 0.748 mmol) with TEA (1.3 eq., 98.4 mg, 0.135 mL, 0.972 mmol) in DCM (2.4 mL) under argon atmosphere. The reaction mixture was stirred for 1h, then diluted with DCM and washed subsequently with saturated solution of NaHCO₃, water (2x) and brine. The organic phase was dried over MgSO₄ and the solvent was evaporated under reduced pressure to yield (propan-2-ylidene)amino 3,4-dimethoxybenzoate (173 mg, 0.733 mmol, 98 %) as a white solid.

¹H NMR (400 MHz, CDCl₃, δ ppm): 7.70 (d, J=8.3 Hz, 1H), 7.58 (s, 1H), 6.90 (d, J=8.3 Hz, 1H), 3.94 (s, 6H), 2.13 (s, 6H)

¹³C NMR (101 MHz, CDCl₃, δ ppm): 164.2, 163.7, 153.2, 148.8, 123.4, 121.6, 112.1, 110.3, 56.0, 22.1, 17.1

MS (ESI) m/z: 238.38 [M+H]⁺.

4-fluorophenyl 3,4-dimethoxybenzoate (R19)



To a solution of 3,4-dimethoxybenzoic acid (1 eq., 400 mg, 2.2 mmol) in THF (9 mL) is added 4-fluorophenol (1 eq., 246 mg, 2.2 mmol) followed by DCC (1 eq., 453 mg, 2.2 mmol) and the solution is stirred at room temperature for 30 minutes. The reaction mixture is diluted with EtOAc, washed with water and the organic phase was dried over anhydrous MgSO₄ and concentrated at reduced pressure. The concentrated solution was maintained overnight at 4 °C to precipitate, then the precipitation was filtered and washed with cold EtOAc to yield **R19** (100 mg, 0.362 mmol, 16 %).

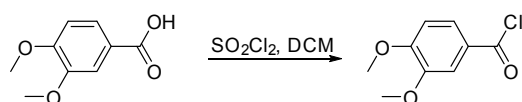
¹H NMR (400 MHz, CDCl₃, δ ppm): 7.86 (dd, J=8.4, 1.9 Hz, 1H), 7.67 (d, J=1.8 Hz, 1H), 7.07 - 7.21 (m, 4H), 6.97 (d, J=8.5 Hz, 1H), 3.97 (s, 3 H), 3.99 (s, 3H)

¹³C NMR (101 MHz, CDCl₃, δ ppm): 148.8, 146.8, 124.4, 123.2, 123.1, 121.6, 116.2, 116.0, 112.4, 110.4, 56.1, 56.1

¹⁹F NMR (376 MHz, CDCl₃, δ ppm): -117.16 (spt, J=4.6)

MS (ESI) m/z: 277.10 [M+H]⁺.

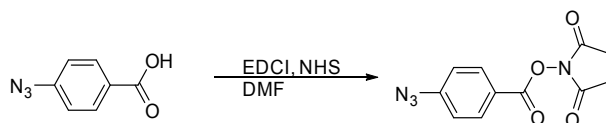
3,4-dimethoxybenzoyl chloride (R20)



SOCl₂ (7 eq., 4.14 g, 2.53 mL, 34.8 mmol) was added to 3,4-dimethoxybenzoic acid (1 eq., 0.90 g, 4.97 mmol) in DCM (10 mL) in a dry flask and the mixture allowed to reflux for 15 min. The excess of thionyl chloride and solvent were then removed at reduced pressure to provide **R20** (0.96 g, 4.82 mmol, 97 %).

¹H NMR (400 MHz, CDCl₃, δ ppm): 7.79 - 7.96 (m, 1 H), 7.55 (s, 1 H), 6.95 (d, J=8.5 Hz, 1 H), 3.82 - 4.08 (m, 6 H)

2,5-dioxopyrrolidin-1-yl 4-azidobenzoate (ABNHS)



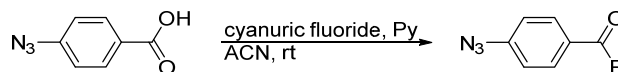
4-azidobenzoic acid (1 eq., 500 mg, 3.06 mmol) was dissolved in DMF (9.76 mL) cooled to 0 °C. To this mixture, EDCI (1.2 eq., 705 mg, 3.68 mmol) was added followed by N-hydroxysuccinimide (1.2 eq., 423 mg, 3.68 mmol). The reaction was stirred in the dark under argon at 0 °C for approximately 1 h and then at room temperature for 15 h. DMF was removed in vacuo. This concentrated mixture was dissolved in 30 ml of EtOAc and then extracted with water (3x 20 ml). The organic layer was dried over MgSO₄, filtered, evaporated and purified using column chromatography (100% EtOAc) to yield 2,5-dioxopyrrolidin-1-yl 4-azidobenzoate (745 mg, 2.86 mmol, 93 %) as a pale yellow coloured product.

¹H NMR (400 MHz, CDCl₃, δ ppm): 8.00 - 8.22 (m, J=8.3 Hz, 2 H), 7.03 - 7.21 (m, J=8.3 Hz, 2 H), 2.90 (br. s., 4 H)

¹³C NMR (101 MHz, CDCl₃, δ ppm): 169.2, 161.0, 146.9, 132.4, 121.3, 119.3, 25.6

MS (ESI) m/z: 283.02 [M+Na]⁺.

4-azidobenzoyl fluoride (ABF)



To 4-azidobenzoic acid (1 eq., 300 mg, 1.84 mmol) in acetonitrile (9 mL), was added pyridine (1 eq., 148 μL, 1.84 mmol). The mixture was stirred at room temperature until a homogeneous solution formed and then cyanuric fluoride (1.35 eq., 213.6 μL, 2.48 mmol) was added. The mixture was allowed to stir at room temperature for 16 h. The reaction mixture was poured onto ice water (20 mL) and diluted with diethyl ether (50 mL). The mixture was transferred to a separatory funnel, the aqueous layer was removed, and the organic layer was washed with water (2 x 10 mL) and brine (10 mL). The organic layer was dried over MgSO₄, filtered and concentrated under reduced pressure to provide the crude residue, which was purified by silica gel flash chromatography (Cyclohexane 2 min, then Cyclohexane to EtOAc in 18 min) to yield **ABF** (200 mg, 1.21 mmol, 66 %) as a pale yellow (*t_m* = 46.6 °C).

¹H NMR (400 MHz, CDCl₃, δ ppm): 8.04 (d, *J* = 8.3 Hz, 3 H), 7.15 (d, *J* = 8.3 Hz, 2 H).

¹³C NMR (101 MHz, CDCl₃, δ ppm): 156.6 (d, *J* = 341.9 Hz), 147.4, 133.3 (d, *J* = 3.9 Hz), 121.1 (d, *J* = 62.6 Hz), 119.5.

¹⁹F NMR (376 MHz, CDCl₃, δ ppm): 17.29.

MS (ESI) m/z: 331.05 [2M+H]⁺.

Synthesis of BCN derivatives

All BCN derivatives were synthesised by co-workers in our laboratory and the corresponding protocols were described in the literature.²²³

REFERENCES

1. Meares, C. F. & American Chemical Society. *Perspectives in bioconjugate chemistry*. (American Chemical Society, 1993).
2. Algar, W. R. in *Chemoselective and Bioorthogonal Ligation Reactions* 1–36 (Wiley-VCH Verlag GmbH & Co. KGaA, 2017). doi:10.1002/9783527683451.ch1
3. Hermanson, G. T. *Bioconjugate Techniques*. *Bioconjugate Techniques* (Elsevier, 2013).
4. Beck, A., Goetsch, L., Dumontet, C. & Corvaia, N. Strategies and challenges for the next generation of antibody–drug conjugates. *Nat. Rev. Drug Discov.* **16**, 315–337 (2017).
5. Chudasama, V., Maruani, A. & Caddick, S. Recent advances in the construction of antibody–drug conjugates. *Nat. Chem.* **8**, 114–119 (2016).
6. Sano, T., Smith, C. & Cantor, C. Immuno-PCR: very sensitive antigen detection by means of specific antibody–DNA conjugates. *Science* **258**, 120–122 (1992).
7. Kazane, S. a. *et al.* Site-specific DNA–antibody conjugates for specific and sensitive immuno-PCR. *Proc. Natl. Acad. Sci.* **109**, 3731–3736 (2012).
8. Cuellar, T. L. *et al.* Systematic evaluation of antibody-mediated siRNA delivery using an industrial platform of THIOMAB–siRNA conjugates. *Nucleic Acids Res.* **43**, 1189–1203 (2015).
9. Mathe, G. ., Tran Ba, L. O. C. . & Bernard, J. Effet sur la leucémie 1210 de la Souris d’une combinaison par diazotation d’A-méthoptérine et de y-globulines de hamsters porteurs de cette leucémie par hétéogreffe. *C.R. Hebd. Séances Acad. Sci., Série B* **246**, 1626–1628 (1958).
10. Perez, H. L. *et al.* Antibody–drug conjugates: Current status and future directions. *Drug Discov. Today* **19**, 869–881 (2014).
11. Trail, P. a *et al.* Cure of xenografted human carcinomas by BR96–doxorubicin immunoconjugates. *Science* **261**, 212–215 (1993).
12. Pietersz, G. a & Krauer, K. Antibody-targeted drugs for the therapy of cancer. *J. Drug Target.* **2**, 183–215 (1994).
13. Bross, P. F. *et al.* Approval summary: Gemtuzumab ozogamicin in relapsed acute myeloid leukemia. *Clinical Cancer Research* **7**, (2001).
14. Younes, A. *et al.* Brentuximab vedotin (SGN-35) for relapsed CD30-positive lymphomas. *N. Engl. J. Med.* **363**, 1812–1821 (2010).
15. Claro, R. A. De, McGinn, K. & Kwitkowski, V. U . S . Food and Drug Administration Approval Summary : Brentuximab Vedotin for the Treatment of Relapsed Hodgkin Lymphoma or Relapsed Systemic Anaplastic Large-Cell Lymphoma U . S . Food and Drug Administration Approval Summary : Lymphoma or Relapsed Sys. *Clin. Cancer Res.* **18**, 5845–5849 (2012).
16. Senter, P. D. & Sievers, E. L. The discovery and development of brentuximab vedotin for use in relapsed Hodgkin lymphoma and systemic anaplastic large cell lymphoma. *Nat. Biotechnol.* **30**, 631–637 (2012).
17. Amiri-Kordestani, L. *et al.* FDA approval: Ado-trastuzumab emtansine for the treatment of patients with HER2-positive metastatic breast cancer. *Clin. Cancer Res.* **20**, 4436–4441 (2014).
18. Ballantyne, A. & Dhillon, S. Trastuzumab emtansine: First global approval. *Drugs* **73**, 755–765 (2013).
19. Pfister, D., Ulmer, N., Klaue, A., Ingold, O. & Morbidelli, M. Modeling the Kinetics of Protein Conjugation Reactions. *Chemie Ing. Tech.* **88**, 1598–1608 (2016).
20. Kim, M. T., Chen, Y., Marhoul, J. & Jacobson, F. Statistical modeling of the drug load distribution on trastuzumab emtansine (Kadcyla), a lysine-linked antibody drug conjugate. *Bioconjug. Chem.* **25**, 1223–1232 (2014).
21. Goldmacher, V. S., Amphlett, G., Wang, L. & Lazar, A. C. Statistics of the Distribution of the

- Abundance of Molecules with Various Drug Loads in Maytansinoid Antibody–Drug Conjugates. *Mol. Pharm.* **12**, 1738–1744 (2015).
22. Hamblett, K. J. *et al.* Effects of drug loading on the antitumor activity of a monoclonal antibody drug conjugate. *Clin. Cancer Res.* **10**, 7063–7070 (2004).
 23. Willner, D. *et al.* (6-Maleimidocaproyl)hydrazone of doxorubicin. A new derivative for the preparation of immunoconjugates of doxorubicin. *Bioconjug. Chem.* **4**, 521–527 (1993).
 24. Doronina, S. O. *et al.* Development of potent monoclonal antibody auristatin conjugates for cancer therapy. *Nat. Biotechnol.* **21**, 778–784 (2003).
 25. Chudasama, V., Maruani, A. & Caddick, S. Recent advances in the construction of antibody–drug conjugates. *Nat. Chem.* **8**, 114–119 (2016).
 26. Sletten, E. M. & Bertozzi, C. R. Bioorthogonal Chemistry: Fishing for Selectivity in a Sea of Functionality. *Angew. Chemie Int. Ed.* **48**, 6974–6998 (2009).
 27. Finn, C. S. M. and M. G., McKay, C. S. & Finn, M. G. Click chemistry in complex mixtures: Bioorthogonal bioconjugation. *Chem. Biol.* **21**, 1075–1101 (2014).
 28. Lang, K. & Chin, J. W. Bioorthogonal reactions for labeling proteins. *ACS Chem. Biol.* **9**, 16–20 (2014).
 29. Kolb, H. C., Finn, M. G. & Sharpless, K. B. Click Chemistry: Diverse Chemical Function from a Few Good Reactions. *Angew. Chemie - Int. Ed.* **40**, 2004–2021 (2001).
 30. Stadtman, E. R. Protein oxidation and aging. *Free Radic. Res.* **40**, 1250–1258 (2006).
 31. Dommerholt, J., Rutjes, P. J. T. & Van Delft, F. L. Strain-Promoted 1,3-Dipolar Cycloaddition of Cycloalkynes and Organic Azides. *Top. Curr. Chem.* **374**, 16 (2016).
 32. Dommerholt, J. *et al.* Highly accelerated inverse electron-demand cycloaddition of electron-deficient azides with aliphatic cyclooctynes. *Nat. Commun.* **5**, 5378–5384 (2014).
 33. Maruani, A., Richards, D. A. & Chudasama, V. Dual modification of biomolecules. *Org. Biomol. Chem.* **14**, 6165–6178 (2016).
 34. Chen, X. & Wu, Y.-W. Selective chemical labeling of proteins. *Org. Biomol. Chem.* **14**, 5417–5439 (2016).
 35. Maruani, A. *et al.* A plug-and-play approach to antibody-based therapeutics via a chemoselective dual click strategy. *Nat. Commun.* **6**, 6645 (2015).
 36. Van Geel, R. *et al.* Chemoenzymatic Conjugation of Toxic Payloads to the Globally Conserved N-Glycan of Native mAbs Provides Homogeneous and Highly Efficacious Antibody–Drug Conjugates. *Bioconjug. Chem.* **26**, 2233–2242 (2015).
 37. Akkapeddi, P. *et al.* Construction of homogeneous antibody–drug conjugates using site-selective protein chemistry. *Chem. Sci.* **7**, 2954–2963 (2016).
 38. Gilis, D., Massar, S., Cerf, N. J. & Rooman, M. Optimality of the genetic code with respect to protein stability and amino-acid frequencies. *Genome Biol.* **2**, 1–12 (2001).
 39. Kramer, R. M., Shende, V. R., Motl, N., Pace, C. N. & Scholtz, J. M. Toward a Molecular Understanding of Protein Solubility: Increased Negative Surface Charge Correlates with Increased Solubility. *Biophys. J.* **102**, 1907–1915 (2012).
 40. Trainor, K., Broom, A. & Meiering, E. M. Exploring the relationships between protein sequence, structure and solubility. *Curr. Opin. Struct. Biol.* **42**, 136–146 (2017).
 41. Hoare, D. G. & Koshland, D. E. A Procedure for the Selective Modification of Carboxyl Groups in Proteins. *J. Am. Chem. Soc.* **2525**, 2057–2058 (1966).
 42. Hoare, D. G. & Koshland, D. E. A Method for the Quantitative Modification and Estimation of Carboxylic Acid Groups in Proteins A Method for the Quantitative Modification of Carboxylic Acid Groups in Proteins. *J. Biol. Chem.* **242**, 2447–2453 (1967).
 43. Totaro, K. A. *et al.* Systematic Investigation of EDC/sNHS-Mediated Bioconjugation Reactions for Carboxylated Peptide Substrates. *Bioconjug. Chem.* **27**, 994–1004 (2016).
 44. Woodward, R. A new synthesis of peptides. *J. Am. Chem. Soc.* **83**, 1010–1012 (1961).
 45. Wade, R., Whisson, M. E. & Szekerke, M. Some Serum Protein Nitrogen Mustard Complexes

- with High Chemotherapeutic Selectivity. *Nature* **215**, 1303–1304 (1967).
46. Rowland, G. F., O’neill, G. J. & Davies, D. a. L. Suppression of tumour growth in mice by a drug–antibody conjugate using a novel approach to linkage. *Nature* **255**, 487–488 (1975).
 47. Hurwitz, E. *et al.* The Covalent Binding of Daunomycin and Adriamycin to Antibodies, with Retention of Both Drug and Antibody Activities. *Cancer Res.* **35**, 1175–1181 (1975).
 48. Winkelhake, J. L. Effects of chemical modification of antibodies on their clearance from the circulation. Addition of simple aliphatic compounds by reductive alkylation and carbodiimide promoted amide formation. *J. Biol. Chem.* **252**, 1865–1868 (1977).
 49. Gautier, V., Boumeester, A. J., Lössl, P. & Heck, A. J. R. Lysine conjugation properties in human IgGs studied by integrating high-resolution native mass spectrometry and bottom-up proteomics. *Proteomics* **0**, 1–10 (2015).
 50. Chen, Y., Kim, M. T.-J., Zheng, L., Deperalta, G. & Jacobson, F. Structural Characterization of Cross-Linked species in Trastuzumab Emtansine (Kadcyla®). *Bioconjug. Chem.* **27**, 2037–2047 (2016).
 51. Rosen, C. B. *et al.* Template-directed covalent conjugation of DNA to native antibodies, transferrin and other metal-binding proteins. *Nat. Chem.* **6**, 804–809 (2014).
 52. Leavell, M. D., Novak, P., Behrens, C. R., Schoeniger, J. S. & Kruppa, G. H. Strategy for selective chemical cross-linking of tyrosine and lysine residues. *J. Am. Soc. Mass Spectrom.* **15**, 1604–1611 (2004).
 53. Chih, H.-W. *et al.* Identification of amino acid residues responsible for the release of free drug from an antibody-drug conjugate utilizing lysine-succinimidyl ester chemistry. *J. Pharm. Sci.* **100**, 2518–25 (2011).
 54. Koniev, O. *et al.* MAPN: First-in-class reagent for kinetically resolved thiol-to-thiol conjugation. *Bioconjug. Chem.* **26**, 1863–1867 (2015).
 55. Miao, Z., Hong, Y., Zhu, T. & Chucholowski, Aleksander, W. Drug-conjugates, conjugation methods, and uses thereof. WO2013173391A1 (2013).
 56. Varadarajan, A., Sharkey, R. M., Goldenberg, D. M. & Hawthorne, M. F. Conjugation of phenyl isothiocyanate derivatives of carborane to antitumor antibody and in vivo localization of conjugates in nude mice. *Bioconjug. Chem.* **2**, 102–110 (1991).
 57. Pei, R. *et al.* A monospecific HLA-B27 fluorescein isothiocyanate-conjugated monoclonal antibody for rapid, simple and accurate HLA-B27 typing. *Tissue Antigens* **41**, 200–203 (1993).
 58. Goding, J. W. Conjugation of antibodies with fluorochromes: Modifications to the standard methods. *J. Immunol. Methods* **13**, 215–226 (1976).
 59. Hudson, R. *et al.* The development and characterisation of porphyrin isothiocyanate–monoclonal antibody conjugates for photoimmunotherapy. *Br. J. Cancer* **92**, 1442–1449 (2005).
 60. Meares, C. F. *et al.* Conjugation of antibodies with bifunctional chelating agents: Isothiocyanate and bromoacetamide reagents, methods of analysis, and subsequent addition of metal ions. *Anal. Biochem.* **142**, 68–78 (1984).
 61. Linder, K. E. *et al.* Technetium labeling of monoclonal antibodies with functionalized BATOs. 1. TcCl(DMG)3PITC [phenyl isothiocyanate]. *Bioconjug. Chem.* **2**, 160–170 (1991).
 62. Mirzadeh, S., Brechbiel, M. W., Atcher, R. W. & Gansow, O. A. Radiometal labeling of immunoproteins: covalent linkage of 2-(4-isothiocyanatobenzyl)diethylenetriaminepentaacetic acid ligands to immunoglobulin. *Bioconjug. Chem.* **1**, 59–65 (1990).
 63. Wilbur, D. S. *et al.* Trifunctional conjugation reagents. Reagents that contain a biotin and a radiometal chelation moiety for application to extracorporeal affinity adsorption of radiolabeled antibodies. *Bioconjug. Chem.* **13**, 1079–1092 (2002).
 64. Dingels, C., Wurm, F., Wagner, M., Klok, H.-A. & Frey, H. Squaric Acid Mediated Chemoselective PEGylation of Proteins: Reactivity of Single-Step-Activated α -Amino

- Poly(ethylene glycol)s. *Chem. - A Eur. J.* **18**, 16828–16835 (2012).
65. Wurm, F. R. *et al.* Be squared: expanding the horizon of squaric acid-mediated conjugations. *Chem. Soc. Rev.* **42**, 8220 (2013).
 66. Ian Storer, R., Aciro, C. & Jones, L. H. Squaramides: physical properties, synthesis and applications. *Chem. Soc. Rev.* **40**, 2330–2346 (2011).
 67. Ximenis, M. *et al.* Kinetic Analysis and Mechanism of the Hydrolytic Degradation of Squaramides and Squaramic Acids. *J. Org. Chem.* **82**, 2160–2170 (2017).
 68. Rodney Hicks, C. J. *et al.* A desferrioxamine B squaramide ester for the incorporation of zirconium-89 into antibodies. *Chem. Commun. Chem. Commun* **52**, 11889–11892 (2016).
 69. Popkov, M., Rader, C., Gonzalez, B., Sinha, S. C. & Barbas, C. F. Small molecule drug activity in melanoma models may be dramatically enhanced with an antibody effector. *Int. J. Cancer* **119**, 1194–1207 (2006).
 70. Li, L.-S. *et al.* Chemical Adaptor Immunotherapy: Design, Synthesis, and Evaluation of Novel Integrin-Targeting Devices. *J. Med. Chem.* **47**, 5630–5640 (2004).
 71. Rader, C., Sinha, S. C., Popkov, M., Lerner, R. A. & Barbas, C. F. Chemically programmed monoclonal antibodies for cancer therapy: adaptor immunotherapy based on a covalent antibody catalyst. *Proc. Natl. Acad. Sci. U. S. A.* **100**, 5396–5400 (2003).
 72. Nicholas, K. M. *et al.* A cofactor approach to copper-dependent catalytic antibodies. *Proc. Natl. Acad. Sci. U. S. A.* **99**, 2648–53 (2002).
 73. Guo, F. *et al.* Breaking the one antibody-one target axiom. *Proc. Natl. Acad. Sci. U. S. A.* **103**, 11009–11014 (2006).
 74. Sinha, S. C., Das, S., Li, L.-S., Lerner, R. A. & Barbas, C. F. Preparation of integrin $\alpha(v)\beta(3)$ -targeting Ab 38C2 constructs. *Nat. Protoc.* **2**, 449–456 (2007).
 75. Doppalapudi, V. R. *et al.* Chemically programmed antibodies: Endothelin receptor targeting CovX-Bodies™. *Bioorg. Med. Chem. Lett.* **17**, 501–506 (2007).
 76. Smyth, M. J., Pietersz, G. A. & McKenzie, I. F. Selective enhancement of antitumor activity of N-acetyl melphalan upon conjugation to monoclonal antibodies. *Cancer Res.* **47**, 62–9 (1987).
 77. Wakankar, A. a. *et al.* Physicochemical stability of the antibody - Drug conjugate trastuzumab-DM1: Changes due to modification and conjugation processes. *Bioconjug. Chem.* **21**, 1588–1595 (2010).
 78. Del Rosario, R. B. & Wahl, R. L. Site-specific radiolabeling of monoclonal antibodies with biotin/streptavidin. *Int. J. Radiat. Appl. Instrumentation. Part B. Nucl. Med. Biol.* **16**, 525–529 (1989).
 79. Li, X. *et al.* Stable and Potent Selenomab-Drug Conjugates. *Cell Chem. Biol.* **24**, 433–442 (2017).
 80. Ponte, J. F. *et al.* Understanding How the Stability of the Thiol-Maleimide Linkage Impacts the Pharmacokinetics of Lysine-Linked Antibody-Maytansinoid Conjugates. *Bioconjug. Chem.* **27**, 1588–1598 (2016).
 81. Baldwin, A. D. & Kiick, K. L. Tunable degradation of maleimide-Thiol adducts in reducing environments. *Bioconjug. Chem.* **22**, 1946–1953 (2011).
 82. Shen, B.-Q. *et al.* Conjugation site modulates the in vivo stability and therapeutic activity of antibody-drug conjugates. *Nat. Biotechnol.* **30**, 184–9 (2012).
 83. Strop, P. *et al.* Location matters: Site of conjugation modulates stability and pharmacokinetics of antibody drug conjugates. *Chem. Biol.* **20**, 161–167 (2013).
 84. Lyon, R. P. P. *et al.* Self-hydrolyzing maleimides improve the stability and pharmacological properties of antibody-drug conjugates. *Nat. Biotechnol.* **32**, 1059–1062 (2014).
 85. Kalia, D., Pawar, S. P. & Thopate, J. S. Stable and Rapid Thiol Bioconjugation by Light-Triggered Thiomaleimide Ring Hydrolysis. *Angew. Chemie Int. Ed.* **56**, 1885–1889 (2017).
 86. Tumey, L. N. *et al.* Mild method for succinimide hydrolysis on ADCs: impact on ADC

- potency, stability, exposure, and efficacy. *Bioconjug. Chem.* **25**, 1871–80 (2014).
87. Fontaine, S. D., Reid, R., Robinson, L., Ashley, G. W. & Santi, D. V. Long-term stabilization of maleimide-thiol conjugates. *Bioconjug. Chem.* **26**, 145–152 (2015).
 88. Christie, R. J. *et al.* Stabilization of cysteine-linked antibody drug conjugates with N-aryl maleimides. *J. Control. Release* **220**, 660–670 (2015).
 89. Kolodych, S. *et al.* CBTF: New amine-to-thiol coupling reagent for preparation of antibody conjugates with increased plasma stability. *Bioconjug. Chem.* **26**, 197–200 (2015).
 90. Koniev, O. *et al.* Selective irreversible chemical tagging of cysteine with 3-arylpropionitriles. *Bioconjug. Chem.* **25**, 202–206 (2014).
 91. Patterson, J. T. *et al.* Improving the serum stability of site-specific antibody conjugates with sulfone linkers. *Bioconjug. Chem.* **25**, 1402–1407 (2014).
 92. Li, L. *et al.* Vinyl sulfone bifunctional derivatives of DOTA allow sulfhydryl- or amino-directed coupling to antibodies. Conjugates retain immunoreactivity and have similar biodistributions. *Bioconjug. Chem.* **13**, 110–115 (2002).
 93. Badescu, G. *et al.* A new reagent for stable thiol-specific conjugation. *Bioconjug. Chem.* **25**, 460–469 (2014).
 94. Toda, N., Asano, S. & Barbas, C. F. Rapid, Stable, Chemoselective Labeling of Thiols with Julia-Kociński-like Reagents: A Serum-Stable Alternative to Maleimide-Based Protein Conjugation. *Angew. Chemie Int. Ed.* **52**, 12592–12596 (2013).
 95. Vinogradova, E. V., Zhang, C., Spokoyny, A. M., Pentelute, B. L. & Buchwald, S. L. Organometallic palladium reagents for cysteine bioconjugation. *Nature* **526**, 687–691 (2015).
 96. Al-Shuaeeb, R. A. A. *et al.* Palladium-Catalyzed Chemoselective and Biocompatible Functionalization of Cysteine-Containing Molecules at Room Temperature. *Chem. - A Eur. J.* **22**, 11365–11370 (2016).
 97. Del Rosario, R. B., Wahl, R. L., Brocchini, S. J., Lawton, R. G. & Smith, R. H. Sulfhydryl Site-Specific Cross-Linking and Labeling of Monoclonal Antibodies by a Fluorescent Equilibrium Transfer Alkylation Cross-Link Reagent. *Bioconjugate Chem* **1**, 51–59 (1990).
 98. Liberatore, F. *et al.* Site-directed chemical modification and cross-linking of a monoclonal antibody using equilibrium transfer alkylating cross-link reagents. *Bioconjugate Chem.* **1**, 36–50 (1990).
 99. Lee, M. T. W. *et al.* Enabling the controlled assembly of antibody conjugates with a loading of two modules without antibody engineering. *Chem. Sci.* **8**, 2056–2060 (2017).
 100. Gupta, N. *et al.* Development of a facile antibody–drug conjugate platform for increased stability and homogeneity. *Chem. Sci.* **40**, 14–23 (2017).
 101. Kuan, S. L., Wang, T. & Weil, T. Site-Selective Disulfide Modification of Proteins: Expanding Diversity beyond the Proteome. *Chem. - A Eur. J.* **22**, 17112–17129 (2016).
 102. Wilbur, D. S., Stray, J. E., Hamlin, D. K., Curtis, D. K. & Vessella, R. L. Monoclonal antibody Fab' fragment cross-linking using equilibrium transfer alkylation reagents. A strategy for site-specific conjugation of diagnostic and therapeutic agents with F(ab')₂ fragments. *Bioconjug Chem* **5**, 220–235 (1994).
 103. Shaunak, S. *et al.* Site-specific PEGylation of native disulfide bonds in therapeutic proteins. *Nat. Chem. Biol.* **2**, 312–313 (2006).
 104. Balan, S. *et al.* Site-specific PEGylation of protein bisulfide bonds using a three-carbon bridge. *Bioconjug. Chem.* **18**, 61–76 (2007).
 105. Choi, J. *et al.* in *PEGylated Protein Drugs: Basic Science and Clinical Applications* 47–73 (Birkhäuser Basel, 2009). doi:10.1007/978-3-7643-8679-5_4
 106. Badescu, G. *et al.* Bridging Disulfides for Stable and Defined Antibody Drug Conjugates. *Bioconjug. Chem.* **25**, 1124–1136 (2014).
 107. Bryant, P. *et al.* In vitro and in vivo evaluation of cysteine rebridged trastuzumab-MMAE antibody drug conjugates with defined drug-to-antibody ratios. *Mol. Pharm.* **12**, 1872–1879

- (2015).
108. Wang, T. *et al.* Water-soluble allyl sulfones for dual site-specific labelling of proteins and cyclic peptides. *Chem. Sci.* **7**, 3234–3239 (2016).
 109. Jones, M. W. *et al.* Polymeric Dibromomaleimides As Extremely Efficient Disulfide Bridging Bioconjugation and Pegylation Agents. *J. Am. Chem. Soc.* **134**, 1847–1852 (2012).
 110. Behrens, C. R. *et al.* Antibody-Drug Conjugates (ADCs) Derived From Interchain Cysteine Cross-Linking Demonstrate Improved Homogeneity and Other Pharmacological Properties Over Conventional Heterogeneous ADCs. *Mol. Pharm.* **12**, 3986–3998 (2015).
 111. Hull, E. A. *et al.* Homogeneous bispecifics by disulfide bridging. *Bioconjug. Chem.* **25**, 1395–1401 (2014).
 112. Morais, M. *et al.* Optimisation of the dibromomaleimide (DBM) platform for native antibody conjugation by accelerated post-conjugation hydrolysis. *Org. Biomol. Chem.* **25**, 1871–1880 (2017).
 113. Castañeda, L. *et al.* Acid-cleavable thiomaleamic acid linker for homogeneous antibody-drug conjugation. *Chem. Commun. (Camb)*. **49**, 8187–9 (2013).
 114. Nunes, J. P. M. *et al.* Functional native disulfide bridging enables delivery of a potent, stable and targeted antibody-drug conjugate (ADC). *Chem. Commun.* **51**, 10624–10627 (2015).
 115. Richards, D. a *et al.* Photochemically re-bridging disulfide bonds and the discovery of a thiomaleimide mediated photodecarboxylation of C-terminal cysteines. *Org. Biomol. Chem.* **14**, 455–459 (2015).
 116. Robinson, E. *et al.* Pyridazinediones deliver potent, stable, targeted and efficacious antibody–drug conjugates (ADCs) with a controlled loading of 4 drugs per antibody. *RSC Adv.* **7**, 9073–9077 (2017).
 117. Lee, M. T. W., Maruani, A., Baker, J. R., Caddick, S. & Chudasama, V. Next-generation disulfide stapling: reduction and functional re-bridging all in one. *Chem. Sci.* **7**, 799–802 (2016).
 118. McGaughey, G. B., Gagné, M. & Rappé, A. K. π -Stacking interactions. Alive and well in proteins. *J. Biol. Chem.* **273**, 15458–15463 (1998).
 119. Tilley, S. D. & Francis, M. B. Tyrosine-selective protein alkylation using π -allylpalladium complexes. *J. Am. Chem. Soc.* **128**, 1080–1081 (2006).
 120. Joshi, N. S., Whitaker, L. R. & Francis, M. B. A three-component Mannich-type reaction for selective tyrosine bioconjugation. *J. Am. Chem. Soc.* **126**, 15942–15943 (2004).
 121. McFarland, J. M., Joshi, N. S. & Francis, M. B. Characterization of a Three-Component Coupling Reaction on Proteins by Isotopic Labeling and Nuclear Magnetic Resonance Spectroscopy. *J. Am. Chem. Soc.* **130**, 7639–7644 (2008).
 122. Romanini, D. W. & Francis, M. B. Attachment of Peptide Building Blocks to Proteins Through Tyrosine Bioconjugation. *Bioconjug. Chem.* **19**, 153–157 (2008).
 123. Seim, K. L., Obermeyer, A. C. & Francis, M. B. Oxidative Modification of Native Protein Residues Using Cerium(IV) Ammonium Nitrate. *J. Am. Chem. Soc.* **133**, 16970–16976 (2011).
 124. Ban, H., Gavrilyuk, J. & Barbas, C. F. Tyrosine bioconjugation through aqueous ene-type reactions: A click-like reaction for tyrosine. *J. Am. Chem. Soc.* **132**, 1523–1525 (2010).
 125. Ban, H. *et al.* Facile and stable linkages through tyrosine: Bioconjugation strategies with the tyrosine-click reaction. *Bioconjug. Chem.* **24**, 520–532 (2013).
 126. Kralovec, J., Singh, M., Mammen, M., Blair, A. H. & Ghose, T. Synthesis of site-specific methotrexate-IgG conjugates. *Cancer Immunol. Immunother.* **29**, 293–302 (1989).
 127. Kölmel, D. K. & Kool, E. T. Oximes and Hydrazones in Bioconjugation: Mechanism and Catalysis. *Chem. Rev.* **117**, 10358–10376 (2017).
 128. Gavrilyuk, J., Ban, H., Nagano, M., Hakamata, W. & Barbas, C. F. Formylbenzene Diazonium Hexafluorophosphate Reagent for Tyrosine-Selective Modification of Proteins and the Introduction of a Bioorthogonal Aldehyde. *Bioconjug. Chem.* **23**, 2321–2328 (2012).

129. Griebenow, N., Greven, S., Lobell, M., Dilmaç, A. M. & Bräse, S. A study on the trastuzumab conjugation at tyrosine using diazonium salts. *RSC Adv.* **5**, 103506–103511 (2015).
130. Sato, S., Nakamura, K. & Nakamura, H. Tyrosine-Specific Chemical Modification with in Situ Hemin-Activated Luminol Derivatives. *ACS Chem. Biol.* **10**, 2633–2640 (2015).
131. Bruins, J. J. *et al.* Inducible, Site-Specific Protein Labeling by Tyrosine Oxidation-Strain-Promoted (4 + 2) Cycloaddition. *Bioconjug. Chem.* **28**, 1189–1193 (2017).
132. Warwicker, J., Charonis, S. & Curtis, R. A. Lysine and arginine content of proteins: Computational analysis suggests a new tool for solubility design. *Mol. Pharm.* **11**, 294–303 (2014).
133. Ahmed, N. & Thornalley, P. J. Peptide Mapping of Human Serum Albumin Modified Minimally by Methylglyoxal in Vitro and in Vivo. *Ann. N. Y. Acad. Sci.* **1043**, 260–266 (2005).
134. Yankeelov Jr., Dempsey Mitchell, J. A. C. T. H. C., Yankeelov, J. A., Mitchell, C. D. & Crawford, T. H. Simple trimerization of 2,3-butanedione yielding a selective reagent for the modification of arginine in proteins. *J. Am. Chem. Soc.* **90**, 1664–1666 (1968).
135. Suckau, D., Mak, M. & Przybylski, M. Protein surface topology-probing by selective chemical modification and mass spectrometric peptide mapping. *Proc. Natl. Acad. Sci. U. S. A.* **89**, 5630–5634 (1992).
136. King, T. P. Selective Chemical Modification of Arginyl Residues. *Biochemistry* **5**, 3454–3459 (1966).
137. Takahashi, K. The Reaction of Phenylglyoxal with Arginine Residues in Proteins. *J. Biol. Chem.* **243**, 6171–6179 (1968).
138. Lo, T. W. C., Westwood, M. E., McLellan, A. C., Selwood, T. & Thornalleys, P. J. Binding and modification of proteins by methylglyoxal under physiological conditions. A kinetic and mechanistic study with N alpha-acetylarginine, N alpha-acetylcysteine, and N alpha-acetyllysine, and bovine serum albumin. *J. Biol. Chem.* **269**, 32299–32305 (1994).
139. Nakaya, K., Horinishi, H. & Shibata, K. States of Amino Acid Residues in Proteins XIV. Glyoxal as a Reagent for Discrimination of Arginine Residues. *J. Biochem.* **61**, 345–351 (1967).
140. Gauthier, M. A. & Klok, H.-A. Arginine-Specific Modification of Proteins with Polyethylene Glycol. *Biomacromolecules* **12**, 482–493 (2011).
141. Oya, T. *et al.* Methylglyoxal Modification of Protein: chemical and immunochemical characterization of methylglyoxal-arginine adducts. *J. Biol. Chem.* **274**, 18492–18502 (1999).
142. Vanoni, M. A., Pilone Simonetta, M., Curti, B., Negri, A. & Ronchi, S. Phenylglyoxal modification of arginines in mammalian D-amino-acid oxidase. *Eur. J. Biochem.* **167**, 261–267 (1987).
143. Stipani, I. *et al.* Inhibition of the Reconstituted Mitochondrial Oxoglutarate Carrier by Arginine-Specific Reagents. *Arch. Biochem. Biophys.* **331**, 48–54 (1996).
144. Mostafa, A. A. *et al.* Plasma protein advanced glycation end products, carboxymethyl cysteine, and carboxyethyl cysteine, are elevated and related to nephropathy in patients with diabetes. *Mol. Cell. Biochem.* **302**, 35–42 (2007).
145. Gao, Y. & Wang, Y. Site-Selective Modifications of Arginine Residues in Human Hemoglobin Induced by Methylglyoxal. *Biochemistry* **45**, 15654–15660 (2006).
146. Hensen, S. M. M. *et al.* Phenylglyoxal-based visualization of citrullinated proteins on western blots. *Molecules* **20**, 6592–6600 (2015).
147. Lewallen, D. M. *et al.* Chemical Proteomic Platform to Identify Citrullinated Proteins. *ACS Chem. Biol.* **10**, 2520–2528 (2015).
148. Clancy, K. W., Weerapana, E. & Thompson, P. R. Detection and identification of protein citrullination in complex biological systems. *Curr. Opin. Chem. Biol.* **30**, 1–6 (2016).
149. Thompson, D. A., Ng, R. & Dawson, P. E. Arginine selective reagents for ligation to peptides and proteins. *J. Pept. Sci.* **22**, 311–319 (2016).

150. Chumsae, C. *et al.* Arginine modifications by methylglyoxal: Discovery in a recombinant monoclonal antibody and contribution to acidic species. *Anal. Chem.* **85**, 11401–11409 (2013).
151. Gong, Y., Andina, D., Nahar, S., Jean-Christophe, L. & Gauthier, M. A. Releasable and Traceless PEGylation of Arginine-rich Antimicrobial Peptides. *Chem. Sci.* **8**, 4082–4086 (2017).
152. Gevaert, K., Van Damme, P., Martens, L. & Vandekerckhove, J. Diagonal reverse-phase chromatography applications in peptide-centric proteomics: Ahead of catalogue-omics? *Anal. Biochem.* **345**, 18–29 (2005).
153. Antos, J. M. & Francis, M. B. Selective tryptophan modification with rhodium carbenoids in aqueous solution. *J. Am. Chem. Soc.* **126**, 10256–10257 (2004).
154. Ruiz-Rodriguez, J., Albericio, F. & Lavilla, R. Postsynthetic modification of peptides: Chemoselective C-arylation of tryptophan residues. *Chem. - A Eur. J.* **16**, 1124–1127 (2010).
155. Popp, B. V. & Ball, Z. T. Structure-selective modification of aromatic side chains with dirhodium metallopeptide catalysts. *J. Am. Chem. Soc.* **132**, 6660–6662 (2010).
156. Williams, T. J., Reay, A. J., Whitwood, A. C. & Fairlamb, I. J. S. A mild and selective Pd-mediated methodology for the synthesis of highly fluorescent 2-arylated tryptophans and tryptophan-containing peptides: a catalytic role for Pd0 nanoparticles? *Chem. Commun.* **50**, 3052–3054 (2014).
157. Hansen, M. B., Hubálek, F., Skrydstrup, T. & Hoeg-Jensen, T. Chemo- and Regioselective Ethynylation of Tryptophan-Containing Peptides and Proteins. *Chem. - A Eur. J.* **22**, 1572–1576 (2016).
158. Seki, Y. *et al.* Transition Metal-Free Tryptophan-Selective Bioconjugation of Proteins. *J. Am. Chem. Soc.* **138**, 10798–10801 (2016).
159. Kramer, J. R. & Deming, T. J. Reversible chemoselective tagging and functionalization of methionine containing peptides. *Chem. Commun.* **49**, 5144–5146 (2013).
160. Boutureira, O. & Bernardes, G. J. L. Advances in chemical protein modification. *Chem. Rev.* **115**, 2174–2195 (2015).
161. Wang, W. *et al.* Impact of methionine oxidation in human IgG1 Fc on serum half-life of monoclonal antibodies. *Mol. Immunol.* **48**, 860–866 (2011).
162. Rademacher, T. W., Homans, S. W., Parekh, R. B. & Dwek, R. A. Immunoglobulin G as a glycoprotein. *Biochem. Soc. Symp.* **51**, 131–148 (1986).
163. Hamann, P. R. *et al.* An anti-MUC1 antibody-calicheamicin conjugate for treatment of solid tumors. Choice of linker and overcoming drug resistance. *Bioconjug. Chem.* **16**, 346–353 (2005).
164. Stan, A. C., Radu, D. L., Casares, S., Bona, C. A. & Brumeanu, T. D. Antineoplastic efficacy of doxorubicin enzymatically assembled on galactose residues of a monoclonal antibody specific for the carcinoembryonic antigen. *Cancer Res.* **59**, 115–121 (1999).
165. Zhou, Q. *et al.* Site-Specific Antibody–Drug Conjugation through Glycoengineering. *Bioconjug. Chem.* **25**, 510–520 (2014).
166. Parsons, T. B. *et al.* Optimal synthetic glycosylation of a therapeutic antibody. *Angew. Chemie - Int. Ed.* **55**, 2361–2367 (2016).
167. Jain, N., Smith, S. W., Ghone, S. & Tomczuk, B. Current ADC Linker Chemistry. *Pharm. Res.* **32**, 3526–3540 (2015).
168. Tsuchikama, K. & An, Z. Antibody-drug conjugates: recent advances in conjugation and linker chemistries. *Protein Cell* 1–14 (2016). doi:10.1007/s13238-016-0323-0
169. Koniev, O. & Wagner, A. Developments and recent advancements in the field of endogenous amino acid selective bond forming reactions for bioconjugation. *Chem. Soc. Rev.* **44**, 5495–5551 (2015).
170. Yoshitake, S., Yamada, Y., Ishikawa, E. & Masseyeff, R. Conjugation of Glucose Oxidase from *Aspergillus niger* and Rabbit Antibodies Using N-Hydroxysuccinimide Ester of N-(4-

- Carboxycyclohexylmethyl)-Maleimide. *Eur. J. Biochem.* **101**, 395–399 (1979).
171. Peeters, J. M., Hazendonk, T. G., Beuvery, E. C. & Tesser, G. I. Comparison of four bifunctional reagents for coupling peptides to proteins and the effect of the three moieties on the immunogenicity of the conjugates. *J. Immunol. Methods* **120**, 133–143 (1989).
 172. Hashida, S. & Ishikawa, E. Use of Normal IgG and its Fragments to Lower the Non-Specific Binding of Fab'-Enzyme Conjugates in Sandwich Enzyme Immunoassay. *Anal. Lett.* **18**, 1143–1155 (1985).
 173. Gould, J. B. & Marks, V. *Nonisotopic Immunoassay*. (Springer US, 1988).
 174. Uto, I. *et al.* Determination of urinary Tamm-Horsfall protein by ELISA using a maleimide method for enzyme-antibody conjugation. *J. Immunol. Methods* **138**, 87–94 (1991).
 175. Vogel, C.-W. *Immunoconjugates: Antibody Conjugates in Radioimaging and Therapy of Cancer*. (Oxford University Press, 1987).
 176. Erickson, H. K. *et al.* Antibody-maytansinoid conjugates are activated in targeted cancer cells by lysosomal degradation and linker-dependent intracellular processing. *Cancer Res.* **66**, 4426–4433 (2006).
 177. Polson, A. G. *et al.* Antibody-drug conjugates targeted to CD79 for the treatment of non-Hodgkin lymphoma. *Blood* **110**, 616–623 (2007).
 178. Tournier, E. J. M., Wallach, J. & Blond, P. Sulfosuccinimidyl 4-(N-maleimidomethyl)-1-cyclohexane carboxylate as a bifunctional immobilization agent. Optimization of the coupling conditions. *Anal. Chim. Acta* **361**, 33–44 (1998).
 179. Gee, K. R., Archer, E. A. & Kang, H. C. 4-Sulfotetrafluorophenyl (STP) esters: New water-soluble amine-reactive reagents for labeling biomolecules. *Tetrahedron Lett.* **40**, 1471–1474 (1999).
 180. Xu, K. *et al.* Characterization of the drug-to-antibody ratio distribution for antibody-drug conjugates in plasma/serum. *Bioanalysis* **5**, 1057–1071 (2013).
 181. Beck, A. *et al.* Cutting-edge mass spectrometry methods for the multi-level structural characterization of antibody-drug conjugates. *Expert review of proteomics* **13**, 157–183 (2016).
 182. Dovgan, I., Kolodych, S., Koniev, O. & Wagner, A. 2-(Maleimidomethyl)-1,3-Dioxanes (MD): a Serum-Stable Self-hydrolysable Hydrophilic Alternative to Classical Maleimide Conjugation. *Sci. Rep.* **6**, 30835 (2016).
 183. Marcoux, J. *et al.* Native mass spectrometry and ion mobility characterization of trastuzumab emtansine, a lysine-linked antibody drug conjugate. *Protein Sci.* **24**, 1210–1223 (2015).
 184. Terral, G., Beck, A. & Cianfèrani, S. Insights from native mass spectrometry and ion mobility-mass spectrometry for antibody and antibody-based product characterization. *J. Chromatogr. B* **1032**, 79–90 (2016).
 185. Koniev, O. Development of new bioselective ligation reactions. (Université de Strasbourg, 2014).
 186. Montalbetti, C. A. G. N. & Falque, V. Amide bond formation and peptide coupling. *Tetrahedron* **61**, 10827–10852 (2005).
 187. Valeur, E. & Bradley, M. Amide bond formation: beyond the myth of coupling reagents. *Chem Soc Rev* **38**, 606–631 (2009).
 188. Al-Warhi, T. I., Al-Hazimi, H. M. A. & El-Faham, A. Recent development in peptide coupling reagents. *J. Saudi Chem. Soc.* **16**, 97–116 (2012).
 189. Woodward, R. B. & Olofson, R. a. The reaction of isoxazolium salts with nucleophiles. *Tetrahedron* **22**, 415–440 (1966).
 190. Llamas, K., Owens, M., Blakeley, R. L. & Zerner, B. N-Ethyl-5-phenylisoxazolium- 3'-sulfonate (Woodward's Reagent K) as a Reagent for Nucleophilic Side Chains of Proteins. *J. Am. Chem. Soc.* **108**, 5543–5548 (1986).
 191. Shiu, H.-Y. *et al.* Electron-Deficient Alkynes as Cleavable Reagents for the Modification of

- Cysteine-Containing Peptides in Aqueous Medium. *Chem. - A Eur. J.* **15**, 3839–3850 (2009).
192. Jafari, M. R., Lakusta, J., Lundgren, R. J. & Derda, R. Allene Functionalized Azobenzene Linker Enables Rapid and Light-Responsive Peptide Macrocyclization. *Bioconjug. Chem.* **27**, 509–514 (2016).
 193. Jedrzejczak, M., Motie, R. E., Satchell, D. P. N., Satchell, R. S. & Wassef, W. N. Kinetics of Aminolysis of some Benzoyl Fluorides and Benzoic Anhydrides in Non-hydroxylic Solvents. *J. Chem. Soc., Perkin Trans. 2* **78**, 1471–1479 (1994).
 194. Prabhu, G., Narendra, N., Basavaprabhu, B., Panduranga, V. & Sureshbabu, V. V. Amino acid fluorides: viable tools for synthesis of peptides, peptidomimetics and enantiopure heterocycles. *RSC Adv.* **5**, 48331–48362 (2015).
 195. Carpino, L. A., Beyermann, M., Wenschuh, H. & Bienert, M. Peptide Synthesis via Amino Acid Halides. *Acc. Chem. Res.* **29**, 268–274 (1996).
 196. Due-Hansen, M. E. *et al.* A Protocol for Amide Bond Formation with Electron Deficient Amines and Sterically Hindered Substrates. *Org. Biomol. Chem.* **14**, 430–433 (2016).
 197. El-Faham, A. & Albericio, F. Peptide Coupling Reagents, More than a Letter Soup. *Chem. Rev.* **111**, 6557–6602 (2011).
 198. Hemantha, H., Chennakrishnareddy, G., Vishwanatha, T. & Sureshbabu, V. One-Pot Synthesis of Ureido Peptides and Urea-Tethered Glycosylated Amino Acids Employing Deoxo-Fluor and TMSN₃. *Synlett* **2009**, 407–410 (2009).
 199. Nagendra, G., Lamani, R. S., Narendra, N. & Sureshbabu, V. V. A convenient synthesis of 1,3,4-thiadiazole and 1,3,4-oxadiazole based peptidomimetics employing diacylhydrazines derived from amino acids. *Tetrahedron Lett.* **51**, 6338–6341 (2010).
 200. Bianco, A., Sonksen, C. P., Roepstorff, P. & Briand, J.-P. Solid-Phase Synthesis and Structural Characterization of Highly Substituted Hydroxyproline-Based 2,5-Diketopiperazines. *J. Org. Chem.* **65**, 2179–2187 (2000).
 201. Hung, K., Harris, P. W. R. & Brimble, M. A. Synthesis of the Peptaibol Framework of the Anticancer Agent Culicinin D: Stereochemical Assignment of the AHMOD Moiety. *Org. Lett.* **14**, 5784–5787 (2012).
 202. Sakamoto, K., Nakahara, Y. & Ito, Y. Combination of silyl carbamate and amino acid fluoride for solid-phase peptide synthesis. *Tetrahedron Lett.* **43**, 1515–1518 (2002).
 203. Sintes, M. *et al.* Electrophilic, Activation-Free Fluorogenic Reagent for Labeling Bioactive Amines. *Bioconjug. Chem.* **27**, 1430–1434 (2016).
 204. Kielland, N., Vendrell, M., Lavilla, R. & Chang, Y.-T. Imaging histamine in live basophils and macrophages with a fluorescent mesoionic acid fluoride. *Chem. Commun.* **48**, 7401 (2012).
 205. Romieu, A. *et al.* The first comparative study of the ability of different hydrophilic groups to water-solubilise fluorescent BODIPY dyes. *New J. Chem.* **37**, 1016–1027 (2013).
 206. Fredriksson, S. *et al.* Protein detection using proximity-dependent DNA ligation assays. *Nat. Biotechnol.* **20**, 473–477 (2002).
 207. Sugo, T. *et al.* Development of antibody-siRNA conjugate targeted to cardiac and skeletal muscles. *J. Control. Release* **237**, 1–13 (2016).
 208. Oh, Y. K. & Park, T. G. siRNA delivery systems for cancer treatment. *Adv. Drug Deliv. Rev.* **61**, 850–862 (2009).
 209. Bumcrot, D., Manoharan, M., Koteliansky, V. & Sah, D. W. Y. RNAi therapeutics: a potential new class of pharmaceutical drugs. *Nat. Chem. Biol.* **2**, 711–719 (2006).
 210. Gunasekaran, K., Nguyen, T. H., Maynard, H. D., Davis, T. P. & Bulmus, V. Conjugation of siRNA with comb-type PEG enhances serum stability and gene silencing efficiency. *Macromol. Rapid Commun.* **32**, 654–659 (2011).
 211. Harris, J. M. & Chess, R. B. Effect of pegylation on pharmaceuticals. *Nat. Rev. Drug Discov.* **2**, 214–221 (2003).
 212. Holder, P. G. & Rabuka, D. in *Biosimilars of Monoclonal Antibodies* 591–640 (John Wiley &

- Sons, Inc., 2016).
213. Lyubchenko, Y. L., Gall, A. A. & Shlyakhtenko, L. S. Visualization of DNA and protein-DNA complexes with atomic force microscopy. *Methods Mol. Biol.* **1117**, 367–384 (2014).
 214. Chen, X., Muthoosamy, K., Pfisterer, A., Neumann, B. & Weil, T. Site-selective lysine modification of native proteins and peptides via kinetically controlled labeling. *Bioconjug. Chem.* **23**, 500–508 (2012).
 215. Versteegen, R. M., Rossin, R., ten Hoeve, W., Janssen, H. M. & Robillard, M. S. Click to Release: Instantaneous Doxorubicin Elimination upon Tetrazine Ligation. *Angew. Chemie Int. Ed.* **52**, 14112–14116 (2013).
 216. Xu, M., Tu, J. & Franzini, R. M. Rapid and efficient tetrazine-induced drug release from highly stable benzonorbornadiene derivatives. *Chem. Commun.* **53**, 6271–6274 (2017).
 217. Rossin, R. *et al.* Triggered Drug Release from an Antibody-Drug Conjugate Using Fast ‘click-to-Release’ Chemistry in Mice. *Bioconjug. Chem.* **27**, 1697–1706 (2016).
 218. Das, M., Jain, R., Agrawal, A. K., Thanki, K. & Jain, S. Macromolecular Bipill of Gemcitabine and Methotrexate Facilitates Tumor-Specific Dual Drug Therapy with Higher Benefit-to-Risk Ratio. *Bioconjug. Chem.* **25**, 501–509 (2014).
 219. Vineberg, J. G. *et al.* Design, Synthesis, and Biological Evaluations of Tumor-Targeting Dual-Warhead Conjugates for a Taxoid–Camptothecin Combination Chemotherapy. *J. Med. Chem.* **57**, 5777–5791 (2014).
 220. Richards, D. A., Maruani, A. & Chudasama, V. Antibody fragments as nanoparticle targeting ligands: a step in the right direction. *Chem. Sci.* **0**, 1–15 (2016).
 221. Guzaev, A. & Lönnberg, H. Bis(hydroxymethylation) of the Active Methylene Group of 1,3-Dicarbonyl and Related Compounds. *Synthesis (Stuttg)*. **1997**, 1281–1284 (1997).
 222. Melnick, M. *et al.* Bis tertiary amide inhibitors of the HIV-1 protease generated via protein structure-based iterative design. *J. Med. Chem.* **39**, 2795–2811 (1996).
 223. Dovgan, I. *et al.* Acyl Fluorides: Fast, Efficient, and Versatile Lysine-Based Protein Conjugation via Plug-and-Play Strategy. *Bioconjug. Chem.* **28**, 1452–1457 (2017).

ANNEXES

Annex 1

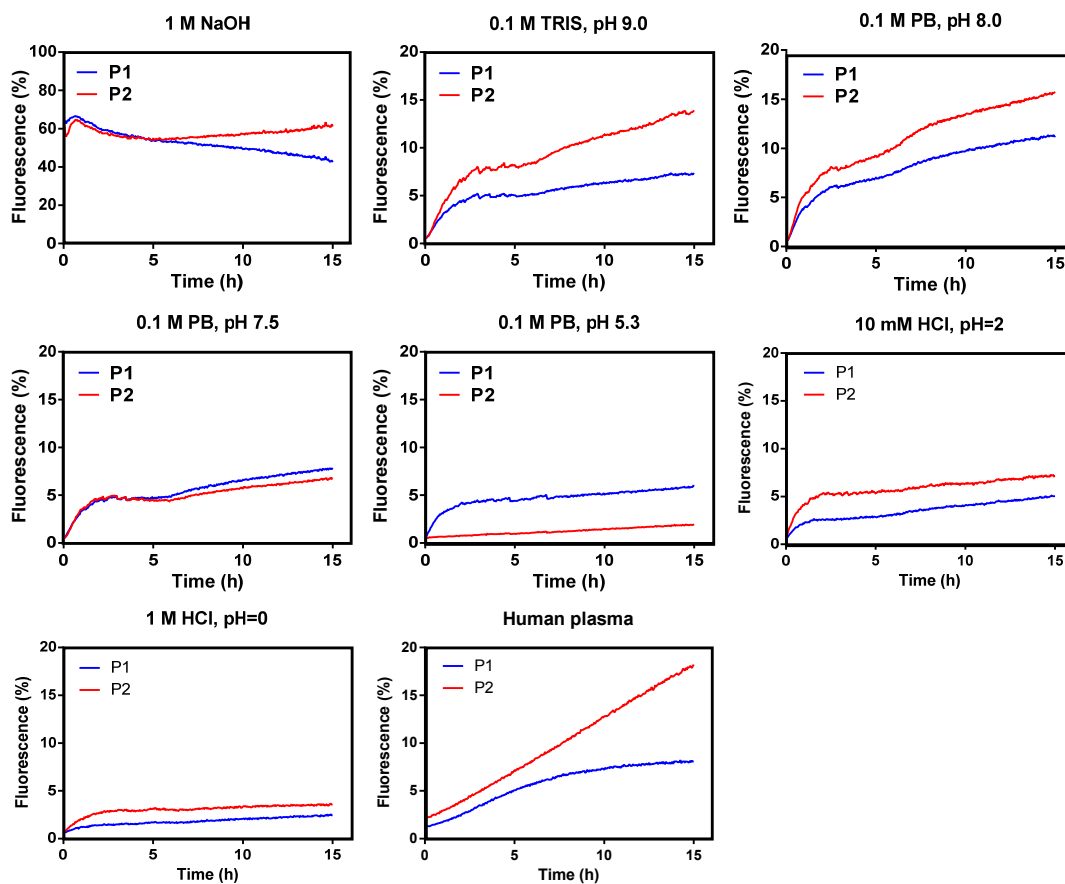


Figure S1. Evolution in time of the fluorescence of MD-based (**P1**) and MCC-based (**P2**) probes ($1\mu\text{M}$) in different media at $37\text{ }^{\circ}\text{C}$. Excitation at 550 nm , emission at 580 nm .

Table S1. Normalised fluorescence of MD-based (**P1**) and MCC-based (**P2**) probes ($1\mu\text{M}$) after 12h and 72h in different media at $37\text{ }^{\circ}\text{C}$.

Condition	Fluorescence of P1 after		Fluorescence of P2 after	
	12h	72h	12h	72h
Plasma, pH 7.4	8%	8%	15%	40%
TRIS 0.1M, pH 9.0	7%	8%	12%	16%
PB 0.1 M, pH 7.4	7%	9%	6%	9%
10mM HCl, pH 2.0	5%	8%	7%	10%
1M HCl, pH 0	2%	5%	4%	5%

Annex 2

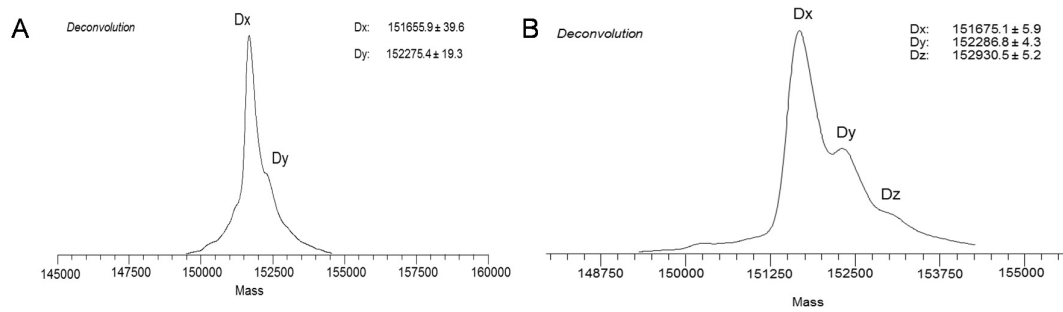


Figure S2. Deconvoluted mass spectra of the deglycosylated ACs. A. Trastuzumab-MD-TAMRA (DoC 8.1). B. Trastuzumab-MCC-TAMRA (DoC 8.3).

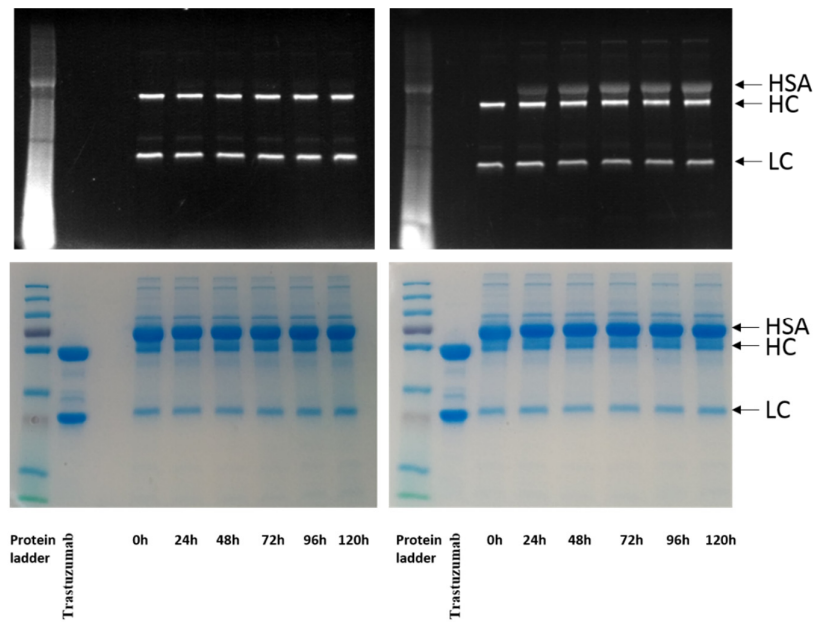


Figure S3. Stability test of C1 (left) and C2 (right) in human plasma Fluorescent gel (up) and CB-stained gel (down).

Annex 3

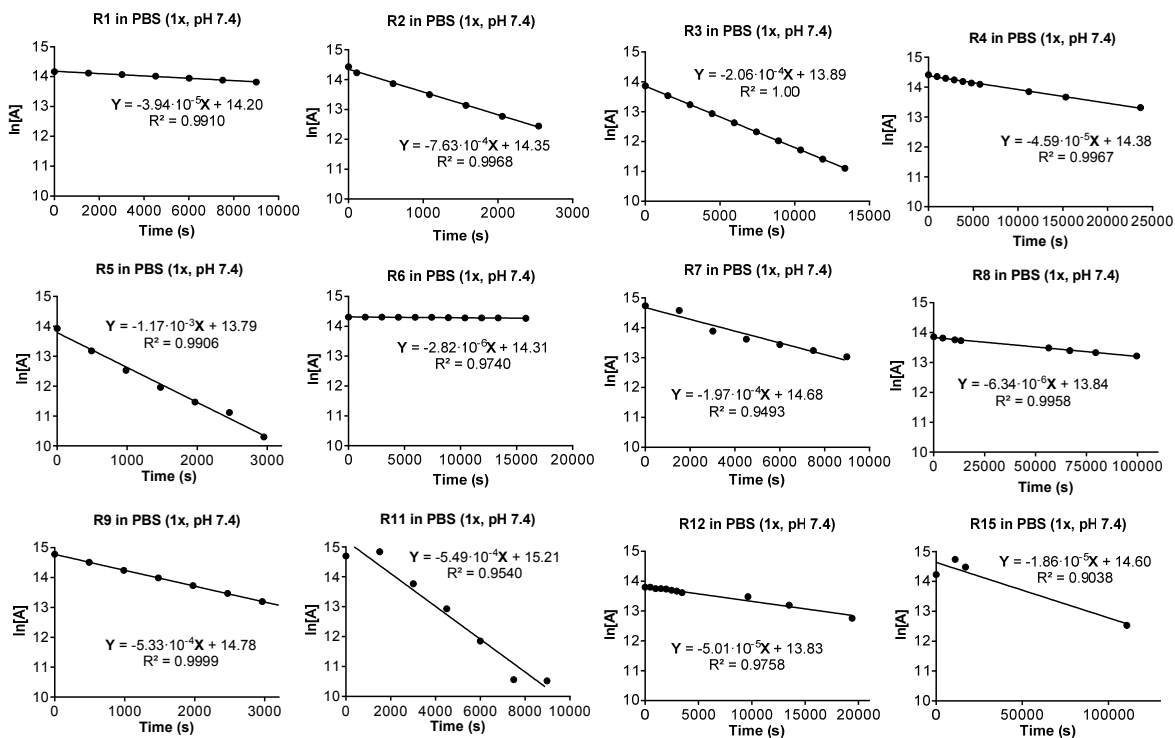


Figure S4. Hydrolytic stability of electrophiles over time monitored by LC-MS at 254 nm.

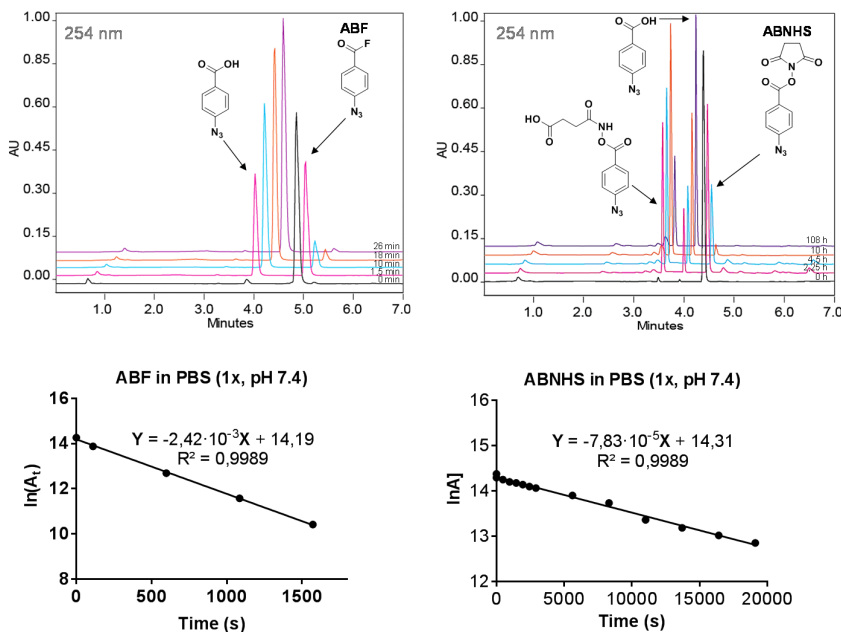


Figure S5. Hydrolysis of ABF and ABNHS in PBS (1x, pH 7.4) monitored by LC-MS at 254 nm and plot of kinetic data.

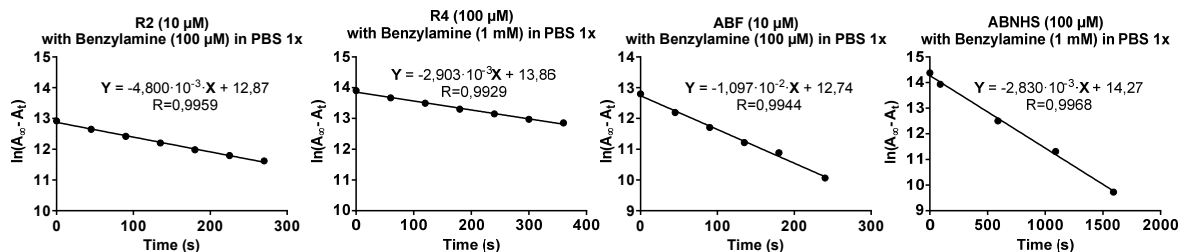


Figure S6. Plot of kinetic data for the aminolysis of **R2**, **R4**, **ABF** and **ABNHS** in PBS (1x, pH 7.4).

Table S2. Rate constants of hydrolysis and aminolysis of the acylating reagents

Compound	Hydrolysis in PBS 1x ^a	Aminolysis with benzylamine in PBS 1x ^a	
	$k_1/10^{-4}, \text{s}^{-1}$	$k_2, \text{L} \cdot \text{mol}^{-1} \cdot \text{s}^{-1}$	$t_{1/2}, \text{min}^b$
DMBF (R2)	7.71	39.80	4.2
DMBNHS (R4)	0.47	2.77	60.2
ABF	24.59	87.95	1.9
ABNHS	0.77	2.72	62

^a reproduced to within $\pm 5\%$; ^b $C_0(\text{BnNH}_2) = C_0(\text{ABF or ABNHS}) = 100 \mu\text{M}$

Table S3. Efficacy of conjugation step using **ABF** or **ABNHS** determined from native-HRMS of **T-TAMRA** conjugates

Conditions			Compound			
Quantity of acylating reagents, equiv.	$t, ^\circ\text{C}$	Time, min	ABNHS		ABF	
			DAR ^a	Efficacy ^b , %	DAR	Efficacy, %
4	4	15	0	0	2.19	54.8
		120	0.16	4.0	2.74	68.5
4	25	15	0.27	6.8	2.87	71.8
		120	1.81	45.3	2.94	73.5
3	25	15	0.19	6.3	2.34	78.0
		120	0.79	26.3	2.31	77.0

^a DAR = average dye to antibody ratio; ^b Efficacy = DAR/Quantity of acylating reagent (equiv.) · 100%

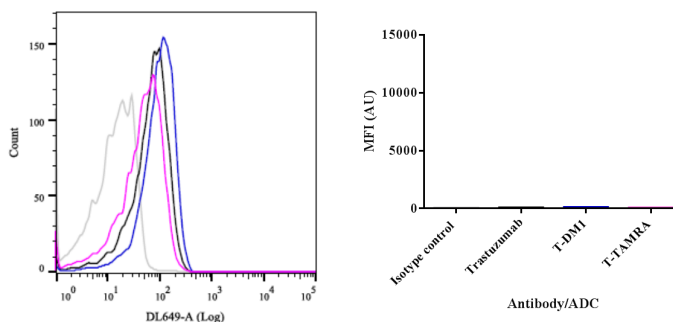


Figure S7. Median fluorescence intensities (MFIs) of ABF-based T-TAMRA (pink), the benchmark T-DM1 (blue) and the native antibody trastuzumab (black) in HER2⁺ MDA-MB-231 cells. Rituximab was used as isotype control (grey). The scale of the bar-plot was adapted to that of Figure 43.

Gel Fluorescence (Cy3 excitation)

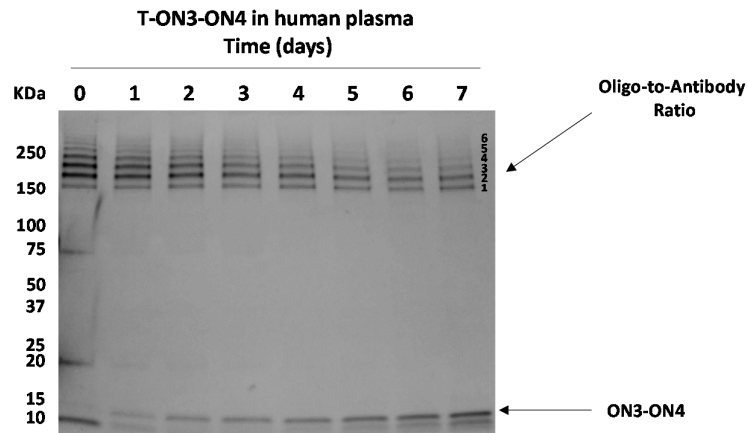


Figure S8. Stability of T-ON3-ON4 in human plasma at 37 °C, fluorescent gel under Cy3 excitation showed appearance of the **ON3-ON4** over time.

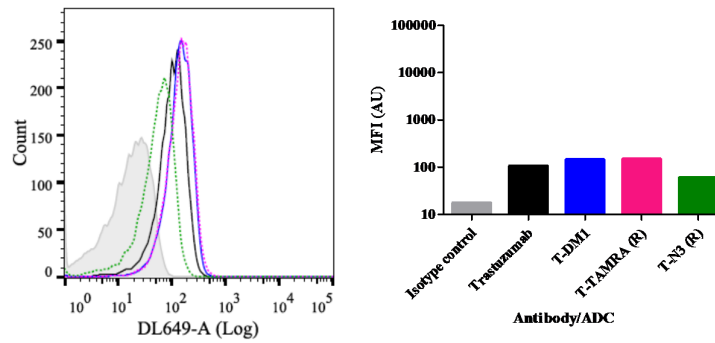
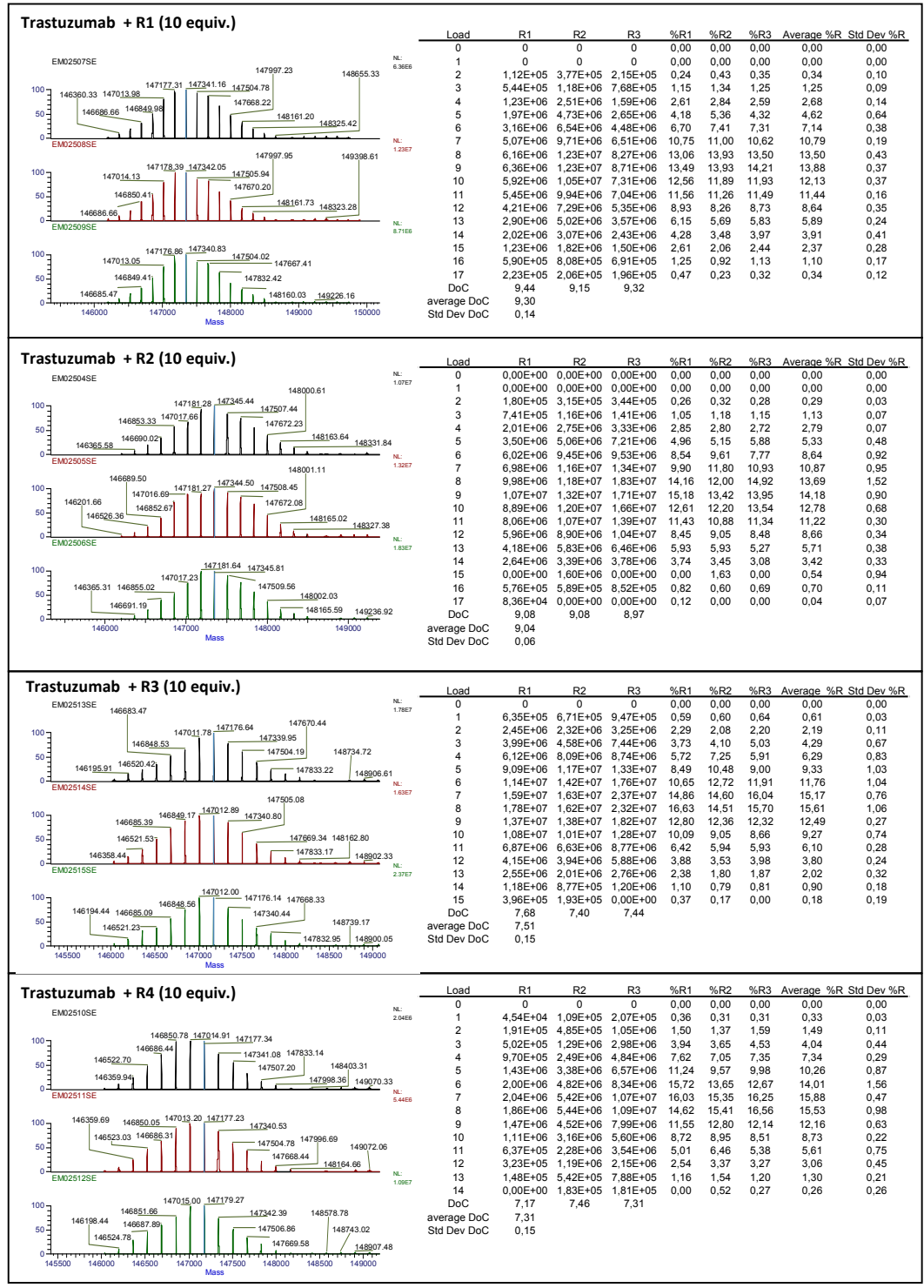


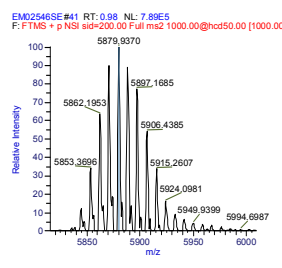
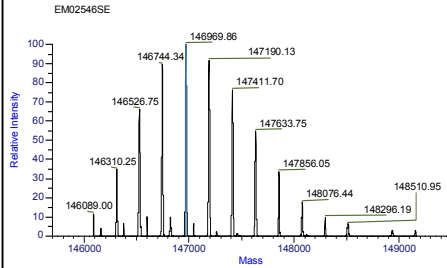
Figure S9. Median fluorescence intensities (MFIs) of trastuzumab (black), the reference T-DM1 (blue), T-TAMRA(R) (pink) and T-N3(R) in HER2- MDA-MB-231 cells. Rituximab was used as isotype control (grey). The scale of the bar-plot was adapted to that of Figure 52.

Annex 4

Native-HRMS spectra

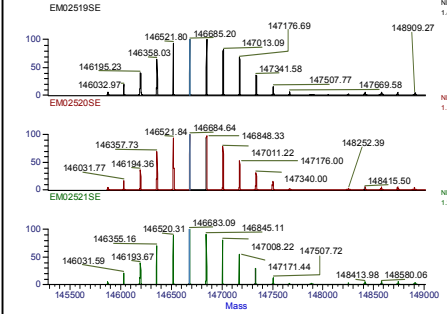


Trastuzumab + R5 (10 equiv.)



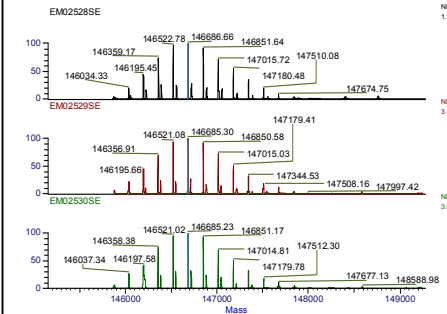
Load	R1	%R1
0	0	0.00
1	1.20E+06	1.94
2	3.62E+06	5.85
3	6.92E+06	11.17
4	9.38E+06	15.15
5	1.05E+07	16.95
6	9.59E+06	15.48
7	7.99E+06	12.90
8	5.73E+06	9.25
9	3.50E+06	5.65
10	1.84E+06	2.97
11	1.01E+06	1.63
12	6.53E+05	1.05
DoC	5.61	
average DoC	5.61	

Trastuzumab + R6 (10 equiv.)



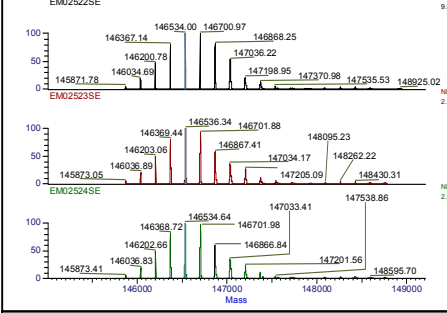
Load	R1	R2	R3	%R1	%R2	%R3	Average %R	Std Dev %R
0	6.13E+05	4.45E+05	5.43E+05	0.66	0.63	0.72	0.67	0.04
1	2.88E+06	1.95E+06	2.64E+06	3.11	2.78	3.50	3.13	0.36
2	5.84E+06	4.32E+06	4.95E+06	6.32	6.16	6.56	6.35	0.20
3	9.57E+06	8.03E+06	8.90E+06	10.35	11.45	11.79	11.20	0.75
4	1.37E+07	1.11E+07	1.14E+07	14.82	15.83	15.11	15.25	0.52
5	1.48E+07	1.19E+07	1.29E+07	16.01	16.97	17.09	16.69	0.59
6	1.47E+07	1.15E+07	1.16E+07	15.90	16.40	15.37	15.89	0.51
7	1.20E+07	9.22E+06	1.02E+07	12.98	13.15	13.52	13.21	0.28
8	9.87E+06	6.09E+06	6.93E+06	10.68	8.68	9.18	9.51	1.04
9	5.36E+06	3.62E+06	3.63E+06	5.80	5.16	4.81	5.26	0.50
10	2.27E+06	1.76E+06	1.53E+06	2.46	2.51	2.03	2.33	0.26
11	8.55E+05	2.02E+05	2.41E+05	0.92	0.29	0.32	0.51	0.36
DoC	5.45	5.32	5.25					
average DoC	5.34							
Std Dev DoC	0.10							

Trastuzumab + R7 (10 equiv.)



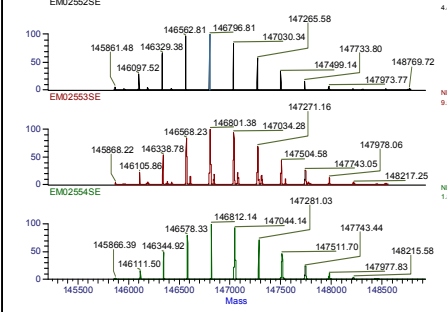
Load	R1	R2	R3	%R1	%R2	%R3	Average %R	Std Dev %R
0	4.16E+04	1.99E+05	1.62E+05	0.40	0.97	0.92	0.76	0.32
1	7.68E+05	1.53E+06	1.21E+06	7.32	7.46	6.85	7.21	0.32
2	1.29E+06	2.39E+06	2.22E+06	12.30	11.65	12.57	12.17	0.47
3	1.69E+06	3.23E+06	2.82E+06	16.11	15.74	15.96	15.94	0.19
4	1.76E+06	3.50E+06	3.00E+06	16.78	17.05	16.98	16.94	0.14
5	1.59E+06	3.17E+06	2.74E+06	15.15	15.45	15.51	15.37	0.19
6	1.25E+06	2.52E+06	2.07E+06	11.91	12.28	11.72	11.97	0.28
7	9.46E+05	1.73E+06	1.51E+06	9.02	8.43	8.55	8.66	0.31
8	6.10E+05	1.12E+06	9.73E+05	5.81	5.46	5.51	5.59	0.19
9	3.24E+05	5.98E+05	5.24E+05	3.09	2.91	2.97	2.99	0.09
10	1.36E+05	3.74E+05	2.88E+05	1.30	1.82	1.63	1.58	0.27
11	5.17E+04	1.21E+05	1.17E+05	0.49	0.59	0.66	0.58	0.09
12	3.43E+04	4.11E+04	2.98E+04	0.33	0.20	0.17	0.23	0.08
DoC	4.54	4.53	4.52					
average DoC	4.53							
Std Dev DoC	0.01							

Trastuzumab + R8 (10 equiv.)



Load	R1	R2	R3	%R1	%R2	%R3	Average %R	Std Dev %R
0	4.33E+05	1.01E+06	1.26E+05	0.84	0.99	1.02	0.95	0.10
1	1.94E+06	4.22E+06	4.96E+05	3.77	4.16	4.01	3.98	0.20
2	4.62E+06	1.04E+07	1.26E+06	8.97	10.24	10.20	9.80	0.73
3	7.97E+06	1.70E+07	2.12E+06	15.47	16.75	17.16	16.46	0.88
4	9.88E+06	2.13E+07	2.59E+06	19.17	20.98	20.96	20.37	1.04
5	9.97E+06	1.96E+07	2.49E+06	19.35	19.31	20.15	19.60	0.48
6	8.07E+06	1.18E+07	1.48E+06	15.66	11.62	11.98	13.09	2.24
7	5.21E+06	7.42E+06	8.52E+05	10.11	7.31	6.90	8.11	1.75
8	1.93E+06	5.71E+06	5.61E+05	3.75	5.62	4.54	4.64	0.94
9	1.08E+06	2.11E+06	2.80E+05	2.10	2.08	2.27	2.15	0.10
10	4.23E+05	9.44E+05	1.00E+05	0.82	0.93	0.81	0.85	0.07
DoC	4.63	4.49	4.45					
average DoC	4.53							
Std Dev DoC	0.09							

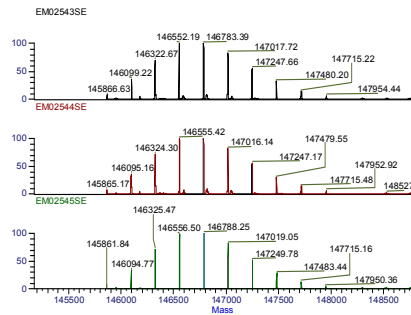
Trastuzumab + R9 (10 equiv.)



Load	R1	R2	R3	%R1	%R2	%R3	Average %R	Std Dev %R
0	2.21E+06	2.56E+05	2.51E+05	1.03	0.53	0.27	0.61	0.38
1	1.24E+07	2.00E+06	2.90E+06	5.76	4.15	3.16	4.36	1.31
2	2.88E+07	5.00E+06	8.98E+06	13.39	10.38	9.79	11.19	1.93
3	4.19E+07	7.90E+06	1.48E+07	19.48	16.40	16.13	17.34	1.86
4	4.41E+07	9.58E+06	1.87E+07	20.50	19.89	20.38	20.26	0.33
5	3.64E+07	8.88E+06	1.72E+07	16.92	18.43	18.75	18.03	0.98
6	2.48E+07	6.56E+06	1.32E+07	11.53	13.62	14.39	13.18	1.48
7	1.42E+07	4.06E+06	8.52E+06	6.60	8.43	9.29	8.11	1.37
8	6.80E+06	2.39E+06	4.37E+06	3.16	4.96	4.76	4.30	0.99
9	2.73E+06	1.12E+06	1.94E+06	1.27	2.33	2.11	1.90	0.56
10	7.76E+05	3.05E+05	7.23E+05	0.36	0.63	0.79	0.59	0.22
11	0.00E+00	1.19E+05	1.55E+05	0.00	0.25	0.17	0.14	0.13
DoC	4.13	4.56	4.65					
average DoC	4.45							
Std Dev DoC	0.28							

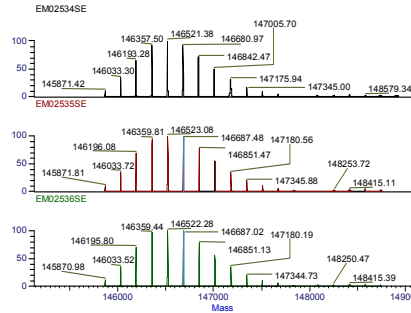


Trastuzumab + R10 (10 equiv.)



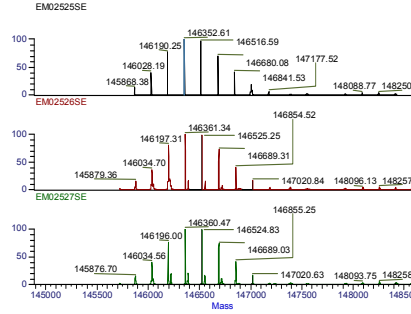
Load	R1	R2	R3	%R1	%R2	%R3	Average %R	Std Dev %R
0	1,22E+06	1,29E+06	1,70E+06	1,43	1,42	1,45	1,43	0,02
1	5,98E+06	6,46E+06	8,11E+06	7,03	7,10	6,91	7,01	0,09
2	1,18E+07	1,30E+07	1,70E+07	13,87	14,29	14,49	14,22	0,32
3	1,69E+07	1,83E+07	2,33E+07	19,86	20,11	19,86	19,94	0,14
4	1,70E+07	1,82E+07	2,42E+07	19,98	20,00	20,63	20,20	0,37
5	1,40E+07	1,48E+07	1,95E+07	16,45	16,26	16,62	16,45	0,18
6	9,39E+06	9,99E+06	1,25E+07	11,04	10,98	10,66	10,89	0,21
7	5,43E+06	5,40E+06	6,83E+06	6,38	5,93	5,82	6,05	0,30
8	2,40E+06	2,60E+06	3,14E+06	2,82	2,86	2,68	2,78	0,10
9	9,62E+05	9,62E+05	1,03E+06	1,13	1,06	0,88	1,02	0,13
DoC	4,00	3,97	3,95					
average DoC				3,97				
Std Dev DoC				0,03				

Trastuzumab + R11 (10 equiv.)



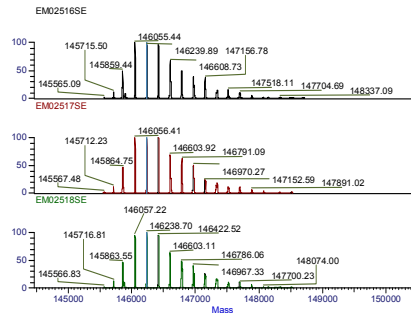
Load	R1	R2	R3	%R1	%R2	%R3	Average %R	Std Dev %R
0	6,05E+06	8,94E+06	8,84E+06	5,90	5,79	5,76	5,82	0,08
1	1,19E+07	1,77E+07	1,78E+07	11,61	11,47	11,59	11,55	0,08
2	1,68E+07	2,47E+07	2,47E+07	16,39	16,00	16,08	16,16	0,20
3	1,84E+07	2,62E+07	2,58E+07	17,95	16,97	16,80	17,24	0,62
4	1,65E+07	2,50E+07	2,50E+07	16,09	16,20	16,26	16,18	0,08
5	1,31E+07	2,01E+07	1,99E+07	12,78	13,02	12,96	12,92	0,13
6	9,03E+06	1,40E+07	1,41E+07	8,81	9,07	9,18	9,02	0,19
7	5,59E+06	8,76E+06	8,72E+06	5,42	5,68	5,68	5,59	0,15
8	3,09E+06	4,95E+06	4,93E+06	2,98	3,21	3,21	3,13	0,13
9	1,53E+06	2,47E+06	2,41E+06	1,49	1,60	1,57	1,55	0,06
10	5,89E+05	1,12E+06	1,10E+06	0,57	0,73	0,72	0,67	0,08
11	0,00E+00	4,01E+05	3,32E+05	0,00	0,26	0,22	0,16	0,14
DoC	3,60	3,69	3,68					
average DoC				3,66				
Std Dev				0,05				

Trastuzumab + R12 (10 equiv.)



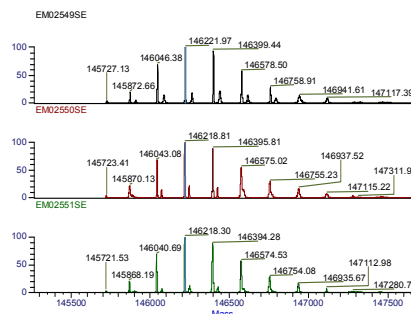
Load	R1	R2	R3	%R1	%R2	%R3	Average %R	Std Dev %R
0	9,80E+05	9,15E+05	1,48E+06	2,69	3,27	3,31	3,09	0,35
1	3,16E+06	2,15E+06	3,64E+06	8,67	7,68	8,14	8,16	0,50
2	6,04E+06	4,60E+06	7,34E+06	16,57	16,43	16,42	16,48	0,09
3	7,99E+06	6,21E+06	9,72E+06	21,93	22,18	21,74	21,95	0,22
4	7,59E+06	6,01E+06	9,55E+06	20,83	21,47	21,36	21,22	0,34
5	5,59E+06	4,44E+06	7,09E+06	15,26	15,86	15,86	15,66	0,35
6	3,25E+06	2,48E+06	4,02E+06	8,92	8,86	8,99	8,92	0,07
7	1,44E+06	9,75E+05	1,62E+06	3,95	3,48	3,62	3,69	0,24
8	4,31E+05	2,14E+05	2,42E+05	1,18	0,76	0,54	0,83	0,33
DoC	3,58	3,56	3,55					
average DoC				3,56				
Std Dev DoC				0,02				

Trastuzumab + R13 (10 equiv.)



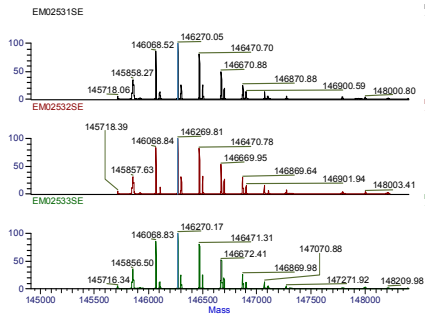
Load	R1	R2	R3	%R1	%R2	%R3	Average %R	Std Dev %R
0	3,50E+06	2,00E+06	3,99E+06	8,47	8,01	8,42	8,30	0,25
1	7,24E+06	4,36E+06	8,09E+06	17,52	17,46	17,07	17,35	0,24
2	6,95E+06	4,22E+06	6,63E+06	16,82	16,90	18,21	17,31	0,78
3	6,90E+06	4,33E+06	8,10E+06	16,69	17,34	17,09	17,04	0,32
4	4,89E+06	2,74E+06	5,46E+06	11,76	10,97	11,52	11,42	0,40
5	3,59E+06	2,71E+06	4,14E+06	8,61	10,85	8,74	9,40	1,26
6	2,67E+06	1,85E+06	3,40E+06	6,46	7,41	7,17	7,01	0,49
7	2,68E+06	9,75E+05	2,18E+06	6,48	3,90	4,56	4,98	1,34
8	7,28E+05	5,68E+05	1,31E+06	1,76	2,27	2,76	2,26	0,50
9	1,09E+06	3,93E+05	5,35E+05	2,64	1,57	1,13	1,78	0,78
10	6,83E+05	4,75E+05	8,33E+05	1,65	1,90	1,76	1,77	0,13
11	3,38E+05	2,35E+05	4,77E+05	0,82	0,94	1,01	0,92	0,10
12	1,33E+05	1,21E+05	1,94E+05	0,32	0,48	0,41	0,41	0,08
13	0,00E+00	0,00E+00	7,26E+04	0,00	0,00	0,15	0,05	0,09
DoC	3,43	3,41	3,37					
average DoC				3,40				
Std Dev DoC				0,03				

Trastuzumab + R14 (10 equiv.)



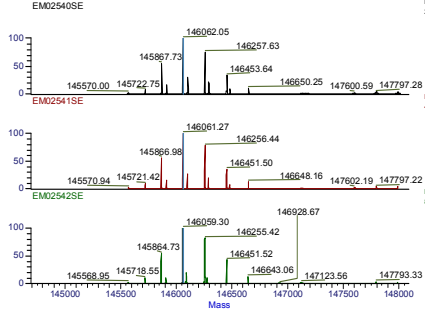
Load	R1	R2	R3	%R1	%R2	%R3	Average %R	Std Dev DoC
0	1,41E+06	9,38E+05	1,96E+06	4,96	5,34	5,23	5,18	0,19
1	5,00E+06	3,07E+07	6,69E+06	17,58	17,46	17,86	17,63	0,20
2	7,36E+06	4,55E+07	9,73E+06	25,88	25,88	25,97	25,91	0,05
3	6,82E+06	4,02E+07	8,56E+06	23,98	22,87	22,85	23,23	0,65
4	4,20E+06	2,45E+07	5,40E+06	14,77	13,94	14,41	14,37	0,42
5	2,05E+06	1,34E+07	2,73E+06	7,21	7,62	7,29	7,37	0,22
6	9,08E+05	7,33E+05	1,43E+06	3,19	4,17	3,82	3,73	0,49
7	5,49E+05	3,50E+06	4,47E+05	1,93	1,99	1,99	1,97	0,04
8	1,41E+05	1,30E+06	2,14E+05	0,50	0,74	0,57	0,60	0,12
DoC	2,73	2,77	2,74					
average DoC				2,74				
Std Dev DoC				0,02				

Trastuzumab + R15 (10 equiv.)



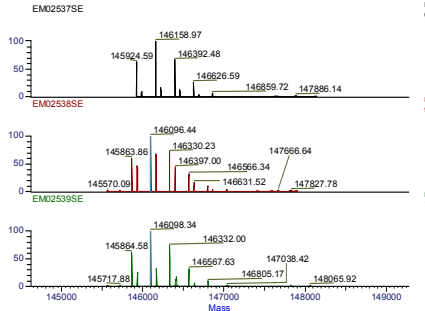
Load	R1	R2	R3	%R1	%R2	%R3	Average %R	Std Dev %R
0	3,51E+06	4,12E+06	3,93E+06	8,74	7,67	8,81	8,41	0,64
1	8,81E+06	1,12E+07	9,65E+06	21,93	20,85	21,64	21,47	0,56
2	1,03E+07	1,36E+07	1,13E+07	25,64	25,32	25,34	25,43	0,18
3	8,15E+06	1,10E+07	9,09E+06	20,29	20,48	20,38	20,38	0,10
4	5,08E+06	7,07E+06	5,76E+06	12,64	13,16	12,92	12,91	0,26
5	2,51E+06	3,90E+06	2,92E+06	6,25	7,26	6,55	6,69	0,52
6	1,30E+06	1,94E+06	1,41E+06	3,24	3,61	3,16	3,34	0,24
7	5,17E+05	8,87E+05	5,32E+05	1,29	1,65	1,19	1,38	0,24
DoC	2,44	2,55	2,45					
average DoC				2,48				
Std Dev DoC				0,06				

Trastuzumab + R16 (10 equiv.)



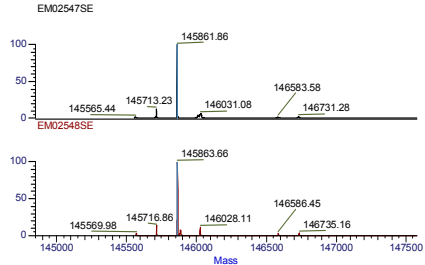
Load	R1	R2	R3	%R1	%R2	%R3	Average %R	Std Dev %R
0	1,58E+07	2,24E+07	4,77E+07	20,06	19,73	18,80	19,53	0,65
1	2,90E+07	4,09E+07	8,75E+07	36,83	36,03	34,49	35,78	1,19
2	2,15E+07	3,14E+07	7,10E+07	27,30	27,66	27,99	27,65	0,34
3	9,53E+06	1,40E+07	3,70E+07	12,10	12,33	14,58	13,01	1,37
4	2,92E+06	4,82E+06	1,05E+07	3,71	4,25	4,14	4,03	0,28
DoC	1,43	1,45	1,51					
average DoC				1,46				
Std Dev DoC				0,04				

Trastuzumab + R17 (10 equiv.)



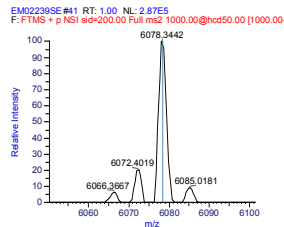
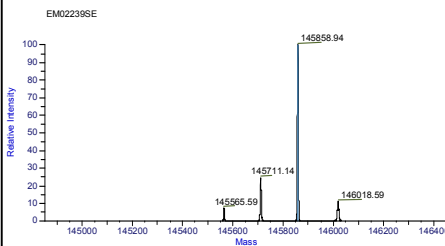
Load	R1	R2	R3	%R1	%R2	%R3	Average %R	Std Dev %R
0	3,74E+06	5,72E+06	6,32E+06	23,94	21,42	21,63	22,33	1,40
1	6,03E+06	9,73E+06	1,05E+07	38,60	36,44	35,94	37,00	1,41
2	3,98E+06	6,92E+06	7,71E+06	25,48	25,92	26,39	25,93	0,46
3	1,49E+06	3,10E+06	3,40E+06	9,54	11,61	11,64	10,93	1,20
4	3,81E+05	9,18E+05	1,08E+06	2,44	3,44	3,70	3,19	0,66
5	0,00E+00	3,10E+05	2,02E+05	0,00	1,16	0,69	0,62	0,58
DoC	1,28	1,43	1,42					
average DoC				1,38				
Std Dev DoC				0,08				

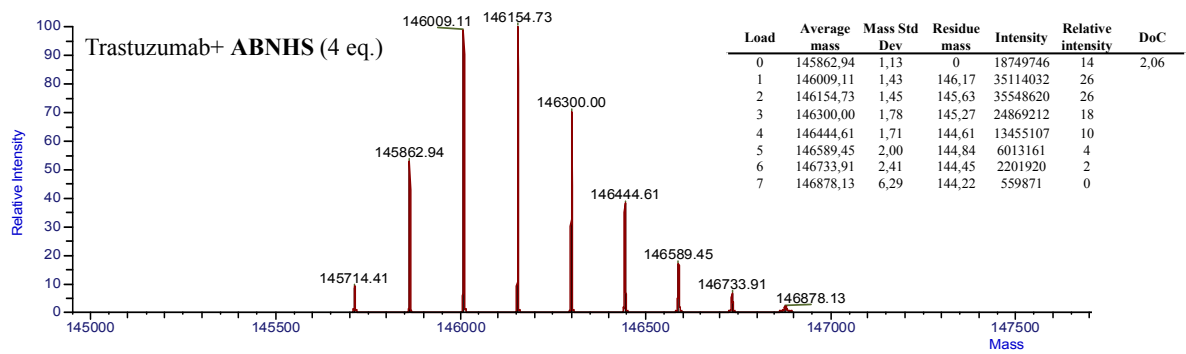
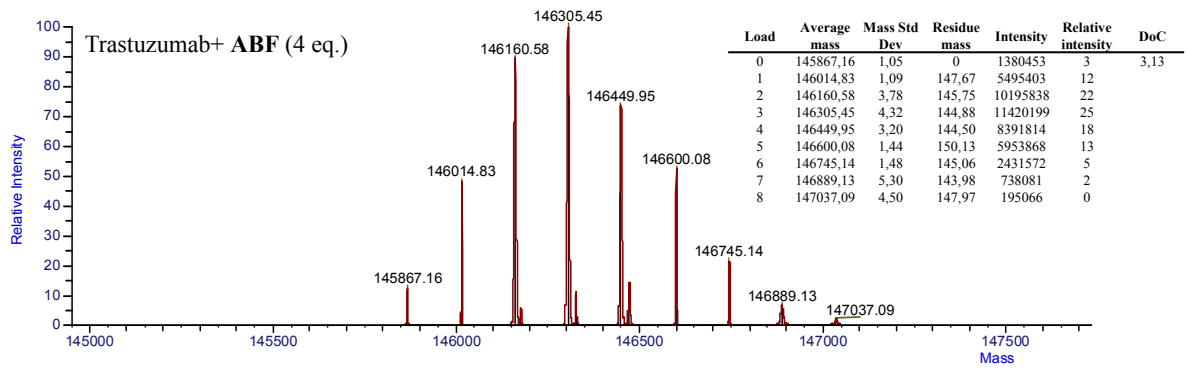
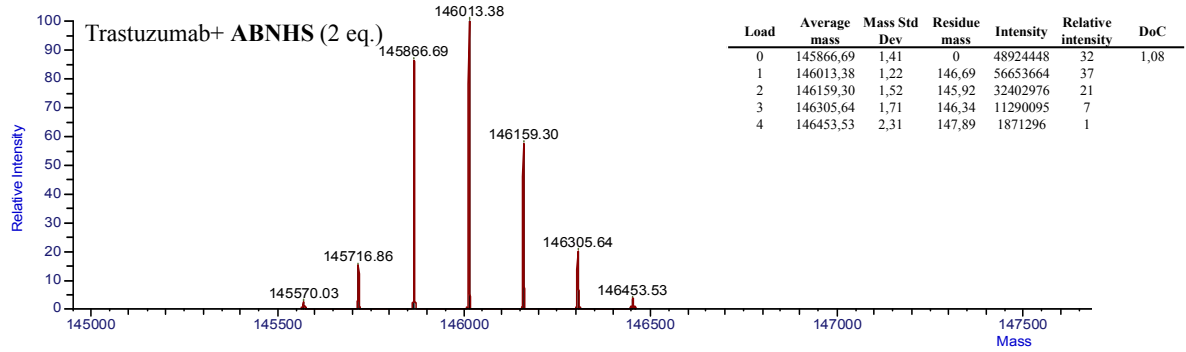
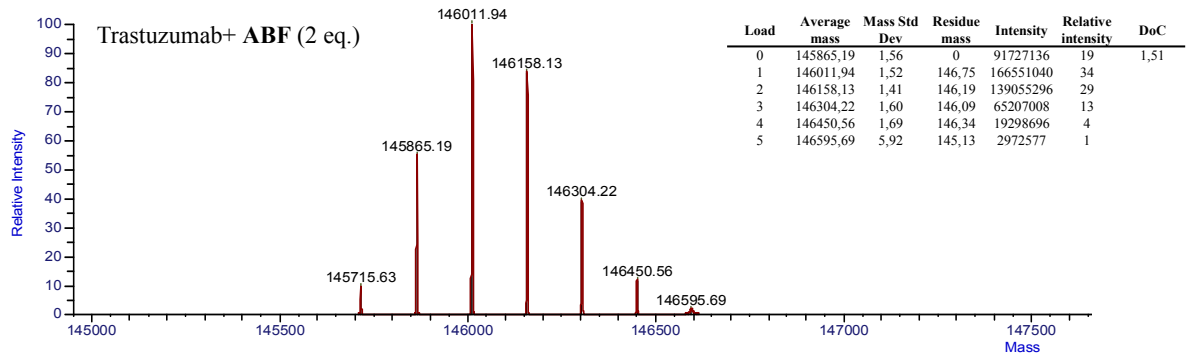
Trastuzumab + R18 (10 equiv.)

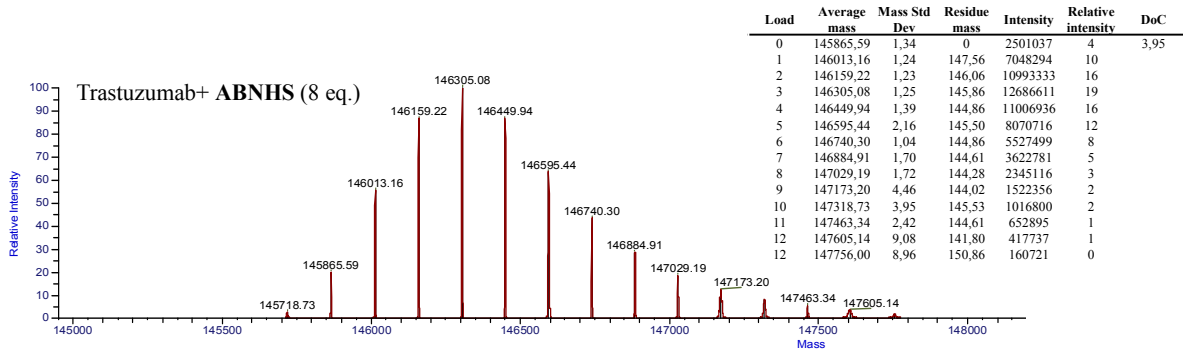
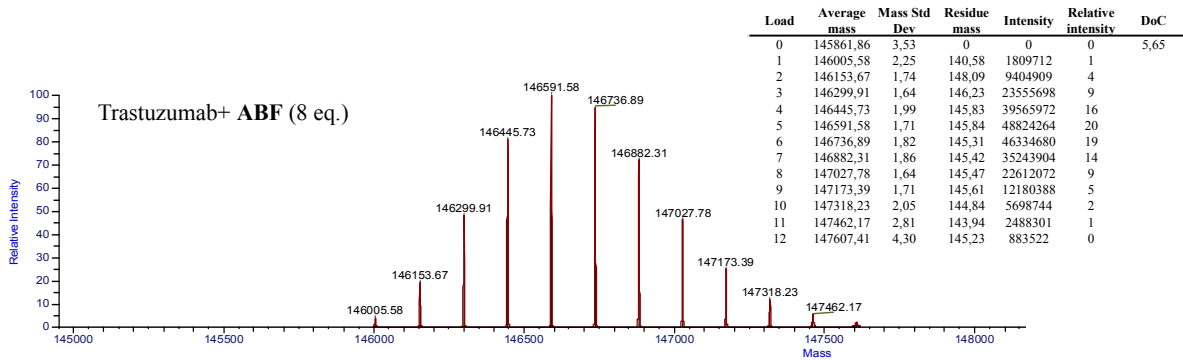
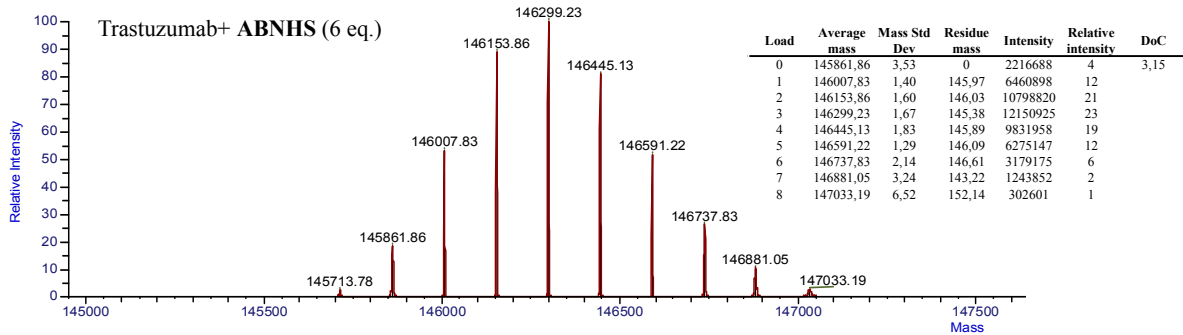
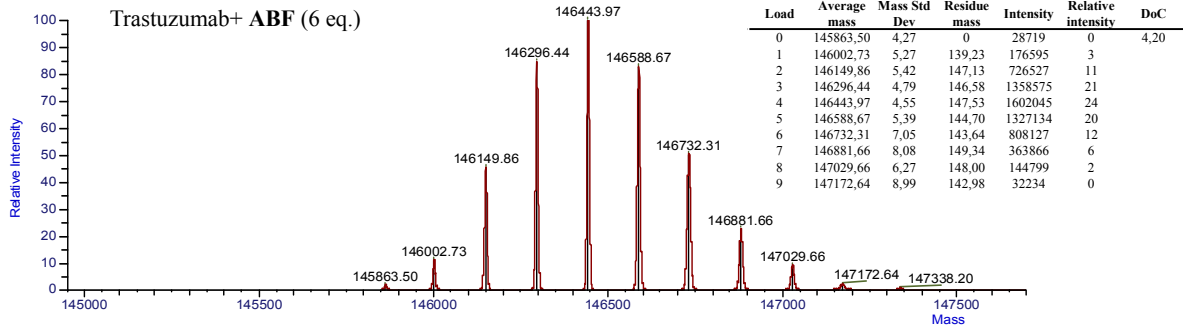


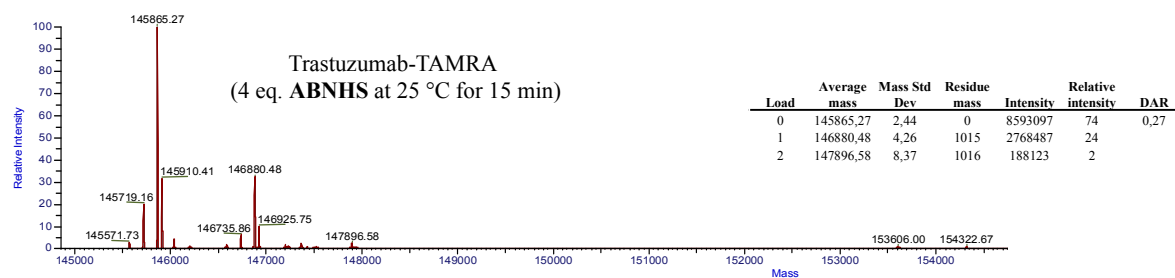
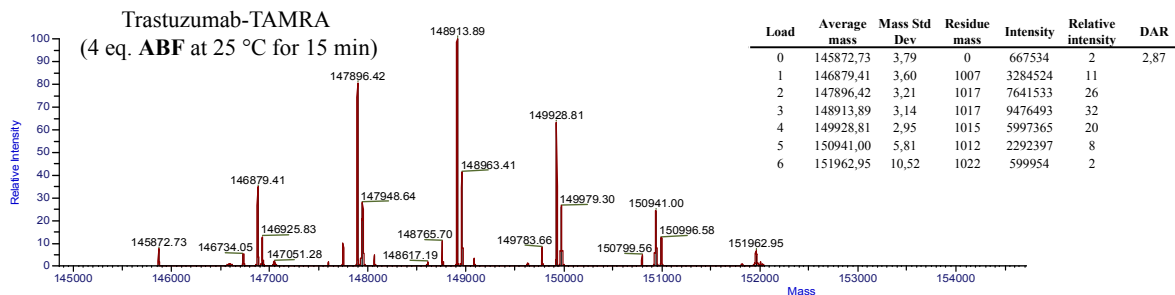
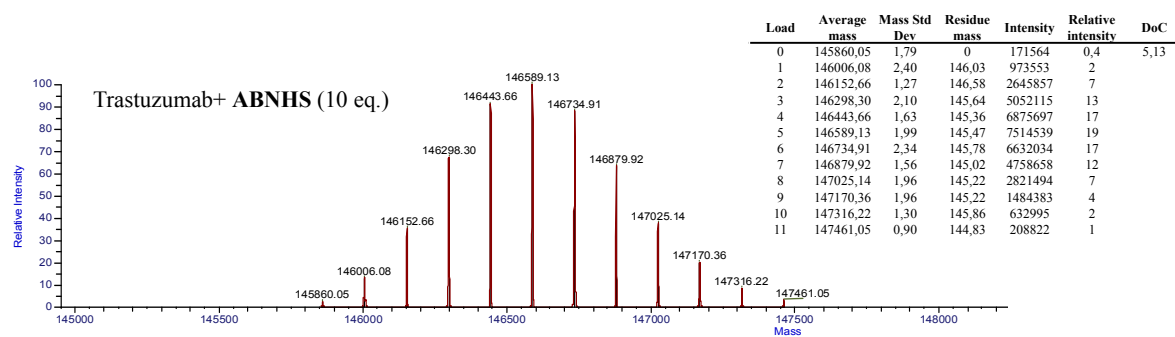
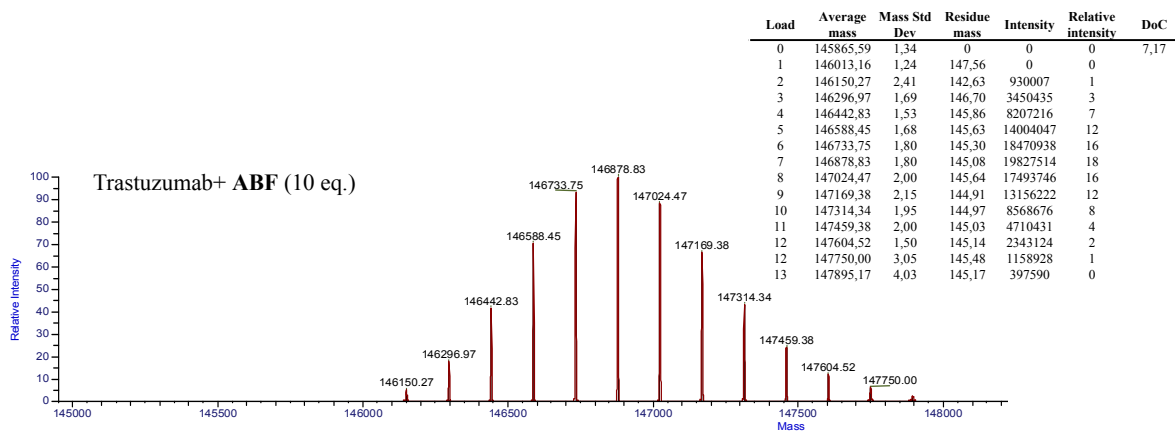
Load	R1	R2
0	3,76E+08	1,91E+08
1	2,25E+07	2,16E+07
DoC	0,06	0,10
average DoC	0,08	

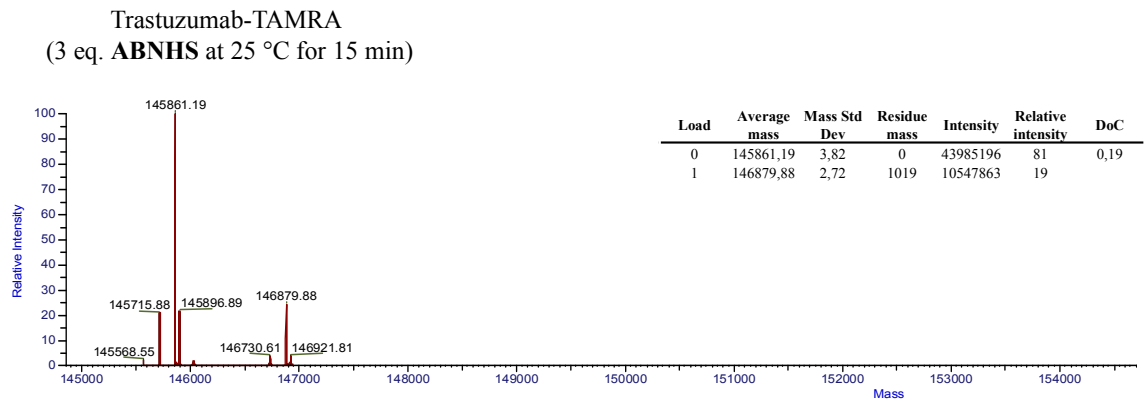
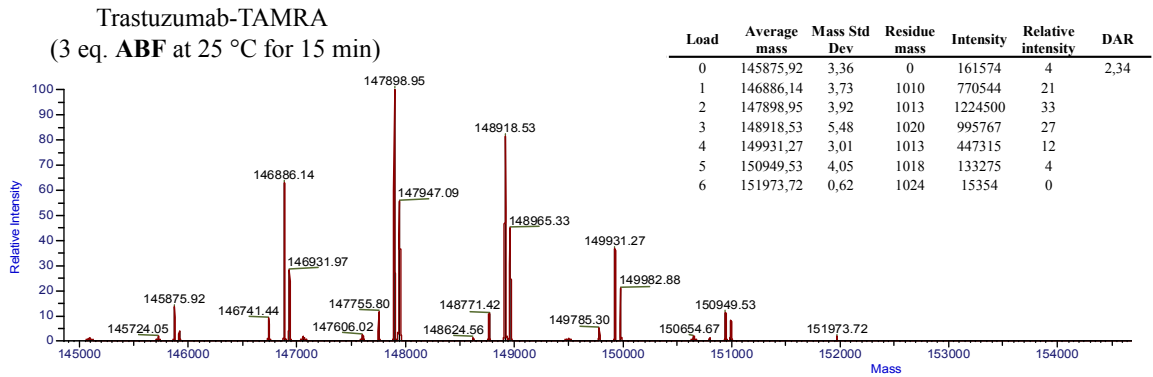
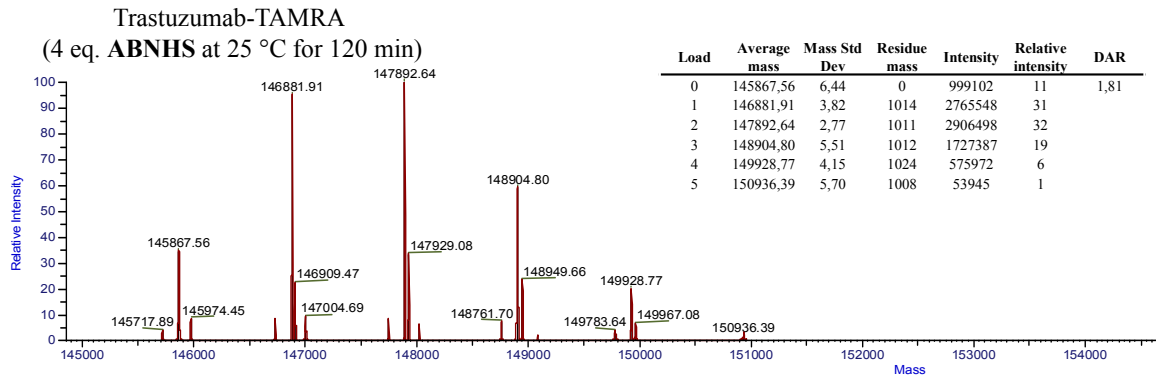
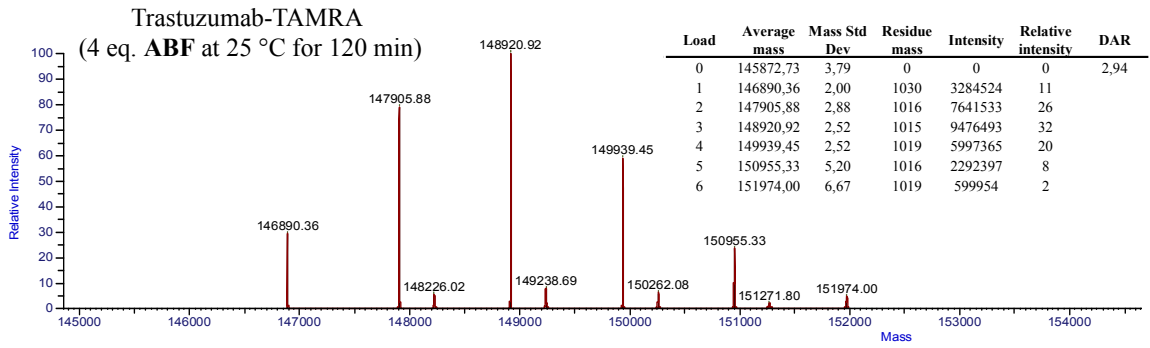
Trastuzumab deglycosylated



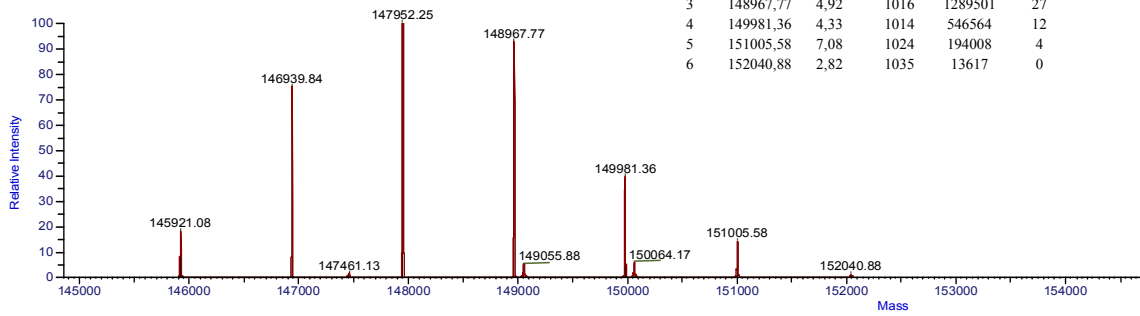






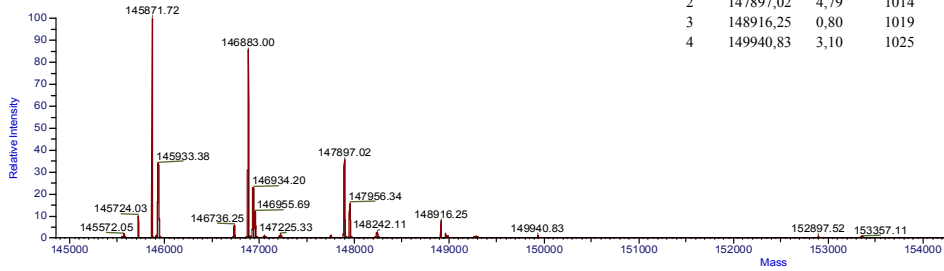


Trastuzumab-TAMRA
(3 eq. ABF at 25 °C for 120 min)

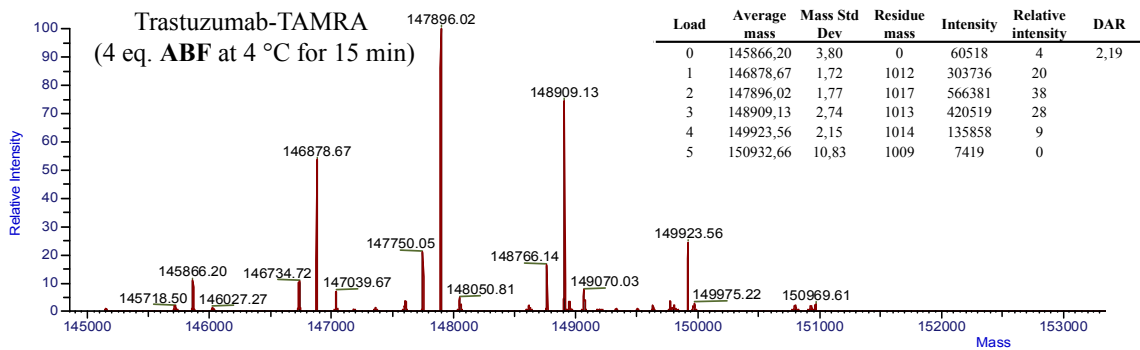


Load	Average mass	Mass Std Dev	Residue mass	Intensity	Relative intensity	DAR
0	145921,08	5,14	0	248942	5	2,31
1	146939,84	3,42	1019	1043288	22	
2	147952,25	3,45	1012	1387507	29	
3	148967,77	4,92	1016	1289501	27	
4	149981,36	4,33	1014	546564	12	
5	151005,58	7,08	1024	194008	4	
6	152040,88	2,82	1035	13617	0	

Trastuzumab-TAMRA
(3 eq. ABNHS at 25 °C for 120 min)

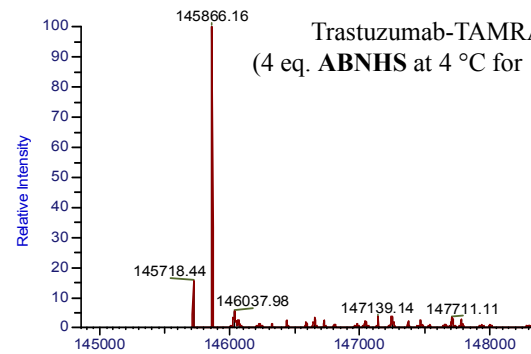


Load	Average mass	Mass Std Dev	Residue mass	Intensity	Relative intensity	DAR
0	145871,72	2,10	0	2740313	44	0,79
1	146883,00	4,09	1011	2343337	37	
2	147897,02	4,79	1014	965235	15	
3	148916,25	0,80	1019	204268	3	
4	149940,83	3,10	1025	26369	0	



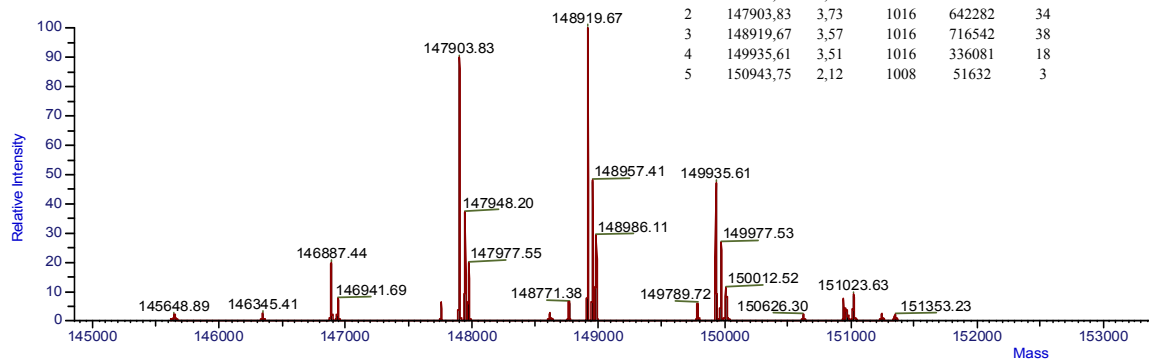
Load	Average mass	Mass Std Dev	Residue mass	Intensity	Relative intensity	DAR
0	145866,20	3,80	0	60518	4	2,19
1	146878,67	1,72	1012	303736	20	
2	147896,02	1,77	1017	566381	38	
3	148909,13	2,74	1013	420519	28	
4	149923,56	2,15	1014	135858	9	
5	150932,66	10,83	1009	7419	0	

Trastuzumab-TAMRA
(4 eq. ABNHS at 4 °C for 15 min)

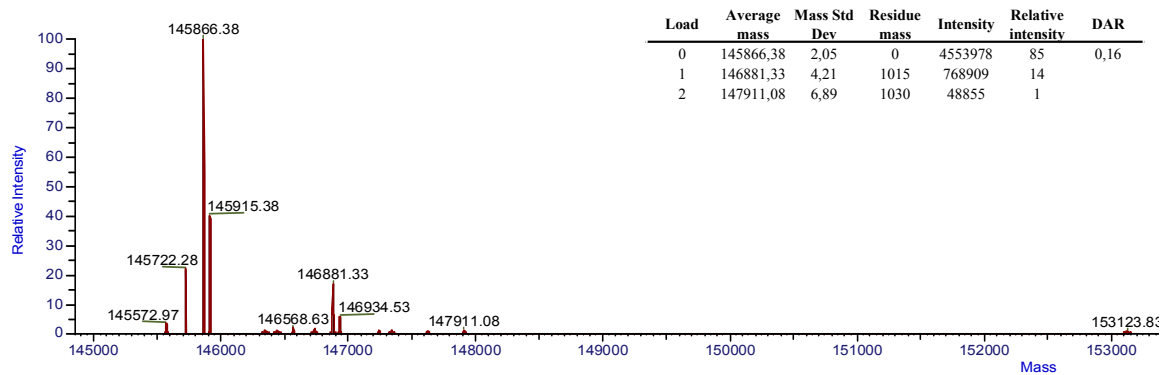


Load	Average mass	Mass Std Dev	Residue mass	Intensity	Relative intensity	DAR
0	145866,20	3,80	0	477534	100	0

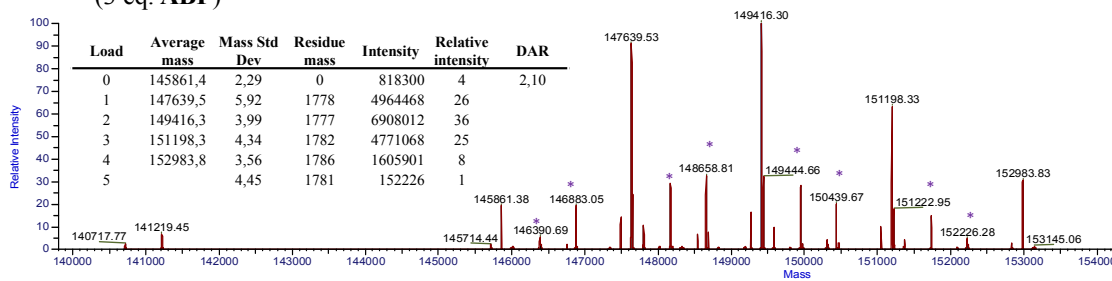
Trastuzumab-TAMRA
(4 eq. ABF at 4 °C for 120 min)



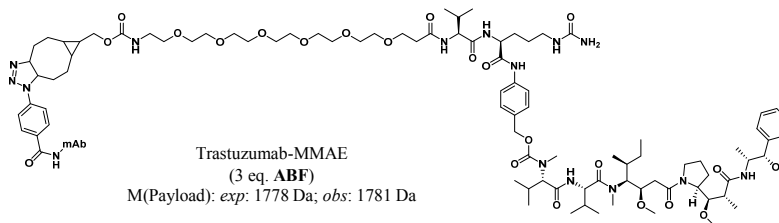
Trastuzumab-TAMRA
(4 eq. ABNHS at 4 °C for 120 min)



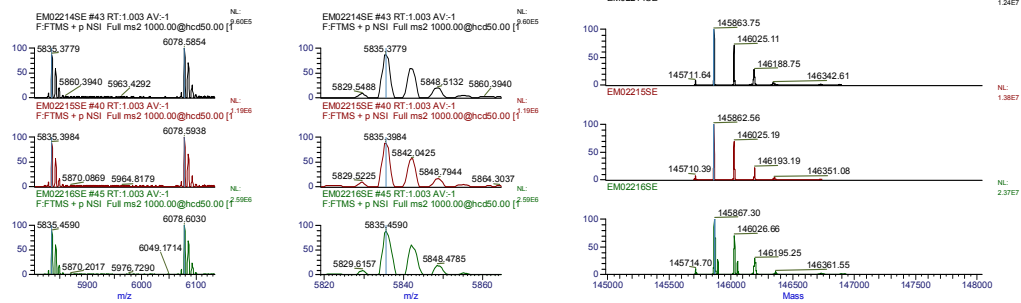
Trastuzumab-MMAE
(3 eq. ABF)



* BCN-PEG_n-COOH (by-product in BCN-MMAE) conjugates with T-N₃

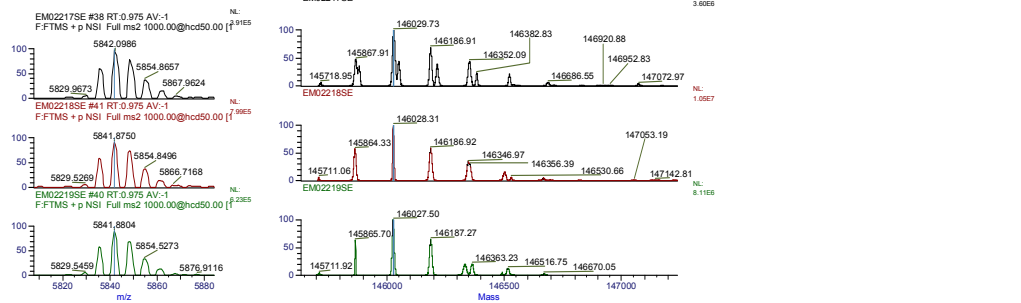


Trastuzumab +APG (2 equiv.)



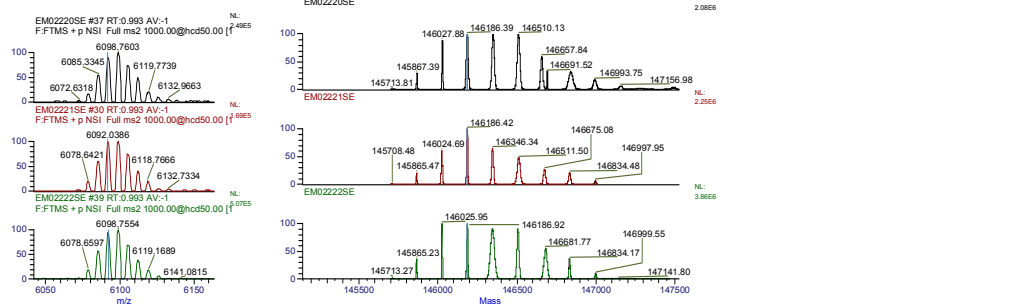
Load	Relative intensity R1	Relative intensity R2	Relative intensity R3	Relative intensity R1(%)	Relative intensity R2(%)	Relative intensity R3(%)	Average R(%)	Std Dev R(%)
0	100,0	100,0	100,0	50	52	49	50	1
1	70,3	67,8	69,9	35	35	34	35	0
2	26,6	21,7	28,4	13	11	14	13	1
3	3,7	3,8	5,0	2	2	2	2	0
DoC	0,7	0,6	0,7					
average DoC	0,67							
Std Dev DoC	0,03							

Trastuzumab + APG (5 equiv.)



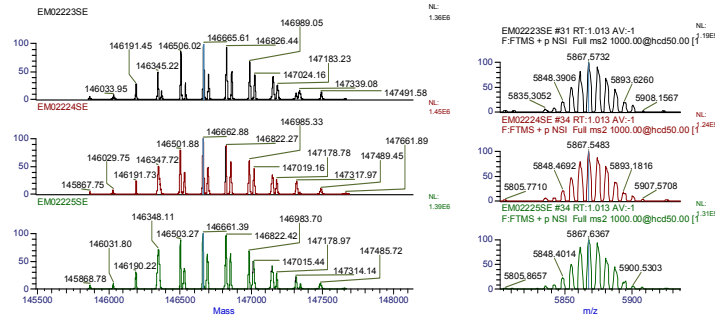
Load	R1	R2	R3	%R1	%R2	%R3	Average %R	Std Dev %R
0	1,70E+06	5,92E+06	5,06E+06	16,48	21,19	23,82	20,50	3,72
1	3,60E+06	1,05E+07	8,11E+06	34,88	37,74	38,13	36,92	1,77
2	2,47E+06	6,06E+06	5,22E+06	23,90	21,72	24,56	23,39	1,49
3	1,56E+06	3,31E+06	1,60E+06	15,07	11,87	7,53	11,49	3,78
4	7,68E+05	1,64E+06	1,03E+06	7,44	5,88	4,85	6,05	1,30
5	2,30E+05	4,49E+05	2,37E+05	2,23	1,61	1,11	1,65	0,56
DoC	1,69	1,48	1,35					
average DoC	1,51							
Std Dev DoC	0,17							

Trastuzumab + APG (10 equiv.)



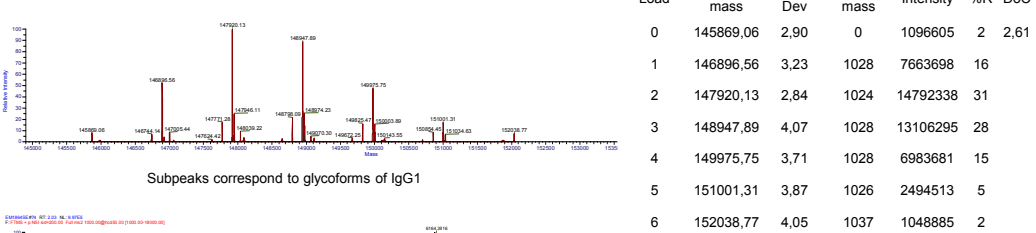
Load	R1	R2	R3	%R1	%R2	%R3	Average %R	Std Dev %R
0	5,99E+05	4,42E+05	1,36E+06	5,45	5,69	6,87	6,01	0,76
1	1,83E+06	1,37E+06	3,86E+06	16,65	17,60	19,47	17,91	1,43
2	2,06E+06	2,25E+06	3,74E+06	18,77	28,97	18,86	22,20	5,86
3	2,05E+06	1,43E+06	3,47E+06	18,67	18,44	17,48	18,19	0,63
4	2,08E+06	1,06E+06	3,49E+06	18,87	13,69	17,60	16,72	2,70
5	1,23E+06	6,04E+05	2,11E+06	11,19	7,78	10,63	9,87	1,83
6	6,48E+05	4,66E+05	1,39E+06	5,89	6,00	7,01	6,30	0,62
7	3,61E+05	1,42E+05	3,75E+05	3,28	1,83	1,89	2,33	0,82
8	1,34E+05	0,00E+00	3,84E+04	1,22	0,00	0,19	0,47	0,65
DoC	3,10	2,73	2,90	100,00	100,00	100,00	100,00	
average DoC	2,91							
Std Dev DoC	0,18							

Trastuzumab + APG (20 equiv.)

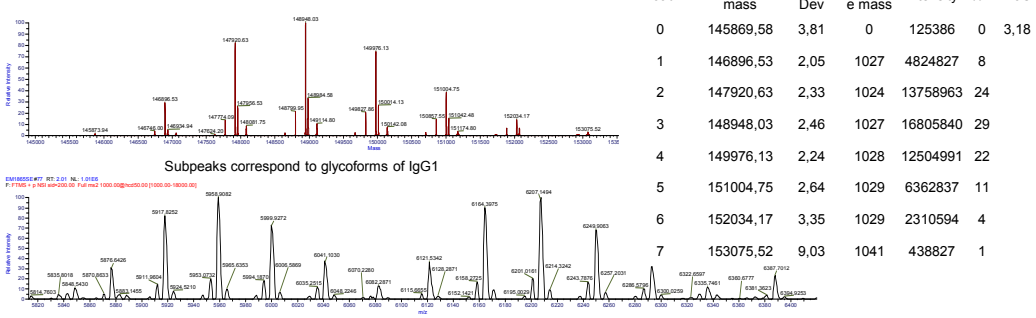


Load	R1	R2	R3	%R1	%R2	%R3	Average %R	Std Dev %R
0	6,93E+04	7,41E+04	9,02E+04	1,03	1,07	1,20	1,10	0,09
1	9,51E+04	1,04E+05	1,26E+05	1,41	1,50	1,68	1,53	0,14
2	3,65E+05	3,25E+05	4,25E+05	5,41	4,69	5,67	5,26	0,51
3	6,57E+05	6,87E+05	9,89E+05	9,73	9,92	13,20	10,95	1,95
4	1,15E+06	1,14E+06	1,21E+06	17,09	16,50	16,21	16,60	0,45
5	1,36E+06	1,45E+06	1,39E+06	20,13	20,98	18,52	19,88	1,25
6	1,27E+06	1,25E+06	1,32E+06	18,75	18,00	17,59	18,11	0,59
7	9,04E+05	8,72E+05	9,34E+05	13,39	12,59	12,46	12,81	0,50
8	5,57E+05	5,08E+05	5,61E+05	8,26	7,33	7,48	7,69	0,50
9	1,42E+05	3,36E+05	2,91E+05	2,11	4,85	3,88	3,61	1,39
10	1,69E+05	1,50E+05	1,37E+05	2,51	2,17	1,83	2,17	0,34
11	12476,91	2,92E+04	2,00E+04	0,18	0,42	0,27	0,29	0,12
DoC	5,29	5,36	5,19					
average DoC	5,28							
Std Dev DoC	0,09							

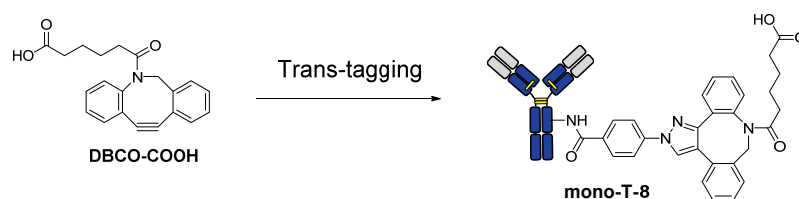
Trastuzumab + APG (8 equiv.) + TAMRA-BCN



Trastuzumab + APG (11 equiv.) + TAMRA-BCN



Annex 5



MS analysis of **mono-T-8**

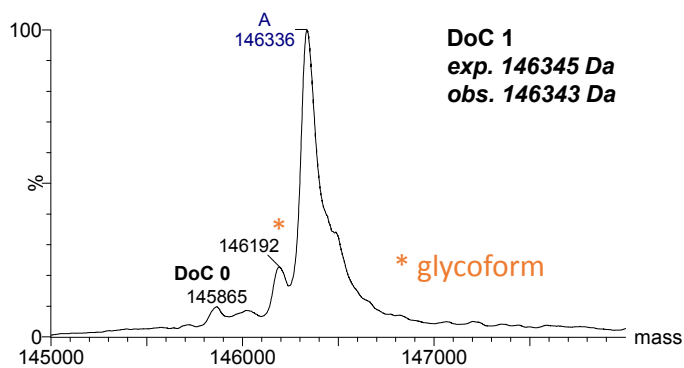


Figure S10. Compound **mono-T-8** was prepared following General procedure A with Trastuzumab as a Protein and DBCO-COOH as a Trans-tagging reagent.

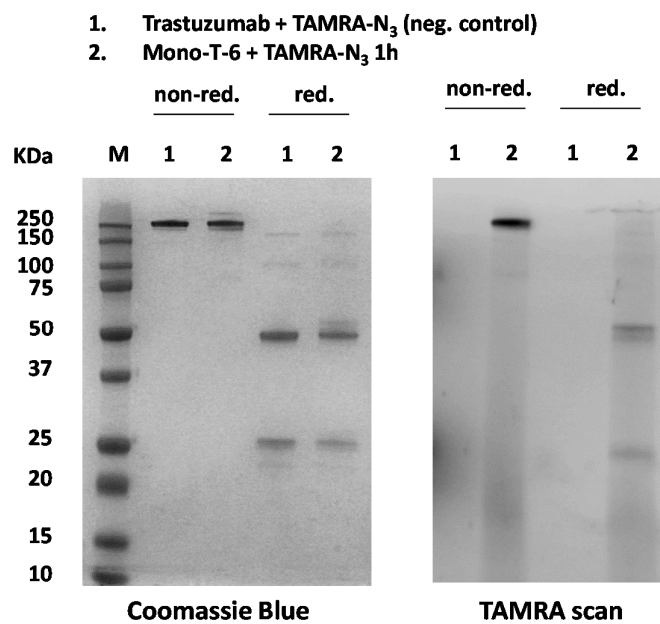


Figure S11. Reduced and non-reduced SDS PAGE of mono-T-6 modification with TAMRA-N₃. Fluorescent gel showed successful post-modification of secondary BCN group in mono-T-6.

Igor DOVGAN

Antibody conjugates: integrated approach towards selective, stable and controllable bioconjugation

Abstract

Within the last decade, antibodies conjugated to cytotoxic drugs or oligonucleotides have gained a great attention in scientific community owing to the unique properties of the antibodies, such as their long circulation time in serum and high selectivity against their target. For instance, antibody conjugates (ACs) are increasingly applied for targeted cancer therapy or bioimaging. Consequently, the development of reliable methodologies for ACs preparation is currently of high demand. However, the controllable conjugation and preparation of ACs with defined structure are still challenging due to high excess and variety of reactive groups in antibody structure, which are accessible for conjugation. Moreover, current linker technologies are based on the maleimide-thiol reaction, yielding adducts, which are unstable during circulation in blood.

This work is focused on chemical approaches for the reliable antibody functionalisation, which enable the preparation of stable ACs with well-defined payload to antibody ratios. The first part is devoted to design and development of maleimide-dioxane reagents as self-hydrolysable and serum-stable alternative to classical maleimide chemistry. The second part is dedicated to a screening approach for evaluation of residue-selective functionalities in reactions with an antibody using high resolution native mass spectrometry. Finally, in the third part the reader is introduced with a novel technology, which enables efficient preparation of stable ACs with a defined degree of conjugation and particularly mono-functionalisation of antibodies.

Keywords: bioconjugation, antibody-drug conjugates, antibody-oligonucleotide conjugates, mono-functionalisation of proteins, arginine modification, lysine tagging

Résumé

Au cours de la dernière décennie, les anticorps conjugués à des médicaments cytotoxiques ou des oligonucléotides ont acquis une grande attention dans la communauté scientifique en raison des propriétés uniques des anticorps, tels que leur long temps de circulation dans le sérum et leur sélectivité élevée par rapport à leur cible. Par exemple, les conjugués d'anticorps (ACs) sont de plus en plus appliqués en thérapie ciblée contre le cancer ou en bioimagerie. Par conséquent, le développement de méthodologies fiables pour la préparation des AC est actuellement en pleine expansion. Cependant, la conjugaison et la préparation contrôlables des ACs avec une structure définie rencontrent encore de nombreux obstacles en raison de l'excès élevé et de la variété des groupes réactifs dans la structure des anticorps, qui sont accessibles pour la conjugaison. En outre, les technologies de liaison actuelles sont basées sur la réaction de maléimide-thiol, produisant des adduits, qui sont instables dans le sang.

Ce travail se concentre sur les approches chimiques pour la fonctionnalisation fiable des anticorps, qui permettent la préparation d'ACs stables présentant un ratio anticorps/principe actif bien défini. La première partie est consacrée à la conception et au développement du réactif maléimide-dioxane, solution auto-hydrolysable et stable dans le sérum, comme alternative à la chimie classique du maléimide. La deuxième partie est consacrée à l'évaluation de la réactivité sélective des différents acides aminés portés par les anticorps par spectrométrie de masse native à haute résolution. Finalement, une nouvelle technologie permettant d'obtenir des ACs stables avec un ratio anticorps/principe actif contrôlé est présentée au lecteur dans une 3^{ème} partie.

Mots-clés: bioconjugaison, conjugués anticorps-principe actif, conjugués anticorps-oligonucléotides, mono fonctionnalisation des protéines, modification de l'arginine, marquage de la lysine

Conjugués d'anticorps : approche intégrative pour une bioconjugaison plus sélective, stable et contrôlable

Conjugués d'anticorps

Parmi une grande variété de bio-conjugués, les conjugués anticorps-médicaments (ADC) ont attiré l'attention de la communauté scientifique au cours de la dernière décennie en tant qu'alternative plus efficace et plus sûre aux chimiothérapies anticancéreuses traditionnelles. L'ADC comprend trois composants : un anticorps monoclonal (mAb) contre les antigènes surexprimés sur les cellules cancéreuses, un médicament hautement cytotoxique avec des valeurs de concentration inhibitrice semi-maximale (IC50) subnanomolaire et un linker liant ces deux entités (Figure 1). Dans l'ADC, l'anticorps agit comme un véhicule permettant l'administration sélective du puissant médicament cytotoxique aux cellules tumorales.

Les conjugués anticorps-oligonucléotides (AOC) constituent un autre type intéressant de conjugué d'anticorps (AC), puisqu'ils sont des outils puissants pour la détection des antigènes en immuno-PCR^{1,2} et sont considérés comme attractifs pour la délivrance spécifique de petites molécules d'ARN interférant dans la cellule.³

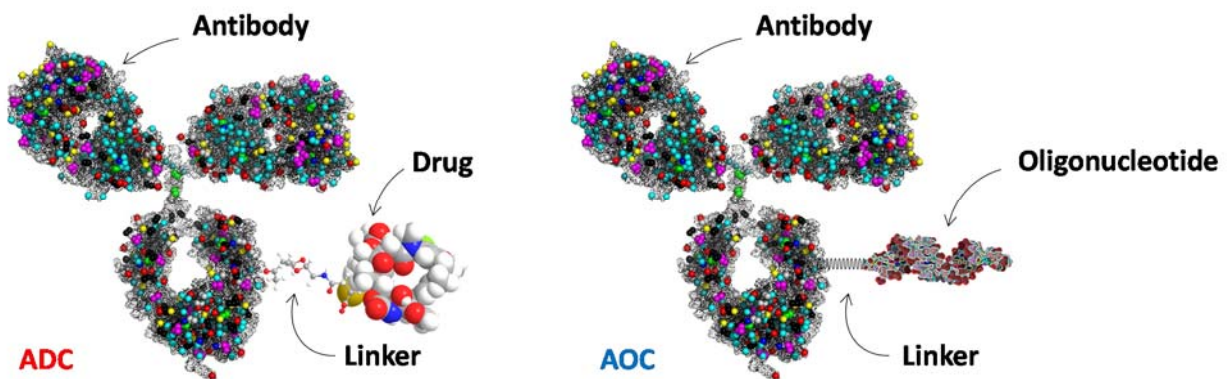


Figure 1. Représentations de conjugués anticorps-médicament (ADC) et de conjugués anticorps-oligonucléotide (AOC).

À cet égard, le développement de méthodologies fiables pour la préparation des AC est actuellement très demandé. La conjugaison contrôlée et la préparation des AC avec une structure définie sont encore difficiles en raison de l'excès de groupes réactifs présents à la surface de

l'anticorps (sur la Figure 1, les points colorés sur l'anticorps représentent ces fonctions réactives vis-à-vis de la bio-conjugaison).

Dans ce travail, nous nous concentrerons sur des approches chimiques pour la fonctionnalisation fiable des anticorps, qui permettent la préparation de conjugués AC stables avec des ratios charge utile / anticorps bien définis. À cette fin, le lecteur devrait tout d'abord être informé de la base de la structure et des propriétés de l'anticorps, qui sont présentés dans les sections suivantes.

Conjugués anticorps-médicament

En 1958, le premier exemple d'attachement covalent d'un agent chimiothérapeutique à un anticorps a été démontré par l'équipe de recherche de Jean Bernard à l'hôpital Héroid à Paris.⁴ En effet, des IgG de hamster ont été fonctionnalisés avec la forme diazotée du méthotrexate et l'ADC obtenu a été testé contre les xénogreffes de leucémie chez le hamster (Figure 2). Il a été montré que cet immuno-conjugué prolongeait significativement la survie des animaux par rapport à l'anticorps non conjugué, au médicament seul, ou à un mélange non covalent de ces derniers. Ainsi, le couplage covalent du méthotrexate à l'anticorps de ciblage a démontré un effet clinique bénéfique. Dans ce cas, les molécules d'anticorps pourraient être considérées comme des "missiles guidés", qui transportent et délivrent des agents cytotoxiques spécifiquement aux cellules ciblées.

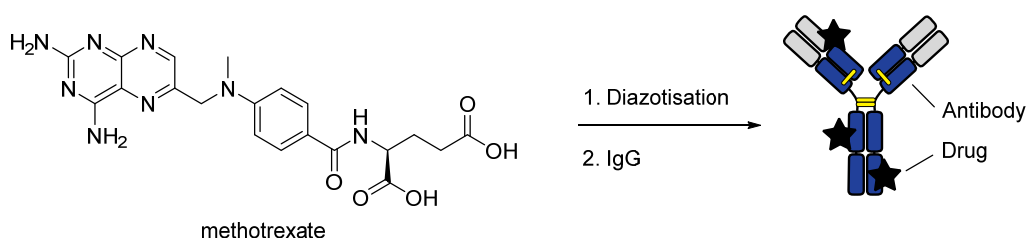


Figure 2. Préparation du premier ADC signalé.

Depuis lors, les technologies de conjugaison d'anticorps et de conception d'ADC n'ont cessé de se développer. Dans les années 1970, des ADC liés de manière covalente et non-covalente ont été testés sur des modèles animaux, suivis moins d'une décennie plus tard par le premier essai clinique sur l'homme avec la vindésine antiméiotique comme charge cytotoxique.⁵ Malgré des résultats prometteurs, ces premières tentatives reposaient exclusivement sur des anticorps murins polyclonaux, qui ont provoqué à l'époque des réactions immunitaires significatives chez l'homme. Ces problèmes ont été surmontés dans les années 1990 en concevant des ADC basés sur des

anticorps monoclonaux (mAbs) chimériques et humanisés.⁶ Par la suite, la sélection rationnelle des cibles et l'augmentation de la puissance des médicaments ont permis d'obtenir des ADC plus efficaces.⁷ Cela a conduit à la première génération d'ADC (Mylotarg®, gemtuzumab ozogamicin, développé par Pfizer) approuvé pour la première fois par la Food and Drug Administration des États-Unis (FDA) en 2000 (Figure 3).⁸

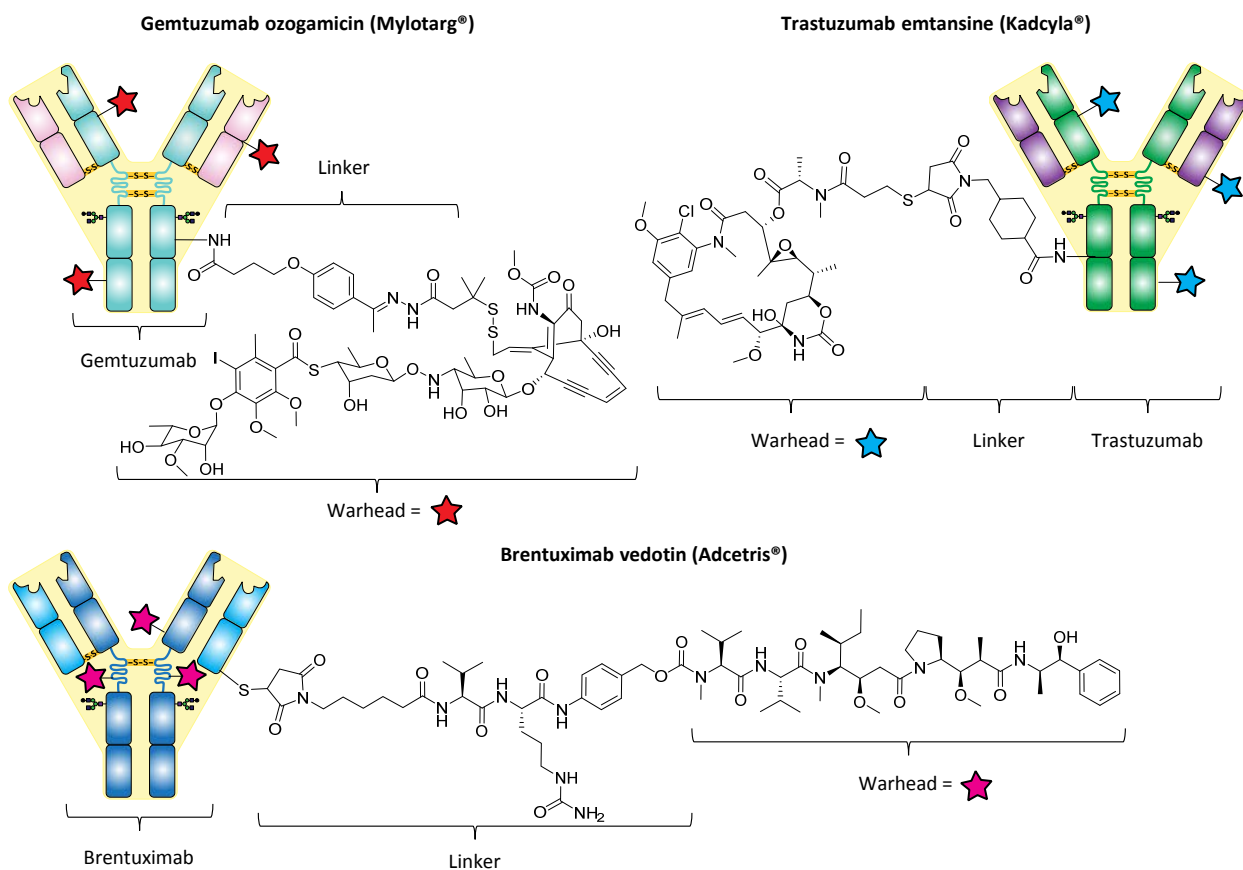


Figure 3. Structures des ADC approuvés par la FDA.

Malgré des résultats cliniques initialement prometteurs, Mylotarg® a été retiré du marché en 2010 en raison d'un manque de bénéfice clinique par rapport à la chimiothérapie standard (début 2017, Pfizer a de nouveau demandé l'approbation des États-Unis et de l'UE). Cependant, très rapidement deux ADC de deuxième génération ont été approuvés par la FDA: l'Adcetris®, brentuximab vedotin (développé par Seattle Genetics)⁹⁻¹¹ en 2011 et le Kadcyla®, trastuzumab emtansine (également connu sous le nom de T-DM1 et ado-trastuzumab emtansine; Roche et Immunogen)^{12,13} en 2013. Actuellement, il y a plus de 60 ADC en essais cliniques et leur marché devrait augmenter dans l'avenir.

L'un des paramètres importants d'un ADC est le rapport moyen médicament / anticorps (DAR moyen), car il détermine la quantité globale de médicament qui peut être administrée aux cellules cibles et peut être directement corrélé à la sécurité et l'efficacité du traitement. Pour la chimie des bio-conjugués en général, ce terme correspond au degré moyen de conjugaison (ci-après, nous le raccourcirons en DoC).

Le Kadcyła® est préparé en attachant le DM1, inhibiteur cytotoxique des microtubules dérivé de la maytansine, aux résidus lysine accessibles de l'anticorps anti-HER2 nommé trastuzumab (ou Herceptin). En raison de la disponibilité de 90 résidus de lysine à la surface du trastuzumab, une telle modification classique et non spécifique conduit à un ADC hautement hétérogène, avec jusqu'à 10^6 espèces distinctes statistiquement possibles lorsque le DAR est de 2 – 4.¹⁴ Selon la spectrométrie de masse (MS), la valeur moyenne de DAR du Kadcyła® est de 3,5 avec un mélange d'anticorps présentant des DAR individuels allant de 0 à 8 (Figure 4). La distribution de la charge de médicament observée peut être décrite statistiquement en utilisant des modèles de distribution de Poisson ou de distribution binomiale.^{15,16} La caractérisation détaillée du profil de distribution est importante, car différentes formes médicamenteuses peuvent avoir des profils pharmacocinétiques et / ou toxicologiques différents.¹⁷

Pour réduire l'hétérogénéité compositionnelle de l'ADC, en 1993, Willner et al. ont exploité une approche basée sur la conjugaison du complexe médicament-linker aux résidus de cystéine générés par la réduction complète des quatre liaisons disulfure inter-chaînes de l'anticorps.¹⁸ En utilisant cette approche, les scientifiques de Seattle Genetics ont préparé un ADC quasi-homogène avec un DAR de 8.¹⁹ Par la suite, il a été montré que les espèces d'anticorps avec des charges de médicaments aussi élevées souffrent d'une faible tolérance, de taux de clairance plasmatique élevés et d'une efficacité réduite *in vivo*.¹⁷ En conséquence, l'Adcetris® a été préparé en utilisant une réduction partielle des ponts disulfures pour obtenir un ADC avec un DAR moyen d'environ 4, ce qui s'est avéré être une valeur optimale en termes d'efficacité et de sécurité. L'Adcetris® contient une toxine synthétique très puissante, la monométhyl auristatine E (MMAE), conjuguée à un anticorps anti-CD30, le brentuximab, *via* un linker valine-citrulline clivable par des protéases. L'approche dirigée par les cystéines a fourni une amélioration significative par rapport aux stratégies de modification de la lysine en termes d'hétérogénéité réduite, tout en donnant malgré tout 15 espèces distinctes présentant une valeur DoC de ~ 4. Une telle modification des résidus de

cystéine laisse également les disulfures originaux non pontés conduisant à des conjugués structurellement désintégrés, ce qui peut diminuer la stabilité de l'ADC.

Il existe un intérêt croissant pour les méthodes de conjugaison spécifique à un nombre restreint de sites de l'anticorps, car elles permettent d'éviter les grandes distributions de DAR. Dans ce contexte, l'ingénierie des anticorps et les approches enzymatiques ont été activement développées.^{20,21} Bien que ces procédés aient été appliqués avec succès pour la préparation d'ADC homogènes, la plupart d'entre eux ne sont pas applicables aux anticorps natifs et nécessitent des techniques d'ingénierie protéique coûteuses.

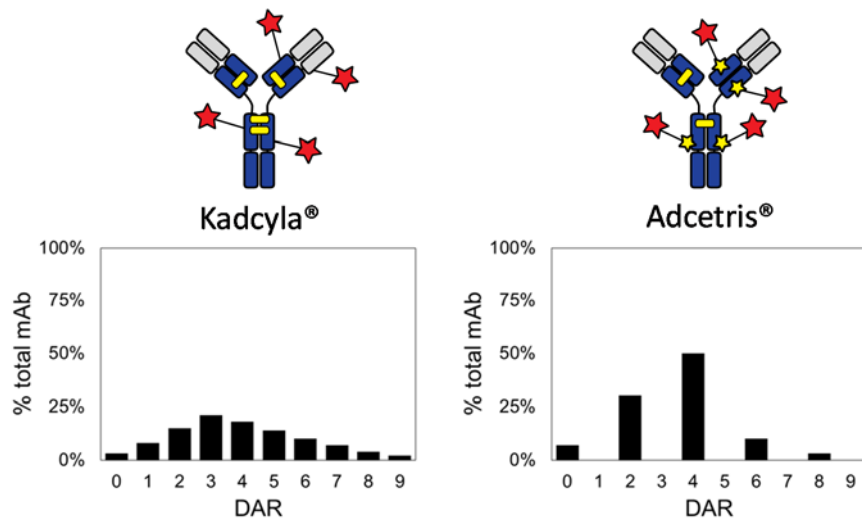


Figure 4. Principaux inconvénients des technologies existantes : hétérogénéité et perte de liaisons disulfure structurelles.

La majorité des ADC en essais cliniques sont basés sur les mêmes technologies de liaison, celles qui ont été utilisées pour la préparation des ADC approuvés par la FDA. Cependant, leurs inconvénients, tels que le manque de sélectivité et / ou la perte d'intégrité structurale, ont forcé les scientifiques à rechercher des stratégies de conjugaison plus stables, plus efficaces et plus contrôlables.

Objectifs

De cette revue, on peut conclure que la majorité des techniques de liaison actuelles pour la conjugaison naturelle d'anticorps ne sont pas idéales et souffrent d'hétérogénéité, de perte de caractéristiques structurelles des anticorps, de faible efficacité et / ou de stabilité.

Ce projet vise à trouver des techniques de bioconjugaison plus fiables et poursuit les objectifs suivants :

- Surmonter la faible stabilité et l'hydrophobicité de la liaison obtenue en utilisant des réactifs hétérobifonctionnels à base de maléimide actuels pour la conjugaison d'anticorps.

- Conception et développement d'un système de criblage général permettant une comparaison fiable de la réactivité de différents groupes fonctionnels avec les anticorps naturels. Pour les groupes présentant les meilleures caractéristiques en termes d'efficacité, de réactivité et / ou de sélectivité, développement des réactifs plug-and-play.

- Améliorer les problèmes d'hétérogénéité, la conception et le développement de stratégies de conjugaison, qui peuvent fournir un contrôle élevé sur la conjugaison donnant des AC avec un degré de conjugaison défini.

Ce projet comprend le développement, la synthèse et l'évaluation biologique de nouvelles technologies de liaison efficaces et polyvalentes pour la préparation d'AC plus stables et mieux définis.

Partie 1. Résultats

Introduction

Le développement de nouveaux linkers et de techniques de conjugaison présente un grand intérêt pour la construction d'immunoconjugués, tels que les conjugués anticorps-médicament (ADC), qui ont été utilisés avec succès en tant que thérapies contre le cancer.^{22,23} La grande majorité des ADC sont préparés en utilisant un linker bi-fonctionnel qui permet deux conjugaisons *via* des fonctions amine et thiol (linker amine-à-thiol).²¹ Jusqu'à présent, le N-succinimidyl-4-(maléimidométhyl)-cyclohexanecarboxylate (SMCC) est le linker amine-thiol le plus utilisé pour la préparation des ADC et autres immunoconjugués.²⁴ SMCC est un réactif hétérobifonctionnel consistant en une fonction maléimide d'un côté pour la réaction de Michael avec des thiols, et de l'autre côté, des esters activés pour une réaction sélective avec des groupes amine. L'un des deux ADC approuvés par la FDA (Food and drug administration) est justement produit en utilisant SMCC comme espaceur.¹³

Bien qu'il soit très utilisé, le linker SMCC souffre d'un certain nombre d'inconvénients, tels que (a) l'instabilité des conjugués à base de SMCC en présence de thiols libres et (b) la nature hydrophobe du linker. Dans le cas des ADC, cela conduit respectivement à (a) une déconjugation

prématurée et un transfert de la toxine vers l'albumine²⁵, et (b) une agrégation accrue pouvant compromettre la pharmacocinétique de l'ADC.²⁶

Pour répondre à la question de la précipitation des réactifs, le composé sulfo-SMCC contenant un groupe sulfonate sur le cycle NHS a été développé.²⁷ Cependant, la structure générale du linker n'a pas changé et, par conséquent, le problème de son hydrophobicité innée (provoquant l'agrégation et la précipitation des bioconjugués) est resté non résolu.

Résultats et discussions

Dans le but de résoudre ce problème, nous avons conçu un nouveau réactif de type SMCC, le 4- (maléimidométhyl) -1,3-dioxane-5-carbonyl oxy) -2,3,5,6-tétrafluoro-benzènesulfonate (MDTF), avec une hydrophilicité accrue au cœur de la structure. Ceci fut obtenu par substitution du cycle cyclohexyle par l'analogue 1,3-dioxane (Figure 5). En ajoutant deux atomes d'oxygène dans la structure, la valeur logP calculée du linker a diminué de 1,67 unité. De plus, nous avons remplacé l'ester activé sulfo-NHS par le 4-sulfotetrafluorophényléther afin d'augmenter la solubilité du produit final dans l'eau, qui est un paramètre important pour les applications biologiques.²⁸

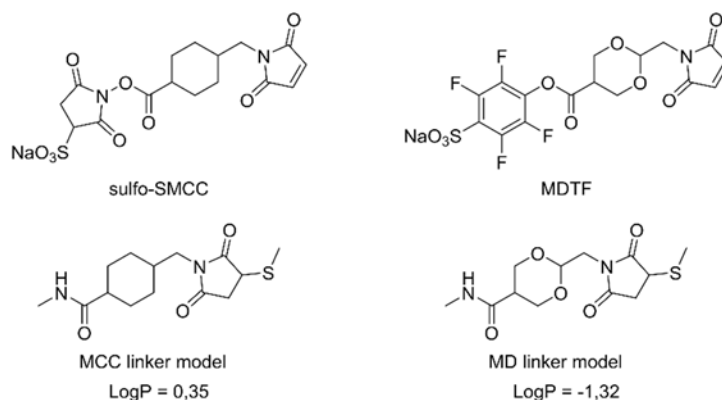


Figure 5. Réactifs SMCC et MDTF, les modèles de linkers et leurs valeurs LogP calculées. Les valeurs de LogP indiquent une plus grande hydrophilicité pour espaceur MD.

Afin d'évaluer la stabilité du linker dans les milieux biologiques et à différents pH, nous avons synthétisé deux sondes FRET, nommées P1 et P2 (Figure 6A), en utilisant les réactifs MDTF et sulfo-SMCC respectivement, ainsi que la conjugaison amine-à-thiol pour coupler un fluorophore-amine (TAMRA-NH₂) et un quencher-thiol (BHQ-2-SH). Ces sondes n'étaient pas fluorescentes, car le quencher et le fluorophore étaient reliés entre eux par un MD ou MCC-linker.

Mais le clivage du linker ou la substitution de BHQ-2-SH par d'autres molécules contenant une fonction thiol, telles que l'albumine de sérum humain (HSA), a entraîné l'apparition du signal de fluorescence.

Pour tester la stabilité des linkers, nous avons incubé les sondes P1 et P2 (1 μ M) dans différents tampons (TRIS, PBS) à différents pH (de 5,5 à 9,0), ainsi que dans le plasma humain et dans HCl 1 M à 37 °C. Il est intéressant de noter que malgré la présence d'une fonction acétal dans sa structure, le linker MD semble être plus stable que le MCC, même à pH 0. On a également constaté que la fluorescence observée pendant l'incubation de P1 dans le plasma humain a atteint un plateau après 12 heures (Figure 6B), tandis que P2 présentait une fluorescence augmentant linéairement. Nous avons démontré que cette augmentation est le résultat d'un échange progressif de BHQ-2-SH par la fonction thiol des protéines HSA présentes dans le plasma humain.²⁹ Cette augmentation de fluorescence linéaire dans P2 a été maintenue pour fournir 40% de clivage de l'espaceur après 72h d'incubation. En revanche, la fluorescence de P1 a demeuré inchangée après avoir atteint un plateau.

En utilisant les sondes FRET, nous avons démontré avec succès une stabilité supérieure des conjugués MD dans le plasma et dans une variété de tampons aqueux. Des études mécanistiques ont révélé que la stabilité accrue est causée par l'hydrolyse rapide du succinimide et induite par le cycle dioxane. Cette hypothèse a été confirmée par une analyse LC-MS du taux d'hydrolyse de la fonction succinimide des sondes P1 et P2 dans le plasma humain à 37 °C. Dans ces conditions, nous avons constaté que la sonde P1 était complètement hydrolysée sous sa forme stable en 29 h. En revanche, la sonde P2 n'était pas propice à l'hydrolyse et seul un minuscule pic (moins de 3%) correspondant à sa forme hydrolysée a été observé après 29 h.

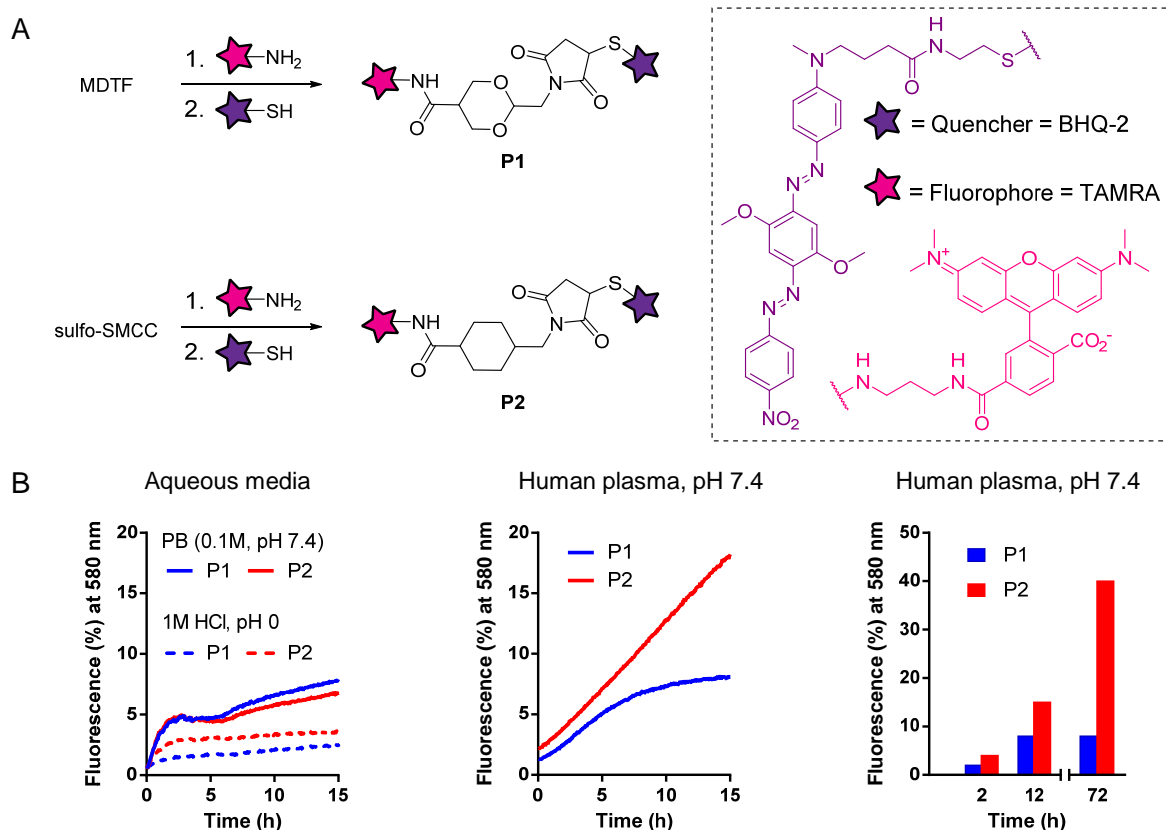


Figure 6. (A) Synthèse de deux sondes FRET, nommées P1 et P2. (B) Stabilité des sondes P1 et P2 (1 μ M) dans le plasma humain à 37 ° C. La fluorescence des sondes P1 et P2 a été étudiée à 580 nm et a été normalisée à la fluorescence d'une solution de TAMRA-NH₂ (1 μ M) et de BHQ-2-SH (1 μ M) dans du plasma humain.

Les linkers de la forme MD semblent donc offrir une possibilité intéressante d'auto-stabilisation des conjugués résultant d'une ouverture du cycle succinimide. Il convient de noter qu'il a déjà été signalé que la stabilisation des conjugués maléimide-à-thiol, obtenue par hydrolyse du cycle succinimide, peut être induite par la modulation du site de conjugaison à un anticorps^{30,31} par un groupe amino adjacent au maléimide,³² en éliminant les substituants N-déficient^{33,34} ou en utilisant des N-aryl-maléimides.³⁵ Dans la plupart des cas, des tampons avec pH élevés sont nécessaires pour obtenir une hydrolyse.^{33,34} De plus, pour permettre l'accès à des conjugués stables dans le sérum, le maléimide peut être remplacé par d'autres groupes réactifs vis-à-vis d'un thiol, tels que le 3-arylpropionitrile^{36,37} ou les sulfates de phényloxadiazoole.³⁸ Alternativement, des méthodes de conjugaison bio-orthogonales peuvent être appliquées.³⁹

Encouragés par ces résultats, nous avons ensuite décidé de tester le réactif MDTF pour la préparation d'un conjugué anticorps-fluorophore et d'évaluer si les propriétés d'auto-hydrolyse

pouvaient être utilisées pour préparer des conjugués stables. À cette fin, une comparaison côte-à-côte avec un réactif sulfo-SMCC a été réalisée (Figure 7).

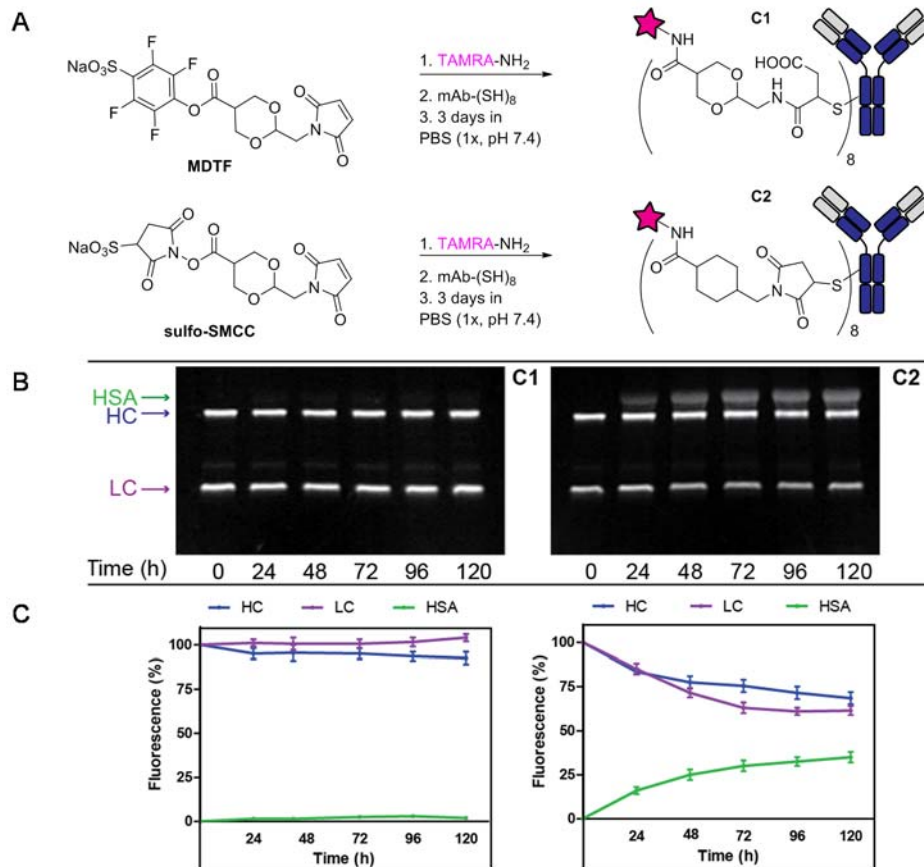


Figure 7. (A) Préparation des conjugués anticorps-fluorophore C1 et C2 par une réaction amine-thiol de MDTF ou sulfo-SMCC avec TAMRA-amine et anti-HER2 anticorps réduit, suivie de l'hydrolyse douce du succinimide dans un tampon PBS (pH 7,5) à 37 °C. (B) L'analyse quantitative de la stabilité du conjugué dans le plasma humain a démontré que 38% du transfert du fluorophore vers la HSA était supérieur à 120 heures pour le conjugué C2 (graphique droit), contrairement à 3% pour le conjugué C1 (graphique gauche).

Premièrement, une réaction entre MDTF ou sulfo-SMCC et TAMRA-NH₂ a été réalisée en utilisant des conditions classiques de conjugaison suivies d'une réaction avec un anticorps anti-HER2 réduit. Les conjugués correspondants ont été purifiés par chromatographie d'exclusion stérique. L'analyse ESI-MS a confirmé la valeur du rapport fluorophore-anticorps de 8 pour les deux conjugués. Pour déclencher l'hydrolyse succinimidylique, les conjugués ont été maintenus dans le tampon PBS à 37 °C pendant 3 jours pour donner les conjugués C1 et C2. Ensuite, les deux conjugués ont été incubés dans du plasma humain pendant cinq jours. Des portions aliquotes

ont été prises toutes les 24 heures et analysées par SDS PAGE. En plus des deux bandes correspondant aux chaînes lourdes (HC) et légères (LC) marquées de l'anticorps, le conjugué MCC a montré l'apparition progressive d'une troisième bande, correspondant au transfert du fluorophore à la HSA.²⁹ L'analyse quantitative par intégration du signal fluorescent de cette bande a montré une dégradation de 38% sur 120 heures pour les conjugués à base de MCC. En revanche, le conjugué C1 n'a pas montré de transfert notable du fluorophore vers la HSA et seulement 3% de dégradation a été observée après 120 heures d'incubation.

Conclusion

En résumé, nous avons développé un nouveau réactif hétérobifonctionnel (MDTF) pour la conjugaison amine-à-thiol qui indique une réactivité similaire à celle des molécules contenant des sulfhydryles en tant que SMCC. La substitution d'un cycle cyclohexylique par un cycle dioxine a augmenté le caractère hydrophile du nouveau linker MD par rapport au linker classique MCC. Fait intéressant, l'espaceur MD a subi une auto-stabilisation dans des conditions douces *via* une ouverture de cycle succinimide. Le linker acide succinamique résultant n'est pas propice à la réaction d'échange de thiol indésirable. Ainsi, une sonde FRET à base de MD incubée dans le plasma humain a montré un taux d'auto-stabilisation considérablement plus élevé que la sonde à base de MCC. Ce processus de stabilisation hydrolytique s'est avéré efficace pour la préparation de conjugués anticorps stables dans le sérum.

Références

- (1) Sano, T., Smith, C., and Cantor, C. (1992) Immuno-PCR: very sensitive antigen detection by means of specific antibody-DNA conjugates. *Science* 258, 120–122.
- (2) Kazane, S. a., Sok, D., Cho, E. H., Uson, M. L., Kuhn, P., Schultz, P. G., and Smider, V. V. (2012) Site-specific DNA-antibody conjugates for specific and sensitive immuno-PCR. *Proc. Natl. Acad. Sci.* 109, 3731–3736.
- (3) Cuellar, T. L., Barnes, D., Nelson, C., Tanguay, J., Yu, S.-F., Wen, X., Scales, S. J., Gesch, J., Davis, D., van Brabant Smith, A., Leake, D., Vandlen, R., and Siebel, C. W. (2015) Systematic evaluation of antibody-mediated siRNA delivery using an industrial platform of THIOMAB-siRNA conjugates. *Nucleic Acids Res.* 43, 1189–1203.
- (4) Mathe, G. ., Tran Ba, L. O. C. ., and Bernard, J. (1958) Effet sur la leucémie 1210 de la Souris d'une combinaison par diazotation d'A-méthoptérine et de γ -globulines de hamsters porteurs de cette leucémie

par hétérogreffe. *C.R. Hebd. Séances Acad. Sci., Série B* 246, 1626–1628.

(5) Perez, H. L., Cardarelli, P. M., Deshpande, S., Gangwar, S., Schroeder, G. M., Vite, G. D., and Borzilleri, R. M. (2014) Antibody-drug conjugates: Current status and future directions. *Drug Discov. Today* 19, 869–881.

(6) Trail, P. a, Willner, D., Lasch, S. J., Henderson, a J., Hofstead, S., Casazza, a M., Firestone, R. a, Hellström, I., and Hellström, K. E. (1993) Cure of xenografted human carcinomas by BR96-doxorubicin immunoconjugates. *Science* 261, 212–215.

(7) Pietersz, G. a, and Krauer, K. (1994) Antibody-targeted drugs for the therapy of cancer. *J. Drug Target.* 2, 183–215.

(8) Bross, P. F., Beitz, J., Chen, G., Xiao Hong Chen, Duffy, E., Kieffer, L., Roy, S., Sridhara, R., Rahman, A., Williams, G., and Pazdur, R. (2001) Approval summary: Gemtuzumab ozogamicin in relapsed acute myeloid leukemia. *Clin. Cancer Res.*

(9) Younes, A., Bartlett, N. L., Leonard, J. P., Kennedy, D. a, Lynch, C. M., Sievers, E. L., and Forero-Torres, A. (2010) Brentuximab vedotin (SGN-35) for relapsed CD30-positive lymphomas. *N. Engl. J. Med.* 363, 1812–1821.

(10) Claro, R. A. De, Mcginn, K., and Kwitkowski, V. (2012) U . S . Food and Drug Administration Approval Summary : Brentuximab Vedotin for the Treatment of Relapsed Hodgkin Lymphoma or Relapsed Systemic Anaplastic Large-Cell Lymphoma U . S . Food and Drug Administration Approval Summary : Lymphoma or Relapsed Sys. *Clin. Cancer Res.* 18, 5845–5849.

(11) Senter, P. D., and Sievers, E. L. (2012) The discovery and development of brentuximab vedotin for use in relapsed Hodgkin lymphoma and systemic anaplastic large cell lymphoma. *Nat. Biotechnol.* 30, 631–637.

(12) Amiri-Kordestani, L., Blumenthal, G. M., Xu, Q. C., Zhang, L., Tang, S. W., Ha, L., Weinberg, W. C., Chi, B., Candau-Chacon, R., Hughes, P., Russell, A. M., Miksinski, S. P., Chen, X. H., McGuinn, W. D., Palmby, T., Schrieber, S. J., Liu, Q., Wang, J., Song, P., Mehrotra, N., Skarupa, L., Clouse, K., Al-Hakim, A., Sridhara, R., Ibrahim, A., Justice, R., Pazdur, R., and Cortazar, P. (2014) FDA approval: Ado-trastuzumab emtansine for the treatment of patients with HER2-positive metastatic breast cancer. *Clin. Cancer Res.* 20, 4436–4441.

(13) Ballantyne, A., and Dhillon, S. (2013) Trastuzumab emtansine: First global approval. *Drugs* 73, 755–765.

(14) Pfister, D., Ulmer, N., Klaue, A., Ingold, O., and Morbidelli, M. (2016) Modeling the Kinetics of Protein Conjugation Reactions. *Chemie Ing. Tech.* 88, 1598–1608.

(15) Kim, M. T., Chen, Y., Marhoul, J., and Jacobson, F. (2014) Statistical modeling of the drug load distribution on trastuzumab emtansine (Kadcyla), a lysine-linked antibody drug conjugate. *Bioconjug.*

Chem. 25, 1223–1232.

(16) Goldmacher, V. S., Amphlett, G., Wang, L., and Lazar, A. C. (2015) Statistics of the Distribution of the Abundance of Molecules with Various Drug Loads in Maytansinoid Antibody–Drug Conjugates. *Mol. Pharm.* 12, 1738–1744.

(17) Hamblett, K. J., Senter, P. D., Chace, D. F., Sun, M. M. C., Lenox, J., Cervený, C. G., Kissler, K. M., Bernhardt, S. X., Kopcha, A. K., Zabinski, R. F., Meyer, D. L., and Francisco, J. A. (2004) Effects of drug loading on the antitumor activity of a monoclonal antibody drug conjugate. *Clin. Cancer Res.* 10, 7063–7070.

(18) Willner, D., Trail, P. A., Hofstead, S. J., King, H. D., Lasch, S. J., Braslawsky, G. R., Greenfield, R. S., Kaneko, T., and Firestone, R. A. (1993) (6-Maleimidocaproyl)hydrazone of doxorubicin. A new derivative for the preparation of immunoconjugates of doxorubicin. *Bioconjug. Chem.* 4, 521–527.

(19) Doronina, S. O., Toki, B. E., Torgov, M. Y., Mendelsohn, B. A., Cervený, C. G., Chace, D. F., DeBlanc, R. L., Gearing, R. P., Bovee, T. D., Siegall, C. B., Francisco, J. a, Wahl, A. F., Meyer, D. L., and Senter, P. D. (2003) Development of potent monoclonal antibody auristatin conjugates for cancer therapy. *Nat. Biotechnol.* 21, 778–784.

(20) Chudasama, V., Maruani, A., and Caddick, S. (2016) Recent advances in the construction of antibody–drug conjugates. *Nat. Chem.* 8, 114–119.

(21) Beck, A., Goetsch, L., Dumontet, C., and Corvaia, N. (2017) Strategies and challenges for the next generation of antibody–drug conjugates. *Nat. Rev. Drug Discov.* 16, 315–337.

(22) Panowski, S., Bhakta, S., Raab, H., Polakis, P., and Junutula, J. R. (2014) Site-specific antibody drug conjugates for cancer therapy. *MAbs* 6, 34–45.

(23) Chudasama, V., Maruani, A., and Caddick, S. (2016) Recent advances in the construction of antibody–drug conjugates. *Nat. Chem.* 8, 114–119.

(24) Koniev, O., and Wagner, A. (2015) Developments and recent advancements in the field of endogenous amino acid selective bond forming reactions for bioconjugation. *Chem. Soc. Rev.* 44, 5495–5551.

(25) Chudasama, V. L., Stark, F. S., Harrold, J. M., Tibbitts, J., Girish, S. R., Gupta, M., Frey, N., and Mager, D. E. (2012) Semi-mechanistic Population Pharmacokinetic Model of Multivalent Trastuzumab Emtansine in Patients with Metastatic Breast cancer. *Clin. Pharmacol. Ther.* 92, 520–527.

(26) Baldwin, A. D., and Kiick, K. L. (2011) Tunable degradation of maleimide–Thiol adducts in reducing environments. *Bioconjug. Chem.* 22, 1946–1953.

(27) Tournier, E. J. M., Wallach, J., and Blond, P. (1998) Sulfosuccinimidyl 4-(N-maleimidomethyl)-1-cyclohexane carboxylate as a bifunctional immobilization agent. Optimization of the coupling conditions. *Anal. Chim. Acta* 361, 33–44.

(28) Gee, K. R., Archer, E. A., and Kang, H. C. (1999) 4-Sulfotetrafluorophenyl (STP) esters: New water-

soluble amine-reactive reagents for labeling biomolecules. *Tetrahedron Lett.* *40*, 1471–1474.

(29) Xu, K., Liu, L., Dere, R., Mai, E., Erickson, R., Hendricks, A., Lin, K., Junutula, J. R., and Kaur, S. (2013) Characterization of the drug-to-antibody ratio distribution for antibody-drug conjugates in plasma/serum. *Bioanalysis* *5*, 1057–1071.

(30) Shen, B.-Q., Xu, K., Liu, L., Raab, H., Bhakta, S., Kenrick, M., Parsons-Reponte, K. L., Tien, J., Yu, S.-F., Mai, E., Li, D., Tibbitts, J., Baudys, J., Saad, O. M., Scales, S. J., McDonald, P. J., Hass, P. E., Eigenbrot, C., Nguyen, T., Solis, W. A., Fuji, R. N., Flagella, K. M., Patel, D., Spencer, S. D., Khawli, L. A., Ebens, A., Wong, W. L., Vandlen, R., Kaur, S., Sliwkowski, M. X., Scheller, R. H., Polakis, P., and Junutula, J. R. (2012) Conjugation site modulates the in vivo stability and therapeutic activity of antibody-drug conjugates. *Nat. Biotechnol.* *30*, 184–9.

(31) Strop, P., Liu, S. H., Dorywalska, M., Delaria, K., Dushin, R. G., Tran, T. T., Ho, W. H., Farias, S., Casas, M. G., Abdiche, Y., Zhou, D., Chandrasekaran, R., Samain, C., Loo, C., Rossi, A., Rickert, M., Krimm, S., Wong, T., Chin, S. M., Yu, J., Dilley, J., Chaparro-Riggers, J., Filzen, G. F., O'Donnell, C. J., Wang, F., Myers, J. S., Pons, J., Shelton, D. L., and Rajpal, A. (2013) Location matters: Site of conjugation modulates stability and pharmacokinetics of antibody drug conjugates. *Chem. Biol.* *20*, 161–167.

(32) Lyon, R. P. P., Setter, J. R. R., Bovee, T. D. D., Doronina, S. O. O., Hunter, J. H. H., Anderson, M. E. E., Balasubramanian, C. L. L., Duniho, S. M. M., Leiske, C. I. I., Li, F., and Senter, P. D. D. (2014) Self-hydrolyzing maleimides improve the stability and pharmacological properties of antibody-drug conjugates. *Nat. Biotechnol.* *32*, 1059–1062.

(33) Tumej, L. N., Charati, M., He, T., Sousa, E., Ma, D., Han, X., Clark, T., Casavant, J., Loganzo, F., Barletta, F., Lucas, J., and Graziani, E. I. (2014) Mild method for succinimide hydrolysis on ADCs: impact on ADC potency, stability, exposure, and efficacy. *Bioconjug. Chem.* *25*, 1871–80.

(34) Fontaine, S. D., Reid, R., Robinson, L., Ashley, G. W., and Santi, D. V. (2015) Long-term stabilization of maleimide-thiol conjugates. *Bioconjug. Chem.* *26*, 145–152.

(35) Christie, R. J., Fleming, R., Bezabeh, B., Woods, R., Mao, S., Harper, J., Joseph, A., Wang, Q., Xu, Z.-Q., Wu, H., Gao, C., and Dimasi, N. (2015) Stabilization of cysteine-linked antibody drug conjugates with N-aryl maleimides. *J. Control. Release* *220*, 660–670.

(36) Kolodych, S., Koniev, O., Baatarkhuu, Z., Bonnefoy, J. Y., Debaene, F., Cianféroni, S., Van Dorsselaer, A., and Wagner, A. (2015) CBTF: New amine-to-thiol coupling reagent for preparation of antibody conjugates with increased plasma stability. *Bioconjug. Chem.* *26*, 197–200.

(37) Koniev, O., Leriche, G., Nothisen, M., Remy, J.-S. S., Strub, J.-M. M., Schaeffer-Reiss, C., Van Dorsselaer, A., Baati, R., and Wagner, A. (2014) Selective irreversible chemical tagging of cysteine with 3-arylpropionitriles. *Bioconjug. Chem.* *25*, 202–206.

(38) Patterson, J. T., Asano, S., Li, X., Rader, C., Barbas, C. F., and Carlos F. Barbas, I. (2014) Improving

the serum stability of site-specific antibody conjugates with sulfone linkers. *Bioconjug. Chem.* 25, 1402–1407.

(39) Lhospice, F., Brégeon, D., Belmant, C., Dennler, P., Chiotellis, A., Fischer, E., Gauthier, L., Boëdec, A., Rispaud, H., Savard-Chambard, S., Represa, A., Schneider, N., Paturel, C., Sapet, M., Delcambre, C., Ingoure, S., Viaud, N., Bonnafous, C., Schibli, R., and Romagné, F. (2015) Site-Specific conjugation of monomethyl auristatin e to Anti-CD30 antibodies improves their pharmacokinetics and therapeutic index in rodent models. *Mol. Pharm.* 12, 1863–1871.